ฤทธิ์ยับยั้งการทำงานของเอนไซม์แอลฟากลูโคซิเดสของสารกลุ่มแลบเดนไดเทอร์ปีนอยด์จากต้นเปล้าหลวง

นางสาว กวิตา ตัณฑุลเวสส

วิทยานิพนธ์นี้เป็นส่วนหนึ่งของการศึกษาตามหลักสูตรปริญญาเภสัชศาสตรมหาบัณฑิต
สาขาวิชาเภสัชเวท ภาควิชาเภสัชเวท
คณะเภสัชศาสตร์ จุฬาลงกรณ์มหาวิทยาลัย
ปีการศึกษา 2549

α-GLUCOSIDASE INHIBITORY ACTIVITY OF LABDANE DITERPENOIDS FROM *CROTON ROXBURGHII*

Miss Kavita Tundulawessa

A Thesis Submitted in Partial Fulfillment of the Requirements

for the Degree of Master of Science in Pharmacy Program in Pharmacognosy

Department of Pharmacognosy

Faculty of Pharmaceutical Sciences

Chulalongkorn University

Academic Year 2006

Thesis Title	α-GLUCOSIDASE INHIBITORY ACTIVITY OF LABDANE DITERPENOIDS FROM *CROTON ROXBURGHII*
By	Miss Kavita Tundulawessa
Field of Study	Pharmacognosy
Thesis Advisor	Associate Professor Chaiyo Chaichantipyuth, Ph. D.

Accepted by the Faculty of Pharmaceutical Sciences, Chulalongkorn University in Partial Fulfillment of the Requirement for the Master's Degree

.....Dean of The Faculty of Pharmaceutical Sciences

(Associate Professor Pornpen Premyothin, Ph. D.)

THESIS COMMITTEE

.....Chairman

(Associate Professor Kittisak Likhitwitayawuid, Ph. D.)

.....Thesis Advisor

(Associate Professor Chaiyo Chaichantipyuth, Ph. D.)

.....Member

(Associate Professor Amorn Petsom, Ph. D.)

.....Member

(Associate Professor Surattana Amnuoypol, Ph. D.)

กวิตา ตัณฑุลเวสส : ฤทธิ์ยับยั้งการทำงานของเอนไซม์แอลฟากลูโคซิเดสของสารกลุ่มแลบเดนไดเทอร์ปีนอยด์จากต้นเปล้าหลวง (α-GLUCOSIDASE INHIBITORY ACTIVITY OF LABDANE DITERPENOIDS FROM *CROTON ROXBURGHII*) อาจารย์ที่ปรึกษา : รศ. ดร. ชัยโย ชัยชาญทิพยุทธ, 152หน้า.

สารประกอบแลบเดนไดเทอร์ปีนอยด์ 5 ชนิด ที่สกัดแยกได้จากเปลือกต้นเปล้าหลวง คือ *ent*-3-oxomanoyl oxide (1), *ent*-1,2-dehydro-3-oxomanoyl oxide (2), *ent*-1,2-dehydro-12α-hydroxy-3-oxomonoyl oxide (3), *ent*-1β-hydroxy-3-oxo-manoyl oxide (4) และ *ent*-3α-hydroxymanoyl oxide (5) และ สารอนุพันธ์ของสารประกอบแลบเดนไดเทอร์ปีนอยด์ 8 ชนิด คือ *ent*-1,2-dehydro-3-oxo-manoyl oxide-14,15-oxirane (6), *ent*-1,2-dehydro-12α-hydroxy-3-oxo-manoyl oxide-14,15-oxirane (7), *ent*-1β-hydroxy-3-oxo-manoyl oxide-14,15-oxirane (8), *ent*-3α-hydroxy-manoyl oxide-14,15-oxirane (9), *ent*-3-oxo-manoyl oxide-14(R),15-diol (10), *ent*-3α-Hydroxy-manoyloxide-14(R),15-diol (11), *ent*-3α,14(R),15-triacetyl-manoyl oxide (12) และ *ent*-3β-hydroxy-manoyl oxide (13) เมื่อนำมาทดสอบการยับยั้งการทำงานของเอนไซม์แอลฟากลูโคซิเดส พบว่า สารประกอบแลบเดนไดเทอร์ปีนอยด์และ สารอนุพันธ์ทั้งหมดมีฤทธิ์ปานกลางในการยับยั้งการทำงานของเอนไซม์ ซึ่งการเติมหมู่ไฮดรอกซีที่คาร์บอนตำแหน่ง 3β (13) จะทำให้ฤทธิ์ยับยั้งการทำงานของเอนไซม์ได้ดีกว่าที่คาร์บอนตำแหน่ง 3α (5) และเมื่อทำปฏิกิริยา epoxidation ที่พันธะคู่ภายนอกวงพบว่ามีผลทำให้การออกฤทธิ์ยับยั้งเอนไซม์เอนไซม์แอลฟากลูโคซิเดสของสารดังกล่าว (6-9) ลดน้อยลงกว่าสารตั้งต้น (2-5)

ภาควิชา.....เภสัชเวท.....
สาขาวิชา....เภสัชเวท.....
ปีการศึกษา...2549.....

ลายมือชื่อนิสิต กวิตา ตัณฑุลเวสส
ลายมือชื่ออาจารย์ที่ปรึกษา ชัยโย ชัยชาญทิพยุทธ

4676552333 MAJOR PHARMACOGNOSY

KEY WORD : *CROTON ROXBURGHII* / LABDANE DITERPENOIDS / α-GLUCOSIDASE

KAVITA TUNDULAWESSA : ALPHA-GLUCOSIDASE INHIBITORY ACTIVITY OF LABDANE DITERPENOIDS FROM *CROTON ROXBURGHII*. THESIS ADVISOR : ASSOCIATE PROFESSOR CHAIYO CHAICHANTIPYUTH, Ph. D. 152 pp.

Five labdane diterpenoids, *ent*-3-oxomanoyl oxide (1), *ent*-1,2-dehydro-3-oxomanoyl oxide (2), *ent*-1,2-dehydro-12α-hydroxy-3-oxomonoyl oxide (3), *ent*-1β-hydroxy-3-oxo-manoyl oxide (4) and *ent*-3α-hydroxymanoyl oxide (5) were isolated from the stem bark of *Croton roxburghii* N.P. Balakr, and they were derivatized to give 8 derivatives, *ent*-1,2-dehydro-3-oxo-manoyl oxide-14,15-oxirane (6), *ent*-1,2-dehydro-12α-hydroxy-3-oxo-manoyl oxide-14,15-oxirane (7), *ent*-1β-hydroxy-3-oxo-manoyl oxide-14,15-oxirane (8), *ent*-3α-hydroxy-manoyl oxide-14,15-oxirane (9), *ent*-3-oxo-manoyl oxide-14(R),15-diol (10), *ent*-3α-hydroxy-manoyloxide-14(R),15-diol (11), *ent*-3α,14(R),15-triacetyl-manoyl oxide (12) and *ent*-3β-hydroxy-manoyl oxide (13). All of the isolated compounds and their derivatives showed moderate α-glucosidase inhibitory activity. Assay for α-glucosidase inhibitory activity showed that 3β-C substituted (13) increased the α-glucosidase inhibitory activities more than 3α-C substituted (5). Epoxidation of the exocyclic double bond (6-9) makes the inhibitory activity reduced.

Department of....Pharmacognosy..... Student's signature.....Kavita Tundulawessa

Field of study.....Pharmacognosy..... Advisor's signature.....

Academic year....2006.....

ACKNOWLEDGEMENTS

The author wishes to express her deepest gratitude to her thesis advisor, Associate Professor Dr. Chaiyo Chaichantipyuth, Department of Pharmacognosy, Faculty of Pharmaceutical Sciences, Chulalongkorn University, for his guidance, suggestions, encouragement and support throughout the course of this study.

Her gratitude is particularly extended to Associate Professor Dr. Amorn Petsom, Department of Chemistry, Faculty of Science, Chulalongkorn University, without whose generous advice, spectroscopic expertise and data supplementation, the completion of this work would not have been possible.

For the provision of laboratory facilities, her most sincere thank goes to the Department of Pharmacognosy, Faculty of Pharmaceutical Sciences, Chulalongkorn University.

The author would also like to acknowledge, with great appreciation, the financial support she received from the Graduate School of Chulalongkorn University.

Her gratitude is also extended to Associate Professor Dr. Kittisak Likhitwitayawuid and Associate Professor Dr. Surattana Amnuoypol for serving as thesis committee members and for their valuable comments and useful suggestions. Moreover, the author would also like to thank Ms. Songchan Phuthong of the Institute of Biotechnology and Genetic Engineering, Chulalongkorn University, for cytotoxic activity test.

A large dept to gratitude is owed to her teachers, friends and all the staff members of the Department of Pharmacognosy, Faculty of Pharmaceutical Sciences, Chulalongkorn University, who kindly offered their assistance, encouragement, and helpful comments throughout this research. Although she has received the generosity of too many of them to list them individually in this page, her appreciation is beyond words.

CONTENTS

CHAPTER Page

CHAPTER Page

LIST OF TABLES

LIST OF FIGURES

Figures Page

Figures Page

Figures Page

Figures Page

LIST OF SCHEMES

Scheme Page

LIST OF ABBREVIATIONS

Ac_2O	=	Acetic anhydride
br	=	Broad (for NMR spectral data)
c	=	Concentration
^{o}C	=	Degree Celcius
$CDCl_3$	=	Deuterated chloroform
$CHCl_3$	=	Chloroform
cm	=	Centimeter
cm^{-1}	=	Reciprocal centimeter (unit of wave number)
^{13}C-NMR	=	Carbon-13-Nuclear Magnetic Resonance
d	=	Doublet (for NMR spectral data)
dd	=	Doublet of doublets (for NMR spectral data)
dia.	=	Diameter
2D	=	Two Dimensional
DEPT	=	Distortionless Enhancement by Polarization Transfer
DNJ	=	Deoxynojirimycin
EtOAc	=	Ethyl Acetate
g	=	Gram
H-HCOSY	=	Homonuclear (Proton-Proton) Correlation Spectroscopy
HMBC	=	H-detected Heteronuclear Multiple Bond Coherence
HMQC	=	H- detected Heteronuclear Multiple Quantum Coherence
H-NMR	=	Proton Nuclear Magnetic Resonance
Hz	=	Hertz
IR	=	Infrared Spectroscopy
J	=	Coupling constant
KBr	=	Potassium bromide
kg	=	Kilogram
L	=	Liter
m	=	Multiplet (for NMR spectral data)
mg	=	Milligram
ml	=	Milliter

mm	=	Millimeter
m-CPBA	=	*m*-chloroperbenzoic acid
MeOH	=	Methanol
MS	=	Mass Spectroscopy
m/z	=	mass-to charge ratio
M^+	=	Molecular ion
NMR	=	Nuclear Magnetic Resonance
NOESY	=	Nuclear Overhauser Enhancement Spectroscopy
No.	=	Number
ppm	=	part per million
q	=	Quartet (for NMR spectral data)
s	=	Singlet (for NMR spectral data)
t	=	Triplet (for NMR spectral data)
TLC	=	Thin Layer Chromatography
UV	=	Ultraviolet Spectroscopy
ν_{max}	=	Wave number at maximum absorption
λ_{max}	=	Wavelength at maximum absorption
δ	=	Chemical Shift
ε	=	Molar absorption
$[\alpha]^{20}_{D}$	=	Specific Rotation at 20° at Sodium D line (589 nm)

CHAPTER I

INTRODUCTION

Croton roxburghii N.P. Balakr. is a plant in Euphorbiaceae family, in the *Croton* genus, commonly known as Plao Yai (central part), Plao Luang (Northern part), Po (Kamphaeng Phet), Khwa-wuu (Karen-Kanchanaburi), Sa-ku-wa (Karen-Mae Hong Son) and Haa-yoeng (Shan-Mae Hong Son)

The plant is a medium size deciduous tree. It is widely distributed throughout Thailand. The calyx and ovary are clothed with minute orbicular silvery scales. The leaves fall between 5.6-12.0 cm. by 13.0-24.0 cm. in size. The leaf is oblong-lanceolate shaped. The Flowers are pale yellowish green and solitary in the axials of minute bracts on long erect racemes. The male flowers are located in the upper part of the racemes and the famales in the lower part. The male flowers are slender, and have the length of pedicels of 4.0 mm. The calyx is more than 6.0 mm. long, and segments are woolly. The twelves stamens are inflexed in bud, and the length of filament is 3.0 mm.. In female flowers, the pedicels are short and stout. It's sepals are more acute than in the male, with densely ciliate margins. The diameter of the fruit is less than 1.3 cm., slightly 3-lobed and clothed with small orbicular and scales. Seeds 8 by 6 mm., ellipsoid, rounded and quite smooth on the back. The pictures of *Croton roxburghii* N.P. Balakr. are shown in Figure 1 (Blatter, Caius and Mhaskar, 1975)

Croton roxburghii N.P. Balakr. is one of the interesting Thai medicinal plants because it is believed that all parts of the plants can be used as medicine. Its leaves are used as a tonic, and the flowers are used as a parasiticide, and the fruits are used as a purgative. The bark is used to treat dyspepsia, and the roots are used as dysentery. Moreover this plant has been used in combination with *C. sublyratus* to treat gastric ulcer and gastric cancer.

The objectives of this research.

1. Isolation of labdane diterpenoids from *Croton roxburghii* N.P. Balakr.
2. Preparation of derivatives of isolated compounds.

3. Examination of the isolated diterpenoids and derivatives for α-glucosidase inhibitory activity.

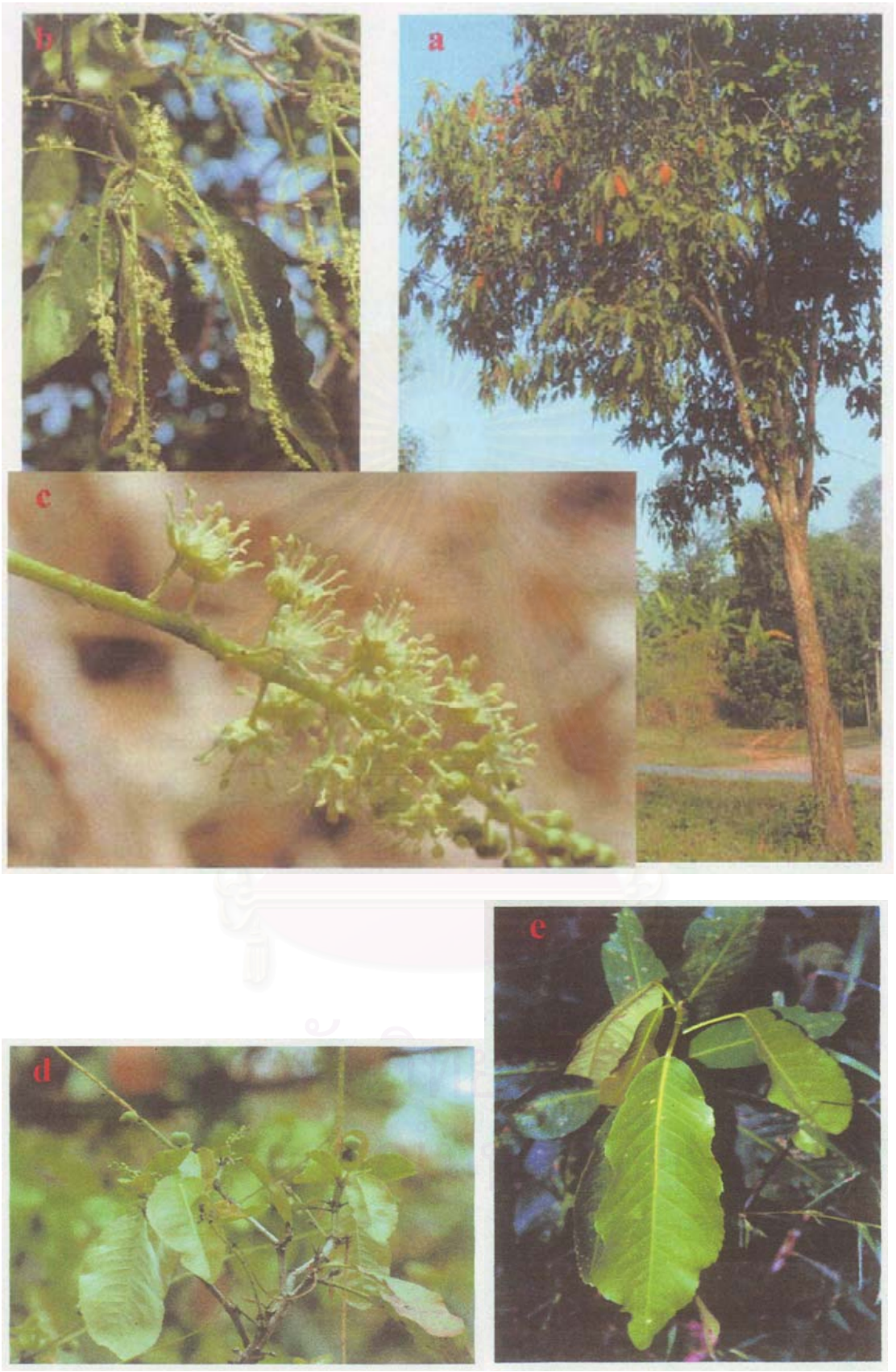

Figure 1. *Croton roxburghii* N.P. Balakr.

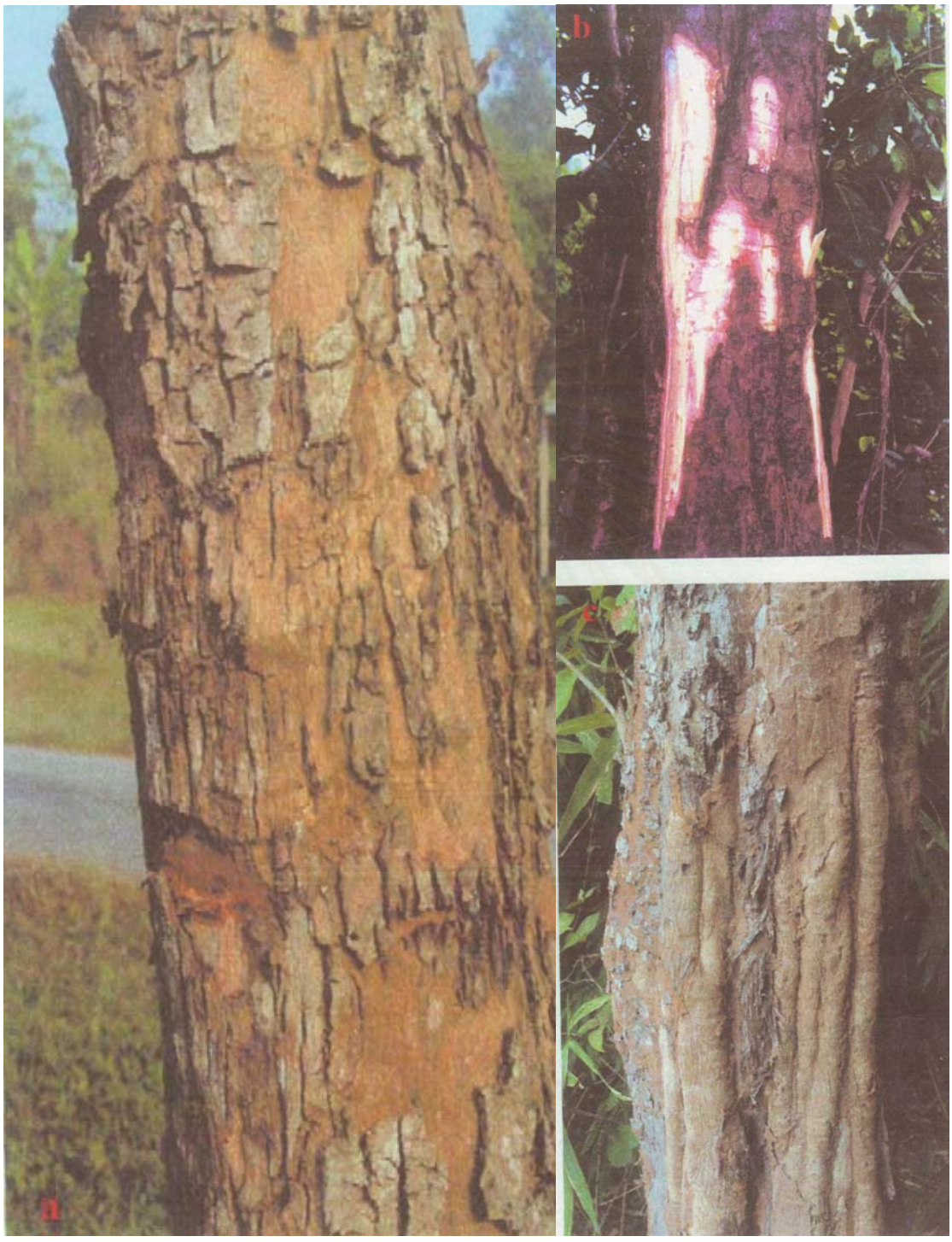

Figure 2. Stem bark of *Croton roxburghii* N.P. Balakr.

CHAPTER II

HISTORICAL

1. Chemical constituents of *Croton roxburghii* N.P. Balakr.

According to previous phytochemical studies, *Croton roxburghii* N.P. Balakr. has been found to be a rich source of diterpenoid compounds. Eight different types of the main diterpenoid skeletons have been isolated from this plant, namely Cembrane, Labdane, Clerodane, Cleistanthane, Pimarane, Abietane, Kaurane, and Trachylobane. In addition to these diterpenoids, triterpenoids, steroids and several other chemical constituents are also present, as summarized in the Table 1.

Table 1. Chemical constituents of *Croton roxburghii* N.P. Balakr.

Consituents	Parts	References
<u>Diterpenoids</u> **1. Cembrane diterpenoids**		
■ crotocembraneic acid **[1]**	stem bark	Surachethapan,1996; Roengsumran *et al.*,1998
■ neocrotocembraneic acid **[2]**	leaves	Achayindee, 1996;
	stem bark	Roengsumran *et al.*,1998.
■ neocrotocembranal **[3]**	stem bark	Roengsumran *et al.*,1999b.
■ poilaneic acid **[4]**	stem bark	Boontha, 2000.
■ (2*E*,7*E*,11*E*) 1-isopropyl-1,4-dihydroxy-4,8-dimethylcyclotetradeca-2,7,11-triene-12-carboxylic acid **[5]**	stem bark	Tanwattanakun,1999.

Table 1. Chemical constituents of *Croton roxburghii* N.P. Balakr.(continued)

Consituents	Parts	References
2. Labdane diterpenoids		
■ *ent*-8(17), 12(*E*),14- labdatrien-18-oic acid **[6]**	stem bark	Pattamadilok, 1998.
■ 12,15-epoxy-8 (17),12,14-labdatriene **[7]**	stem bark	Pattamadilok, 1998.
■ labda-7,12 (*E*) 14-triene **[8]**	stem bark	Roengsumran *et al.*,1999a.
■ labda-7,12 (*E*) 14-triene-17-al **[9]**	stem bark	Roengsumran *et al.*,1999a.
■ labda-7,12 (*E*) 14-triene-17-ol **[10]**	stem bark	Roengsumran *et al.*,1999a.
■ labda-7,12 (*E*) 14-triene-17-oic acid **[11]**	stem bark	Roengsumran *et al.*,1999a.
■ labda-7,13 (*Z*)-diene-17,12-olide **[12]**	stem bark	Baiagern, 1999.
■ labda-7,13 (*Z*)-diene-17,12-olide-16-ol **[13]**	stem bark	Baiagern, 1999.
■ 2-acetoxy-labda-8(17),12 (*E*),14-triene-3-ol **[14]**	stem bark	Kuptiyanuwat, 1999. Roengsumran *et al.*, 2001.
■ 3-acetoxy-labda-8(17),12 (*E*),14-triene-2-ol **[15]**	stem bark	Kuptiyanuwat, 1999. Roengsumran *et al.*, 2001.

Table 1. Chemical constituents of *Croton roxburghii* N.P. Balakr.(continued)

Consituents	Parts	References
■ labda-8(17),12 (*E*),14-triene -2,3-diol **[16]**	stem bark	Kuptiyanuwat, 1999. Roengsumran *et al*., 2001.
■ 12 (*E*), 14-labdadiene-7,8-diol **[17]**	stem bark	Boontha, 2000.
■ 6-acetoxy-12 (*E*), 14-labdadiene-7,8-diol **[18]**	stem bark	Boontha, 2000.
■ 12 (*E*), 14-labdadiene-6,7,8-triol **[19]**	stem bark	Boontha, 2000.
■ nidorellol **[20]**	stem bark	Roengsumran *et al*.,2002.
3. Clerodane diterpenoids ■ (-)-hardwickiic acid **[21]**	root bark wood	Aiyar and Seshadri, 1972b.
	stem bark	Aiyar and Seshadri, 1972a; Surachethapan, 1996; Baiagern, 1999; Sirimongkhon, 2000; Sriyangnok, 2000.
■ 11-dehydro-(-)-hardwickiic acid **[22]**	stem bark	Aiyar and Seshadri, 1972a.
	root bark wood	Aiyar and Seshadri, 1972b.

Table 1. Chemical constituents of *Croton roxburghii* N.P. Balakr.(continued)

Consituents	Parts	References
■ (-)-20-benxyloxyhardwickiic acid **[23]**	stem bark	Baiagern, 1999.
■ methyl-15,16-epoxy-12-oxo-3,13(16),14-clerodatriene-20,19-olide-17-oate **[24]**	stem bark	Tanwattanakun, 1999.
■ crovatin **[25]**	stem bark	Siriwat, 1999.
■ croblongifolin **[26]**	stem bark	Roengsumran *et al.*,2002.
4. Cleistanthane diterpenoid ■ 3,4-*seco*-cleistantha-4(18),13(17),15-trien-3-oic acid **[27]**	stem bark	Siriwat, 1999; Sriyangnok,2000.
5. Pimarane diterpenoids ■ oblongifoliol **[28]**	stem bark	Rao *et al.*,1968.
	root bark wood	Aiyar and Seshadri, 1972b.
■ 19-deoxyoblongifoliol **[29]**	stem bark	Rao *et al.*,1968.
	root bark wood	Aiyar and Seshadri, 1972b.

Table 1. Chemical constituents of *Croton roxburghii* N.P. Balakr.(continued)

Consituents	Parts	References
■ 3-deoxyoblongifoliol **[30]**	stem bark	Aiyar and Seshadri, 1971a.
	root bark wood	Aiyar and Seshadri, 1972b.
■ oblongifolic acid **[31]**	stem bark	Aiyar and Seshadri, 1970.
	root bark wood	Aiyar and Seshadri, 1972b.
■ *ent*-isopimara-7,15-diene **[32]**	stem bark	Aiyar and Seshadri, 1971b.
	root bark wood	Aiyar and Seshadri, 1972b.
■ *ent*-isopimara-7,15-diene-19-aldehyde **[33]**	stem bark	Aiyar and Seshadri, 1971b.
	root bark wood	Aiyar and Seshadri, 1972b.
■ 19-hydroxy-*ent*-isopimara-7,15-diene **[34]**	stem bark	Aiyar and Seshadri, 1971b.
■ (-)-pimara-9(11),15-diene-19-oic acid **[35]**	stem bark	Tanwattanakun, 1999.
■ (-)-pimara-9(11),15-diene-19-ol **[36]**	stem bark	Tanwattanakun, 1999.

Table 1. Chemical constituents of *Croton roxburghii* N.P. Balakr.(continued)

Consituents	Parts	References
6. Abeitane diterpenoid		
■ abeita-7,13-diene-3-one **[37]**	stem bark	Sriyangnok, 2000.
7.Kaurane diterpenoid		
■ *ent*-kaur-16-en-19-oic acid **[38]**	stem bark	Pattamadilok, 1998; Sirimongkhon, 2000.
8. Trachylobane diterpenoid		
■ trachyloban-19-oic acid **[39]**	stem bark	Boontha, 2000.
<u>Triterpenoid</u>		
■ acetyl aleuritolic acid **[40]**	stem bark	Aiyar and Seshadri, 1971c
<u>Steroids</u>		
■ campesterol **[41]**	wood stem bark	Chaicharoenpong, 1996 Pattamadilok, 1998
■ stigmasterol **[42]**	wood leaves stem bark	Chaicharoenpong, 1996 Achayindee, 1996 Pattamadilok, 1998
■ β-sitosterol **[43]**	stem bark wood leaves	Rao et al., 1968 Chaicharoenpong, 1996 Achayindee, 1996

Table 1. Chemical constituents of *Croton roxburghii* N.P. Balakr.(continued)

Consituents	Parts	References
<u>Steroid Glucosides</u> ■ stigmasteryl-3-O-β-D-glucopyranoside **[44]**	wood	Chaicharoenpong, 1996
■ β-sitosteryl-3-O-β-D-glucopyranoside **[45]**	wood	Chaicharoenpong, 1996
■ campesteryl-3-O-β-D-glucopyranoside **[46]**	wood	Chaicharoenpong, 1996
<u>Coumarin</u> ■ 7-hydroxy-6-methoxycoumarin (Scopoletin) **[47]**	wood	Chaicharoenpong, 1996
<u>Miscellaneous</u> ■ mixture of long chain aliphatic hydrocarbon (C_{27}-C_{33})	wood leaves	Chaicharoenpong, 1996 Achayindee, 1996
■ mixture of long chain aliphatic carboxylic acid (C_{18}, C_{22}-C_{34})	wood	Chaicharoenpong, 1996
■ mixture of long chain alcohol (C_{28}-$C_{29,}$ C_{31}-$C_{32,}$ C_{34})	leaves	Achayindee, 1996
■ 6,10,14-trimethyl-2-pentadecanone **[48]**	leaves	Achayindee, 1996
■ potassium chloride	leaves	Achayindee, 1996

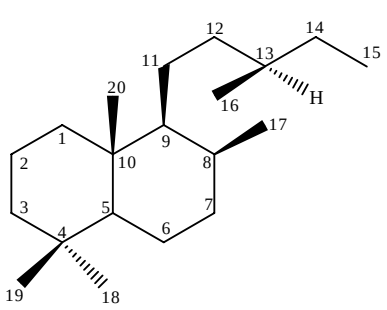

Labdane

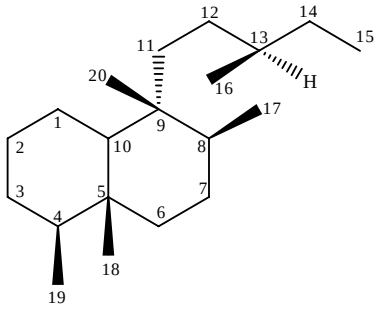

Clerodane

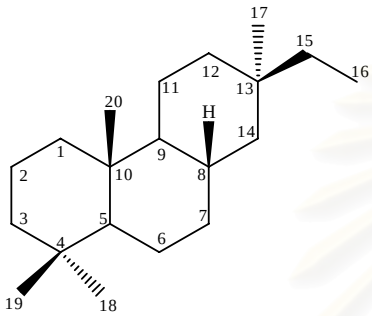

Pimarane

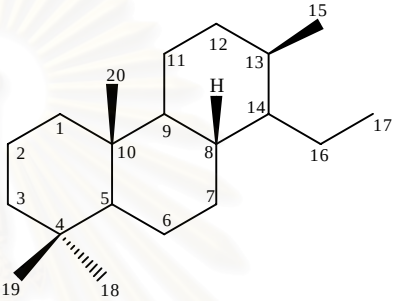

Cleistanthane

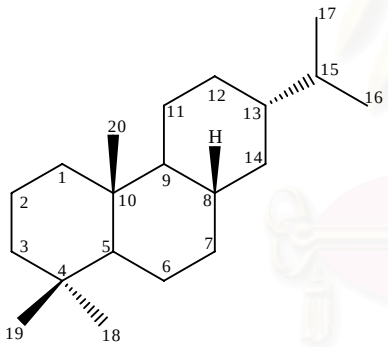

Abietane

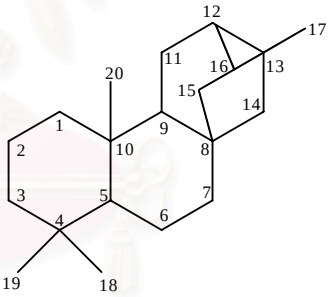

Trachylobane

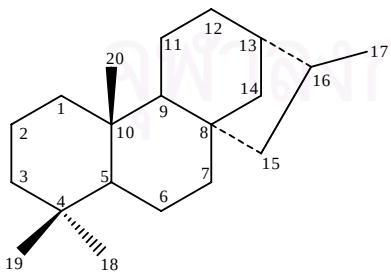

Kaurane

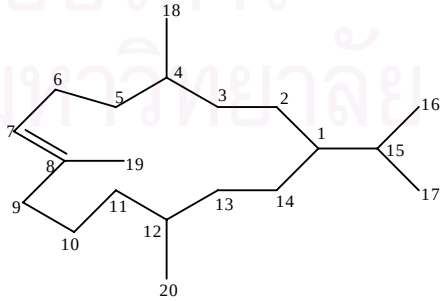

Cembrane

Figure 3. Basic structures of diterpenoid compounds in *C. roxburghii* N.P. Balakr.

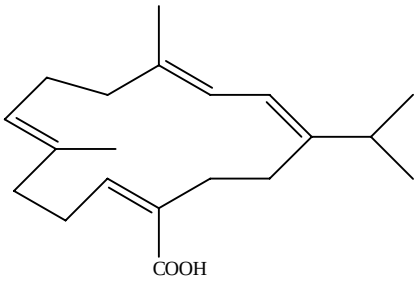

crotocembraneic acid **[1]**

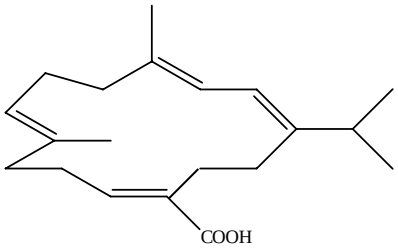

neocrotocembraneic acid **[2]**

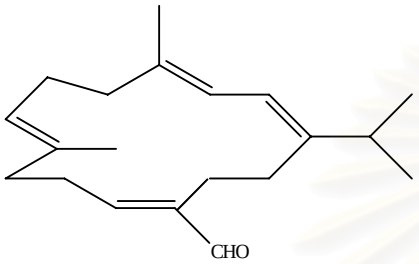

neocrotocembranal **[3]**

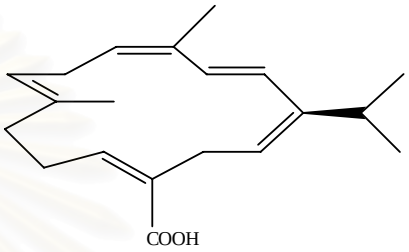

poilaneic acid **[4]**

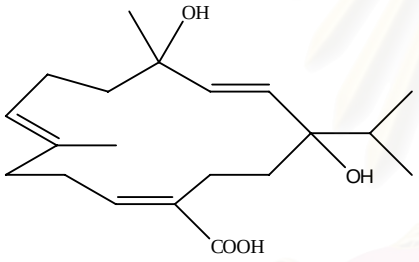

(2*E*,7*E*,11*E*) 1-isopropyl-1,4-dihydroxy-4,8-dimethylcyclotetradeca-2,7,11-triene-carboxylic acid **[5]**

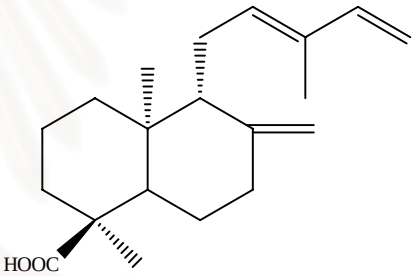

ent-8(17), 12(*E*),14- 12labdatrien-18-oic acid **[6]**

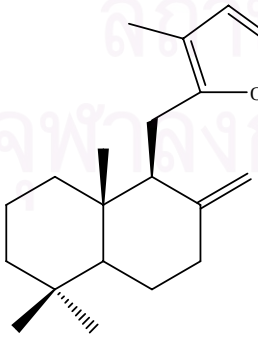

12,15-epoxy-8 (17),12,14- labdatriene **[7]**

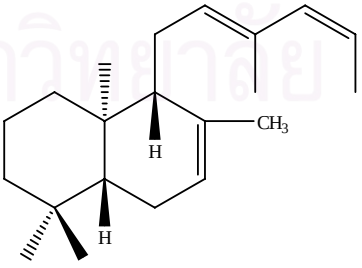

labda-7,12 (*E*) 14-triene **[8]**

Figure 4. Structural of chemical constituents of *C. roxburghii*.

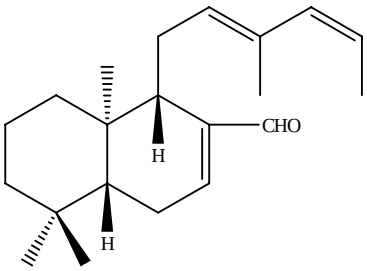

labda-7,12 (*E*)14-triene-17-al **[9]**

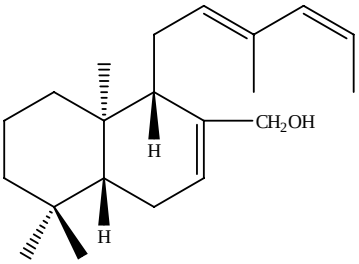

labda-7,12 (*E*)14-triene-17-ol **[10]**

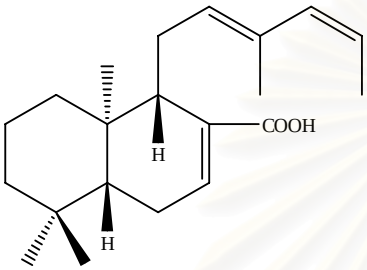

labda-7,12 (*E*)14-triene-17-oic acid **[11]**

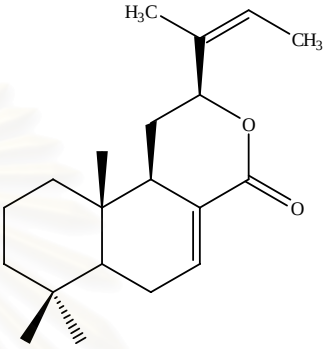

labda-7,13 (*Z*)-diene-17,12-olide **[12]**

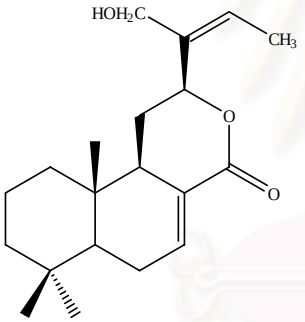

labda-7,13 (*Z*)-diene-17,12-olide-16-ol **[13]**

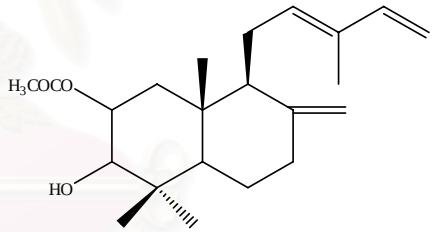

2-acetoxy-labda-8(17),12 (*E*),14-triene-3-ol **[14]**

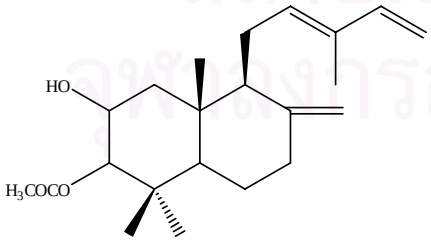

3-acetoxy-labda-8(17),12 (*E*),14-triene-2-ol **[15]**

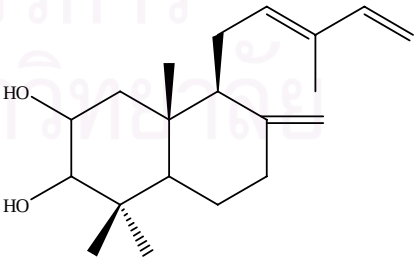

labda-8(17),12 (*E*),14-triene -2,3-diol **[16]**

Figure 4. Structural of chemical constituents of *C. roxburghii*. (continued)

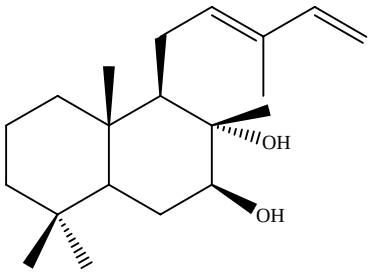

12 (*E*), 14-labdadiene-7,8-diol **[17]**

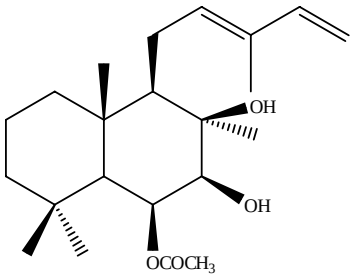

6-acetoxy-12 (*E*), 14-labdadiene-7,8-diol **[18]**

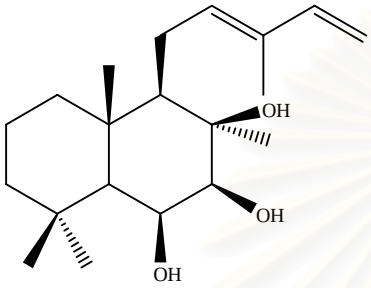

12 (*E*), 14-labdadiene-6,7,8-triol **[19]**

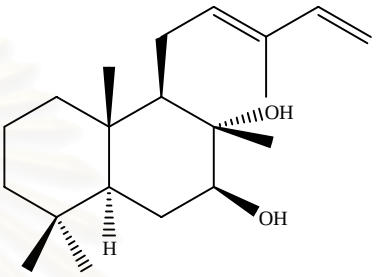

nidorellol **[20]**

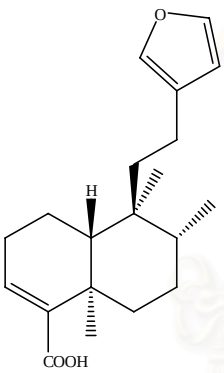

(-)-hardwickiic acid **[21]**

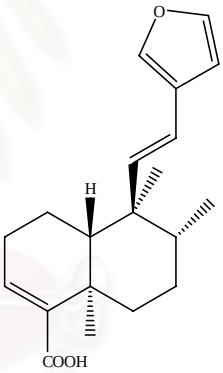

11-dehydro-(-)-hardwickiic acid **[22]**

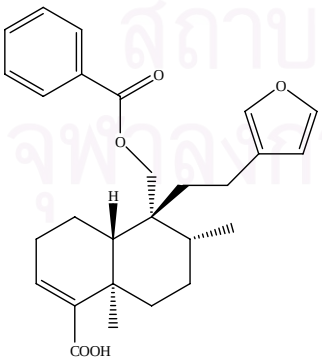

(-)-20-benxyloxyhardwickiic acid **[23]**

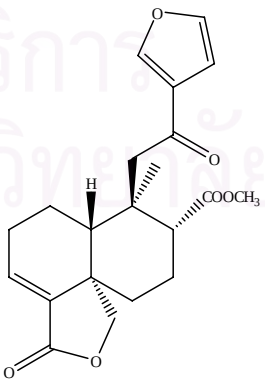

Methyl-15,16-epoxy-12-oxo-3,13(16),
14-clerodatriene-20,19-olide-17-oate **[24]**

Figure 4. Structural of chemical constituents of *C. roxburghii*. (continued)

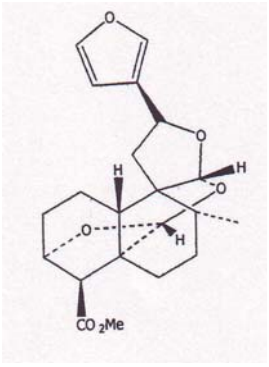

crovatin **[25]**

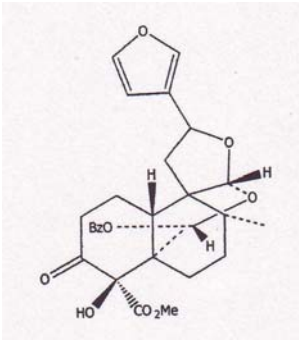

croblongifolin **[26]**

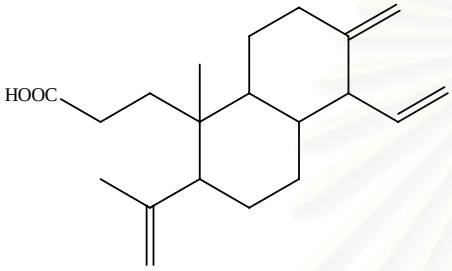

3,4-*seco*-cleistantha-4(18),13(17),
15-trien-3-oic acid **[27]**

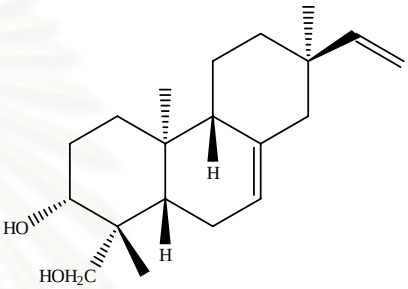

oblongifoliol **[28]**

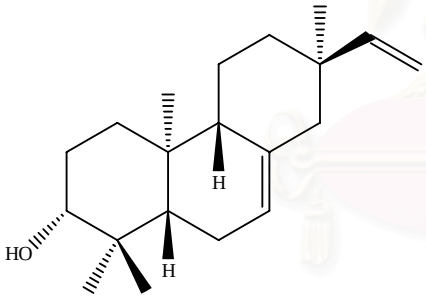

19-deoxyoblongifoliol **[29]**

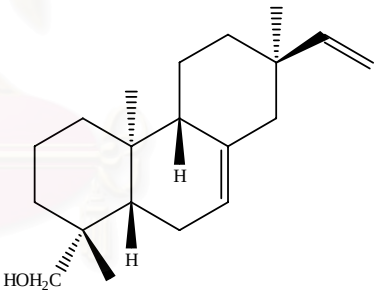

3-deoxyoblongifoliol **[30]**

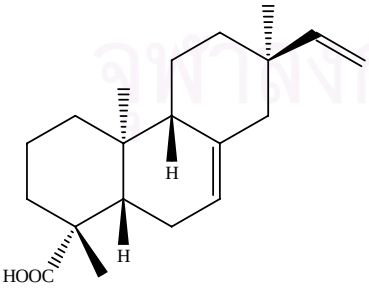

oblongifolic acid **[31]**

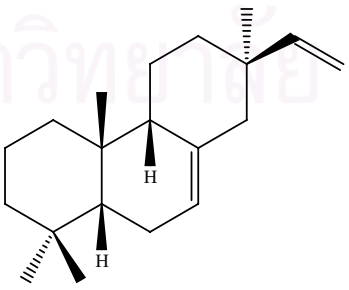

ent-isopimara-7,15-diene **[32]**

Figure 4. Structural of chemical constituents of *C. roxburghii*. (continued)

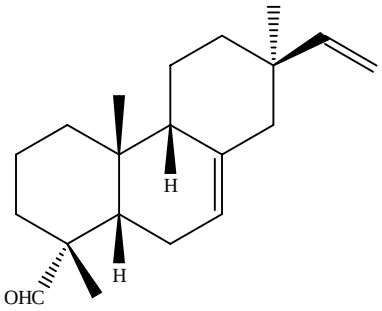

ent-isopimara-7,15-diene-19-aldehyde **[33]**

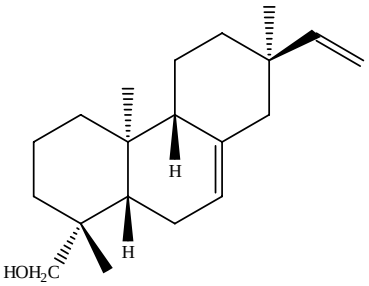

19-hydroxy-*ent*-isopimara-7,15-diene **[34]**

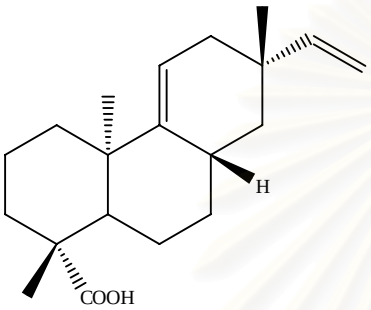

(-)-pimara-9(11),15-diene-19-oic acid **[35]**

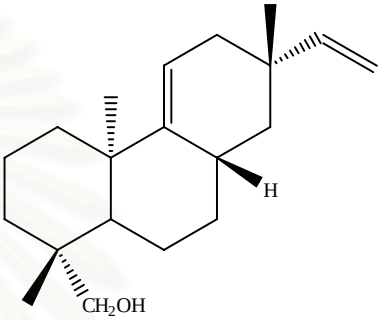

(-)-pimara-9(11),15-diene-19-ol **[36]**

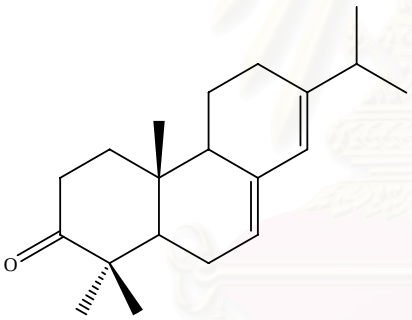

abeita-7,13-diene-3-one **[37]**

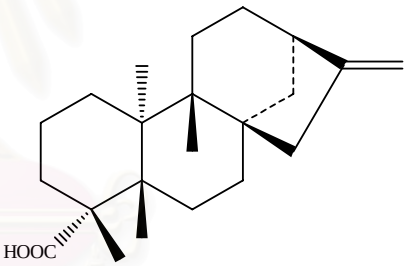

ent-kaur-16-en-19-oic acid **[38]**

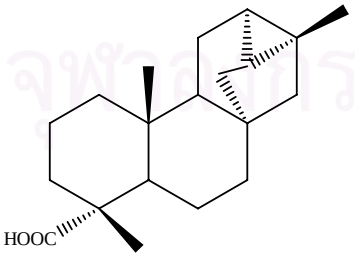

trachyloban-19-oic acid **[39]**

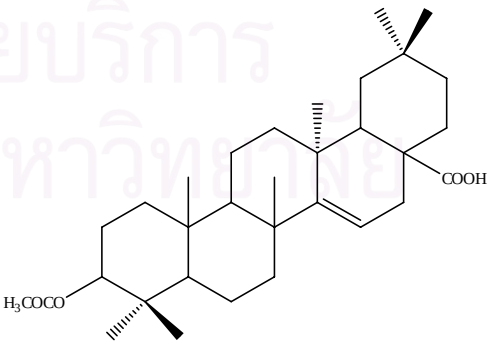

acetyl aleuritolic acid **[40]**

Figure 4. Structural of chemical constituents of *C. roxburghii*. (continued)

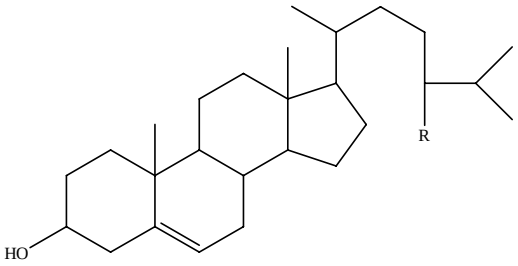

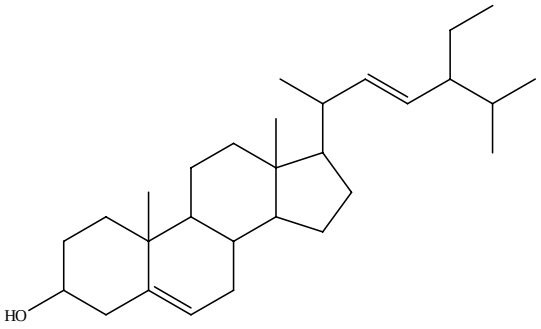

campesterol: R= C_2H_5 **[41]**

stigmasterol **[42]**

β-sitosterol : R= CH_3 **[43]**

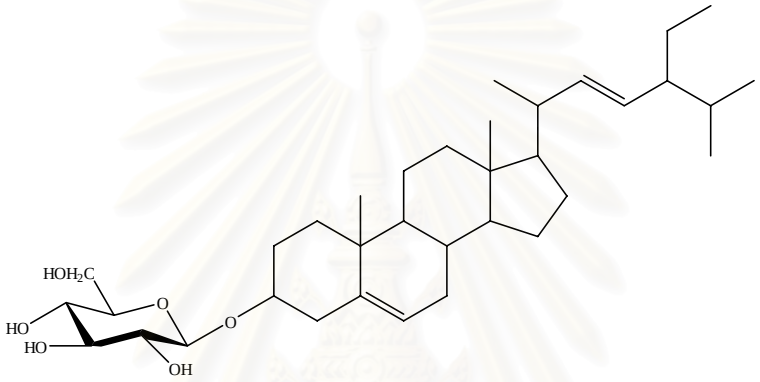

stigmasteryl-3-O-β-D-glucopyranoside **[44]**

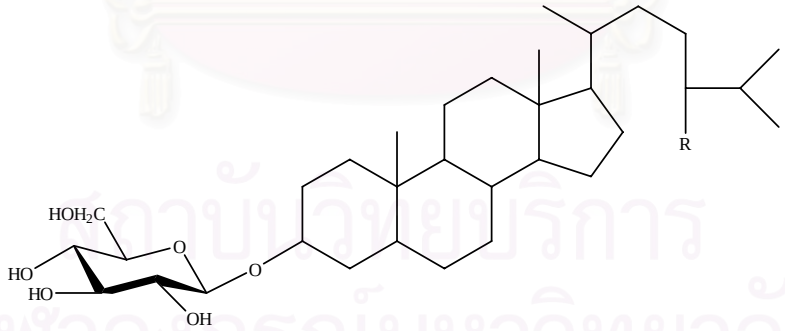

β-sitosteryl-3-O-β-D-glucopyranoside ; R= C_2H_5 **[45]**

campesteryl-3-O-β-D-glucopyranoside : R= CH_3 **[46]**

Figure 4. Structural of chemical constituents of *C. roxburghii*. (continued)

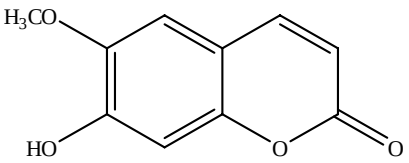

7-hydroxy-6-methoxycoumarin (Scopoletin) **[47]**

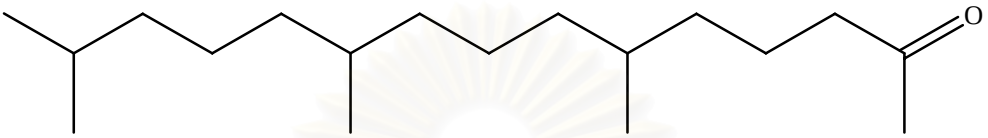

6,10,14-trimethyl-2-pentadecanone **[48]**

Figure 4. Structural of chemical constituents of *C. roxburghii*. (continued)

2. Biological activies of diterpenoids compounds from *Croton roxburghii* N.P. Balakr.

Diterpenoids compounds isolated from *C. roxburghii* have been investigated for many biological activities such as cytotoxicity, antimicrobial, antiplatelet aggregation, cAMP phosphodiesterase inhibition, antioxidant and antibacterial. The biological activities which have been reported as potent are cytotoxicity, antiplatelet aggregation, antimicrobial and insecticidal activities.

2.1 Cytotoxic activity

Some of the diterpene compounds listed in Table 2 have shown to exhibit in vitro cytotoxicity against many human tumor cell lines, as below.

Table2. Cytotoxic activity of some diterpene compounds from *C. roxburghii*

Compounds	IC_{50}(μg/mL)					References
	KATO-3	SW620	BT474	HEP-G2	CHAGO	
[13]	7.1	6.5	>10	5	6.4	Baiagern, 1999.
[14]	5.7	7.1	>10	>10	>10	Roengsumran *et al.*, 2001.
[15]	3.3	>10	5.9	>10	>10	Roengsumran *et al.*, 2001.
[16]	2.2	2.7	4.6	3.7	3.3	Roengsumran *et al.*, 2001.
[26]	0.35	0.47	0.12	0.35	0.24	Roengsumran *et al.*, 2002.
[36]	6.5	5.9	>10	6.7	6.1	Tanwattanakun, 1999.

[13] = labda-7,13 (*Z*)-diene-17,12-olide-16-ol

[14] = 2-acetoxy-labda-8 (17),12 (*E*),14-triene-3-ol

[15] = 3-acetoxy-labda-8 (17),12 (*E*),14-triene-2-ol

[16] = labda-8(17),12 (*E*),14-triene -2,3-diol

[26] = croblongifolin

[36] = (-)-pimara-9(11),15-diene-19-ol

Tumor Cell Lines:

KATO-3 = human gastric carcinoma

SW620 = human colon adenocarcinoma

BT474 = human breast ductal carcinoma

HEP-G2 = human liver hepatoblastoma

CHAGO = human undifferentiated lung carcinoma

From the data in Table 2 it is very interesting to note that, among the three structurally related labdane diterpenes **[14-16]**, **[14]** and **[15]** were less active but more selective than **[16]**. The presence of the acetyl group is believed to be the cause of this, since it is likely that an acetylation of these compound could decrease their ability to form hydrogen bond with certain receptor on tumor cells and made them more selective but less active (Roengsumran et al., 2001). Furthermore, neocrotocembranol **[3]** exhibited cytotoxicity against P-388 cells (lymphoid neoplasm) *in vitro* with and IC_{50} value of 6.48 (μg/mL)(Roengsumran *et al*.,1999b).

2.2 Antiplatelet aggregation

Another notable compound derived from this plant, is neocrotocembranol **[3]**. This compound inhibited platelet aggregation induced by thrombin with an IC_{50} value of

47.21 (μg/mL). However, two other cembranoid diterpenes, crotocembraneic acid **[1]** and neocrotocembraneic acid **[2]**, showed no inhibitory effect on platelet aggregation. Thus, the reactive aldehyde functionality was proposed as playing an important part in this effect. (Roengsumran et al.,1999b).

2.3 Insecticidal activity

(-)-Hardwickiic acid **[21]**, a well-known clerodane diterpene, has been reported as having insecticidal activity against *Alphis craccivora* (Aphidae). The compound, at a dose of 5 ppm/insect, caused 62% mortality of adult female aphids after 24 hours (Bandara et al., 1987).

2.4 Antimicrobial activity

The clerodane diterpene compound, (-)-hardwickiic acid **[21]** exhibited antimicrobial activity against gram-positive bacteria (*Bacillus subtilis*, *Staphylococcus aureus*) and *Mycobacterium smegmatis*. (Jame, Slice and Edilberto, 1991).

2.5 Inhibition of cAMP phosphodiesterase activity

Cembranoid compounds, crotocembraneic acid **[1]** and neocrotocembraneic acid **[2]** have been reported to act as inhibitors of cAMP phosphodiesterase activity (Singtothong, 1999).

3. Biogenetic pathway of diterpenoids in *Croton roxburghii* N.P. Balakr.

The diterpenes are C 20 compounds biogenetically derived from geranylgeranyl pyrophosphate. The notable feature of diterpene structures is the fascinating variation encountered in their skeletons, which accounts for the division of these compounds into several types. The following correlation chart shows the main diterpene skeletons found in *Croton roxburghii* N.P. Balakr. (Devon and Scott, 1972)

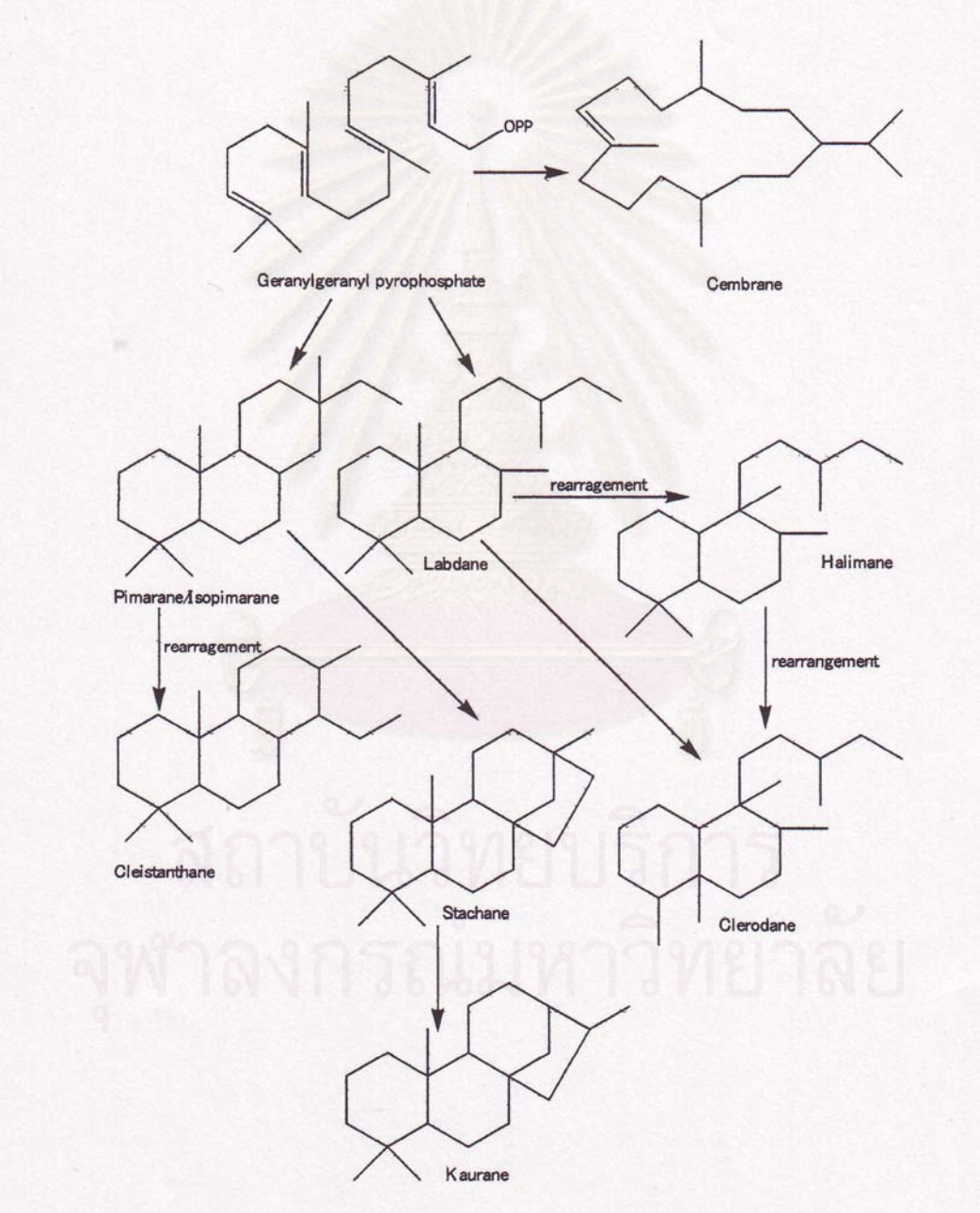

Scheme 1. Biogenetic pathway of diterpenoid compounds in *C. roxburghii*

4. Antidiabetic agents ; α-glucosidase inhibitors

In the 1970s, it was realized that inhibition of all or some of the intestinal disaccharidases and pancreatic α-amylase by inhibitors could regulate the absorption of carbohydrate and these inhibitors could be used therapeutically in the oral treatment of the non-insulin dependent diabetes mellitus (type II diabetes). The *Actiniplanes* strain SE 50 yields a potent sucrase inhibitor, acarbose, which inhibits pig intestinal sucrase with IC_{50} value of 0.5 μM,

In 1984, the validamycin A-producing organism *Streptomyces hygroscopicus* var. *limoneus* was reported to coproduce valiolamine, which is a potent inhibitor of pig intestinal maltase and sucrase with IC_{50} values of 2.2 and 0.049 μM, respectively. Numerous *N*-substituted valiolamine derivatives were synthesized to enhance its α-glucosidase inhibitory activity *in vitro* and the very simple derivative voglibose (AO128) which was obtained by reductive amination of valionamine with dihydroxyacetone, was selected as the potential oral antidiabetic agent. Its IC_{50} values toward maltase and sucrase were 0.015 μM and 0.046 μM, respectively.

In 1966, nojirimycin was discovered as the first glucose analog with nitrogen atom in place of the ring oxygen. Nojirimycin was first described as an antibiotic produced by *Streptomyces roseochromogenes* R-468 and *S. lavendulae* SF-425 and shown to be a potent inhibitor of α- and β-glucosidase from various sources. However, because this iminosugar with the hydroxyl group at C-1 is fairly unstable, it is usually stored as bisulfite adducts or it may be reduced by catalytic hydrogenation with a platinum catalyst or by $NaBH_4$ to 1-deoxynojirimycin (DNJ). DNJ was later isolated from the roots of mulberry trees and called molanoline. Despite the excellent α-glucosidase inhibitory activity *in vitro*, its efficacy *in vivo* was only moderate. Therefore, a large number of DNJ derivatives were prepared in the hope of increasing the *in vivo* activity. Thus miglitol was selected as the most favorable inhibitor out of a large number of in vitro active agents. In 1996, miglitol was granted clearance by the U.S. Food and Drug Administration (FDA) and was introduced onto the market in 1999 as a more potent second-generation α-glucosidase inhibitor with fewer gastrointestinal side effects.

Salacia reticulata Wight, known as kothalahimbutu in Singhalese and distributed in Sri Lanka and Indian forests, has been used as a supplementary food in Japan to prevent obesity and diabetes. Traditionally, ayurvedic medicine advised that a person suffering from diabetes should drink water left overnight in a mug carved from kothalahimbutu wood. Salacinol and Kotalanol have been identified as α-glucosidase inhibiting component from the water-soluble fraction of the roots and stems of *S. reticulate*. The IC_{50} values of salacinol toward rat intestinal maltase, sucrase, and isomaltase are 3.2, 0.84, and 0.59 μg/ml, respectively. The inhibitory activities toward maltase and sucrase are nearly equal to those of acarbose and that toward isomaltase is much more potent than that of acarbose. Kotalanol shows a more potent inhibitory activity than salacinol and acarbose toward sucrase. Furthermore salacinol has been found to more strongly inhibit the increase of serum glucose levels in sucrose-loaded rats than acarbose. The use of dietary supplement to prevent or treat diabetes will increase dramatically as knowledge about bioactive components of food in health increases. (Asano, 2003)

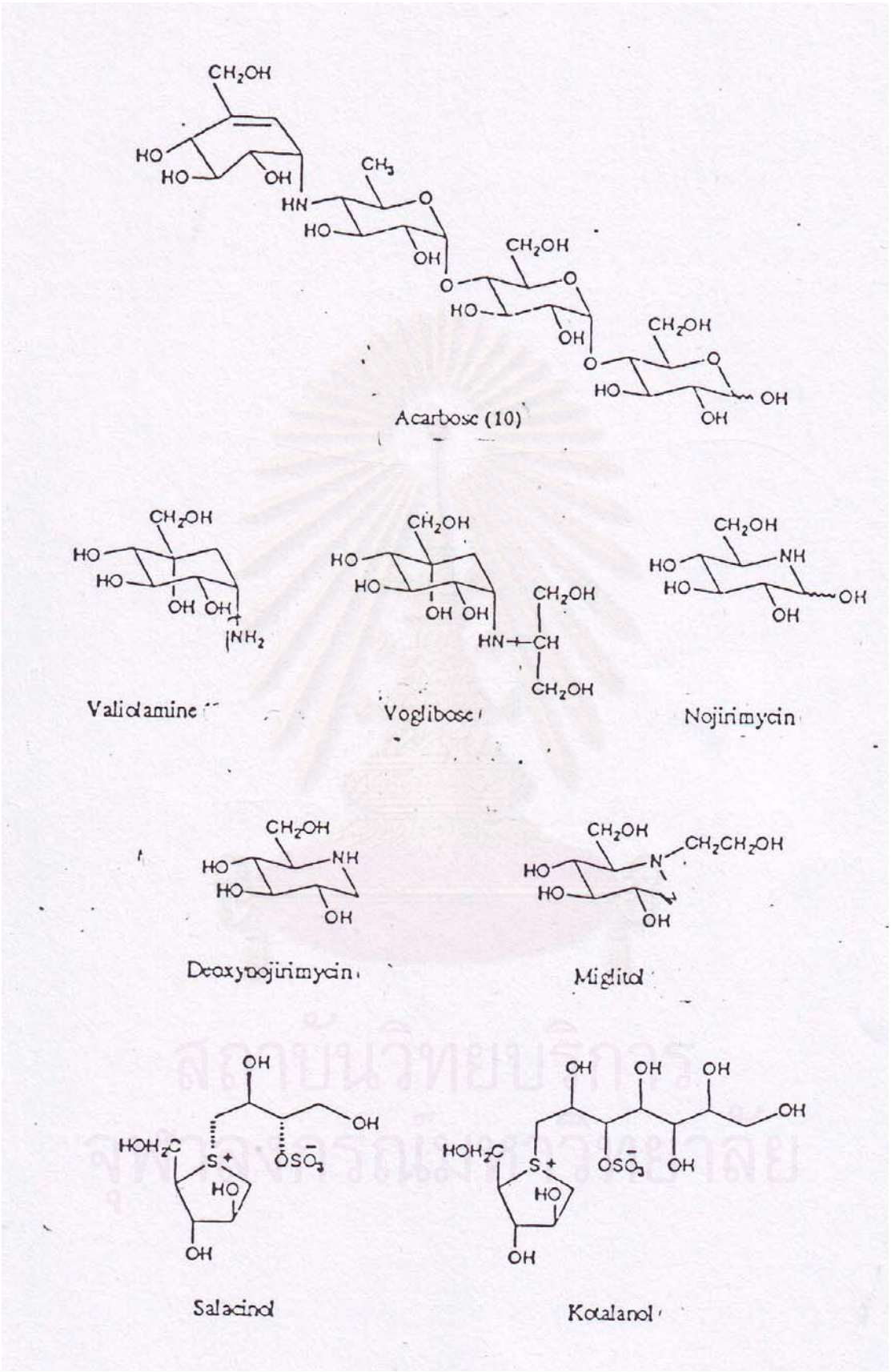

Figure 5. Structural of Antidiabetic agents ; α-glucosidase inhibitors

CHAPTER III

EXPERIMENTAL

1. Source of Plant Material

The stem bark of *Croton roxburghii* N.P. Balakr was collected from,Loei province,Thailand.The plant material was authenticated by comparison with the voucher specimen No. BKF 084729, deposited in the herbarium of Royal Forest Department, Bangkan, Bangkok, Thailand.

2. General Techniques

2.1 Analytical Thin Layer Chromatography (TLC)

Technique : One dimension, ascending

Adsorbent : Silica gel 60 F_{254} precoated plate (E.Merck)

Layer thickness : 0.2 mm.

Developing distance : 6.0 cm.

Temperature : Laboratory room temperature (30-35^{O}C)

Detection : 1. Ultraviolet light at wavelength of 254 nm.

2. Iodine vapour

2.2 Column Chromatography

2.2.1 Conventional Column Chromatography

Adsorbent : 1. Silica gel 60 (No.7734)(E.Merck)
Particle size 0.063-0.200 nm. (70-230 mesh ASTM)

2. Silica gel 60 (No.9385)(E.Merck)
Particle size 0.040-0.063 nm. (230-400 mesh ASTM)

Packing method : Wet packing

Sample loading : The sample was dissolved in a small amount of eluent, and then applied gently on top of the column.

Detection: Fractions were examined using TLC technique. In order to detect the compounds in each, the TLC plate was observed under UV light at wavelength of 254 nm and then exposed to iodine vapour.

2.2.2 Flash Column Chromatography

Adsorbent : 1. Silica gel 60 (No.7734)(E.Merck)
Particle size 0.063-0.200 nm. (70-230 mesh ASTM)
2. Silica gel 60 (No.9385)(E.Merck)
Particle size 0.040-0.063 nm. (230-400 mesh ASTM)

Packing method : Wet packing

Sample loading : The sample was dissolved in a small amount of eluent, and then applied gently on top of the column.

Detection : Fractions were examined using TLC technique. In order to detect the compounds in each, the TLC plate was observed under UV light at wavelength of 254 nm and then exposed to iodine vapour.

2.3 Spectroscopic Techniques

2.3.1 Ultraviolet(UV) absortption Spectra

UV spectra were obtained on a Shimadzu UV-160A UV/VIS spectrophotometer at Faculty of Pharmaceutical Sciences, Chulalongkorn Univesity.

2.3.2 Mass Spectra (MS)

Time of Flight spectra (TOF) of isolated compounds were obtained on a Micromass Platform II mass spectrometer at 70 eV. at The National Science and Technology Development Agency of Thailand.

2.3.3 Nuclear Magnetic Resonance (NMR) Spectra

^{1}H NMR spectra and ^{13}C NMR spectra of isolated compounds were recorded at 300 MHz, on a JEOL JMN (Alpha series) Spectrometer at the Department of Organic Chemistry, Faculty of Sciences, Srinakarinwirot University.

Deuterated chloroform and deuterated methanol were used as the NMR solvent throughout this study. Spectral data were reported in ppm scale using the solvent chemical shift as the reference frequency.

3. Extraction and Isolation

3.1 Extraction of the stem bark of *Croton roxburghii* N.P. Balakr

The dried, powdered stem bark of *Croton roxburghii* N.P. Balakr (2 kg.) was macerated twice with hexane (2 x 2 L) for three days. The obtained extract was evaporated under reduced pressure at a temperature of approximately 40^{O}C to give 213.7 g of hexane extract (10.69 % w/w)

3.2 Isolation

3.2.1 Isolation of compounds

The crude hexane extract (10 g) was chromatographed on a conventional silica gel column (silica gel 60, No.7734, 100 g), eluted initially with hexane and increasing the polarity of eluent by gradually adding ethyl acetate to 100%, to yield various fractions of 10 mL each. The fractions that showed similar TLC patterns were combined, and then evaporated to give starting materials *ent*-3-oxo-manoyl oxide (compound **1**, 0.38 g), *ent*-1,2-dehydro-3-oxo-manoyl oxide (compound **2**, 0.95 g), *ent*-1,2-dehydro-12α -hydroxy-3-oxo-manoyl oxide (compound **3**, 0.11 g), *ent*-1β-hydroxy-3-oxo-manoyl oxide (compound **4**, 0.14 g), and *ent*-3α -hydroxy-manoyl oxide (compound **5**, 0.32 g)

4. Synthesis and Isolation

4.1 Epoxidation

4.1.1 *ent*-1,2-dehydro-3-oxo-manoyl oxide-14,15-oxirane

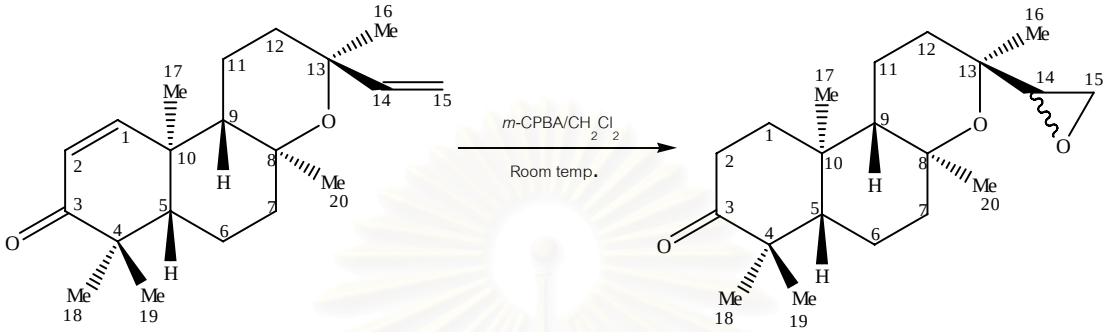

Compound **2** Compound **6**

To a solution of compound **2** (*ent*-1,2-dehydro-3-oxo-manoyl oxide, 0.302 g, 1 mmole) in methylene chloride (3 mL) was added *m*-chloroperbenzoic acid (*m*-CPBA, 0.1742 g, 1.2 mmole) at 0^{O}C. The mixture was stirred for 1 hour and then 2 days at room temperature. The solution was treated with saturated aqueous $NaHCO_3$ and 10% sodium sulfite and extracted with CH_2Cl_2. The organic layer was dried with Na_2SO_4 and concentrated to give a residue containing crude epoxide compound **6**, which was purified by TLC (silica gel, 15% ethyl acetate in hexane as developing solvent) to give compound **6** containing *ent*-1,2-dehydro-3-oxo-manoyl oxide-14(R),15-oxirane and *ent*-1,2-dehydro-3-oxo-manoyl oxide-14(S),15-oxirane (0.261 g,81.76%) as colourless crystals.

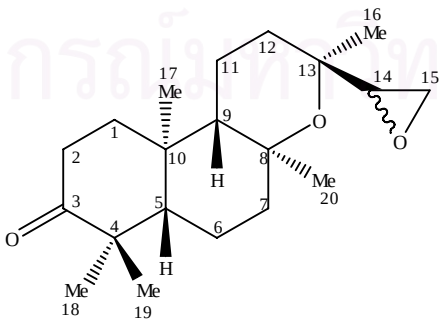

Compound **6**

TOF MS : $C_{20}H_{30}O_3$+Na : 341.2086

^{1}H and ^{13}C NMR ($CDCl_3$)

$C^{\#}$	δ_C	δ_H	HMBC
1	157.57	7.10 (d, J = 10.4 Hz)	C-20
2	125.9	5.86 (d, J = 10.4 Hz)	-
3	205	-	-
4	44.67	-	-
5	52.01	1.78 (m)	-
6	20.09	1.52 (m), 1.70 (m)	-
7	41.887	1.53 (m), 1.92 (m)	-
8	71.60	-	-
9	51.19	1.62 (m)	-
10	39.18	-	-
11	15.36	1.70 (m), 1.84 (m)	-
12	33.79	1.72 (m), 1.90 (m)	-
13	76.6	-	-
14	59.71	2.79 (m)	C-12, C-15, C-16
15	43.79	2.64 (m)	C-13, C-14
16	27.64	1.22 (s)	C-12, C-13, C-14
17	24.75	1.38 (s)	-
18	24.48	1.16 (s)	-
19	21.27	1.08 (s)	-
20	18.74	1.05 (s)	-

4.1.2 *ent*-1,2-dehydro-12α-hydroxy-3-oxo-manoyl oxide-14,15-oxirane

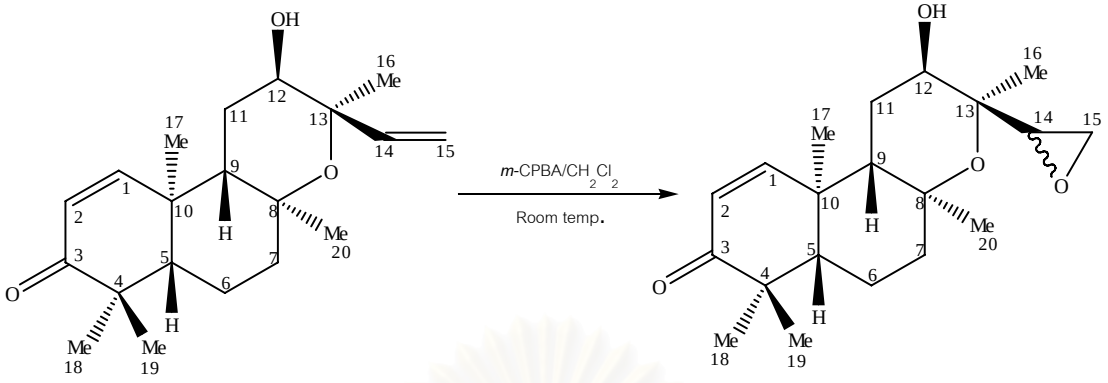

Compound **3** Compound **7**

To a solution of compound **3** (*ent*-1,2-dehydro-12α -hydroxy-3-oxo-manoyl oxide, 0.090 g, 0.283 mmole) in methylene chloride (3 mL) was added *m*-chloroperbenzoic acid (*m*-CPBA, 0.1742 g, 1.2 mmole) at 0^{O}C. The mixture was treated in the same manner as described in section 4.1.1 to give a residue containing crude epoxide compound **7**, which was purified by TLC (silica gel, 47% ethyl acetate in hexane as developing solvent) to give compound **7** containing 1,2-dehydro-12α-hydroxy-3-oxo-manoyl oxide-14(R),15-oxirane and 1,2-dehydro-12α-hydroxy-3-oxo-manoyl oxide-14(S),15-oxirane (0.066 g, 69.82%) as colourless crystals.

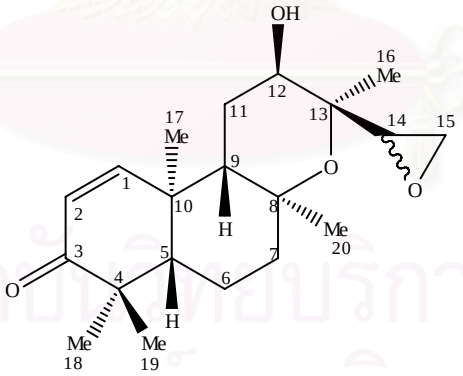

Compound **7**

TOF-MS : $C_{20}H_{30}O_4$+H : 335.2224

^{1}H and ^{13}C NMR ($CDCl_3$)

C#	δ_C	δ_H	HMBC
1	157.15	7.127 (d, J=10.4 Hz)	C-2, C-20
2	126.01	5.862 (d, J=10.4 Hz)	C-1

3	205	-	C-1, C-2
4	44.63	-	C-19
5	53.18	1.85 (m)	C-19
6	20.44	1.52 (m), 1.72 (m)	-
7	41.6	1.75 (m), 1.92 (m)	-
8	75.0	-	-
9	44.05	2.05 (m)	C-8, C-12
10	38.79	-	-
11	24.42	1.85 (m), 1.94 (m)	-
12	72.8	4.0 (q, broad)	C-14
13	73.0	-	C-12, C-15, C-16
14	56.5	3.01 (m)	C-12, C-15
15	44.63	2.88 (m)	C-14
		2.78 (m)	-
16	27.68	1.125 (s)	C-14
17	24.85	1.29 (s)	
18	25.31	1.15 (s)	
19	20.081	1.09 (s)	
20	18.9	1.01 (s)	

4.1.3 *ent*-1β-hydroxy-3-oxo-manoyl oxide-14,15-oxirane

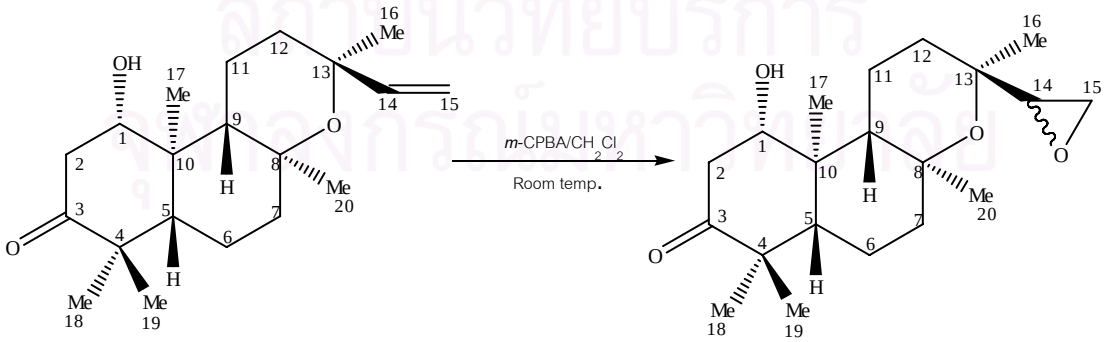

Compound **4**

Compound **8**

To a solution of compound **4** (*ent*-1β-hydroxy-3-oxo-manoyl oxide, 0.16 g, 0.50 mmole) in methylene chloride (3 mL) was added *m*-chloroperbenzoic acid (*m*-CPBA, 0.1742 g, 1.2 mmole) at 0^{O}C. The mixture was treated in the same manner as described in section 4.1.1 to give a residue containing crude epoxide compound **8**, which was purified by TLC (silica gel, 42% ethyl acetate in hexane as developing solvent) to give compound **8** containing *ent*-1β-hydroxy-3-oxo-manoyl oxide-14(R),15-oxirane and *ent*-1β-hydroxy-3-oxo-manoyl oxide-14(S),15-oxirane (0.13 g, 77.2%) as colourless crystals.

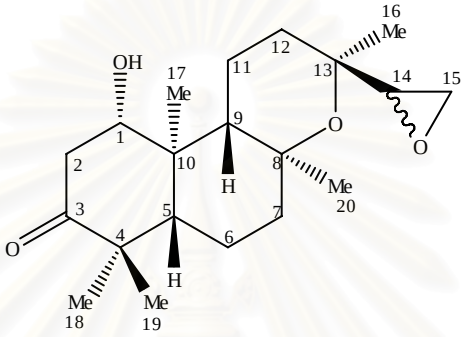

Compound **8**

TOF-MS : $C_{20}H_{32}O_4$+H : 337.2371

^{1}H and ^{13}C NMR ($CDCl_3$)

C#	δ_C	δ_H	HMBC
1	41.45	2.9 (q; J=8, 4 Hz)	C-2, C-3
2	33.63	2.3 (q; J= 8, 4 Hz)	C-1, C-3
		2.35 (q; J= 8, 4 Hz)	
3	214.98	-	C-2, C-3,C-18, C-19
4	47.1	-	-
5	57.4	1.49 (m)	-
6	20.44	1.50 (m), 1.56 (m)	-
7	45.08	2.32 (m)	-
8	74.68	-	C-16
9	56.47	1.52 (m)	
10	42.39	-	-
11	17.17	1.55 (m), 2.18(m)	-

12	77.7	4.1 (q, broad)	C-20
13	71.3	-	C-14
14	59.8	2.64 (m)	C-13, C-15
15	43.8	2.86 (m)	C-13, C-14, C-17
		2.75 (m)	
16	27.47	1.25 (s)	C-8
17	24.61	1.18 (s)	C-15
18	24.2	1.04 (s)	C-3
19	20.08	1.00 (s)	C-3
20	10.99	0.80 (s)	C-12

4.1.4 *ent*-3α-hydroxy-manoyl oxide-14,15-oxirane

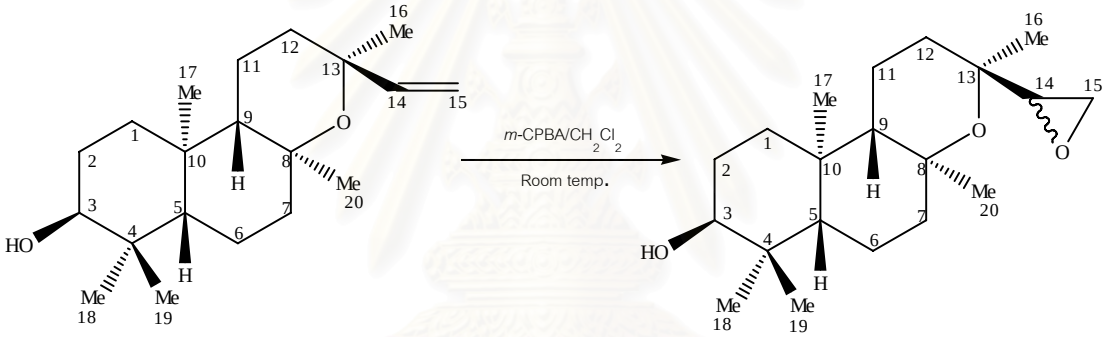

Compound **5** Compound **9**

To a solution of compound **5** (*ent*-3α -hydroxy-manoyl oxide, 0.204 g, 0.671 mmole) in methylene chloride (3 mL) was added *m*-chloroperbenzoic acid (*m*-CPBA, 0.1742 g, 1.2 mmole) at 0^{O}C. The mixture was treated in the same manner as described in section 4.1.1 to give a residue containing crude epoxide compound **9**, which was purified by TLC (silica gel, 47% ethyl acetate in hexane as developing solvent) to give compound **9** containing *ent*-3α-hydroxy-manoyl oxide-14(R),15-oxirane and *ent*-3α-hydroxy-manoyl oxide-14(S),15-oxirane (0.181 g, 84.20%) as colourless crystals.

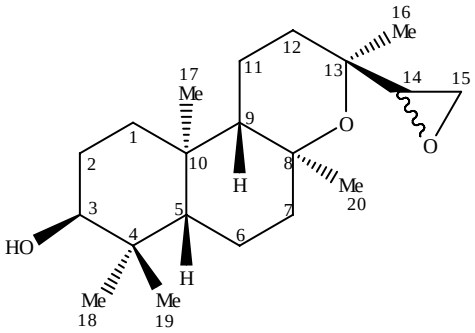

Compound **9**

TOF-MS : $C_{20}H_{34}O_3$ + Na = 345.2406

^{1}H and ^{13}C NMR ($CDCl_3$)

C#	δ_C	δ_H	HMBC
1	32.23	1.32 (m);1.35 (m)	-
2	25.23	1.58 (m); 1.94 (m)	-
3	76.08	3.41 (d, J=2.7 Hz)	
4	37.56	-	-
5	56.8	1.44 (m)	-
6	19.46	1.30 (m), 1.54 (m)	-
7	42.7	1.49 (m), 1.84 (m)	-
8	70.87	-	C-14, C-15
9	48.88	1.46 (m)	-
10	36.69	-	-
11	15.36	1.41 (m), 1.63 (m)	-
12	33.67	1.62 (m), 1.75 (m)	C-14, C-8
13	76.6	-	-
14	59.9	2.70 (dd, J = 5.1 Hz,	C-8, C-15
		J = 2.4 Hz)	-
15	43.85	2.87 (dd, J = 11 Hz,	C-8, C-12,
		J = 5.1 Hz)	C-14
		2.63 (dd, J = 11 Hz,	-
		J = 1.9 Hz)	-
16	28.24	1.29 (s)	C-8

17	24.30	1.33 (s)	-
18	24.88	1.04 (s)	-
19	21.79	0.91 (s)	-
20	15.57	0.9 (s)	-

4.2 Oxidation

4.2.1 *ent*-3-oxo-manoyl oxide-14(R),15-diol

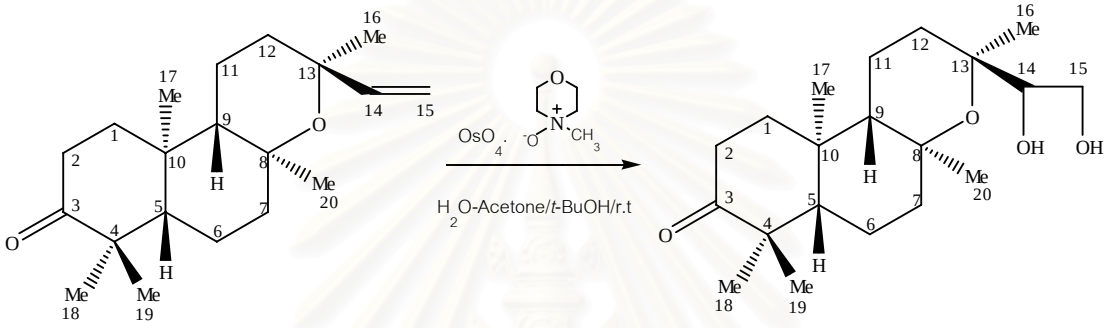

Compound **1** Compound **10**

A solution of *N*-methyl morpholine *N*-oxide hydrate (NMO, 50% in water,320 mg) and acetone (3 mL) was treated with Osmium tetroxide (OsO_4, 12.7 mg, 0.05 mmole) in *tert*-butyl alcohol (3 mL). After 15 min at room temperature, compound **1** (*ent*-3-oxo-manoyl oxide 0.315 g, 1.036 mmole) in acetone (2 mL) was added dropwise to the solution. The reaction was slightly exothermic and was maintained at room temperature for 2 days. The solution became dark brown. The solution mixture was treated with saturated aqueous $Na_2S_2O_3$ and was stirred for 30 min. The mixture was extracted with EtOAc. After drying with Na_2SO_4, the solvent was removed and the residue was purified by column chromatography with *n*-Hexane-EtOAc-Acetone (8:1.5:0.5) to give compound **10** (34 mg, 9.70%) as a yellow liquid.

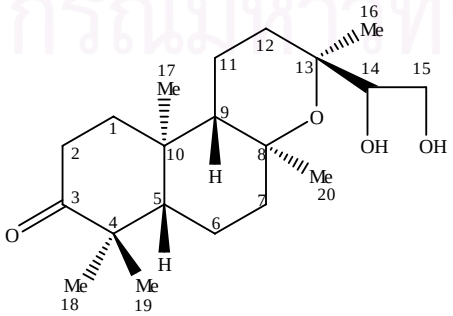

Compound **10**

TOF-MS : $C_{20}H_{34}O_4$ + Na = 361.48

^{1}H and ^{13}C NMR ($CDCl_3$)

C#	δ_C	δ_H	HMBC
1	32.77	1.45 (m)	C-3
2	29.67	2.43 (m)	C-3
3	214.57	-	C-1, C-2, C18, C-19
4	47.1	-	C-18, C-19
5	48.8	1.50 (m)	-
6	19.51	1.05 (m)	-
7	42.18	1.48 (m)	-
8	75.79	-	C-16, C-13
9	49.9	1.40 (m)	-
10	40.46	-	-
11	14.8	0.91 (m)	-
12	31.49	1.66-1.71(m)	-
13	77.44	-	C-8, C-17
14	71.68	3.798 (dd, J = 11 Hz, J = 5 Hz)	-
15	63.08	3.37 (dd, J = 11 Hz, J = 5 Hz) 3.1(m)	-
16	25.15	1.29 (s)	C-8
17	23.83	1.34 (s)	C-13
18	24.01	1.09 (s)	C-19
19	20.85	1.04 (s)	C-18
20	15.69	0.92 (s)	-

4.2.2 *ent*-3α-hydroxy-manoyloxide-14(R),15-diol

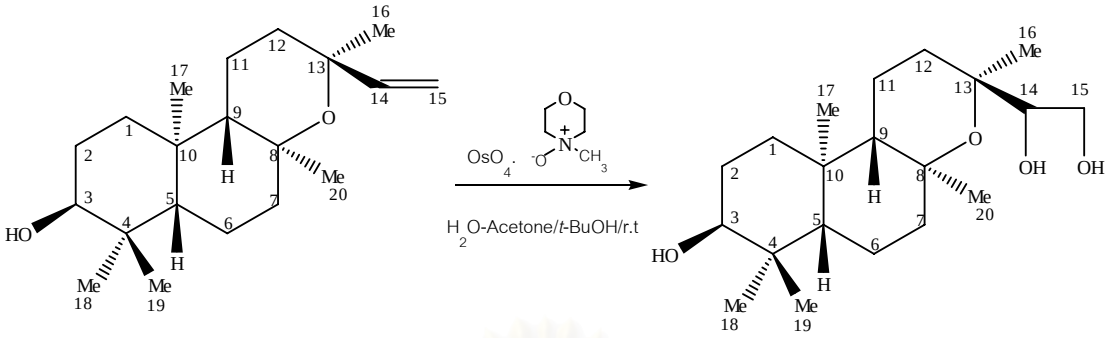

Compound **5** Compound **11**

A solution of *N*-methyl morpholine *N*-oxide hydrate (50% in water,320 mg) and acetone (3 mL) was treated with Osmium tetroxide (12.7 mg, 0.05 mmole) in *tert*-butyl alcohol (3 mL). After 15 min at room temperature, compound **5** (*ent*-3α-hydroxy-manoyl oxide,0.311 g, 1.016 mmole) in acetone (2 mL) was added dropwise to the solution. The reaction was slightly exothermic and was maintained at room temperature for 2 days. The solution became dark brown. The solution mixture was treated with saturated aqueous $Na_2S_2O_3$ and was stirred for 30 min. The mixture was extracted with EtOAc. After drying with Na_2SO_4, the solvent was removed and the residue was purified by column chromatography with *n*-Hexane-CH_2Cl_2-Acetone (3:2:2.5) to give compound **11** (16 mg, 46.25%) as a yellow liquid.

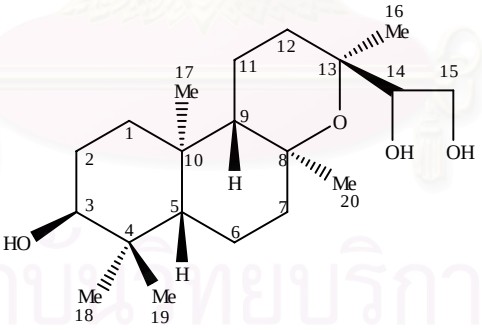

Compound **11**

TOF-MS : $C_{20}H_{36}O_4$+Na = 363.2502

^{1}H and ^{13}C NMR ($CDCl_3$)

C#	δ_C	δ_H	HMBC
1	32.27	1.32 (m),	-
		1.35 (m)	-
2	24.93	1.58 (m),	-
		1.94 (m)	-
3	79.5	3.41 (d, J = 2.4 Hz)	C-5
4	37.20	-	-
5	57.97	1.78 (m)	C-3
6	19.10	1.52 (m)	-
		1.70 (m)	-
7	42.82	1.53 (m)	-
		1.92 (m)	-
8	75.11	-	C-16
9	48.81	1.44 (m)	-
10	36.40	-	C-20
11	14.46	1.42-1.62 (m)	-
12	34.30	1.62-1.77 (m)	-
13	78.7	-	C-14, C-15
14	75.4	3.78 (m),	C-8, C-13, C-15
		3.5 (m)	C-8, C-13, C-15
15	62.53	3.32 (m),	C-8, C-13, C-14
		3.33 (m)	C-8, C-13, C-14
16	27.63	1.28 (s)	C-8, C-13
17	23.69	1.30 (s)	-
18	24.01	0.95 (s)	-
19	21.41	0.83 (s)	-
20	14.90	0.80 (s)	C-1, C-5, C-10

4.3 Acetylation ; *ent*-3 α,14(R),15-Triacetyl-manoyl oxide

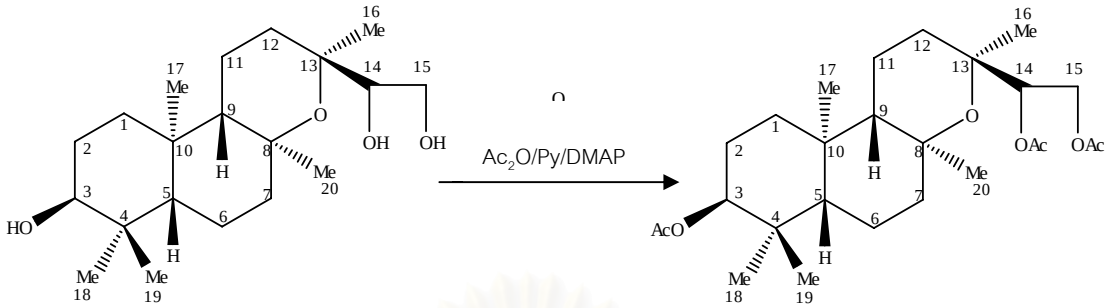

Compound **11** Compound **12**

To a solution of compound **11** (*ent*-3α-hydroxy-manoyl oxide-14,15-diol, 0.162 g, 0.479 mmole) in pyridine (4 mL) were added DMAP (170 mg, 1.35 mmol) and acetic anhydride (230 mg, 2.25 mmol). The reaction was stirred at room temperature for 2 days. The solvent was removed in vacuo. A saturated aqueous $NaHCO_3$ solution was added to the residue, and the mixture was extracted with diethyl ether. The organic layer was dried with Na_2SO_4, and the solvent was removed. Purification by column chromatography with *n*-Hexane-EtOAc(1:4) gave compound **12** (0.042 mg, 16.70%) as a yellow liquid.

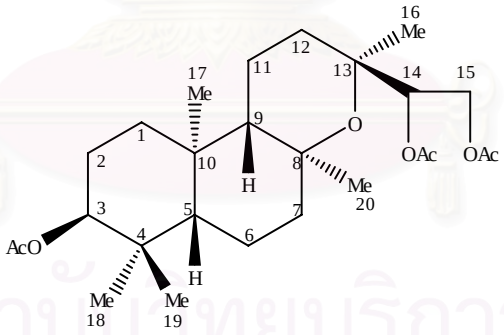

Compound **12**

TOF-MS: $C_{26}H_{42}O_7$ = 489.07

^1H and ^{13}C NMR (CD_3OD)

C#	δ_C	δ_H	HMBC
1	31.7	1.32 (m), 1.35 (m)	C-20
2	21.75	1.8 (m)	-

3	77.01	4.50 (d, J = 2.5 Hz)	-
4	35.7	-	-
5	56.6	1.42 (m)	C-20
6	18.23	1.3 (m)	-
7	41.57	1.51 (m),1.83 (dt, J = 12.0, 3.2 Hz)	C-8
8	72.3	-	C-7
9	49.07	1.44 (m)	C-10
10	35.5	-	C-9
11	13.72	1.42 (m), 1.62 (m)	-
12	33.68	1.61 (m), 1.77 (m)	-
13	74.19	-	-
14	75.89	4.02 (dd, J = 17 Hz, J = 11 Hz)	C-8, C-13
15	62.7	4.88 (dd, J = 17 Hz, J = 9 Hz) 4.39 (dd, J = 11 Hz J = 9 Hz)	C-8,
16	26.83	1.07 (s)	C-8, C-9
17	23.61	1.12 (s)	-
18	24.01	0.75 (s)	-
19	22.04	0.70 (s)	-
20	14.53	0.65 (s)	-
21, 22, 23	169.45 ,169.68, 170.13	-	-
24	19.91	1.99(s)	-
25	20.07	2.004(s)	-
26	20.4	2.0(s)	-

4.4 Reduction : *ent*-3β-hydroxy-manoyl oxide

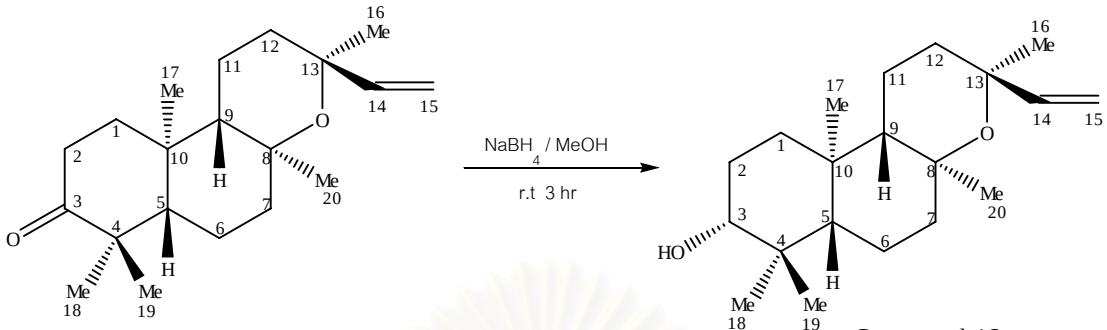

Compound **1** Compound **13**

Sodium borohydride (0.5 g, 13.21 mmol was dissolved in MeOH 3 mL), and the solution was stirred at 0^{O}C. Then the solution of compound **1** (3-oxo-manoyl oxide 0.615 g, 2.02 mmole) in MeOH (2 mL) was added dropwise to the solution. The reaction was slightly exothermic and was maintained at 0^{O}C for 30 mins, raised to the room temperature, and stirred for 3 hrs. The solution mixture was treated with saturated aqueous $NaHCO_3$ and was stirred for 30 min. The mixture was extracted with EtOAc. After drying with Na_2SO_4, the solvent was removed and the residue was purified by column chromatography with *n*-Hexane-EtOAc (4:1) to give compound **13** (0.3 g, 48.51%) as a solid.

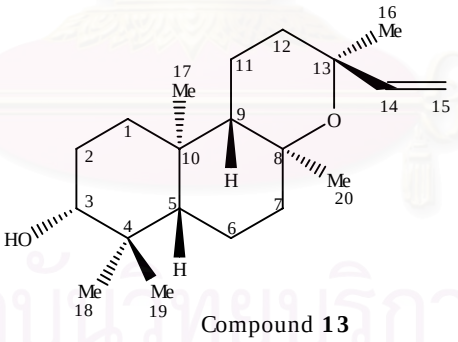

Compound **13**

TOF-MS: $C_{20}H_{34}O_2$ + Na = 333.1103

^{1}H and ^{13}C NMR ($CDCl_3$)

C#	δ_C	δ_H	HMBC
1	37.2	1.45 (m)	C-18, C-19
2	27.2	1.6 (m)	C-19
3	78.8	3.2 (dd, J = 11 Hz, 4.8 Hz)	C-18, C-19

4	38.8	-	-
5	55.2	1.25 (m)	C-19
6	19.51	1.05 (m), 1.08(m)	-
7	43.1	1.48 (m), 1.86 (m)	C-16
8	73	-	C-16
9	55.4	1.40 (m)	-
10	36.7	-	-
11	15.39	0.91(m)	C-20
12	35.6	1.66 (m),1.80 (m)	C-13
13	75	-	C-14
14	147.6	5.8 (dd, J = 17 Hz, 10.8 Hz)	C-13, C-8
15	110.3	4.9 (dd, J = 10.8 Hz, 1.3Hz)	-
		5.15 (dd, J = 17 Hz, 1.3Hz)	-
16	25.4	1.2 (s)	C-8, C-14
17	23.01	1.28 (s)	-
18	28.4	0.96 (s)	C-19
19	15.47	0.3 (s)	-
20	15.2	0.2 (s)	-

5. Biological activity test

5.1 Cytotoxicity test

Cytotoxicity test was carried out at the Institute of Biotechnology and Genetic Engineering. Bioassay of cytotoxicity activity against human tumor cell culture *in vitro* was performed by the MTT [3-(4,5-dimethylthaizol-2-yl)-2,5-diphenylterazolium bromide] colorimetric method (Carmichael *et al*., 1987). In principle, the viable cell number/well is directly proportional to the production of formazan which, following solubilization, can be measured spectrophotometrically.

The human tumor cell line was harvested from exponential-phase maintenance culture (T-75 cm^2 flask), counted by trypan blue exclusion, and dispensed within replicate 96-well culture plates in 100 μl volumes using a repeating pipette. Following a 24 h incubation at 37^OC, with 5%CO_2, 100% relative humidity, 100 μl of culture medium containing sample was dispensed within appropriate well (control group, N=6; each sample treatment group, N=3). Peripheral wells of each plate (lacking cell) were utilized for sample blank (N=2) and medium/tetrazolium reagent blank (N=6) background determination. Culture plates were then incubated for 4 days prior to the addition of tetrazolium reagent. MTT stock solution was prepared as follows: 5 mg MTT/mL PBS was steriled and filtered with 0.45 μm filtered units. MTT working solution was prepared just prior to culture application by diluting MTT stock solution 1:5 (v/v) in prewarmed standard culture medium. MTT working solution (50 μl) was added to each culture well resulting in 50 μg MTT/250 μl total medium volume and cultures were incubated at 37^OC for 4 to 24 h depending upon individual cell line requirements. Following incubation, cell monolayers and formazan were inspected microscopically: culture plates containing suspension lines or detached cells were centrifuged at low speed for 5 min. All 10-20 μl of culture medium supernatant was removed from wells by slow aspiration through a blunt 18-guage needle and replaced with 150 μl of DMSO using a pipette. Following through formazan solubilization, the absorbance of each well was measured using a microculture plate reader at 540 nm (single wavelength, calibration factor = 1.00)

Cell line growth and growth inhibition were expressed in terms of mean ($\pm$ 1 SD) absorbance units and / or percentage of control absorbance($\pm$ 1 SD %) following subtraction of mean background absorbance.

Samples were also tested for cytotoxic activity towards 5 cancer cell lines, including HEP-G2 (hepatoma), SW 620 (colon), Chago (lung), Kato-3 (gastric) and BT 474 (breast), following the experimental method for bioassay of cytotoxic activity.

5.2 α-glucosidase inhibitory activity

The inhibitory effect of each compound on α-glucosidase activity was measured according to the literature procedure (Matsui, T *et al*., 1996). Briefly, α-glucosidase from baker's yeast was assayed using 0.1 M phosphate buffer at pH 6.9, and 1 mM *p*-nitrophenyl-α-D-glucopyranoside (PNP-G) was used as a substrate. The concentration of the enzymes was 1 U/mL in each experiment. α-Glucosidase (40 μL) was incubated in the absence or presence of various sample (concentration 1 mg/mL, 10 μL) at 37°C. The preincubation time was specified at 10 min and PNP-G solution (950 μL) was added to the mixture. The reaction was carried out at 37°C for 20 min, and then 1 mL of 1M Na_2CO_3 was added to terminate the reaction. Enzymatic activity was quantified by measuring the absorbance at 405 nm. 1-deoxynorjorimycin was used as the positive control in this study.

CHAPTER IV

RESULTS AND DISCUSSION

1. Structure Determination

1.1 Identification of Isolated Compounds

The separation of crude hexane extract gave five compound including *ent*-3-oxo-manoyl oxide (compound **1**), *ent*-1,2-dehydro-3-oxo-manoyl oxide (compound **2**), *ent*-1,2-dehydro-12α -hydroxy-3-oxo-manoyl oxide (compound **3**), *ent*-1β-hydroxy-3-oxo-manoyl oxide (compound **4**), and *ent*-3α-hydroxy-manoyl oxide (compound **5**). Identifications of these compounds were done by TLC comparison with authentic samples.

1.2 Structure determination of compound 6

Compound **6** was obtained as colourless needles (0.261 g) with melting point of 157- 159^{O}C (CH_2Cl_2-Hexane). The ^{1}H- NMR spectrum (Figure 6) of compound **6** showed five methyl groups at δ_H 1.05(3H, s; H-20), 1.08(3H, s; H-19), 1.16(3H, s; H-18), 1.22(3H, s; H-16), 1.38(3H, s; H-17) and two olefinic protons at δ_H 5.86(1H, d; H-2), 7.10(1H, d; H-1).

The two of olefinic protons of starting material at δ_H 5.89 (1H, dd; J=17.6, 10.8Hz; H-14) and 4.94 (1H, dd; J=10.6, 1.4Hz; H15a or b), 5.16 (1H, dd; J=17.2, 1.4Hz; H15a or b) became to be a methine proton at 2.79 (1H, m; H-14) and two methylene protons at δ_H 2.64 (2H, m; H-15).

The ^{13}C-NMR spectrum (Figure 7) of compound **6** showed twenty carbon resonances, with a pair of olefinic carbons (δ_C 125.9, 157.15; C-2, C-1). The pair of olefinic carbons (δ_C 147.4, 110.7; C-14, C-15) of the starting material (compound **2**) became the corresponding epoxide carbons, one methine carbon at δ_C 59.7 (C-14) and one methylene carbon at δ_C 43.79 (C-15).

In DEPT experiments (Figure 8), all of carbon signals are as similarly related to the carbon signals of the starting material compound **2** (*ent*-1,2-dehydro-3-oxo-manoyl oxide) except that the signals at δ_C 147.4 (C-14), 110.7 (C-15) disappeared. The two new signals at δ_C 43.79 (C-15), and δ_C 59.7 (C-14) showed their proximity to the oxygen atom of the oxirane ring in the molecule.

In the TOF-MS spectrum (Figure 12) compound **6** gave a peak $[M+Na]^+$ as the base peak at *m/z* 341.2093. The molecular formula of compound was assigned as $C_{20}H_{30}O_3$.

2D-NMR techniques were then used to assist in the interpretation of the structure of this compound. In the HMBC spectrum (Figure 11), the methyl at δ_H1.22 ppm (H-16) correlated with the epoxide moiety at δ_C 59.71 ppm (C-14). The methine at δ_H 2.64ppm (H-14) correlated with δ_C 76.6 ppm (C-13) and δ_C 59.71 ppm (C-14).The methylene at δ_H 2.79 ppm (H-15) correlated with δ_C 76.6 ppm (C-13) and δ_C 59.71 ppm (C-14).

1.3 Structure determination of compound **7**

Compound **7** was obtained as colourless needles (0.066 g) with melting point of 147- 150^{O}C (CH_2Cl_2-Hexane). The ^{1}H- NMR spectrum (Figure 13) of compound **7** showed five methyl groups at δ_H 0.8 (3H, s; H-20), 1.00 (3H, s; H-19), 1.04 (3H, s; H-18), 1.25 (3H, s; H-16), 1.18 (3H, s; H-17) and two olefinic protons at δ_H 5.86 (1H, d; H-2), 7.127 (1H, d; H-1).

The two of olefinic protons of starting material (compound 3) at δ_H 5.81 (1H, dd; J=17.6, 10.8Hz;H-14) and 5.26 (1H, dd; J=10.6, 1.4Hz; H15a or b, 5.44(1H, dd; J=17.2, 1.4Hz; H15a or b) became a methine proton at δ_H 3.01 (1H, m; H-14) and two methylene protons at δ_H 2.78, 2.88 (2H, m; H-15).

The ^{13}C-NMR spectrum (Figure14) of compound **7** showed twenty carbon resonances, with a pair of olefinic carbons (δ_C 126.01, 157.15 ; C-2,C-1). The pair of olefinic carbons (δ_C 142.5, 115.8; C-14, C-15) of starting material (compound 3)

became the corresponding epoxide carbons, with one methine carbon at δ_C 56.5 (C-14) and one methylene carbon at δ_C 44.63 (C-15).

In DEPT experiments (Figure15), all of carbon signals are as similarly related to the carbon signals of the starting material compound **3** (*ent*-1,2-dehydro-12α -hydroxy-3-oxo-manoyl oxide) except that the signals at δ_C 142.5 (C-14), 115.8 (C-15) disappeared. The two new signals at δ_C 56.5 (C-15), and δ_C 44.63 (C-14) showed their proximity to the oxygen atom of the oxirane ring in the molecule.

In the TOF-MS spectrum (Figure19) compound **7** gave a pseudo molecular ion peak $[M+H]^+$ as the base peak at m/z 335.2224. The molecular formula of compound was assigned as $C_{20}H_{30}O_4$.

The 2D-NMR techniques were then used to assist in the interpretation of the structure of this compound. In the HMBC spectrum (Figure18), the methyl at δ_H1.125 ppm (H-16) correlated with the epoxide moiety at δ_C 56.5 ppm (C-14). The methine at δ_H 2.64 ppm (H-14) correlated with δ_C 73.0 ppm (C-13) and δ_C 56.5 ppm (C-14).The methylene at δ_H 2.75, 2.86 ppm (H-15) correlated with δ_C 73.0 ppm (C-13), δ_C 56.5 ppm (C-14). and δ_C 24.85 ppm (C-17).

1.4 Structure determination of compound 8

Compound **8** was obtained as colourless needles (0.181 g) with melting point of 178-180^{O}C (EtOAc-Hexane). The ^{1}H- NMR spectrum (Figure20) of compound **8** showed five methyl groups at δ_H 0.8 (3H, s; H-20), 1.0 (3H, s; H-19), 1.04 (3H, s; H-18), 1.25 (3H, s; H-16), 1.18 (3H, s; H-17).

It also showed six of methylene protons at δ_H 2.94 (m),1.58 (m; H-11), 2.3 (m), 2.35 (m; H-12), 1.50 (m), 1.56 (m; H-6), 2.32 (m; H-7), 1.55 (m), 2.18 (m; H-2), and new ones at δ_H 2.75 (m), 2.86 (m; H15).

Four of methine protons at δ_H 1.49 (m; H-5), 1.52 (m; H-9), 14.1 (broad; H-12) and a new one at δ_H 2.64 (m; H-14) were observed.

The ^{13}C-NMR spectrum (Figure21) of compound **8** showed twenty carbon resonances, most of which were similar to the starting material (compound **4**), except that the pair of olefinic carbons (δ_C147.8 and 110.4 at C-14 and C-15) became the corresponding epoxide carbons with one methine at δ_C 59.9 (C-14) and one methylene at δ_C 43.85 (C-15).

In DEPT experiments (Figure22), most of carbon signals were as similarly related to the carbon signals of the starting material compound **4** (*ent*-1β-hydroxy-3-oxo-manoyl oxide) except that the signals at δ_C 147.6 (C-14), 110.5 (C-15) disappeared. The two new signals at δ_C 43.8 (C-15), and δ_C 59.8 (C-14) showed their proximity to the oxygen atom of the oxirane ring in the molecule.

In the TOF-MS spectrum (Figure 25) compound 8 gave $C_{20}H_{32}O_4$ a molecular ion peak $[M+H]^+$ as the base peak at *m/z* 337.2371. The molecular formula of compound was assigned as $C_{20}H_{32}O_4$.

2D-NMR techniques were then used to assist in the interpretation of the structure of this compound. In the HMBC spectrum (Figure 24), the methyl protons at δ_H 1.18 ppm (H-17) correlated with δ_C 43.8 ppm (C-15). The methine proton at δ_H 2.64 ppm (H-14) correlated with δ_C 43.8 ppm (C-15) and δ_C 71.3 ppm (C-13) The methylene at δ_H 2.75, 2.86 ppm (H-15) correlated with δ_C 59.8 ppm(C-14), δ_C 71.3 ppm(C-13) and δ_C 24.61 ppm (C-17).

1.5 Structure determination of compound **9**

Compound **9** was obtained as colourless needles (0.181 g) with melting point of 142-144^{O}C (EtOAc-Hexane). The ^{1}H- NMR spectrum (Figure 26) of compound **9** showed five methyl groups at δ_H 0.9 (3H, s; H-20), 0.91 (3H, s; H-19), 1.04 (3H, s; H-18), 1.29 (3H, s; H-16), 1.33 (3H, s; H-17).

It also showed six methylene protons at δ_H 1.32-1.35 (m; H-1), 1.58-1.94 (m; H-2), 1.30-1.57 (m; H-6), 1.49-1.84 (m; H-7), 1.42-1.1.62 (m; H-11), 1.61-1.77 (m; H-12)

and new ones δ_H 2.87 (1H, dd; J=11, 5.1 Hz; H15a or b) , 2.63 (1H, dd; J= 11, 1.9 Hz; H15a or b).

In addition, it exhibited four methine protons at δ_H 1.49 (m; H-5),1.52 (m; H-9) 4.1 (broad; H-12), and a new one at δ_H 2.64 (m; H-14).

The ^{13}C-NMR spectrum (Figure 26) of compound **10** showed twenty carbon resonances, similar to the starting material (compound **5**), except that the pair of olefinic carbons (δ_C147.6 and 110.5 at C-14 and C-15) became the corresponding of epoxide carbons, with one methine at δ_C 59.8 (C-14) and a new one methylene at δ_C 43.8 (C-15).

In DEPT experiments (Figure 28), most of carbon signals were similar to the carbon signals of the starting material compound **5** (*ent*-12α-hydroxy-3-oxo-manoyl oxide) except that the signals at δ_C 147.6 (C-14), 110.5 (C-15) disappeared. The two new signals at δ_C 59.8 (C-15), and δ_C 43.8 (C-14) showed their proximity to the oxygen atom of the oxirane ring in the molecule.

In the TOF-MS spectrum (Figure 32) compound **9** gave $C_{20}H_{34}O_3$ + Na at *m/z* = 345.2406. The base peak was $[M+Na]^+$ at *m/z* = 345.2406. The molecular formula of compound was assigned as $C_{20}H_{34}O_3$.

2D-NMR techniques were then used to assist in the interpretation of the structure of this compound. In the HMBC spectrum (Figure31), the methyl protons at δ_H 2.7 ppm (H-14) correlated with δ_C 43.85 ppm (C-15) and δ_C 70.87 ppm (C-8). The methylene at δ_H 2.63, 2.87 ppm (H-15) correlated with δ_C 70.87 ppm (C-8), δ_C 56.5 ppm (C-14). and δ_C 33.68 ppm (C-12).

1.6 Structure determination of compound **10**

Compound **10** was obtained as a yellow liquid (34 mg). The ^{1}H- NMR spectrum (Figure33) of compound **10** showed five methyl groups at δ_H 0.9 (3H, s; H-20), 1.03 (3H, s; H-19), 1.09 (3H, s; H-18), 1.29 (3H, s; H-16), 1.34 (3H, s; H-17).

It also showed seven of methylene protons at δ_H 1.45 (m; H-1), 2.43 (m; H-2), 1.50 (m), 1.05 (m; H-6), 1.48 (m; H-7), 0.9 (m; H-11), 1.66-1.71 (m; H-12) and new methylene at δ_H 3.62(m), 3.76(m; H15).

In addition, it showed three methine protons at δ_H 1.50 (m; H-5), 1.40 (m; H-9) and a new one at δ_H 4.008 (dd; J = 11.4 , 5 Hz, H-14).

The ^{13}C-NMR spectrum (Figure34) of compound **10** showed twenty carbon resonances, similar to the starting material (compound **1**), except that the pair of olefinic carbons (δ_C147.6 and 110.4 at C-14 and C-15) became carbons of diol structure with one methine carbon at δ_C 71.68 (C-14) and a new methylene carbon at δ_C 63.08 (C-15).

In DEPT experiments (Figure 35), most of carbon signals were similar to the carbon signals of the starting material compound **1** (*ent*-3-oxo-manoyl oxide) except thatthe signals at δ_C 147.6 (C-14), 110.4 (C-15) disappeared. The two new signals at δ_C 63.08 (C-15), and δ_C 71.68 (C-14) showed their proximity to the oxygen atoms of the diol in the molecule.

In the TOF-MS spectrum (Figure 38), compound **10** gave $C_{20}H_{34}O_4$ + Na at *m/z* = 361.48. The base peak was $[M+Na]^+$ at *m/z* 361.48. The molecular formula of compound was assigned as $C_{20}H_{34}O_4$.

2D-NMR techniques were then used to assist in the interpretation of the structure of this compound. In the HMBC spectrum (Figure36), the methyl protons at δ_H 1.09 ppm (H-18) and δ_H 1.04 ppm (H-19) correlated with δ_C 214.57 ppm (C-3) the carbonyl moiety. The methyl proton at δ_H 1.34 ppm (H-17) correlated with δ_C 31.49 ppm (C-12), δ_C 75.79 ppm (C-8) and δ_C 77.44 ppm (C-13). The methyl protons at δ_H 1.29 ppm (H-16) correlated with δ_C 75.79 ppm (C-8).

1.7 Structure determination of compound **11**

Compound **11** was obtained as a yellow liquid (16 mg). The ^{1}H- NMR spectrum (Figure39) of compound **11** showed five methyl groups at δ_H 0.8 ppm (3H, s; H-20), 0.83 (3H, s; H-19), 0.95 (3H, s; H-18), 1.28 (3H, s; H-16), 0.83 (3H, s; H-17).

There were seven methylene protons at δ_H 1.32 ppm (m), 1.35 (m; H-1), 1.58 (m), 1.94 (m; H-2),1.3 (m), 1.57 (m; H-6), 1.49 (m), 1.83 (m; H-7), 1.42 (m),1.62 (m; H-11), 1.62 (m), 1.77 (m; H-12) and new ones at δ_H 3.32 (m), 3.33 (m; H15).

There were four methine protons at δ_H 3.41 ppm (d; J=2.4; H-3), 1.42 (m; H-5), 1.44 (m; H-9) and new ones at δ_H 3.5 (m), 3.77 (m; H-14).

The ^{13}C-NMR spectrum (Figure40) of compound **11** showed twenty carbon resonances, similar to the starting material (compound **5**), except that the pair of olefinic carbons (δ_C147.6 and 110.5 at C-14 and C-15) became the corresponding diol carbons, with one methine at δ_C 77(C-14) and one methylene at δ_C 62.5 (C-15).

In DEPT experiment (Figure 41), most of carbon signal were similar to the carbon signals of the starting material compound **5** (*ent*-3α-hydroxy-manoyl oxide) except that the signals at δ_C 147.6 (C-14), 110.5 (C-15) disappeared. The two new signals at δ_C 62.5 (C-15), and δ_C 77 (C-14) showed their proximity to the oxygen atoms of diol in the molecule.

In the TOF-MS spectrum (Figure 45) compound 11 gave $C_{20}H_{36}O_4$ + Na at *m/z* = 363.2507. The base peak was $[M+Na]^+$ at *m/z* 363.2507. The molecular formula of compound was assigned as $C_{20}H_{36}O_4$.

2D-NMR techniques were then used to assist in the interpretation of the structure of this compound. In the HMBC spectrum (Figure 44), methyl protons at δ_H 1.28 (s) ppm (H-16) correlated with δ_C 75.11 ppm (C-8) the quarternary carbon. This quarternary carbon (C-8) correlated with δ_C 77 ppm (C-14), δ_C 62.53 ppm (C-15) and δ_C 27.63 ppm (C-16). The methylene proton at δ_H 3.2, 3.33 ppm (H-15) correlated with δ_C 78.7

ppm (C-13). The methine proton at δ_H 3.5, 3.77ppm (H-14) correlated with δ_C 75.11 ppm (C-8), δ_C 78.7 ppm (C-13), δ_C 62.53 ppm (C-15).

1.8 Structure determination of compound **12**

Compound **12** was obtained as a yellow liquid (0.042 mg). The ^{1}H- NMR spectrum (Figure 46) of compound **12** showed eight methyl groups at δ_H 0.65 ppm (3H, s; H-20), 1.12 (3H, s; H-19), 0.70 (3H, s; H-18), 1.07 (3H, s; H-16), 0.75 (3H, s; H-17) and three methyl acetate groups at δ_H 1.995 (3H, s; H-24), 2.004 (3H, s; H-25), 2.019 (3H, s; H-26).

There were seven methylene protons at δ_H 1.32 ppm (m; H-1), 1.8 (q; J=2.5 Hz; H-2),1.30 (m; H-6), 1.51(m), 1.83 (dt; J=12, 3.2 Hz; H-7), 1.42 (m),1.62 (m; H-11), 1.62(m), 1.77 (m; H-12) and a new methylene at δ_H 4.39 (dd, J = 11, 9 Hz), 4.88 (dd; J = 17, 9 Hz; H15).

There were four methine protons at δ_H 4.509 ppm (d; J=2.5; H-3), 1.42 (m; H-5),1.44 (m; H-9) and a new one at δ_H 4.02 (dd; J=17, 11 Hz; H-14).

The ^{13}C-NMR spectrum (Figure 47) of compound **12** show twenty six carbon resonances, similar to the starting material (compound **11**), except that the three acetate groups (six carbons, including three of carbonyl carbons and three methyl groups) at δ_C 169.45, 169.68 and 170.13 ppm (C-21, C-22, C-23) of carbonyl carbons and at δ_C 19.91, 20.07 and 20.4 ppm (C-24, C-25, C-26) of the three new methyl carbons. These observations showed that full acetylation was successful on the three hydroxy groups at δ_C 77.01 ppm (C-3), 77 (C-14) and 62.7 (C-15).

In DEPT experiments (Figure 48), most of carbon signals were similar the carbon signals of the starting material compound **11** (*ent*-3α-hydroxy-manoyl oxide-14(R),15-diol) except that the signals at δ_C 147.6 (C-14), 110.5 (C-15) disappeared. The two new signals at δ_C 62.5 (C-15), and δ_C 77 (C-14) showed their proximity to the oxygen atoms of the diol in the molecule.

In the TOF-MS spectrum (Figure 52) compound 12 gave $C_{26}H_{42}O_7$ + Na at *m/z* = 489.07. The base peak was $[M+Na]^+$ at *m/z* 489.07. The molecular formula of compound was assigned as $C_{26}H_{42}O_7$.

2D-NMR techniques were then used to assist in the interpretation of the structure of this compound. In the HMBC spectrum (Figure 51), methyl protons at δ_H 1.07 ppm (s; H-16) correlated with δ_C 72.3 ppm (C-8), a quarternary carbon. This quarternary carbon (C-8) correlated with δ_C75.89 ppm (C-14), δ_C 62.7 ppm (C-15) and δ_C 26.83 ppm (C-16). The methylene proton at δ_H 4.39 ppm (dd; J=11, 9 Hz), 4.88 ppm (dd; J=17, 9 Hz; H-15) correlated with δ_C 74.19 ppm (C-13).

The methine proton at δ_H 4.02 ppm (dd; J=17, 11 Hz; H-14) correlated with δ_C 72.3 ppm (C-8), δ_C 74.19 ppm (C-13), δ_C 62.7 ppm (C-15).

1.9 Structure determination of compound **13**

Compound **13** was obtained as a white solid (0.3 g). The ^{1}H- NMR spectrum (Figure 53) of compound **13** showed eight methyl groups at δ_H 0.91 ppm (3H, s; H-20), 1.03 (3H, s; H-19), 1.09 (3H, s; H-18), 1.29 (3H, s; H-16), 1.34 (3H, s; H-17).

There were six methylene protons at δ_H 1.45 ppm (m; H-1), 1.6 (m; H-2), 1.05(m),1.08 (m; H-6), 1.48 (m), 1.86(m; H-7), 0.91 (m; H-11), 1.66 (m),1.80 (m; H-12).

There were three methine protons at δ_H 1.50 ppm (m; H-5), 1.40 (m; H-9), and a new one at δ_H 3.6 ppm (dd; J=11, 8 Hz; H-3). Three olefinic protons at δ_H 5.8 ppm (dd; J=17, 10.8 Hz; H-14), 4.9 ppm (dd; J= 10.8, 1.3 Hz; H-15a), 5.15 ppm (dd; J=17, 1.3 Hz; H-15b).

The ^{13}C-NMR spectrum (Figure 54) of compound **13** showed twenty carbon resonances, similar to the starting material (compound **1**), except the new methine carbon, generated by reduction with sodium borohydride at δ_C 78.8 ppm (C-3). These observations showed that the disappearance of carbonyl carbon (compound 1) at δ_C 217.2 ppm (C-3) which became the methine oxygenated carbon at δ_C 78.8 ppm (C-3).

In DEPT experiments (Figure 55), most of carbon signals were similar to the carbon signals of the starting material compound **1** (*ent*-3-oxo-manoyl oxide) except that the signals of carbonyl carbon moiety at δ_C 217.2 ppm (C-3) disappeared. The new oxygenated carbon signals at δ_C 78.8 ppm (C-3) showed their proximity the oxygen atom of alcohol in the molecule.

In the TOF-MS spectrum (Figure 59) compound **13** gave $C_{20}H_{34}O_2$ + Na at *m/z* 333.1103. The base peak was $[M+Na]^+$ at *m/z* 333.1103. The molecular formula of compound was assigned as $C_{20}H_{34}O_2$.

2D-NMR techniques were then used to assist in the interpretation of the structure of this compound. The ^{13}C-^{1}H COSY (Figure 56) and HMQC; (Figure 59) spectra helped to identify protons with carbon to which they are attached. The methine proton at δ_H 3.2 ppm (dd; J= 11, 4.8 Hz; H-3) correlated with carbon atom at δ_C 78.8 ppm (C-3).

The HMBC (Figure 58), methyl protons at δ_H 1.2 ppm (s; H-16) correlated with δ_C 147.6 ppm (C-14) and the quarternary carbon δ_C 73 ppm (C-8). The other quarternary carbon (C-13) correlated with olefinic carbon at δ_C 147.6 ppm (C-14). The methyl protons at δ_H 0.9 ppm (s; H-19) correlated with δ_C 55.2 ppm (C-5) and the δ_C 28.4 ppm (C-18).

2. Cytotoxic Activity Test of Isolated Compounds and their derivatives.

Bioassay of cytotoxic activity against human cell cultures *in vitro* was performed by the MTT [3-(4,5-dimethylthiazol-2-yl)-2,5-diphenyltetrazoliumbromide] colorimetric method. Each isolate was evaluated in a test for cytotoxicity against BT474 (breast carcinoma), CHAGO (lung carcinoma), HEP-G2 (hepatocarcinoma), KATO-3 (gastric carcinoma), and SW620 (colon carcinoma). Doxorubicin hydrochloride was used as a positive control.

The results from Table 3 showed that the compounds **1-13** were inactive as indicated by the percent survival of cancer cell lines more than 50% in BT 474 (human

breast ductal carcinoma), CHAGO (human undifferentiated lung carcinoma), HEP-G2 (human liver hepatoblastoma), KATO-3 (human gastric carcinoma), SW620 (human colon adenocarcinoma).

Table 3 Cytotoxicity data of the derivatives from *C. roxburghii*.

sample	Percent Survival(%)				
	SW620	BT 474	KATO-3	HEP-G2	CHAGO
Compound 1	96	103	84	109	103
Compound2	96	91	74	100	101
Compound3	96	127	96	98	101
Compound4	98	92	96	108	101
Compound5	96	103	96	102	101
Compound6	96	77	91	100	101
Compound7	94	82	97	101	98
Compound8	94	94	97	91	100
Compound9	94	91	69	74	102
Compound10	93	81	99	91	102
Compound11	95	75	98	93	100
Compound12	94	91	95	100	102
Compound13	95	89	99	83	100
Doxorubicin	100	100	100	100	100

3. α-glucosidase inhibitory activity

In this study, the α-glucosidase inhibitory activity of compounds **1-13** were reported. Table 4 showed the % inhibition determined at 1 mg/mL concentration of test compound.

Table 4 Inhibitory activities of the derivatives from *C. roxburghii*.

Sample	% inhibition
Compound 1	44.32
Compound 2	49.03
Compound 3	43.21
Compound 4	46.26
Compound 5	55.12
Compound 6	37.25
Compound 7	37.79
Compound 8	37.59
Compound 9	38.71
Compound 10	42.31
Compound 11	42.41
Compound 12	40.21
Compound13	65.58
1-deoxynojirimycin	79.08

The results for the structure-activity relationship studies showed that 3β-C hydroxy substituted of compound **1** (compound **13**) increased the α-glucosidase inhibitory activities more than 3α-C hydroxy substituted (compound **5**). Epoxidation of the exocyclic double bond makes the inhibitory activity reduced.

In summary, most of the compounds (compound **1-13**) determined for α-glucosidase inhibitory activities showed moderate α-glucosidase inhibitory activities.

CHAPTER V

CONCLUSION

From the stem bark of *Croton roxburghii* N.P. Balakr. (Euphorbiaceae) , five diterpene compounds have been isolated. They were identified by TLC in comparision with previous reports. Compounds **1-5** were identified as *ent*-3-oxo-manoyl oxide, *ent*-1,2-dehydro-3-oxo-manoyl oxide, *ent*-1,2-dehydro-12α-hydroxy-3-oxo-manoyl oxide, *ent*-1β-hydroxy-3-oxo-manoyl oxide, and *ent*-3α-hydroxy-manoyl oxide, respectively. The derivatives **6-13**, were *ent*-1,2-dehydro-3-oxo-manoyl oxide-14,15-oxirane, *ent*-1,2-dehydro-12α-hydroxy-3-oxo-manoyl oxide-14,15-oxirane, *ent*-1β-hydroxy-3-oxo-manoyl oxide-14,15-oxirane, *ent*-3α-hydroxy-manoyl oxide-14,15-oxirane, *ent*-3-oxo-manoyl oxide-14(R),15-diol, *ent*-3α-Hydroxy-manoyloxide-14(R),15-diol, *ent*-3α,14(R),15-triacetyl-manoyl oxide and *ent*-3β-hydroxy-manoyl oxide, respectively. Its showed no cytotoxic activity in BT 474 (human breast ductal carcinoma), CHAGO (human undifferentiated lung carcinoma), HEP-G2 (human liver hepatoblastoma), KATO-3 (human gastric carcinoma), SW620 (human colon adenocarcinoma). most of the compounds (compound **1-13**) determined for α-glucosidase inhibitory activities showed moderate α-glucosidase inhibitory activities. Epoxidation of the exocyclic double bond makes the inhibitory activity reduced. The 3β-C hydroxy substituted of compound **1** (compound **13**) increased the α-glucosidase inhibitory activities more than 3α-C hydroxy substituted (compound **5**).

REFERENCES

Achayindee, S. 1996. Chemical constituents of leaf of *Croton oblongifolius* Roxb. Master Thesis, Department of Chemistry, Faculty of Science, Chulalongkorn University.

Adisakwattana, S., Sookkongwaree, K., and Roengsumran, S. 2004. Structure-activity relationships of trans-cinnamic acid derivatives on α-glucosidase inhibition. Bioorg. Med. Chem. Lett. 14:2893-2896

Aiyar, V.N., and Seshadri, T.R. 1970. Components of *Croton oblongifolius* Roxb. III Constitution of oblongifolic acid. Tetrahedron. 26: 5275-5279.

Aiyar, V.N., and Seshadri, T.R. 1971a. Chemical components of *Croton oblongifolius* Roxb. Part V. Indian J. Chem. 9: 613-614.

Aiyar, V.N., and Seshadri, T.R. 1971b. Chemical components of *Croton oblongifolius* Roxb. Part IV Constitution of oblongifoliol and deoxyoblongifoliol. Indian J. Chem. 9: 1055-1059.

Aiyar, V.N., and Seshadri, T.R. 1971c. Isolation of acetyl aleuritolic acid from *Croton oblongifolius* Roxb. Indian J. Chem. 9: 1028-1029.

Aiyar, V.N., and Seshadri, T.R. 1972a . Chemical components of *Croton oblongifolius* Roxb. Curr. Sci. 41: 839-840.

Asano, N. 2003. Glycosidase inhibitors: update and perspectives on practical use. Glycobiology. 13: 93R*104R.

Baiagern, S. 1999. Chemical and biological activity from stem bark of *Croton oblongifolius* Roxb. From Amphor Muang, Udonthani province. Master thesis, Department of chemistry, Faculty of Science, Chulalongkorn University.

Bandara, B. M. R., Wimalasiri, W. R. and Bandara, K. A. N. P. 1987. Isolation and insecticidal activity of (-)-hardwickiic acid from *Croton aromaticus*. Planta Med. 53: 575

Blatter, E., Caius, J.F. and Mhaskar, K.S. 1975. Indian Medicinal Plants. Vol.III 2nd edition. Delhi: Jayyed Press.

Bohlmann, F. and Fritz, U. 1978. New diterpene and acetylene derivatives of Nidorellarten. Phytochemistry. 17: 1769-1772.

Bunta, B. 2000. Chemical and biological activity from stem bark of *Croton oblongifolius* Roxb. From Amphor Muang, Prachup Khiri Khan province. Master thesis, Department of chemistry, Faculty of Science, Chulalongkorn University.

Cabrera, E., Garcia-Granados, A. and Aranzazu Quecuty, M. 1988. Terpenoids from *Sideritis varoi*. Phytochemistry. 27 183-185

Chaicharoenpong, C. 1996. Chemical constituents of wood of *Croton oblongifolius* Roxb. Master thesis, Department of chemistry, Faculty of Science, Chulalongkorn University.

Chaichantipyuth, C. 2005. New labdane diterpenoids from *Croton oblongifolius* and their cytotoxic activity. Ph. D. thesis, Laboratory of Medicinal Organic Chemistry, Graduate School of Pharmaceutical Sciences, Chiba University.

Devon, T. K. and scott, A. I. 1972. Handbook of naturally iccurring compounds. New York and London: Academic press.

Fraga, B. M., Gonzalez, P., Hernansez, M. G. and Suarez, S. 1999. Formation of 2,3 – seco acids in the biotransformation of the diterpene ribenone by *Gibberella fujikuroi*. Tetrahedron. 55:1781-1792.

Israngkura Na Ayutthaya, A. 2002. Chemical constituents of the stem bark of *Croton oblongifolius* Roxb. From Loei province.Master thesis, Department of pharmacognosy, Faculty of Pharmaceutical Science, Chulalongkorn University.

Jame, D. M., Slice, S. C. and Edilberto, R. S. 1991. Antimicrobial diterpenes of *Croton oblongifolius* Roxb: Hardwickiic and 3,4-secotrachylobanoic acid. J. Nat. Prod. 54: 1625-1633.

Kuptiyanuwat, N. 1999. Chemical and biological activity from *Croton oblongifolius* Roxb. From Amphor Wang Sa Pung, Loei province.Master thesis, Department of chemistry, Faculty of Science, Chulalongkorn University.

Pattamadilok, D. 1988. Chemical constituents of the stem bark of *Croton oblongifolius* Roxb. From Chainat province. Master thesis, Department of pharmacognosy, Faculty of Pharmaceutical Science, Chulalongkorn University.

Rao, P. S., Sachdev, T. R., and Singh, H. B. 1968. Isolation and constitution of oblongifoliol, a new diterpene of *Croton oblongifolius* Roxb. Tetrahedron Lett. 45: 4685-4688.

Roengsumran, S., Achayindee, S., Petsom, A., Pudhom, K., Singtotong, P., Sur achetapan, C., and Vilaivan, T. 1998 Two new cembranoids from *Croton oblongifolius* Roxb. J. Nat. Prod. 61:652-654.

Roengsumran, S., Petsom, A., Sommit, D., and Vilaivan, T. 1999a. Labdane diterpenoids from *Croton oblongifolius* Roxb. Phytochemistry 50: 449-453.

Roengsumran, S., Singtotong, P., Pudhom, K., Ngamrojnavanich, N., Petsom, A., and Chaichantipyuth, C. 1999b. Neocrotocembranal from *Croton oblongifolius* Roxb. J. Nat. Prod. 62: 1163-1164.

Roengsumran, S., Petsom, A., Kuptiyanuwat, N., Vilaivan, T., Ngamrojnavanich, N., Chaichantipyuth, C. and Phuthong, S. 2001. Cytotoxic labdane diterpenoids from *Croton oblongifolius* Roxb. Phytochemistry 56: 103-107.

Singh, M., Pal, M. and Sharma, R. P. 1999. Biological activity of the labdane diterpenes. Planta Med. 65: 2-8.

Sirimongkon, S. 2000. Kaurane diterpenes from stem bark of *Croton oblongifolius* Roxb. from Amphor Kui Buri, Prachub Khiri Khan province. Master Thesis. Department of chemistry, Faculty of Science, Chulalongkorn University.

Siriwat, K. 1999. Chemical and biological activity from stem bark of *Croton oblongifolius* Roxb. from Amphor Dan Sai, Loie province. Master Thesis. Department of chemistry, Faculty of Science, Chulalongkorn University.

Sriyangnok, S. 2000. Chemical and biological activity from stem bark of *Croton oblongifolius* Roxb. From Amphor Pranburi, Prachuap Khiri Khan province. Master Thesis. Department of chemistry, Faculty of Science, Chulalongkorn University.

Surachethapan, C. 1996. Chemical constituents of stem bark of *Croton oblongifolius* Roxb. Master thesis. Department of chemistry, Faculty of Science, Chulalongkorn University.

Tanwattanakun, T. 1999. Chemical and biological activity from stem bark of *Croton oblongifolius* Roxb. From Amphor Muang, Uttaradit province Master thesis. Department of chemistry, Faculty of Science, Chulalongkorn University.

APPENDIX

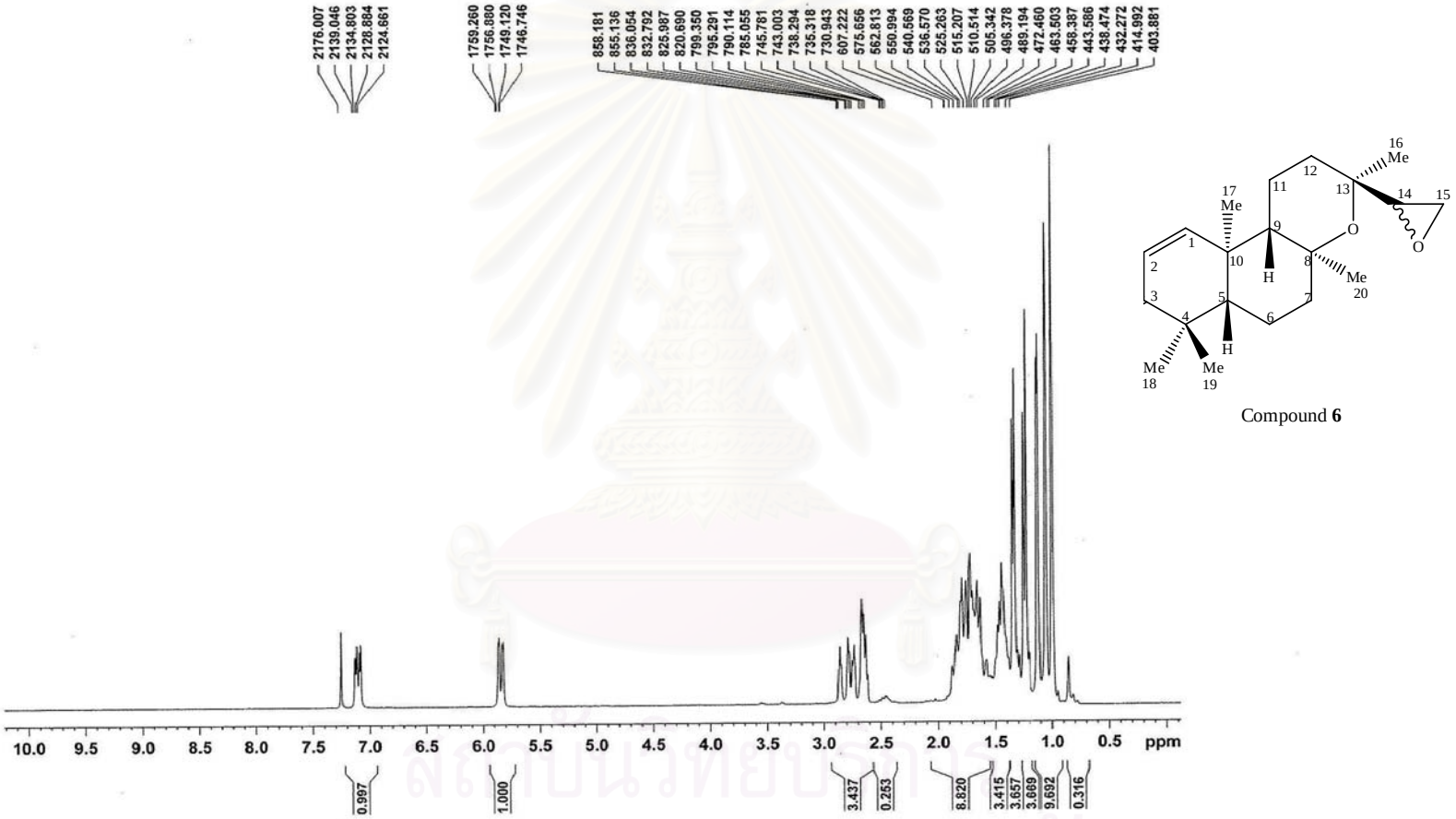

Compound **6**

Figure 6 The 300 MHz ^{1}H-NMR spectrum of compound **6** (in $CDCl_3$)

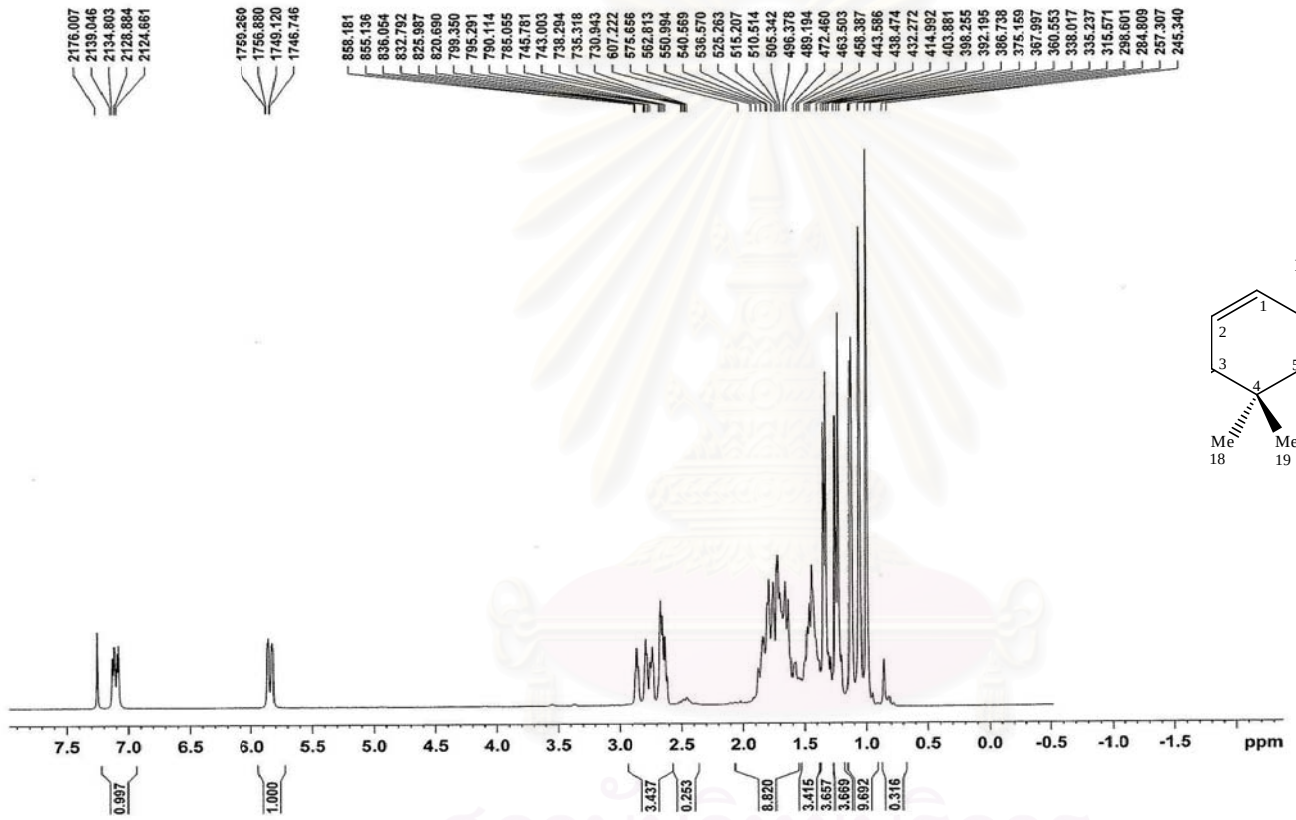

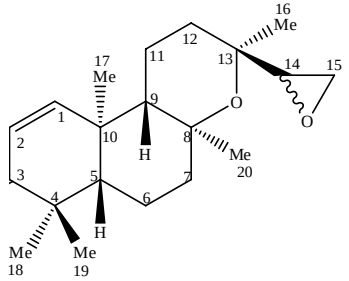

Compound **6**

Figure 6a The 300 MHz ^{1}H-NMR spectrum of compound **6** (in $CDCl_3$)

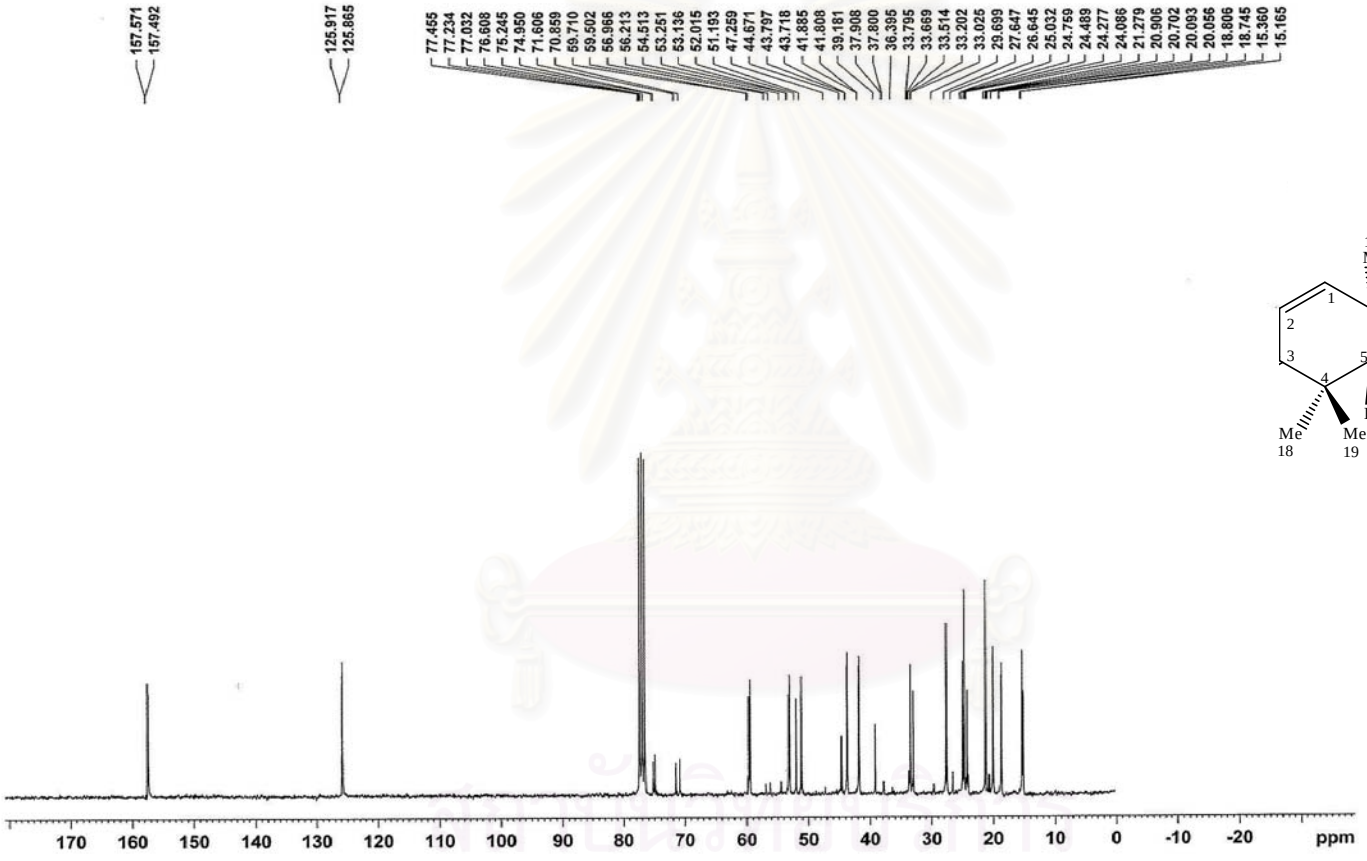

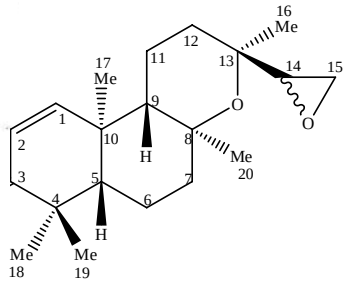

Compound **6**

Figure 7 The 75 MHz ^{13}C-NMR spectrum of compound **6** (in $CDCl_3$)

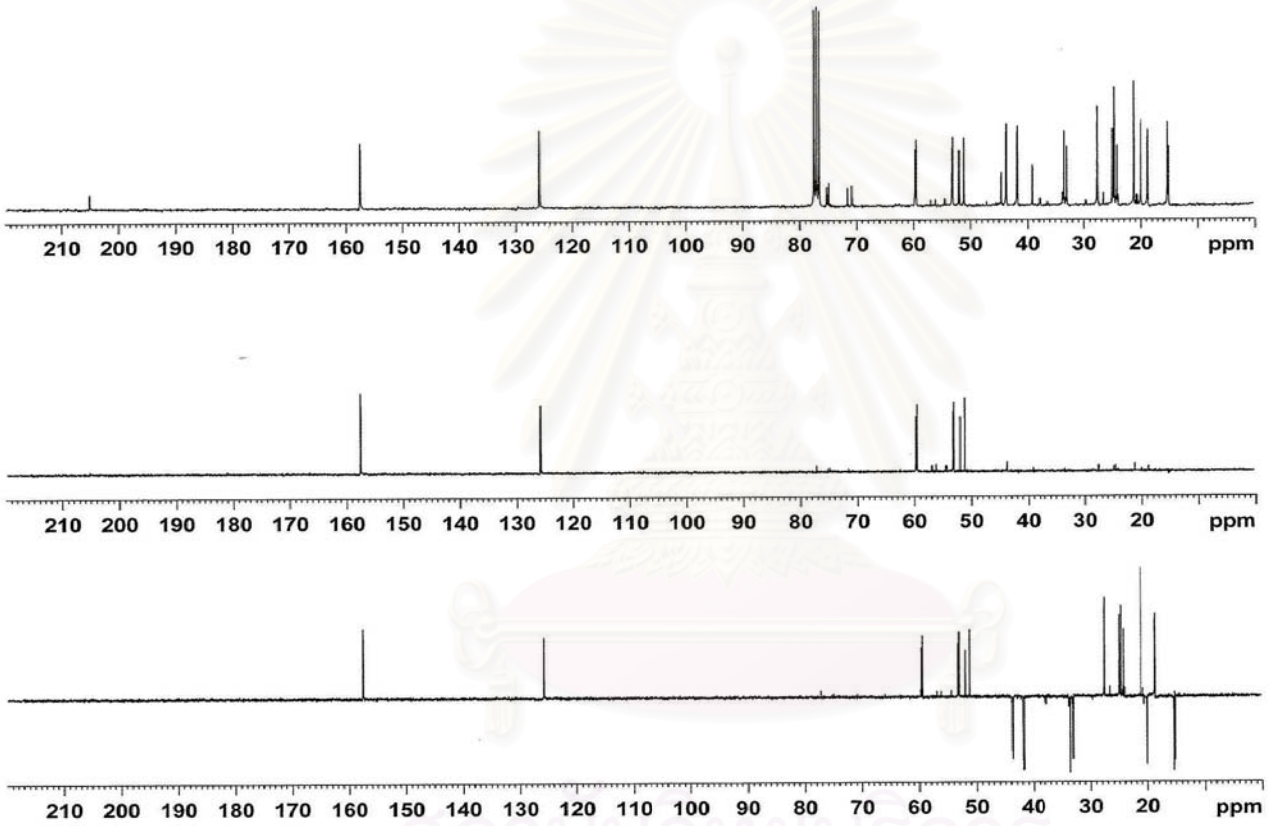

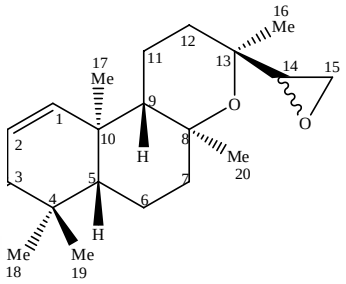

Compound **6**

Figure 8 The 75 MHz ^{13}C-NMR, DEPT-90 and DEPT-135 spectra of compound **6**

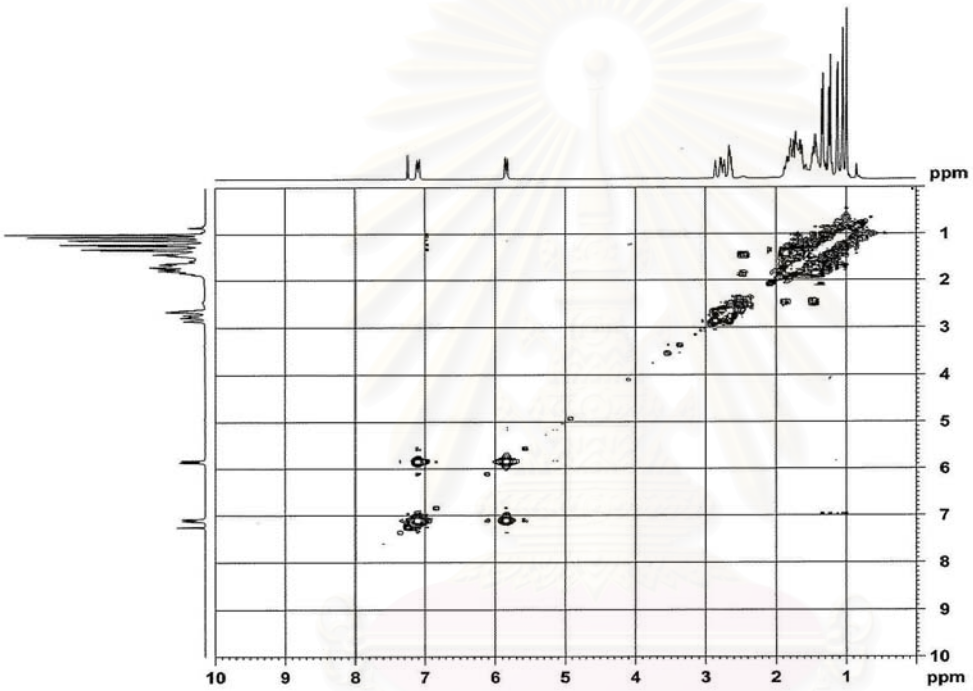

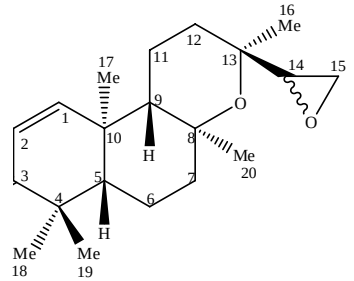

Compound **6**

Figure 9 The 300 MHz ^{1}H-^{1}H COSY NMR spectrum of compound 6

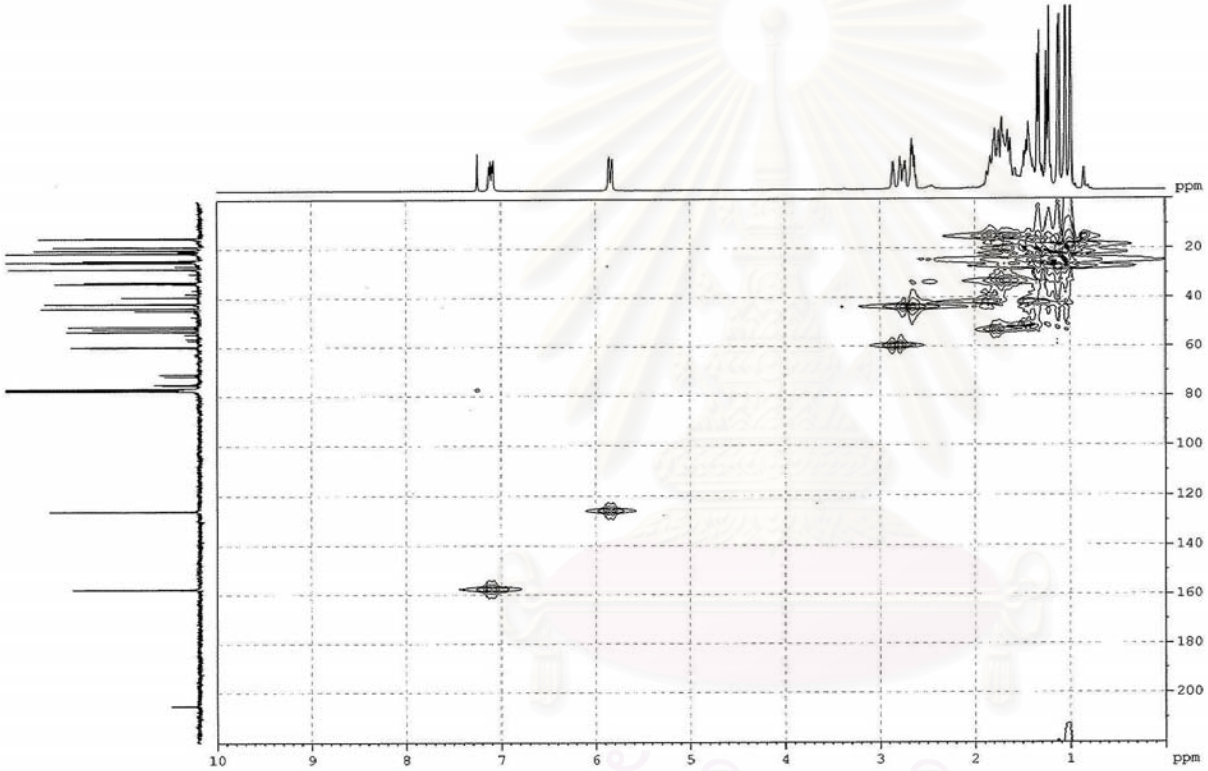

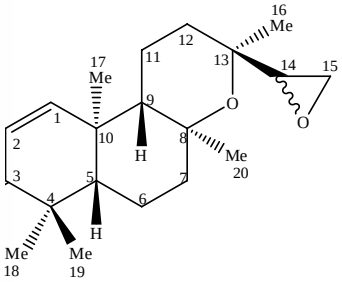

Compound **6**

Figure 10 The 300 MHz HMQC NMR spectrum of compound 6

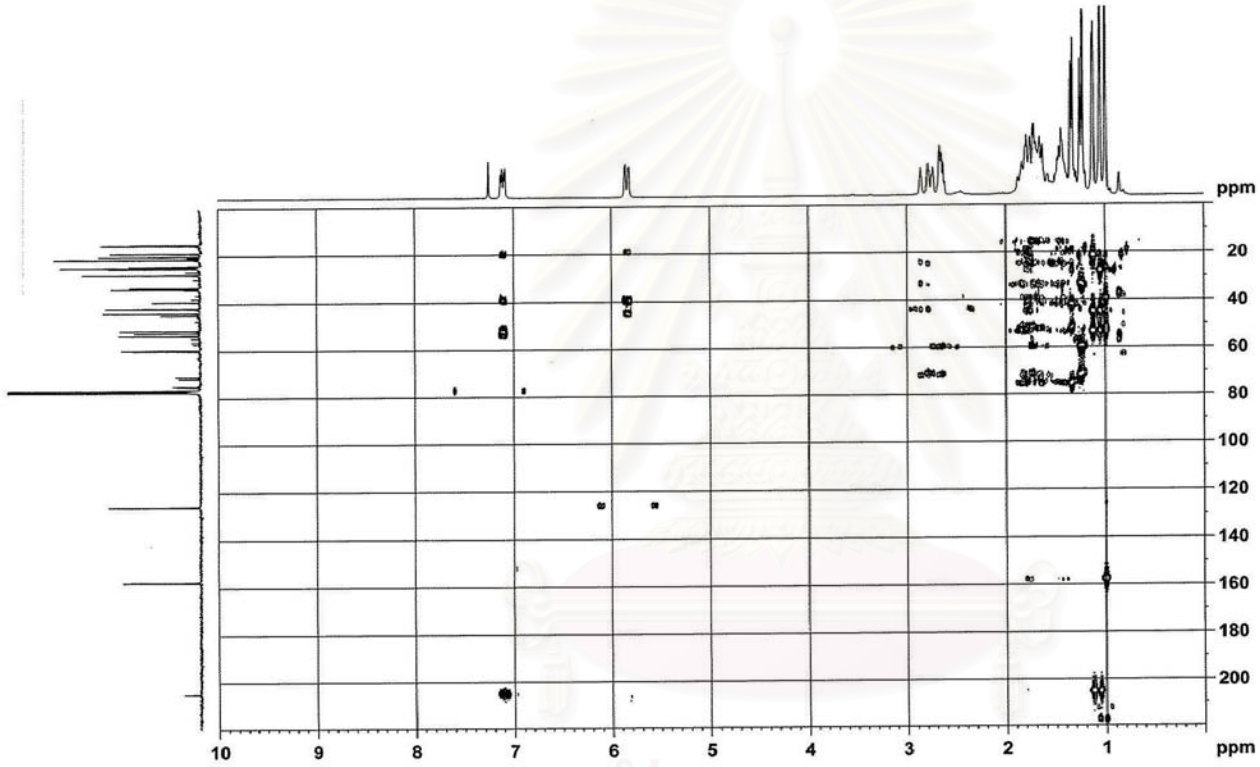

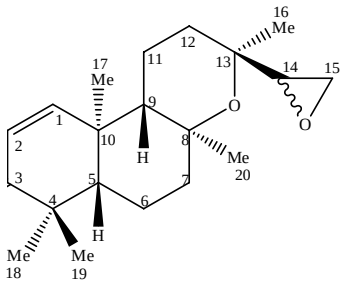

Compound **6**

Figure 11 The 300 MHz HMBC spectrum of compound **6** (in $CDCl_3$)

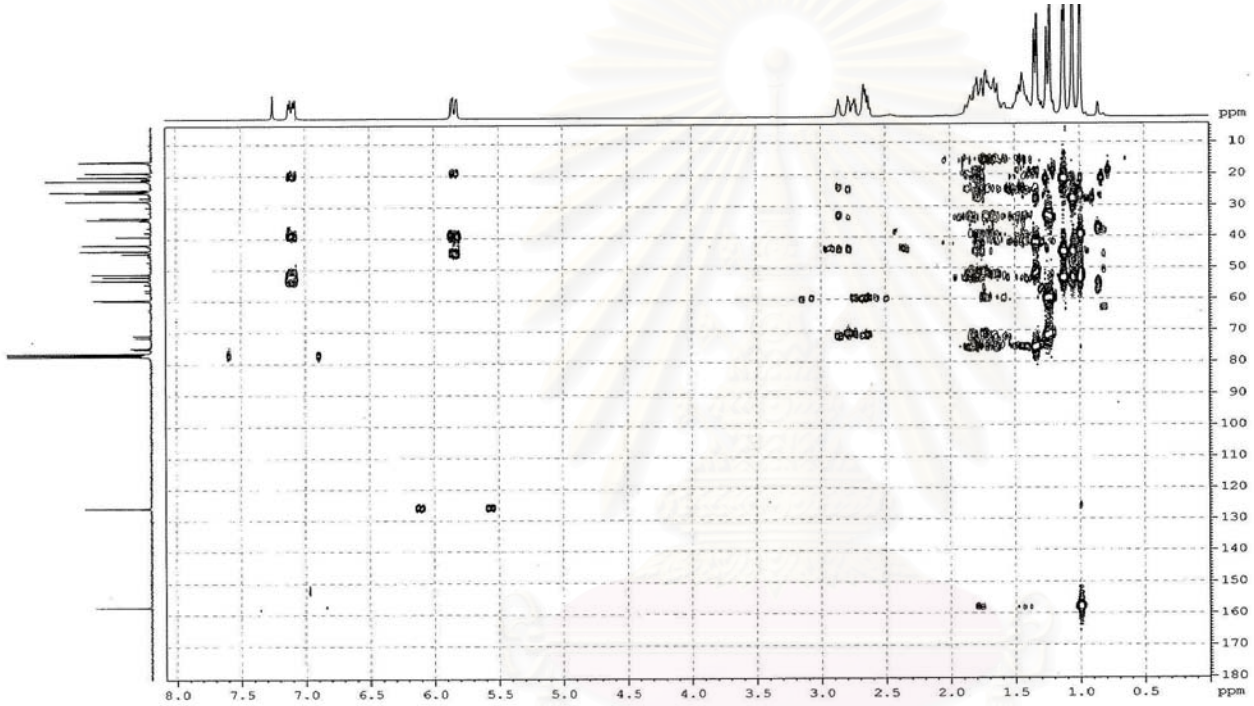

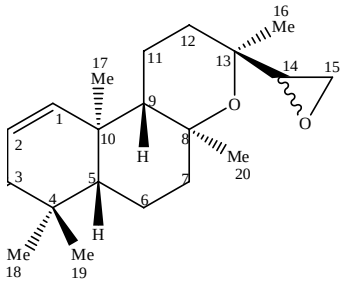

Compound **6**

Figure 11a The expanded 300 MHz HMBC spectrum of compound **6** (in $CDCl_3$)

(δ_H8.0-0.5 ppm, δ_C10 -160 ppm)

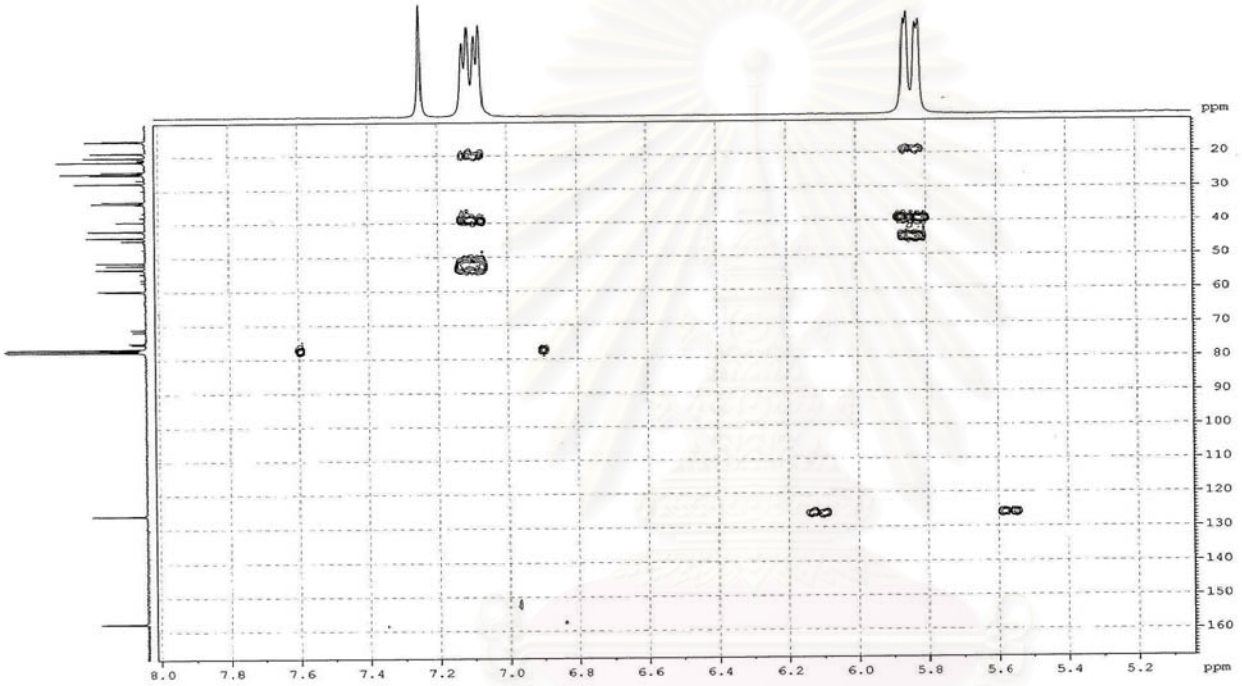

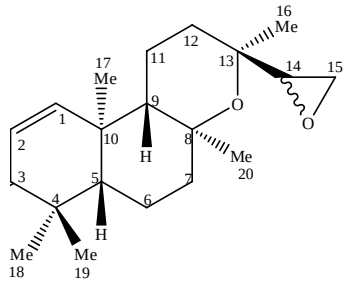

Compound **6**

Figure 11b The expanded 300 MHz HMBC spectrum of compound **6** (in $CDCl_3$)

(δ_H8.0-5.2 ppm, δ_C10 -160 ppm)

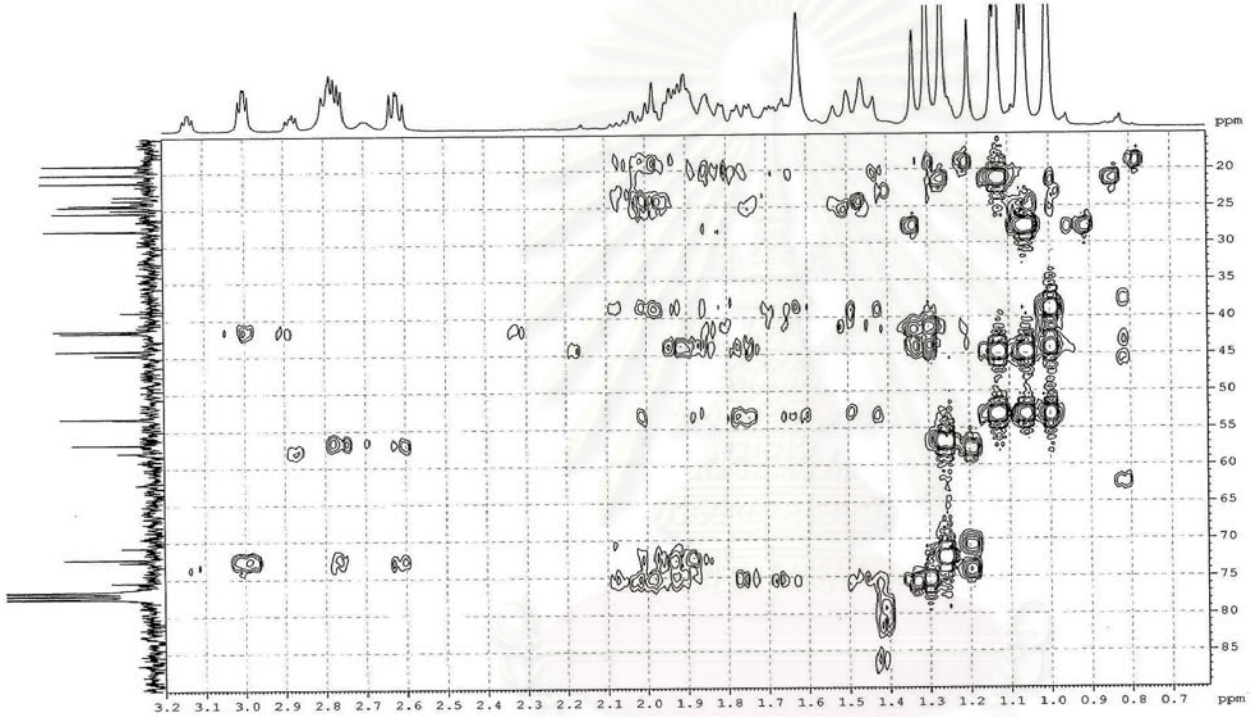

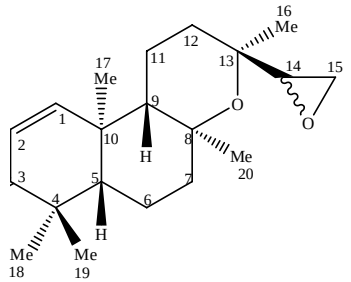

Compound **6**

Figure 11c The expanded 300 MHz HMBC spectrum of compound **6** (in $CDCl_3$)

(δ_H3.2-0.7 ppm, δ_C15 -85 ppm)

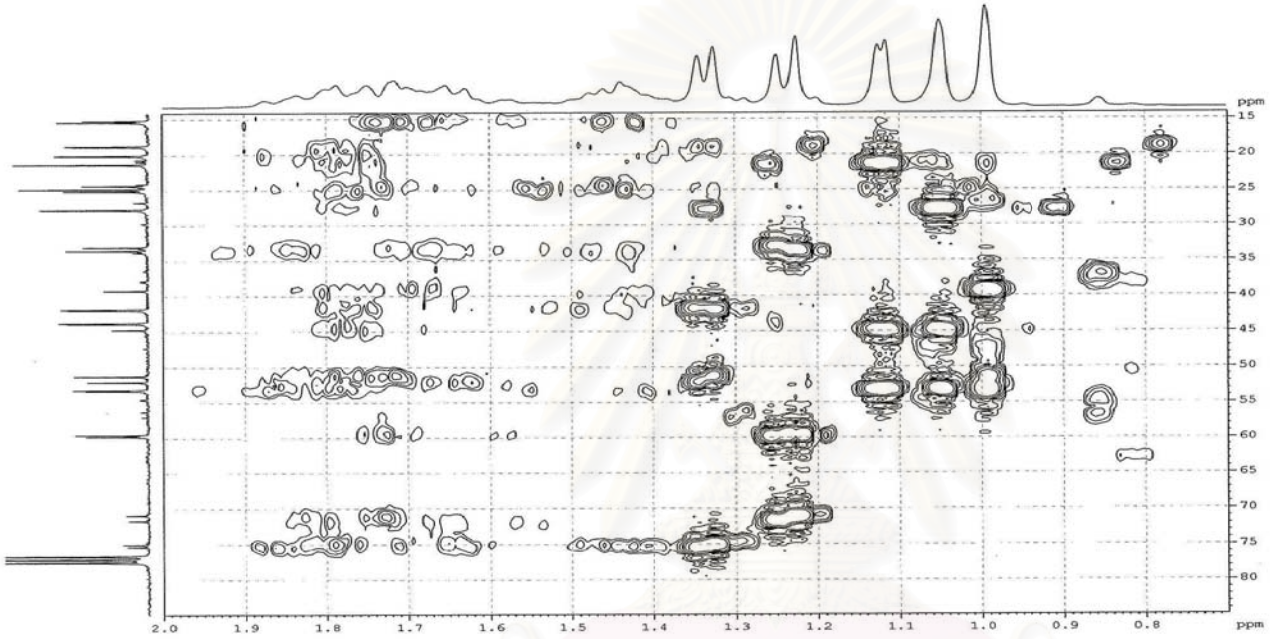

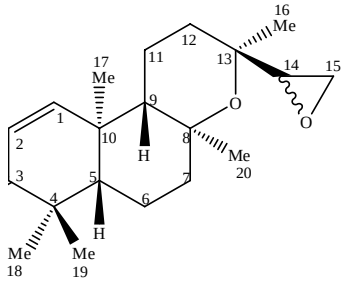

Compound **6**

Figure 11d The expanded 300 MHz HMBC spectrum of compound **6** (in $CDCl_3$)

(δ_H2.0-0.7 ppm, δ_C15 -85 ppm)

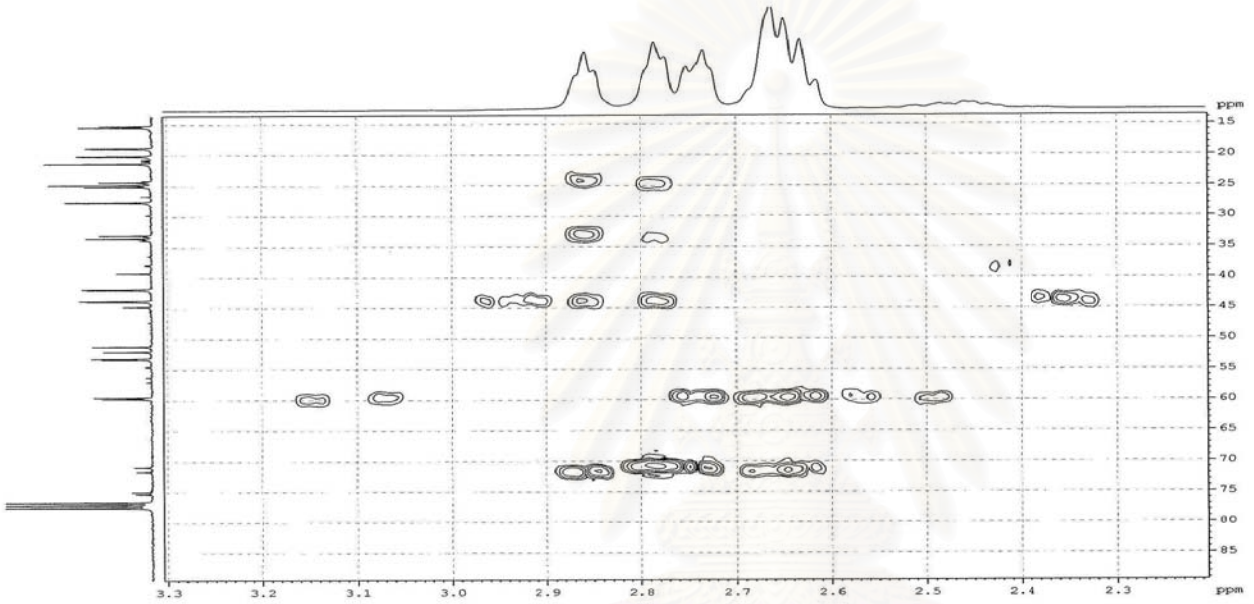

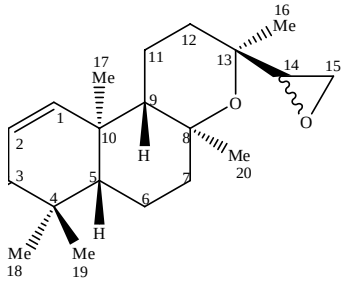

Compound **6**

Figure 11e The expanded 300 MHz HMBC spectrum of compound **6** (in $CDCl_3$)

(δ_H3.3-2.3 ppm, δ_C15 -85ppm)

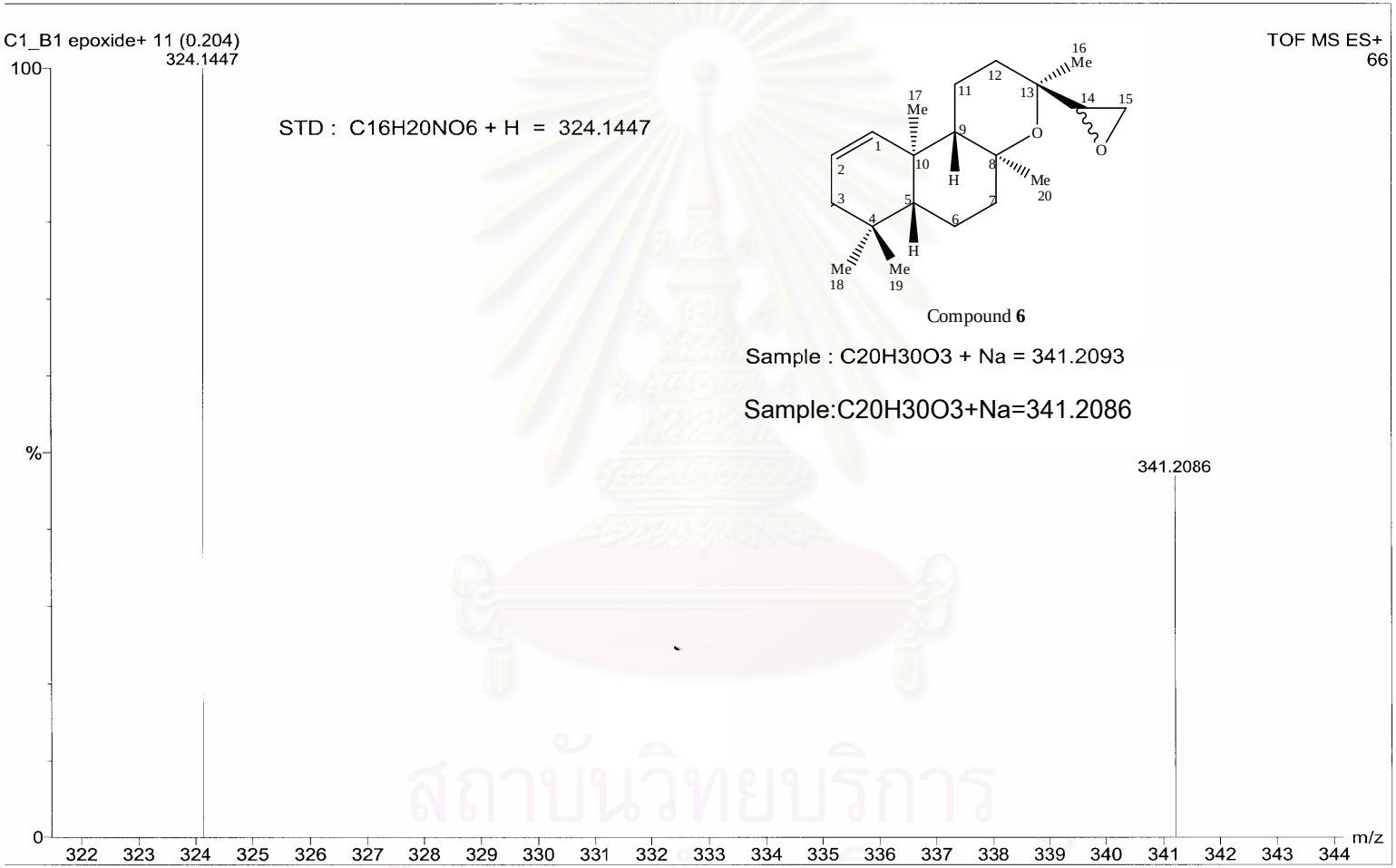

Figure 12 The TOF-MS spectrum of compound 6

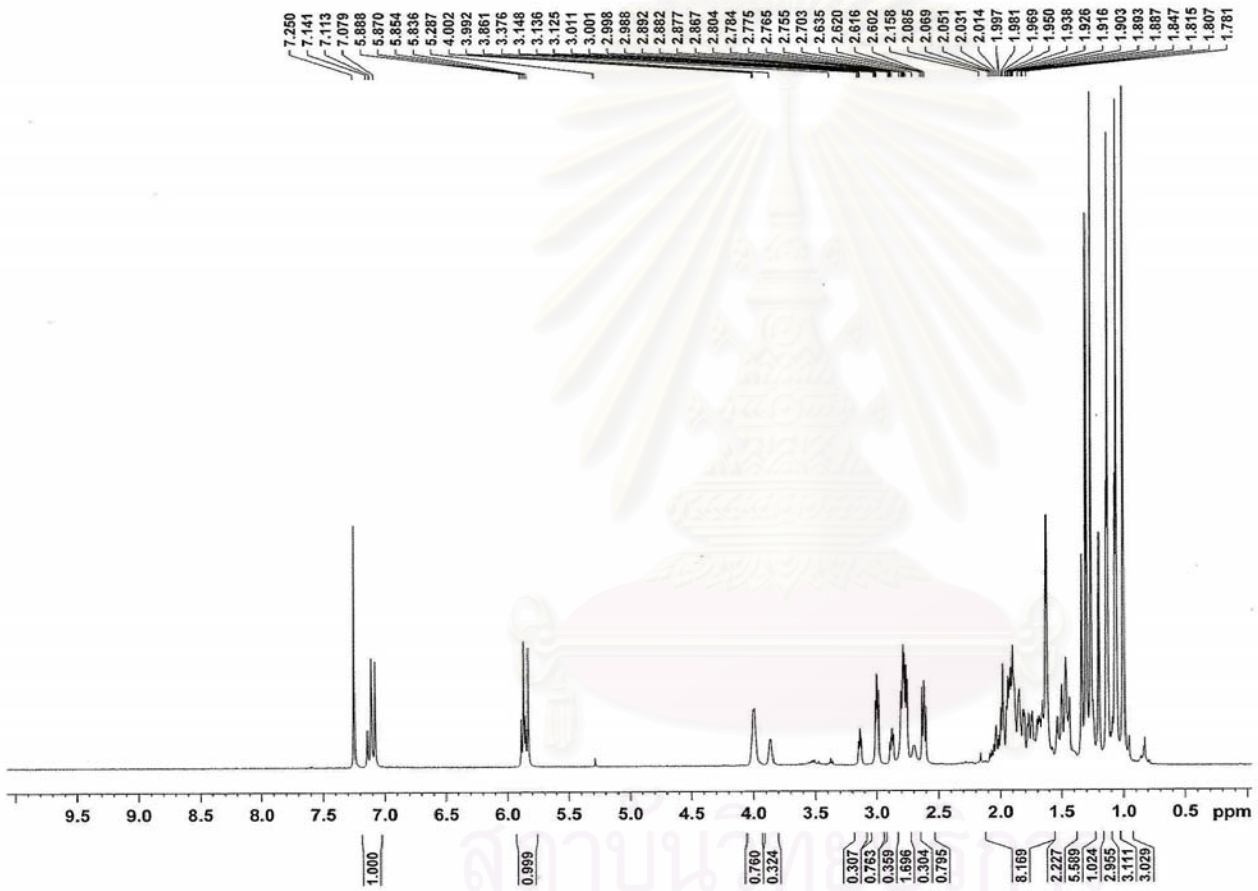

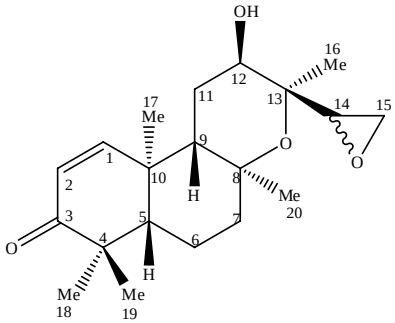

Compound **7**

Figure 13 The 300 MHz ^{1}H-NMR spectrum of compound **7** (in $CDCl_3$)

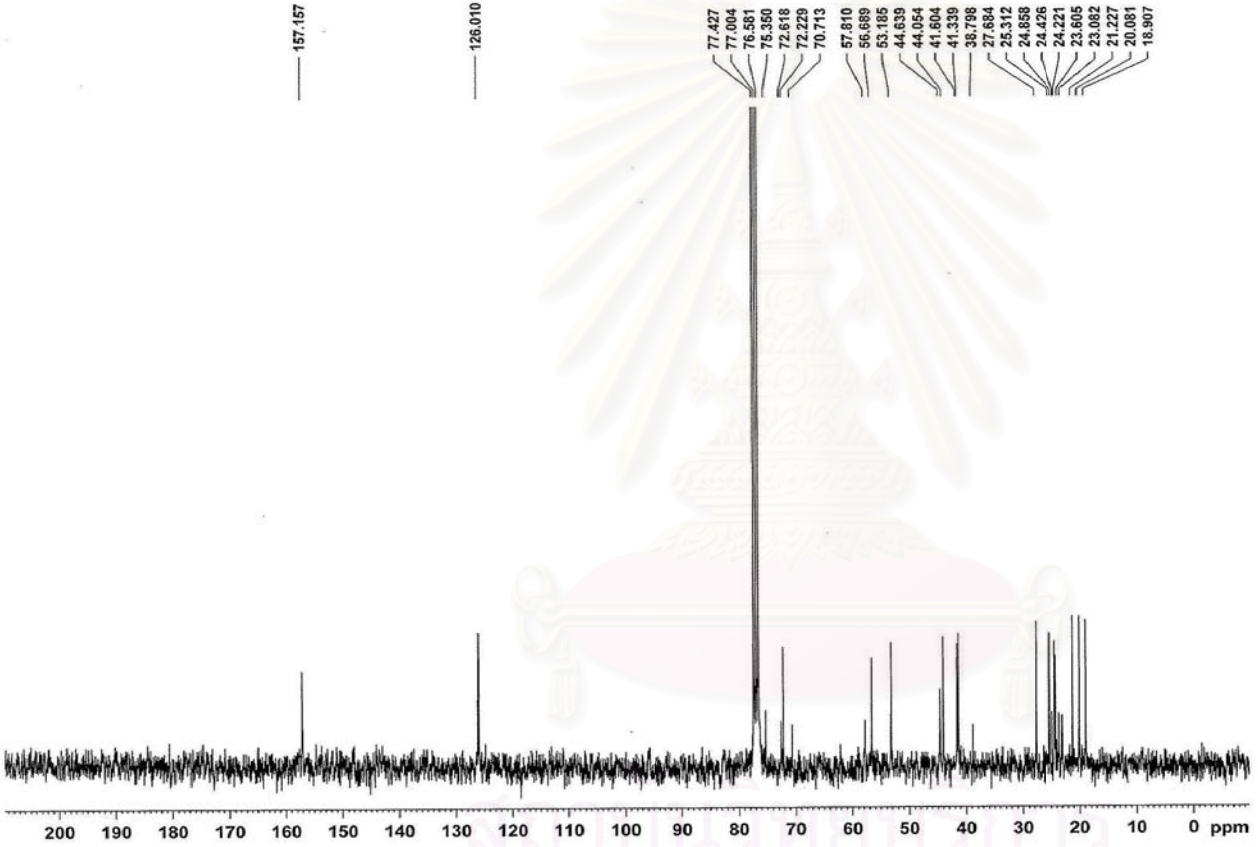

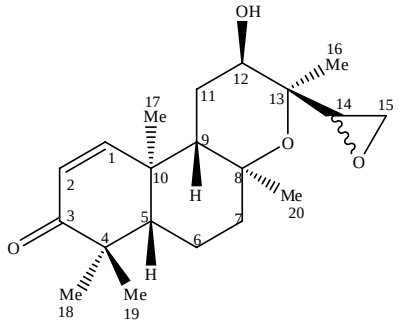

Compound **7**

Figure 14 The 75 MHz ^{13}C-NMR spectrum of compound **7** (in $CDCl_3$)

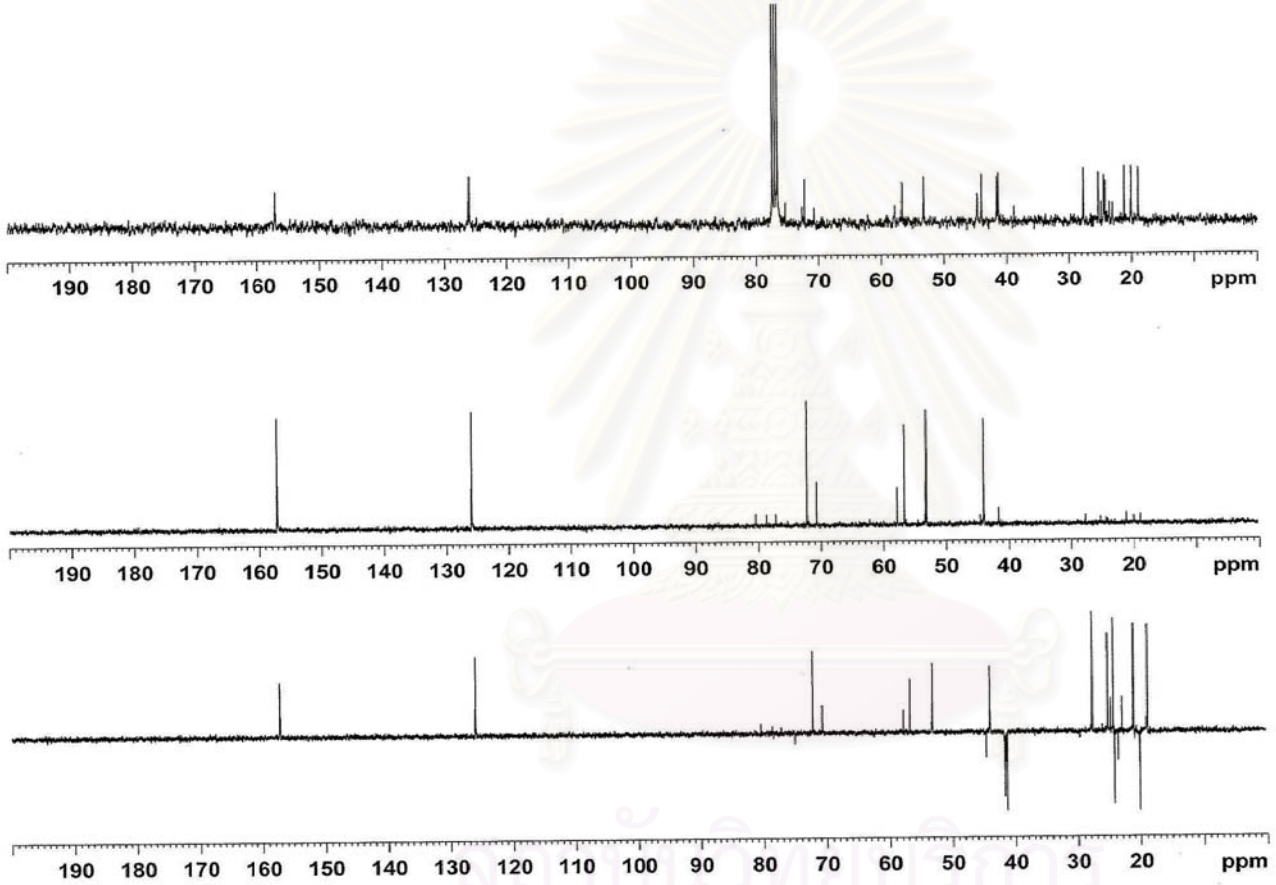

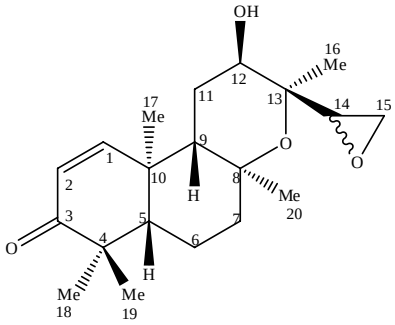

Compound **7**

Figure 15 The 75 MHz ^{13}C-NMR, DEPT-90 and DEPT-135 spectra of compound **7**

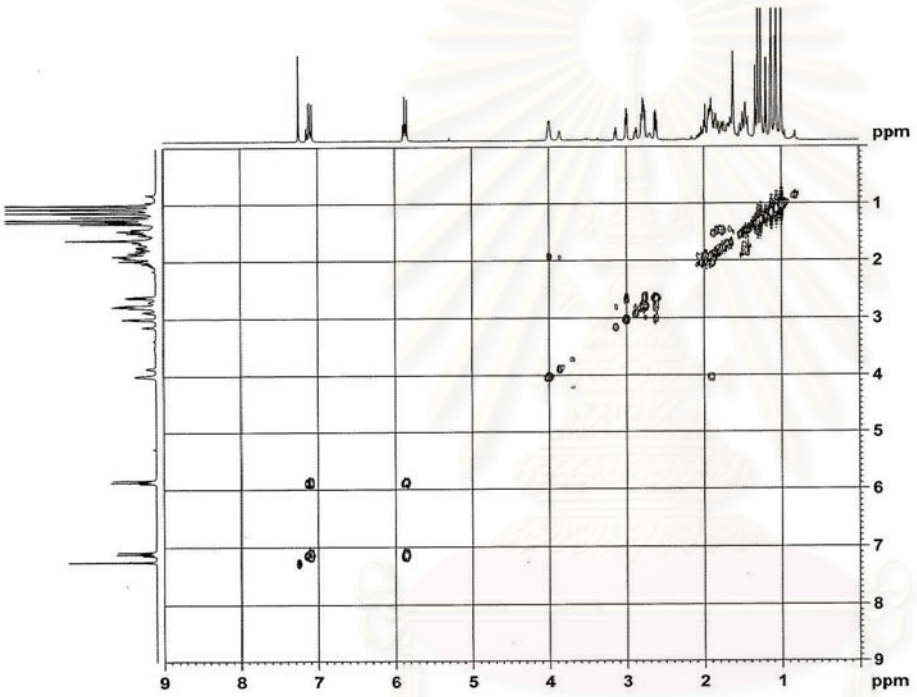

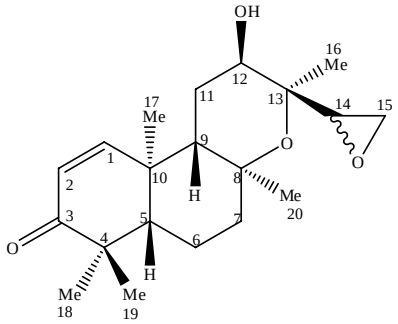

Compound **7**

Figure 16 The 300 MHz ^{1}H-^{1}H COSY NMR spectrum of compound **7**

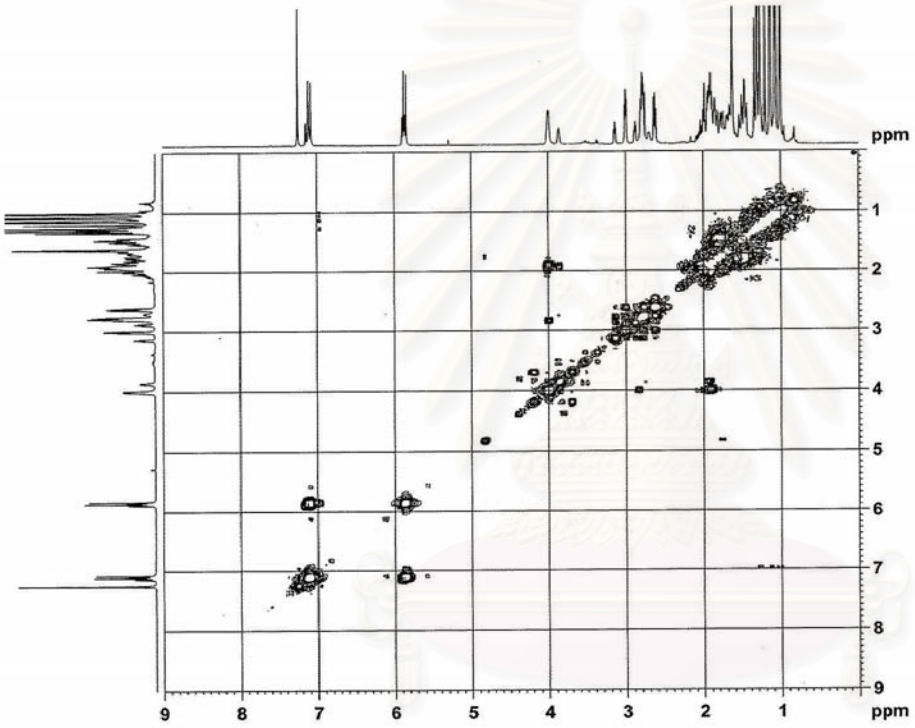

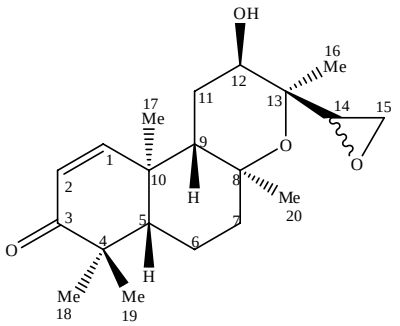

Compound **7**

Figure 16a The expanded 300 MHz ^{1}H-^{1}H COSY NMR spectrum of compound **7**

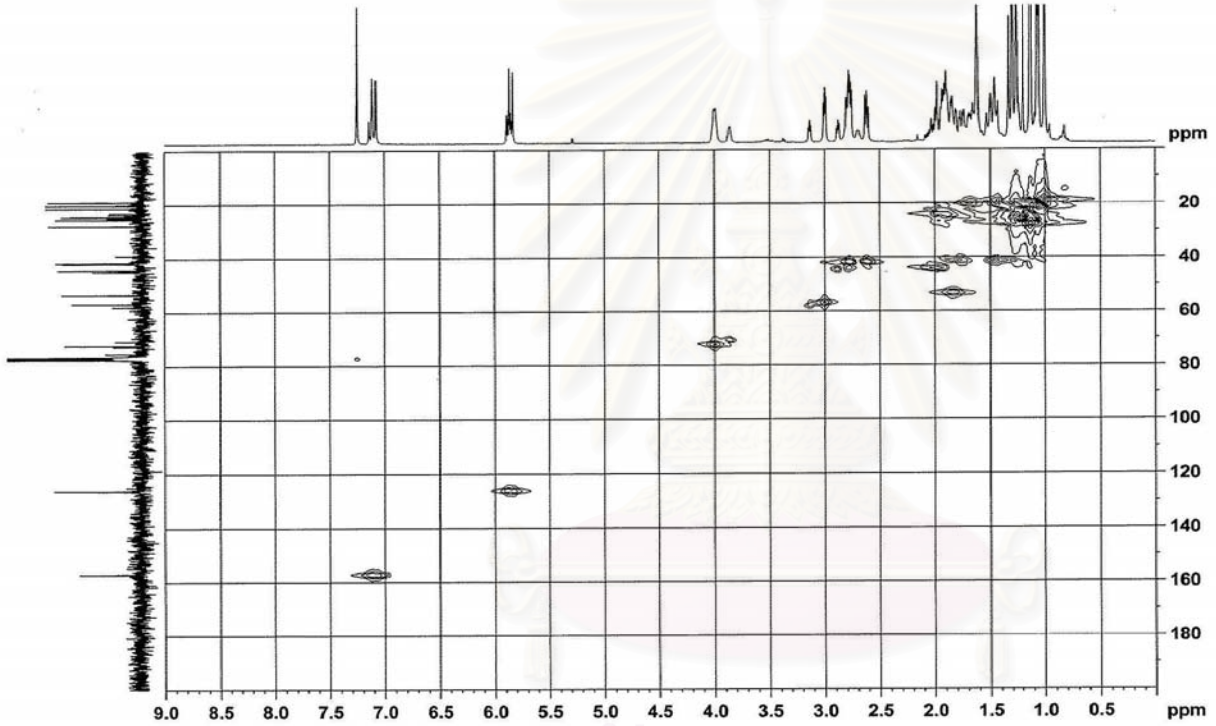

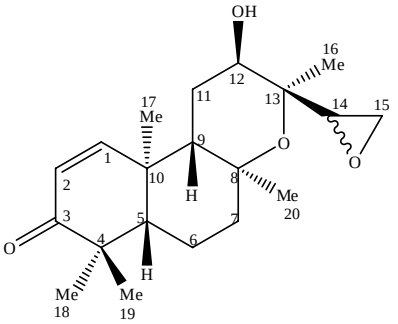

Compound **7**

Figure 17 The 300 MHz HMQC spectrum of compound **7** (in $CDCl_3$)

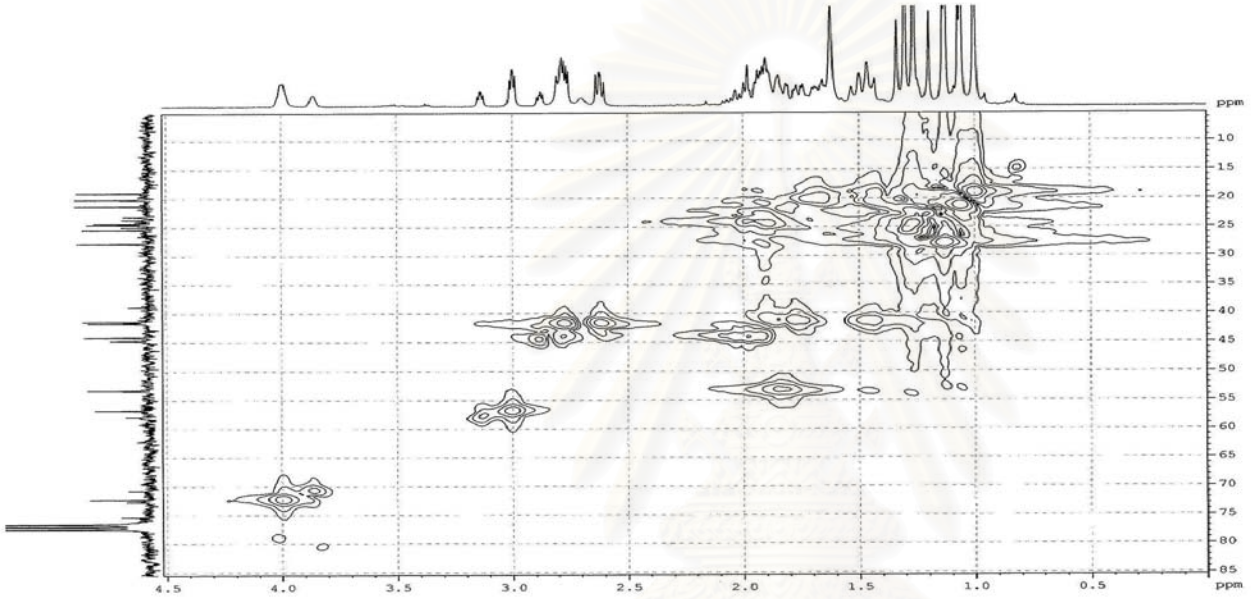

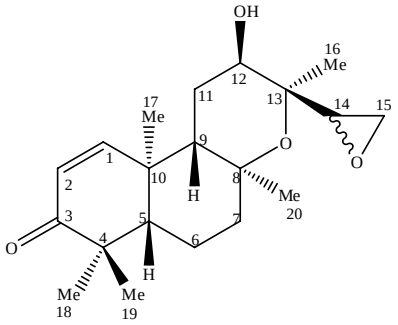

Compound **7**

Figure 17a The expanded 300 MHz HMQC spectrum of compound **7** (in $CDCl_3$)

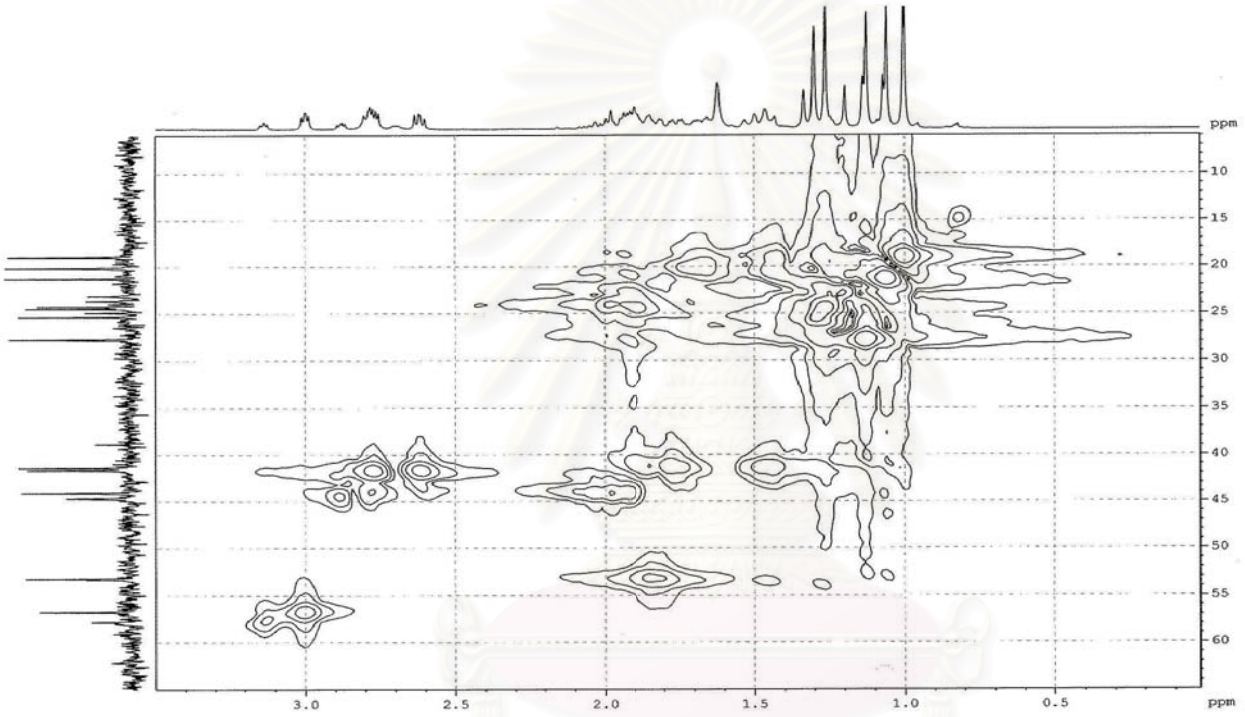

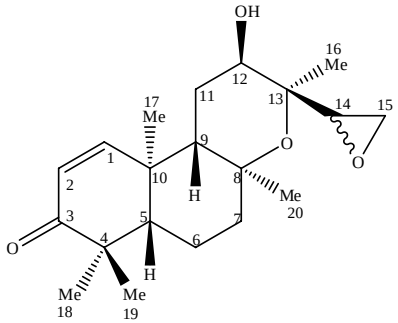

Compound **7**

Figure 17b The expanded 300 MHz HMQC spectrum of compound **7** (in $CDCl_3$)

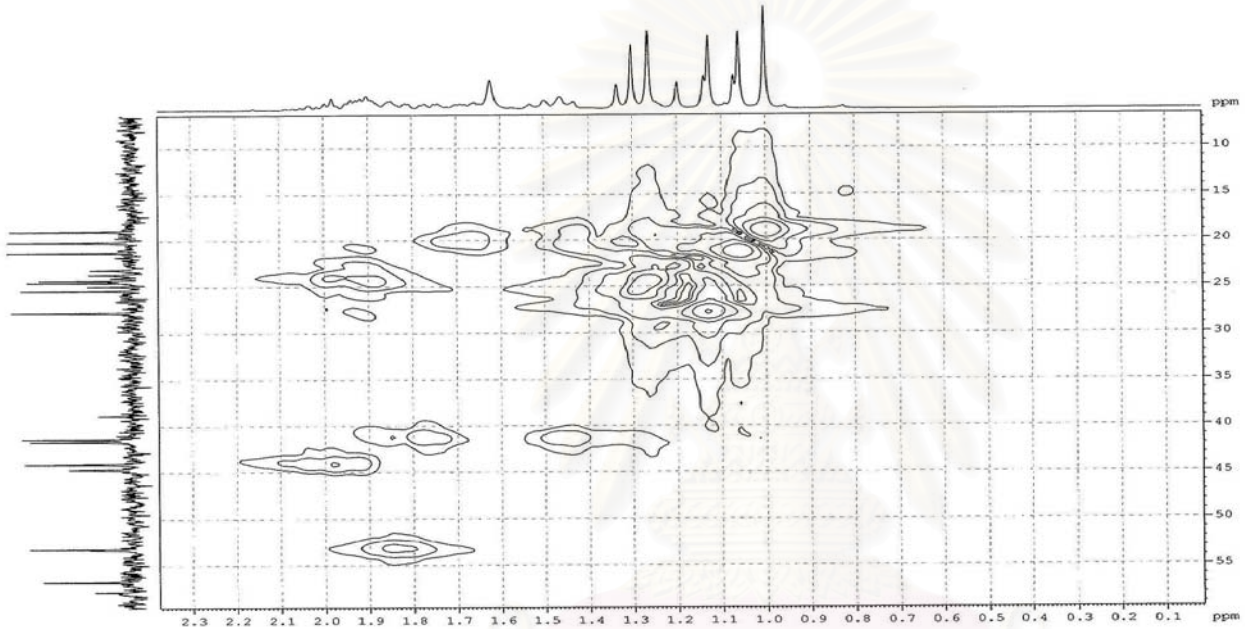

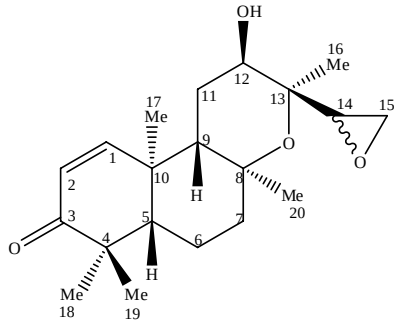

Compound **7**

Figure 17c The expanded 300 MHz HMQC spectrum of compound **7** (in $CDCl_3$)

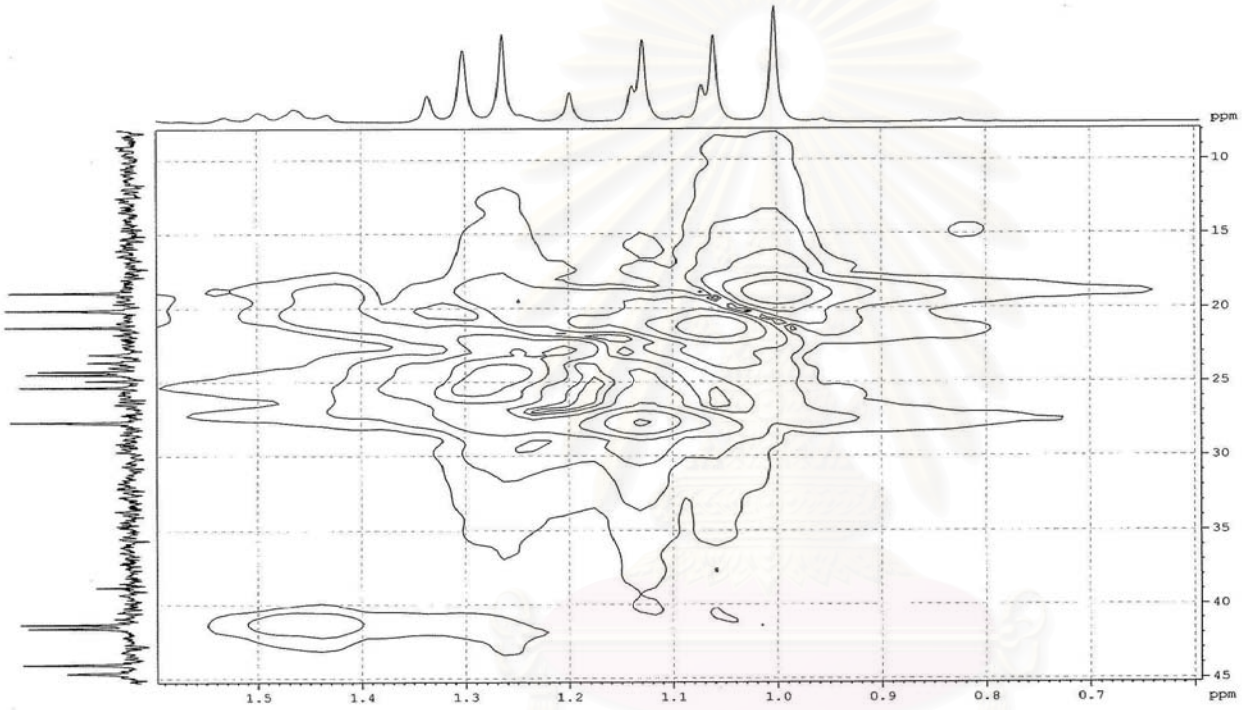

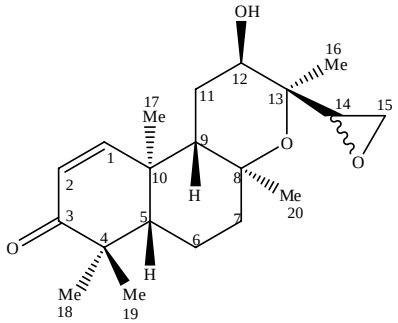

Compound **7**

Figure 17d The expanded 300 MHz HMQC spectrum of compound **7** (in $CDCl_3$)

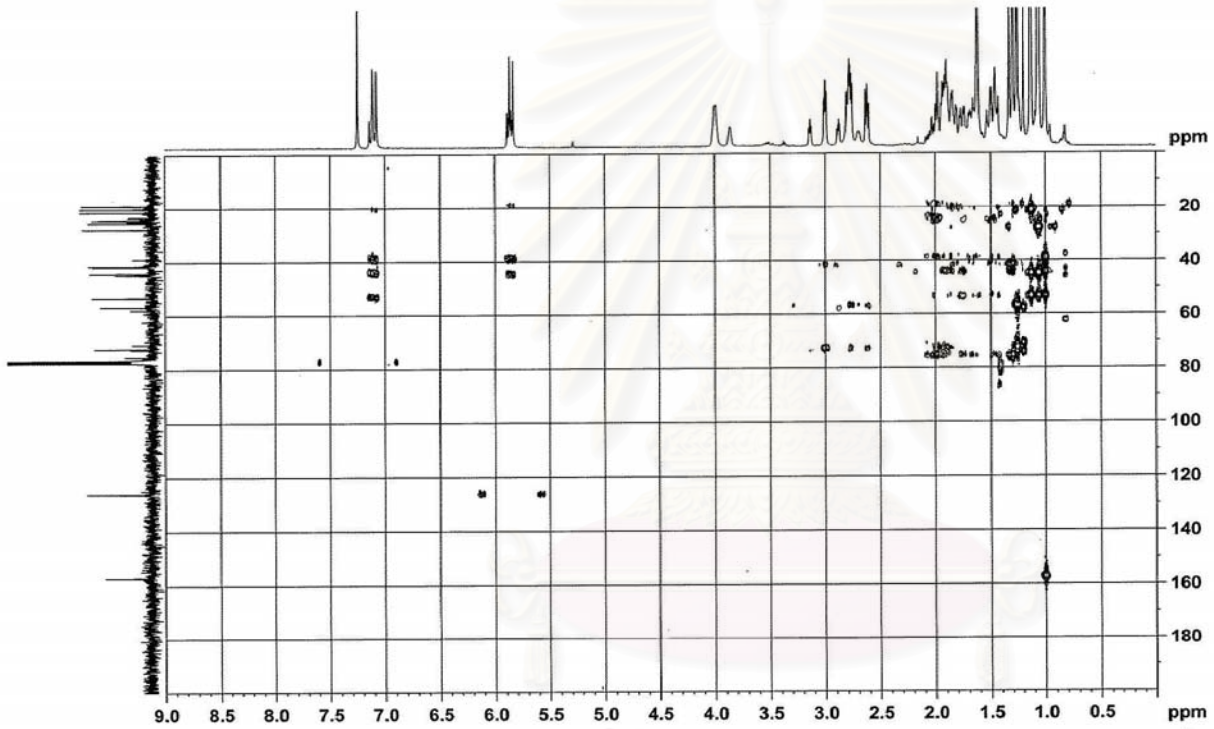

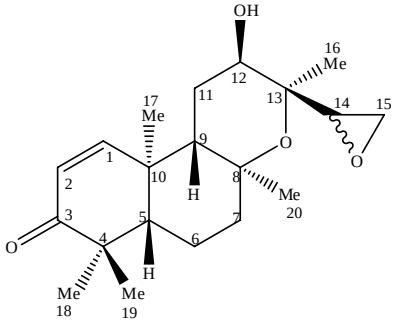

Compound **7**

Figure 18 The 300 MHz HMBC spectrum of compound **7** (in $CDCl_3$)

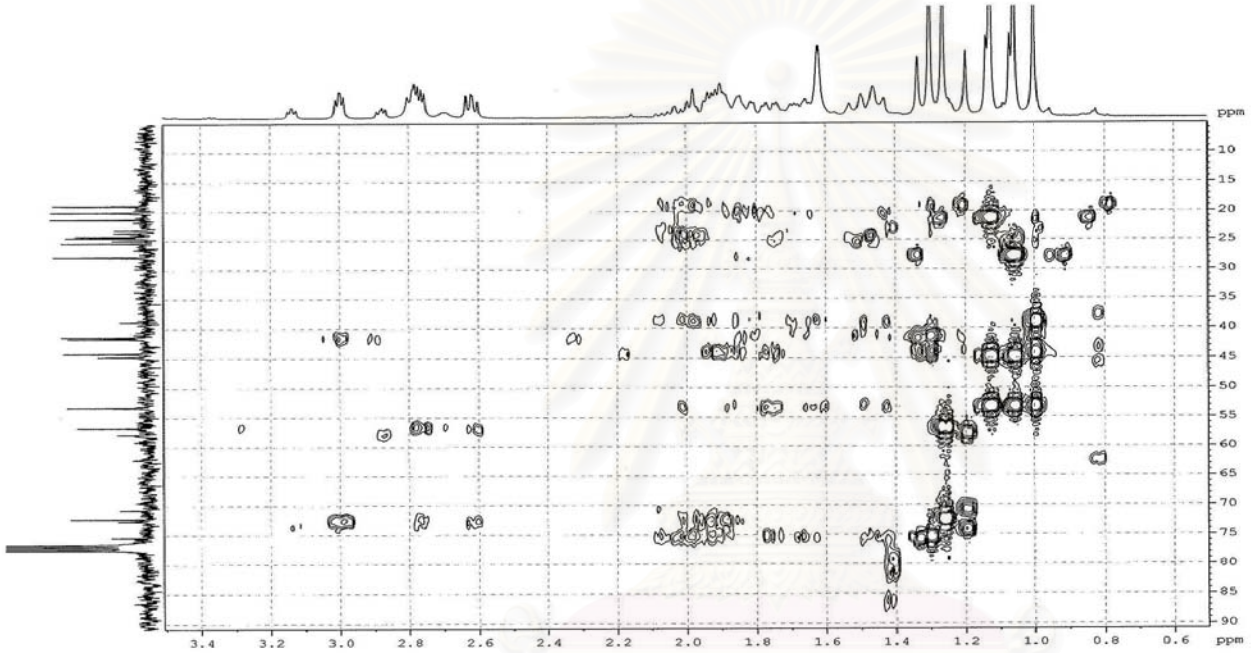

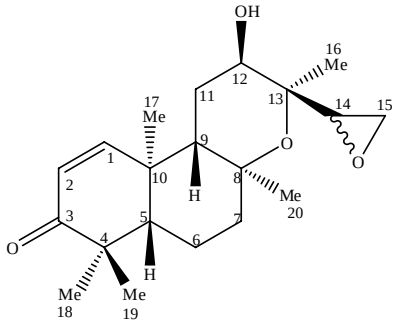

Compound **7**

Figure 18a The expanded 300 MHz HMBC spectrum of compound **7** (in $CDCl_3$)

(δ_H3.4-0.5 ppm, δ_C10 -90 ppm)

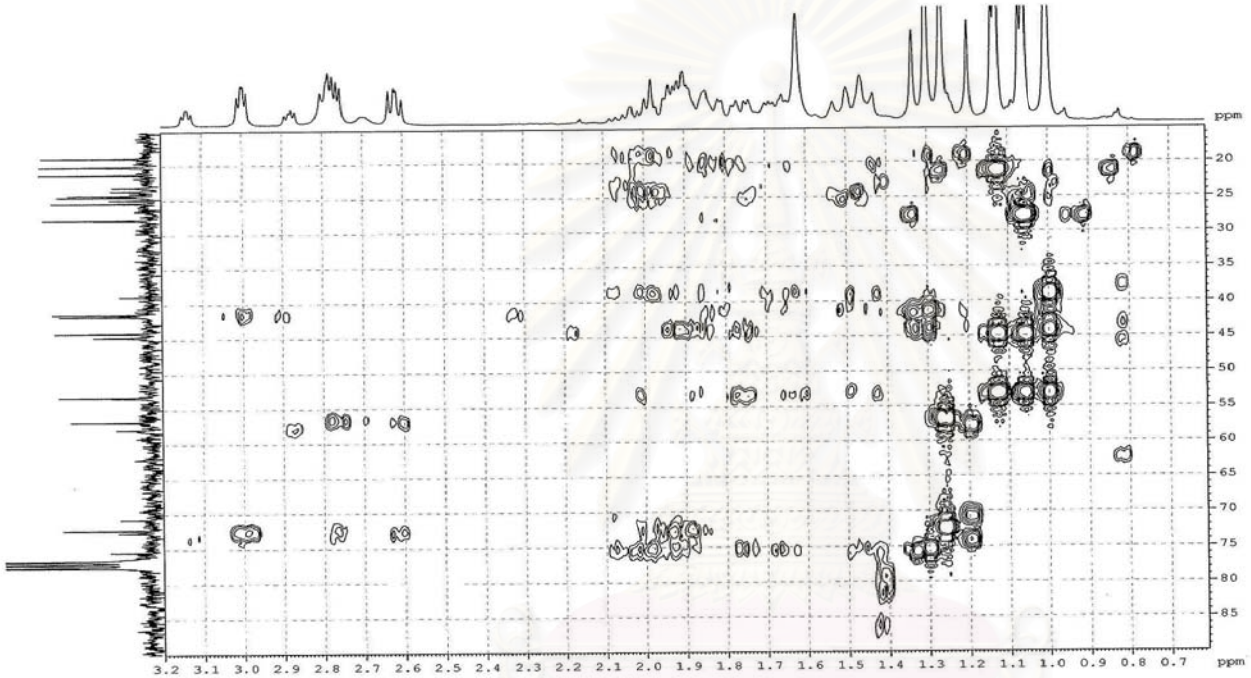

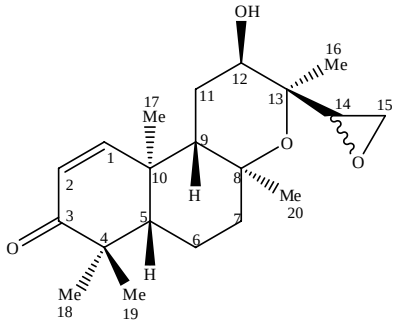

Compound **7**

Figure 18b The expanded 300 MHz HMBC spectrum of compound **7** (in $CDCl_3$)

(δ_H3.2-0.7 ppm, δ_C15 -90 ppm)

89

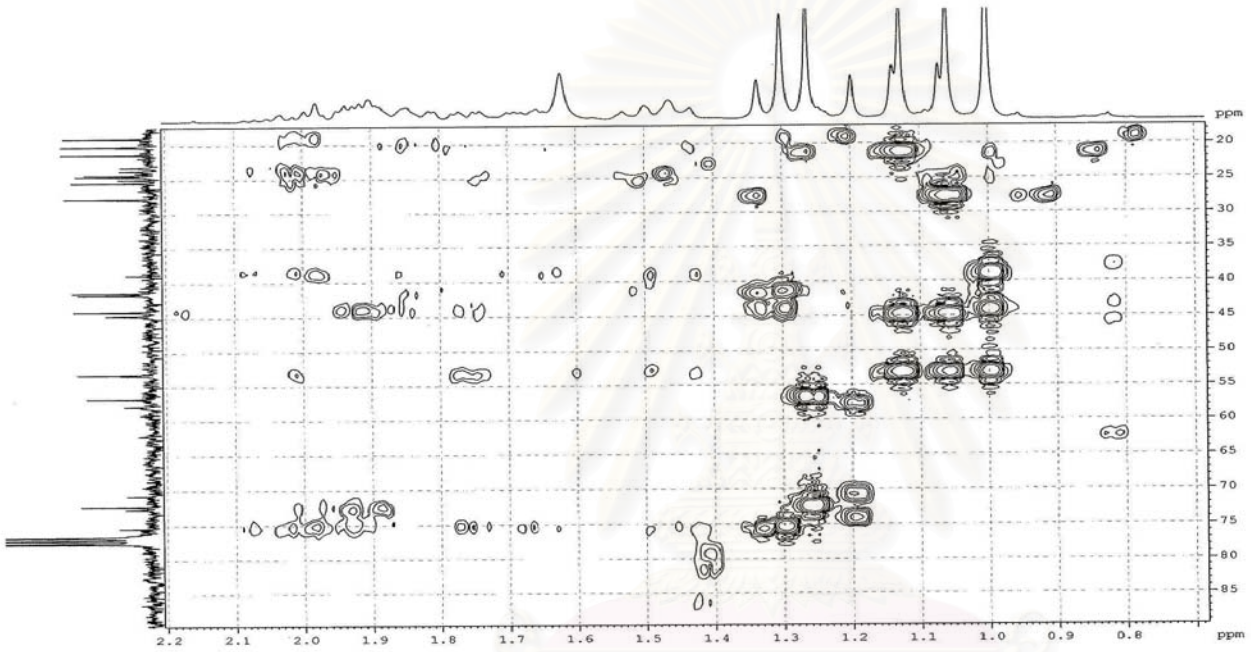

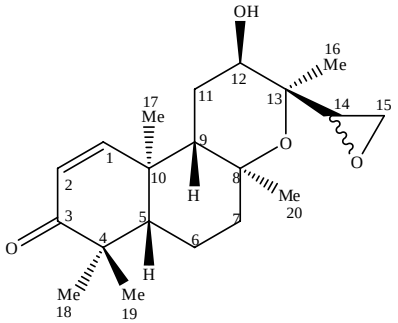

Compound **7**

Figure 18c The expand 300 MHz HMBC spectrum of compound **7** (in $CDCl_3$)

(δ_H2.2-0.7 ppm, δ_C15 -90 ppm)

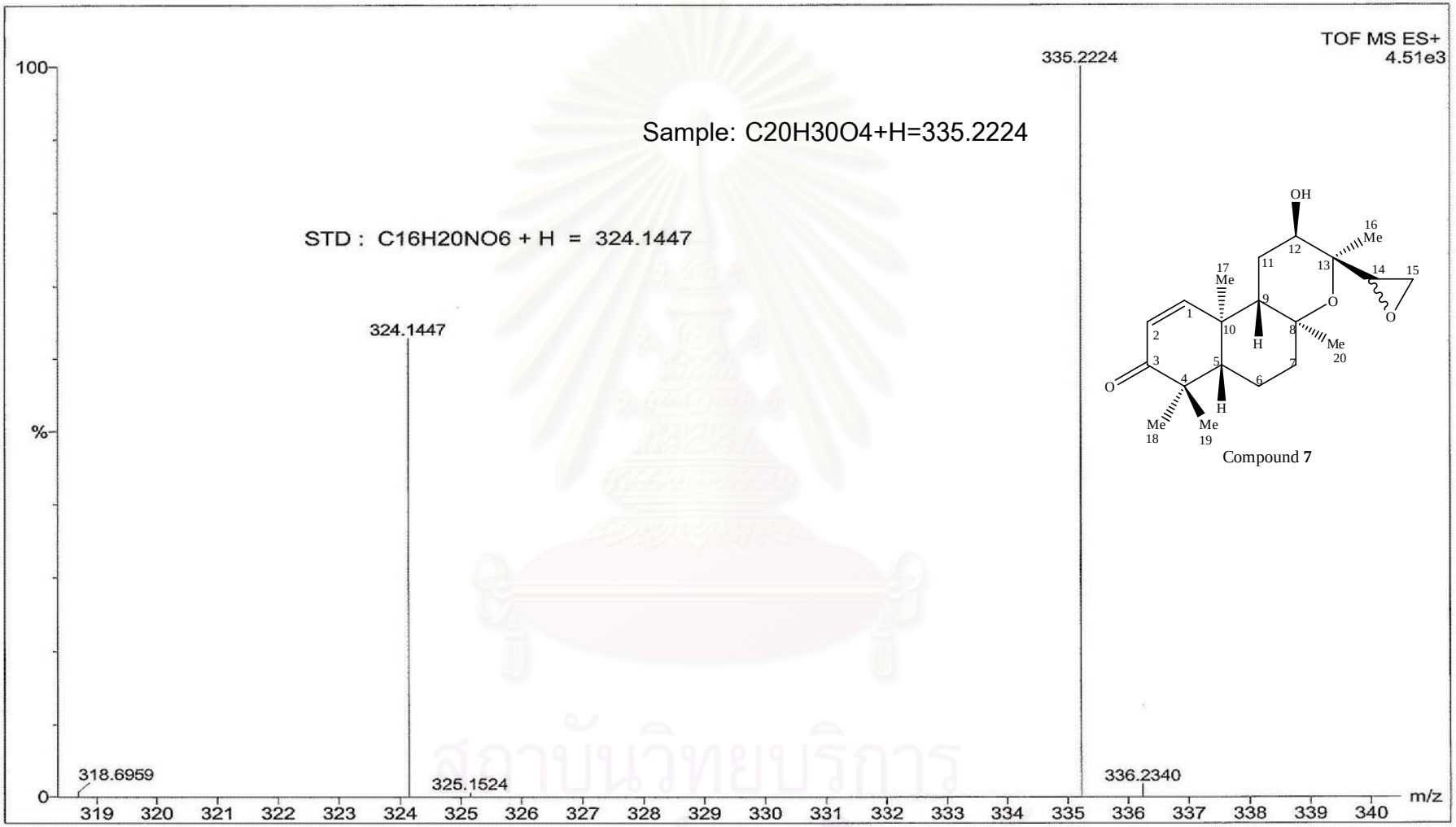

Compound **7**

Figure 19 The TOF-MS spectrum of compound **7**

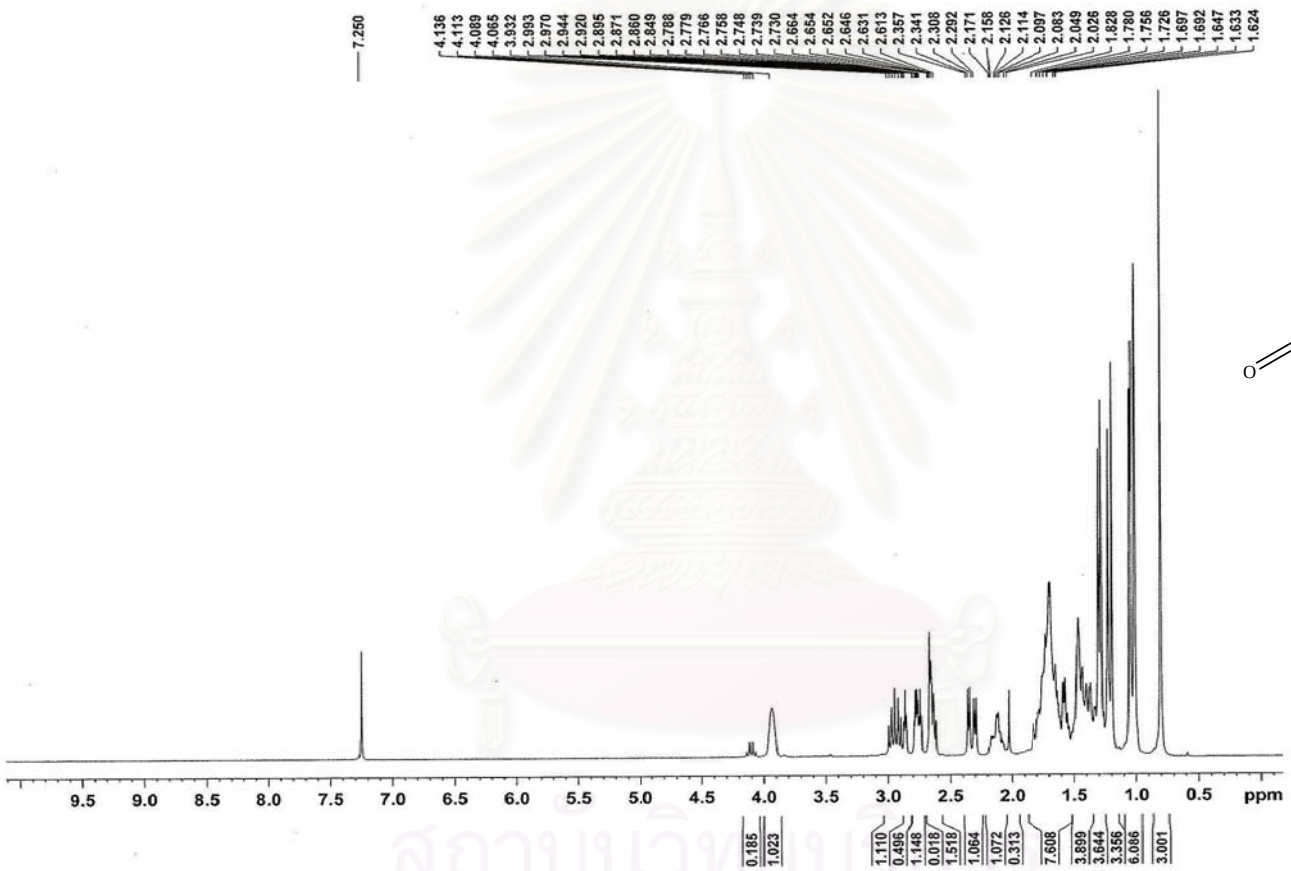

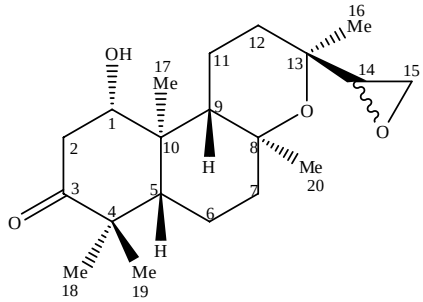

Compound **8**

Figure 20 The 300 MHz ^{1}H-NMR spectrum of compound **8** (in $CDCl_3$)

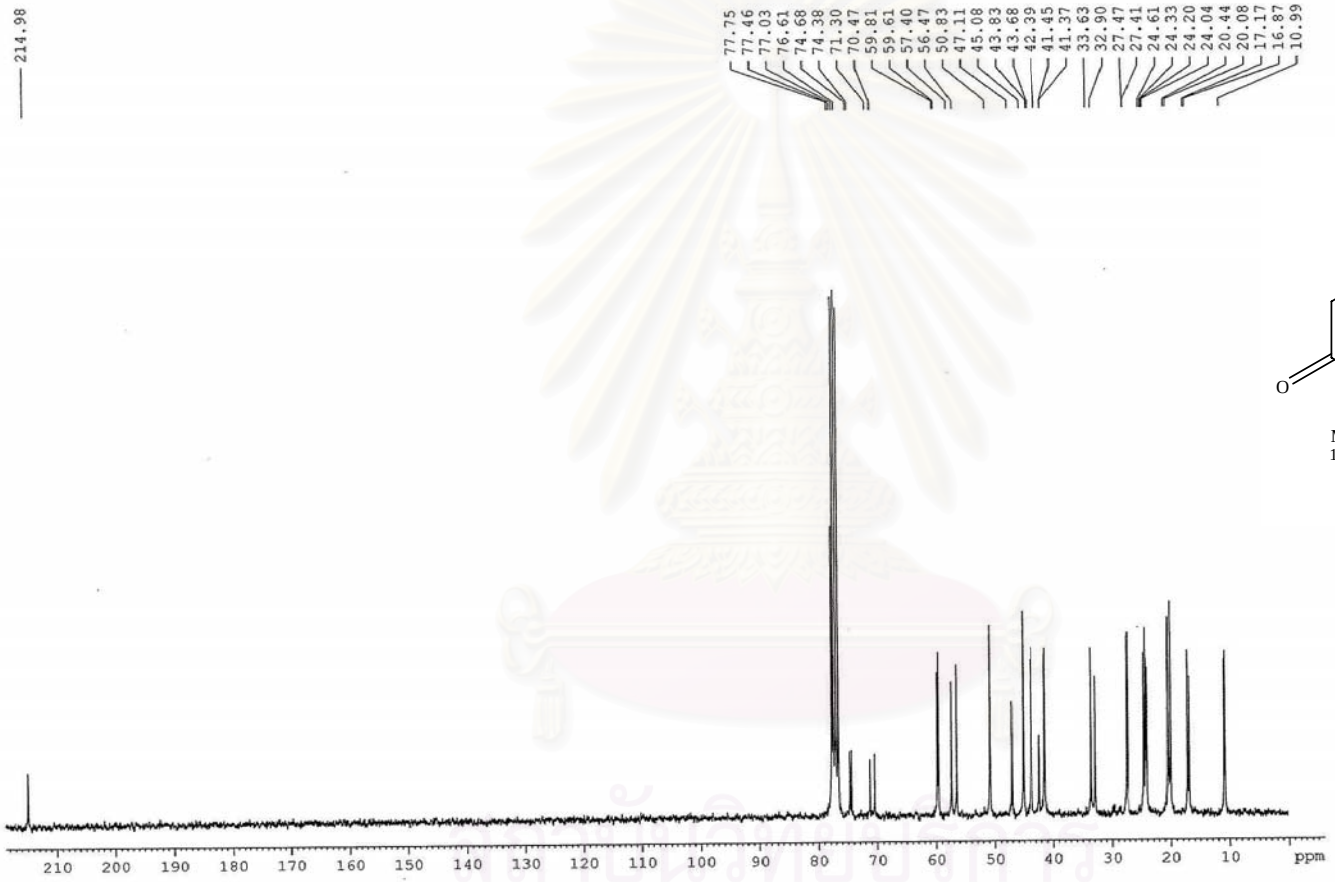

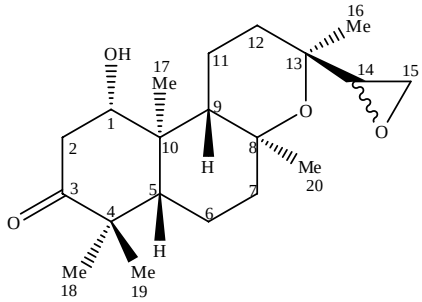

Compound **8**

Figure 21 The 75 MHz ^{13}C-NMR spectrum of compound **8** (in $CDCl_3$)

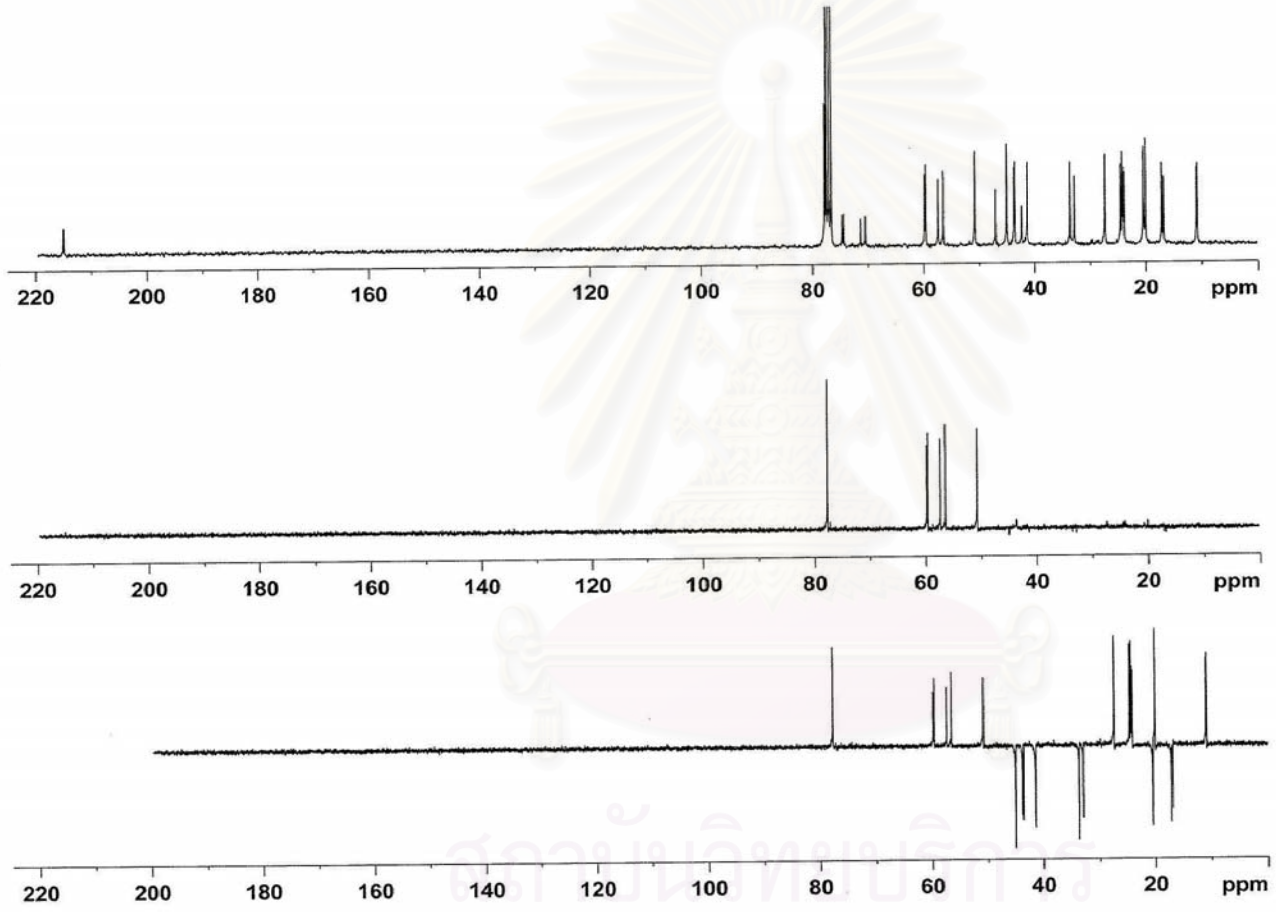

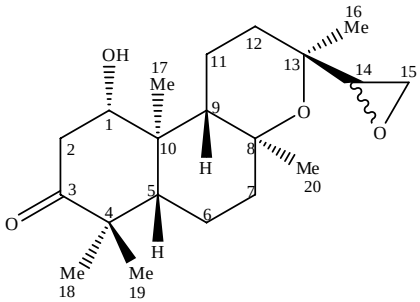

Compound **8**

Figure 22 The 75 MHz ^{13}C-NMR, DEPT-90 and DEPT-135 spectra of compound **8**

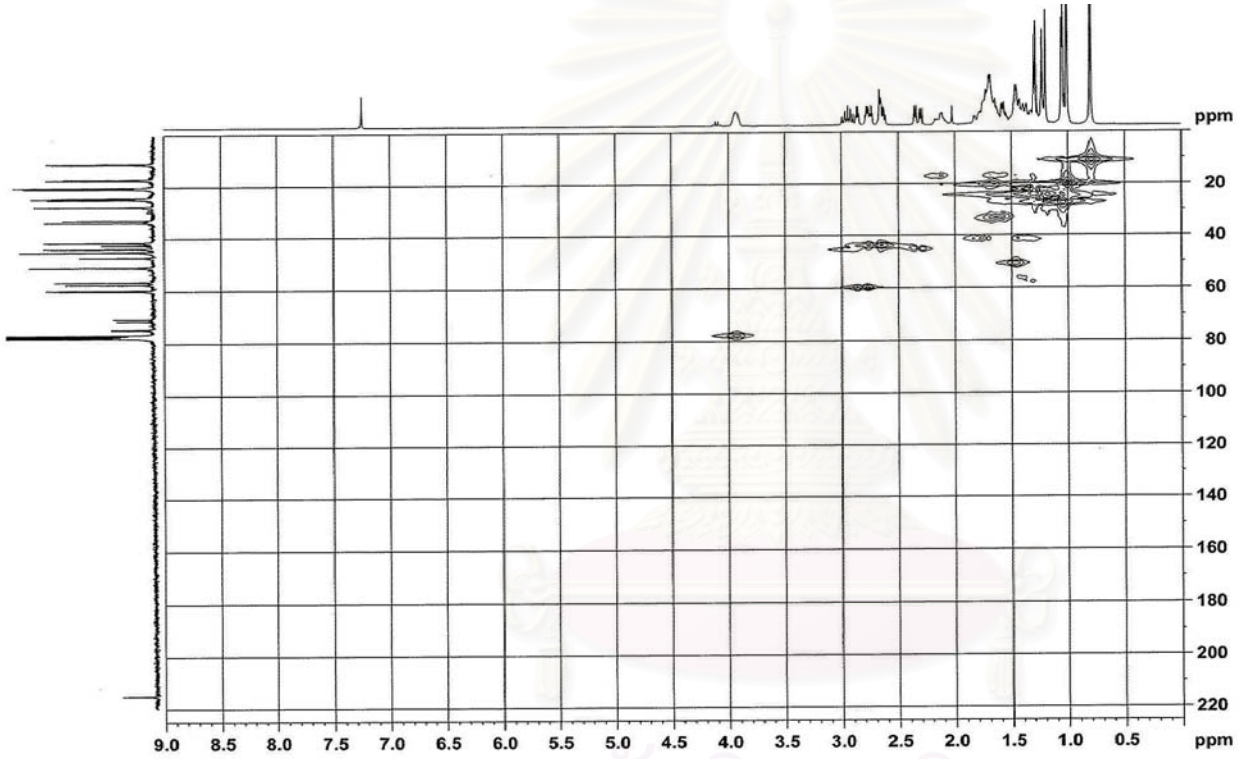

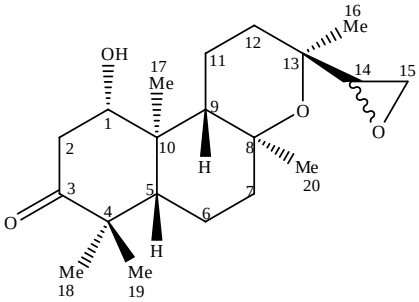

Compound **8**

Figure 23 The 300 MHz HMQC NMR spectrum of compound 8

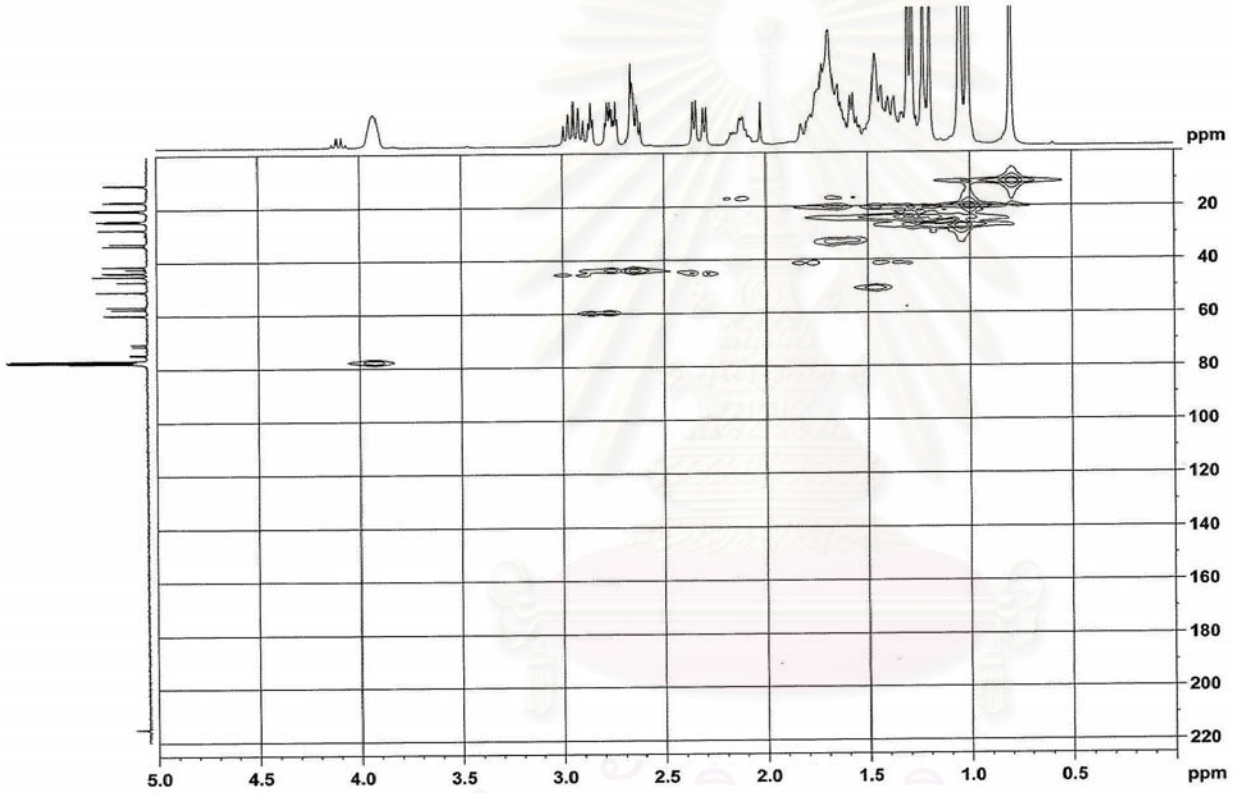

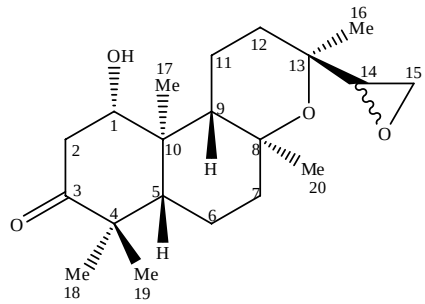

Compound **8**

Figure 23a The expanded 300 MHz HMQC NMR spectrum of compound **8**

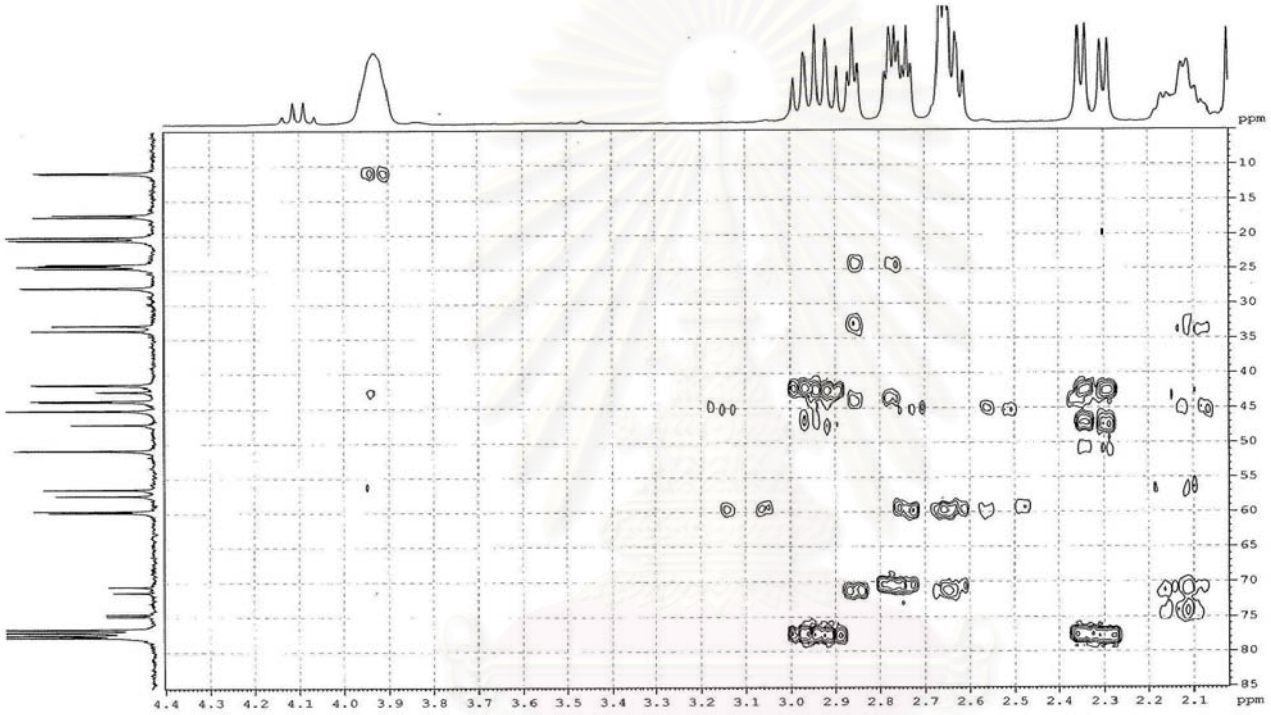

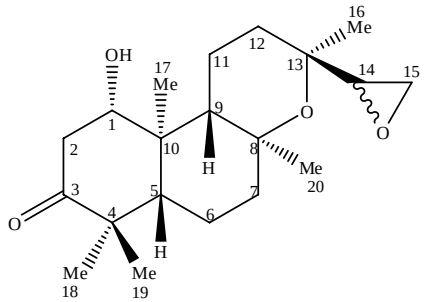

Compound **8**

Figure 24 The 300 MHz HMBC spectrum of compound **8** (in $CDCl_3$)

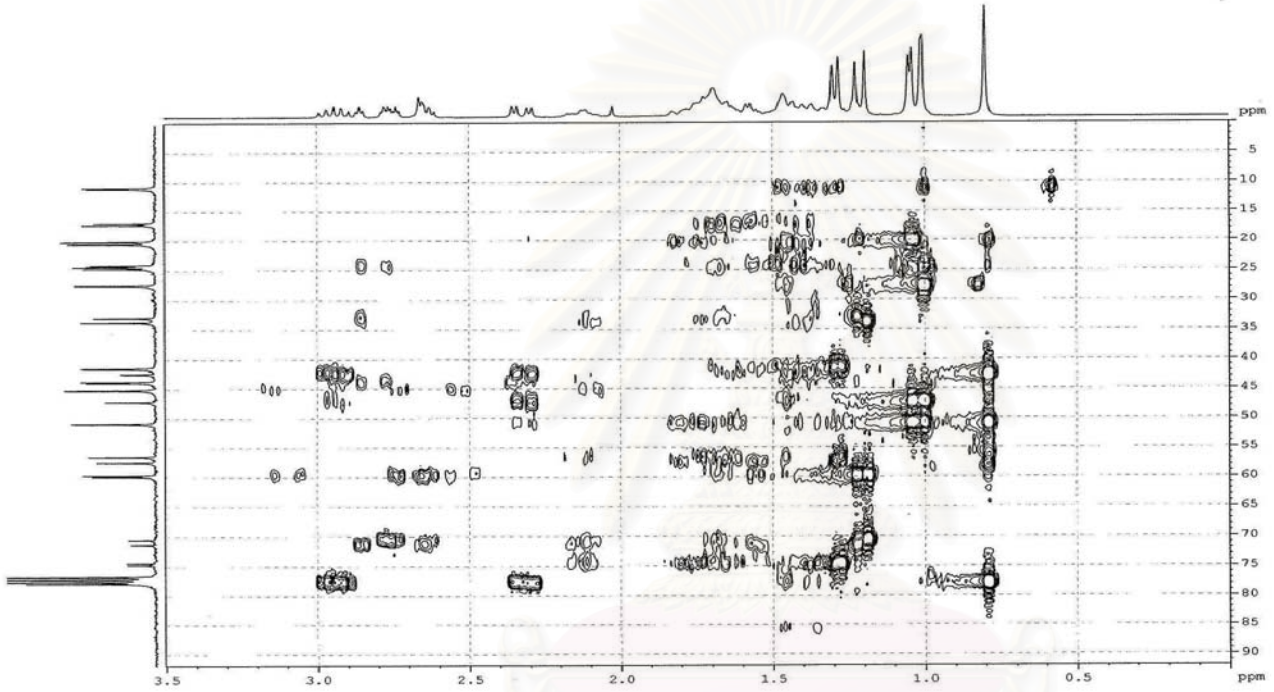

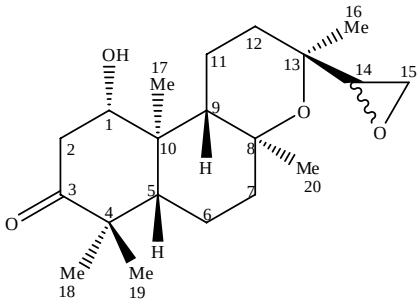

Compound **8**

Figure 24a The expanded 300 MHz HMBC spectrum of compound **8** (in $CDCl_3$)

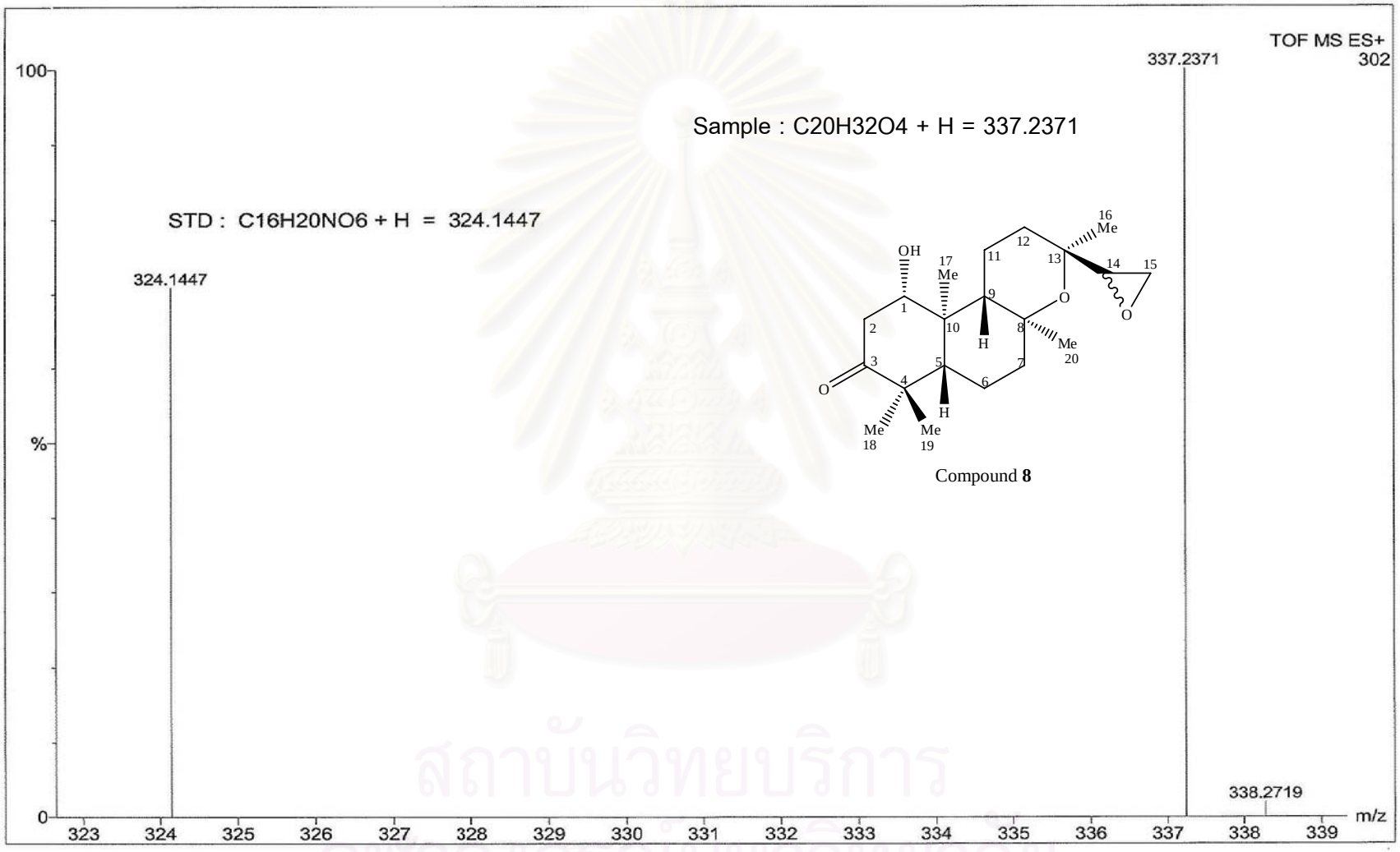

Compound **8**

Figure 25 The TOF-MS spectrum of compound **8**

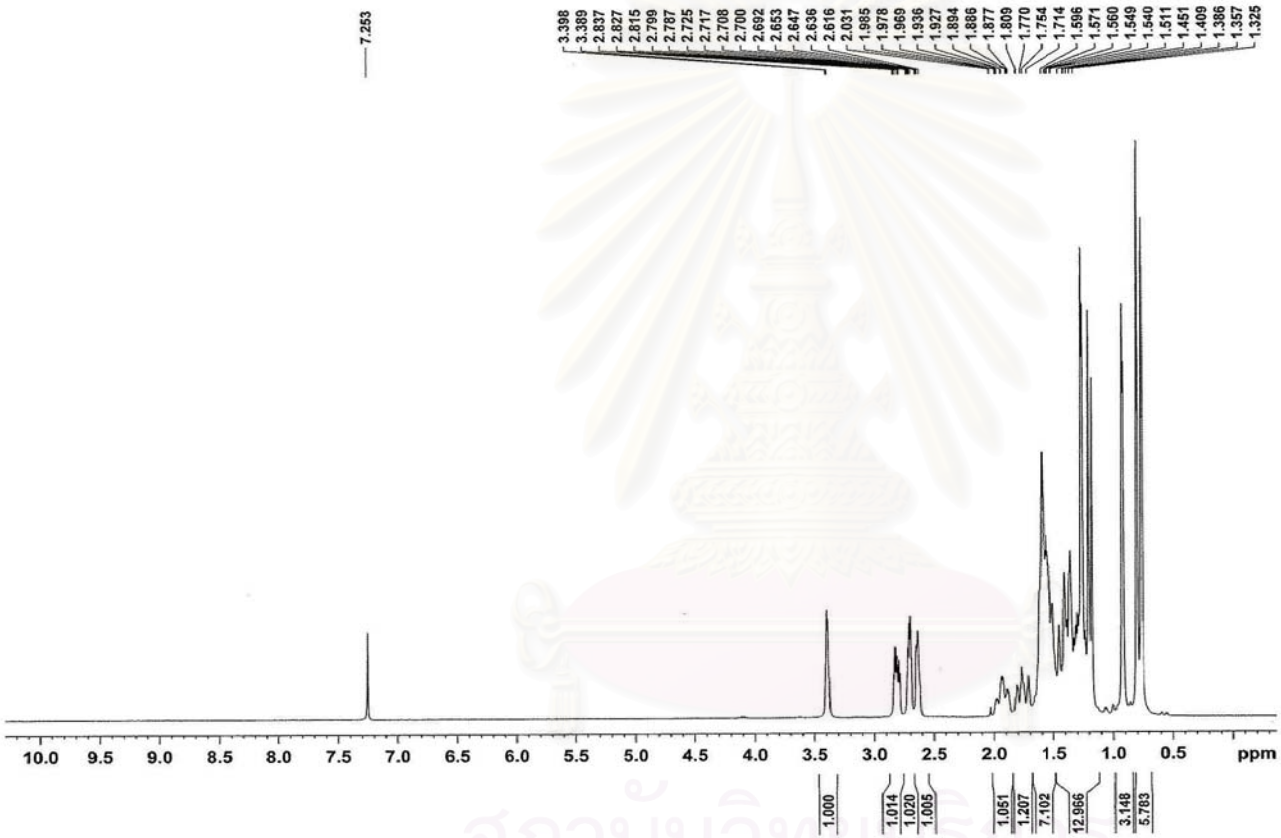

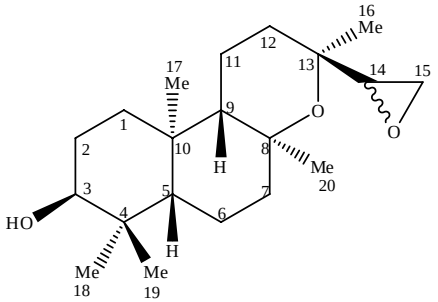

Compound **9**

Figure 26 The 300 MHz ^{1}H-NMR spectrum of compound **9** (in $CDCl_3$)

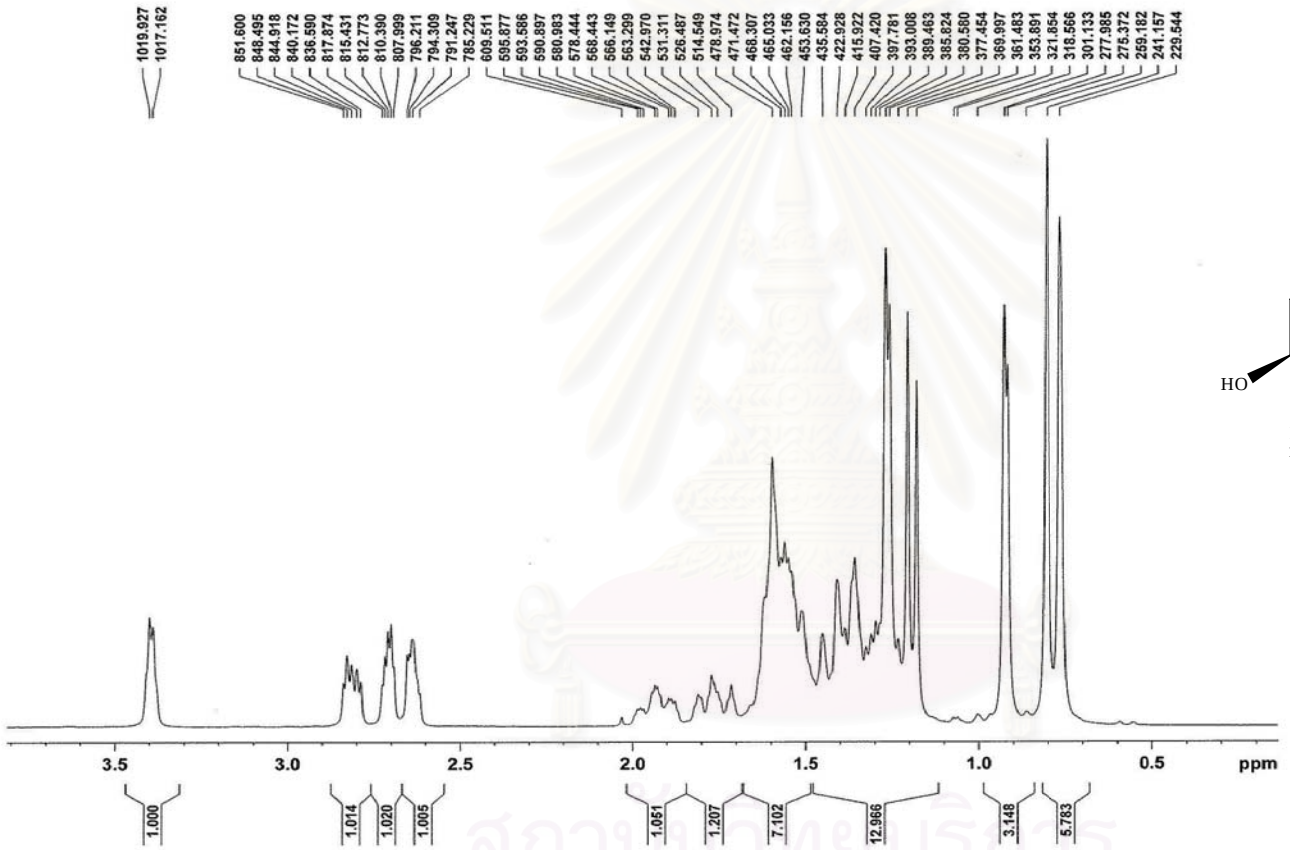

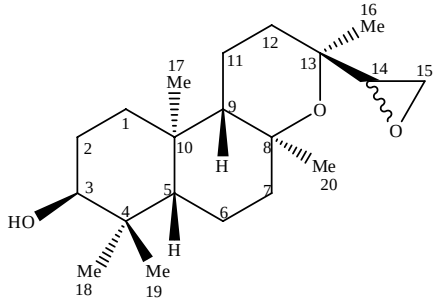

Compound **9**

Figure 26a The expanded 300 MHz ^{1}H-NMR spectrum of compound **9** (in $CDCl_3$)

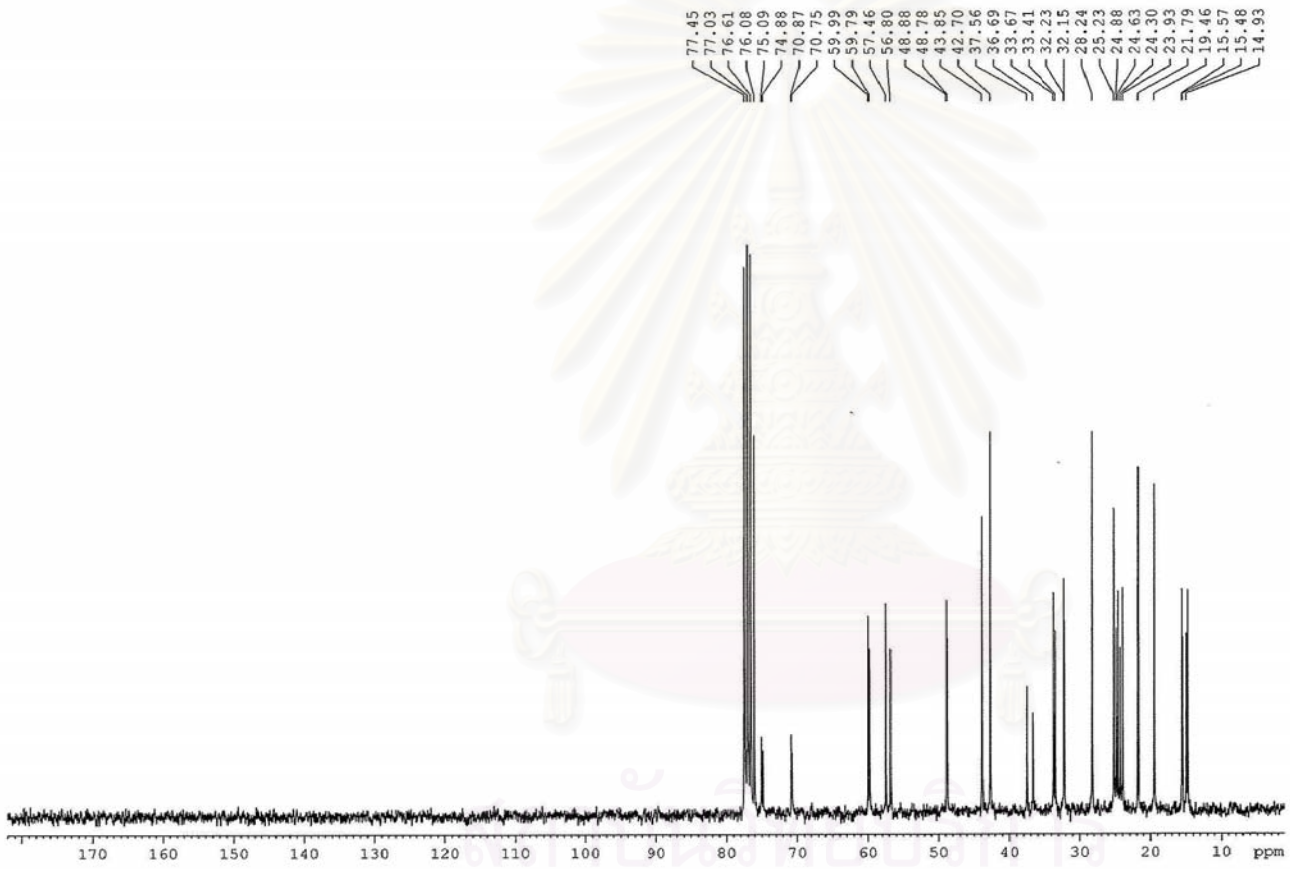

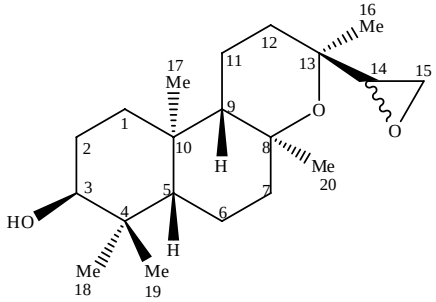

Compound **9**

Figure 26a The 75 MHz ^{13}C-NMR spectrum of compound **9** (in $CDCl_3$)

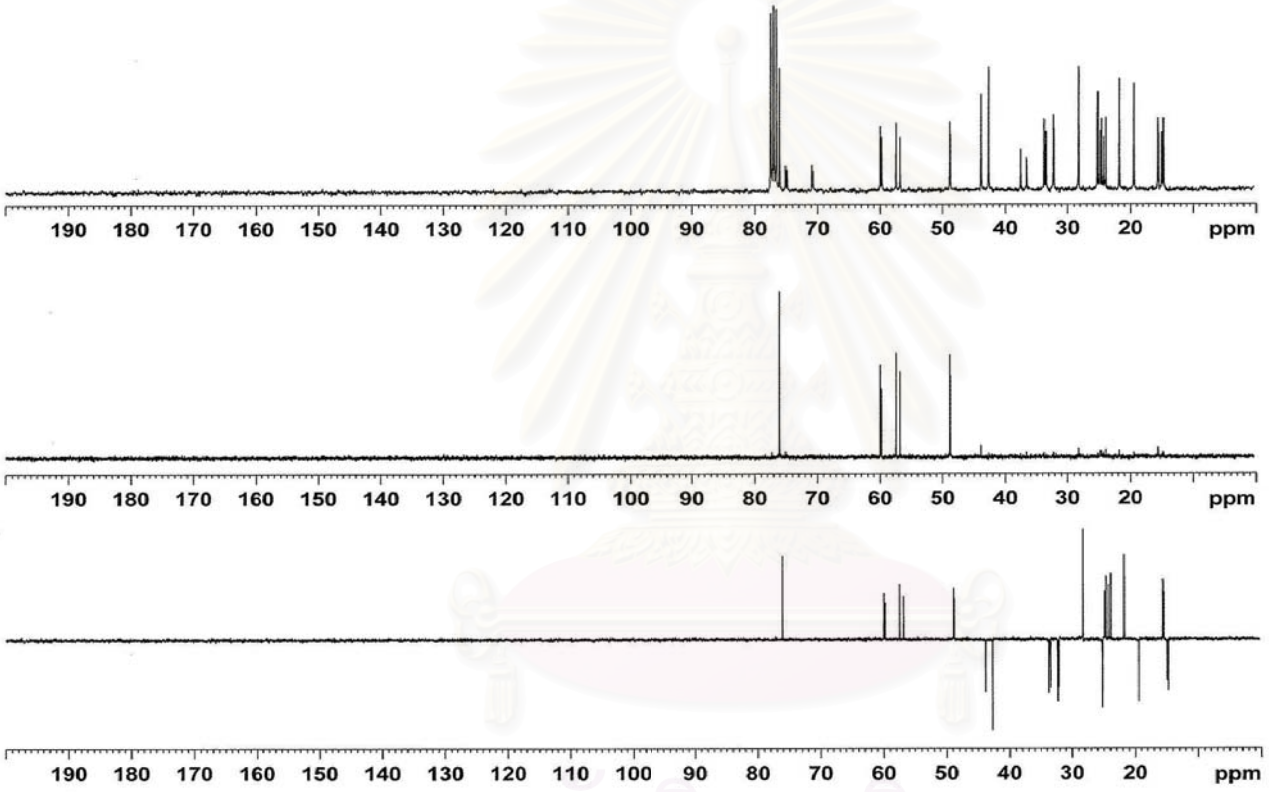

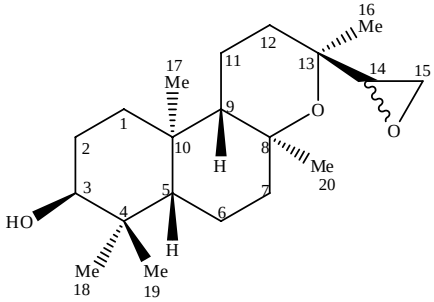

Compound **9**

Figure 28 The 75 MHz ^{13}C-NMR, DEPT-90 and DEPT-135 spectra of compound **9**

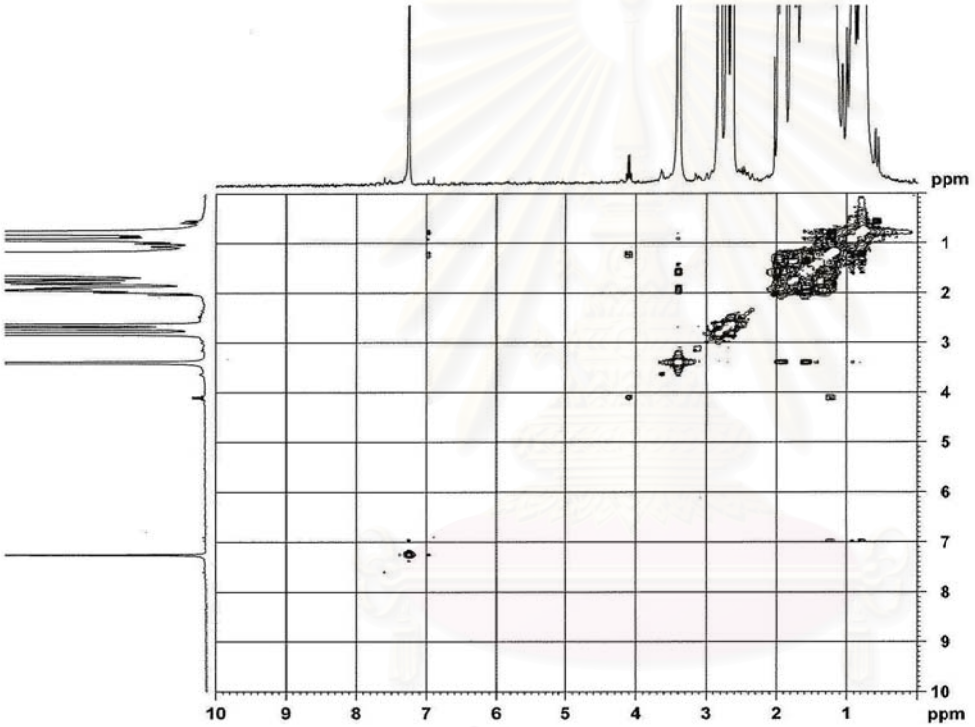

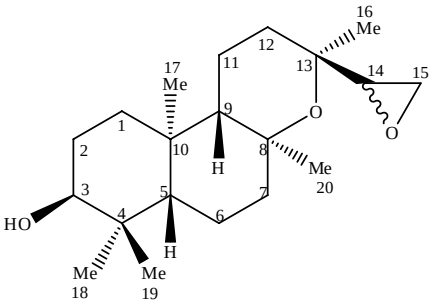

Compound **9**

Figure 29 The 300 MHz ^{1}H-^{1}H COSY spectrum of compound **9** (in $CDCl_3$)

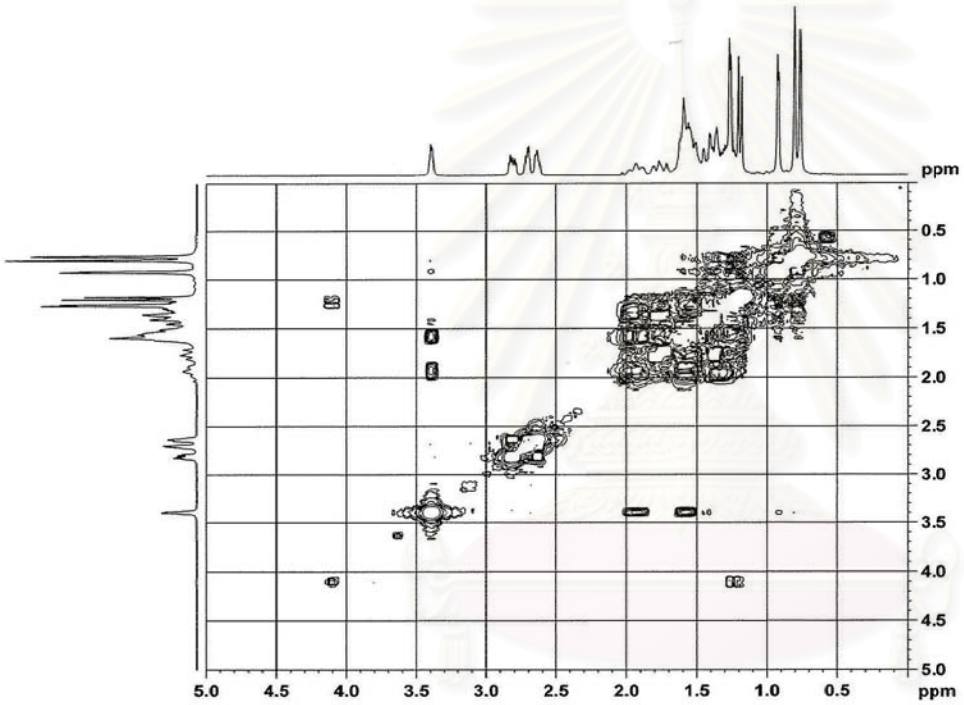

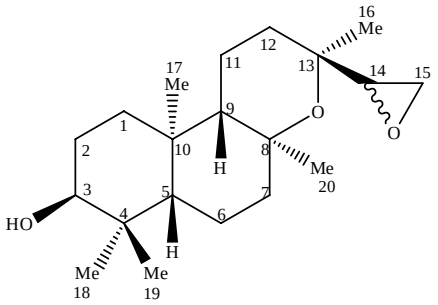

Compound **9**

Figure 29a The expanded 300 MHz ^{1}H-^{1}H COSY spectrum of compound **9** (in $CDCl_3$)

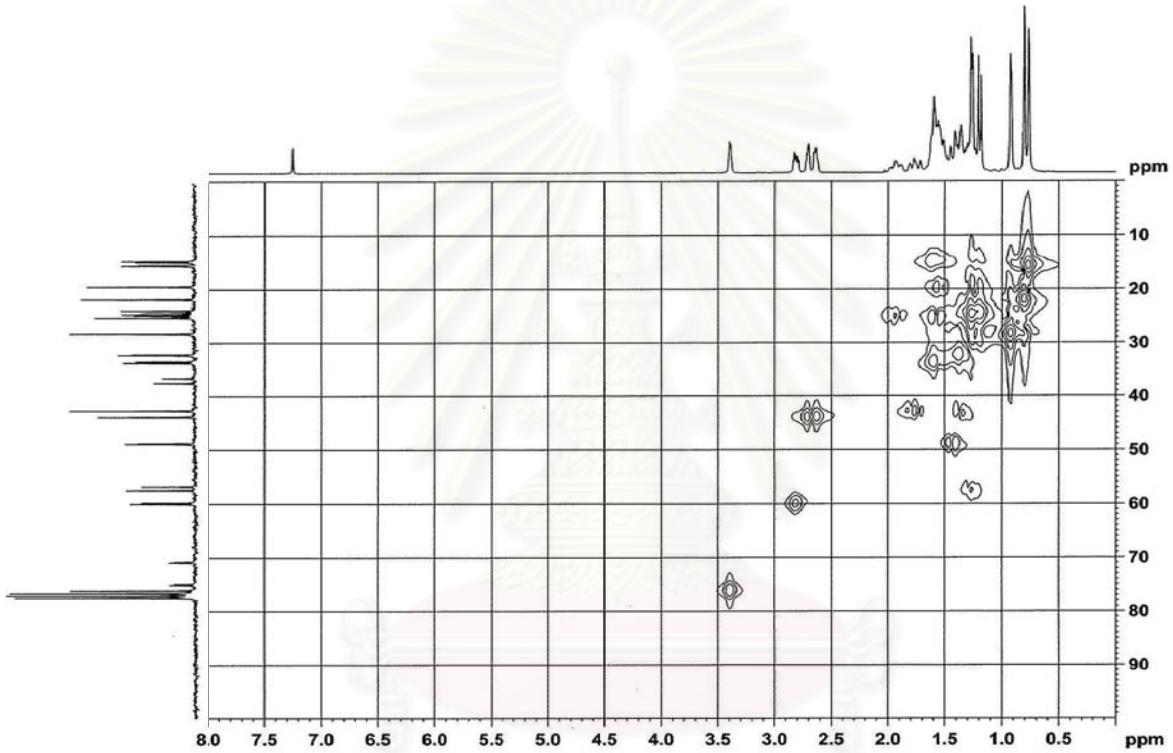

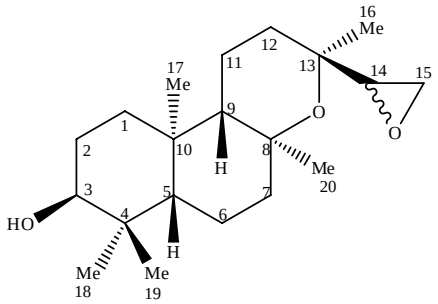

Compound **9**

Figure 30 The 300 MHz HMQC spectrum of compound **9** (in $CDCl_3$)

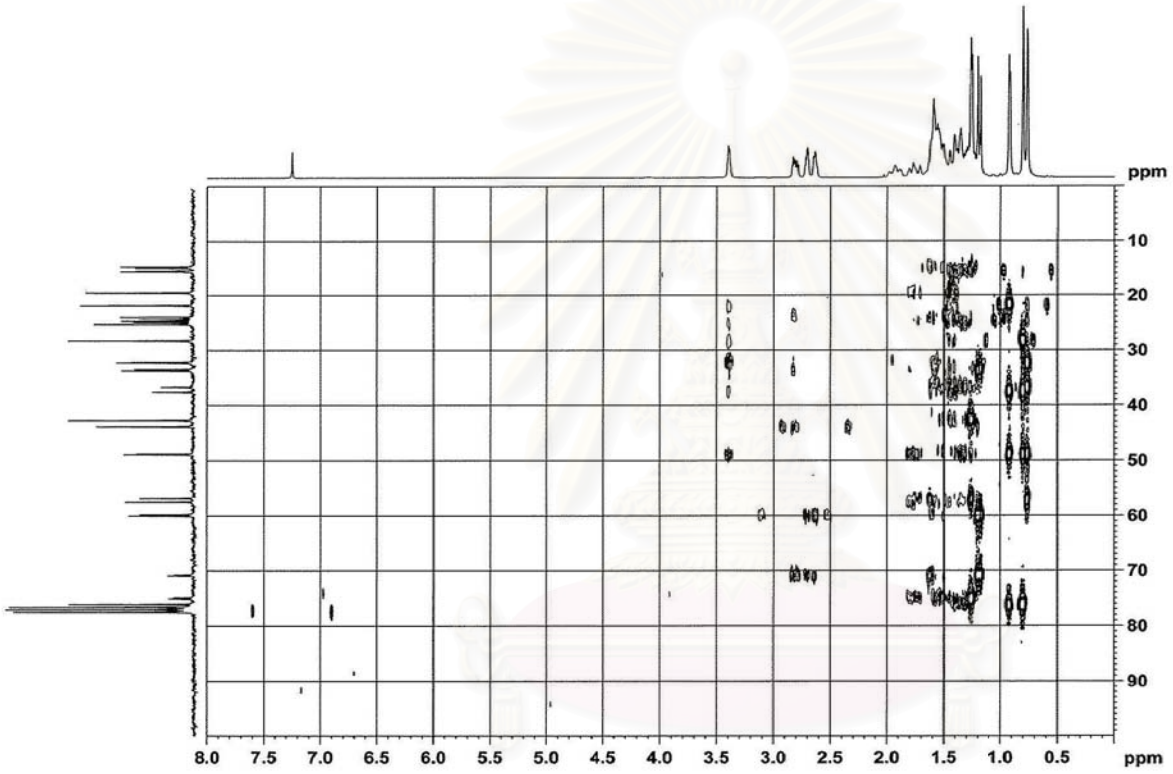

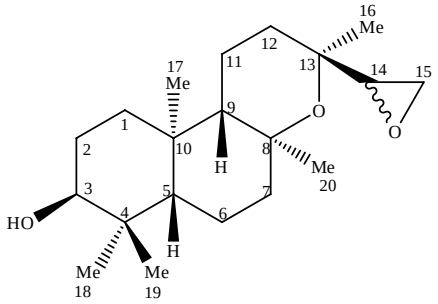

Compound **9**

Figure 31 The 300 MHz HMBC spectrum of compound 9 (in $CDCl_3$)

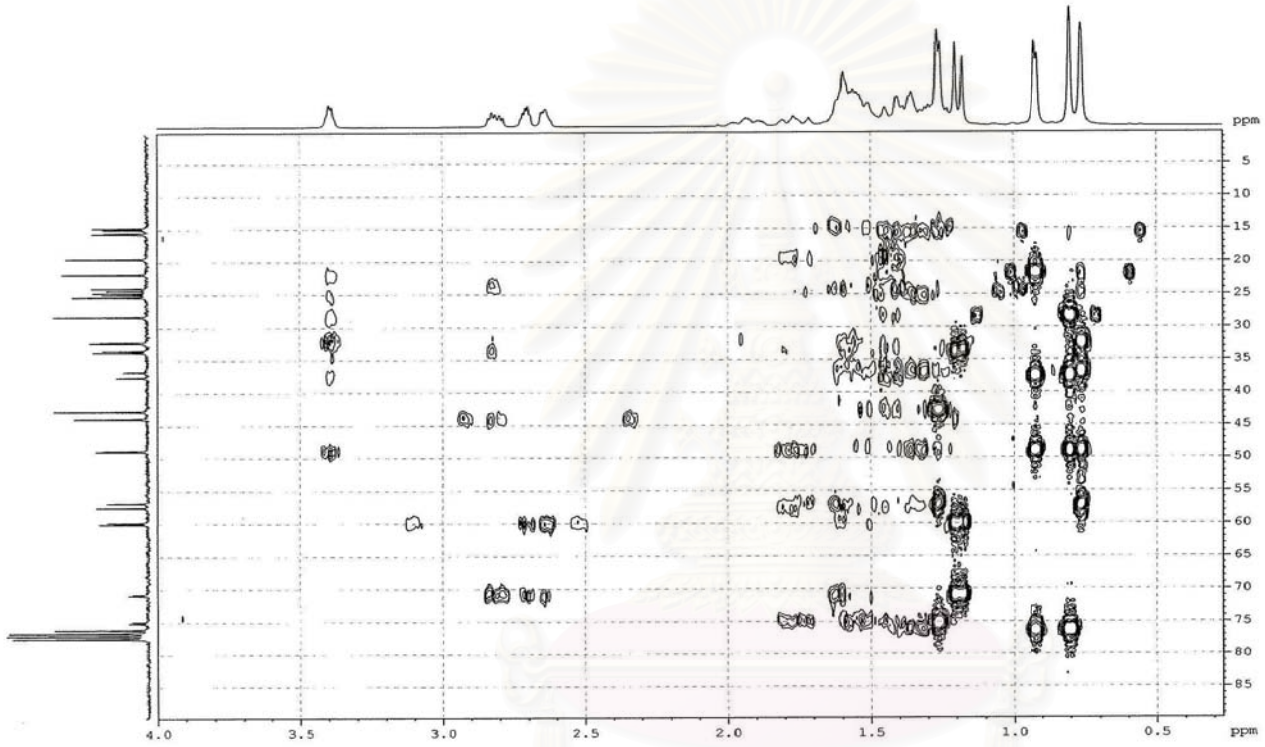

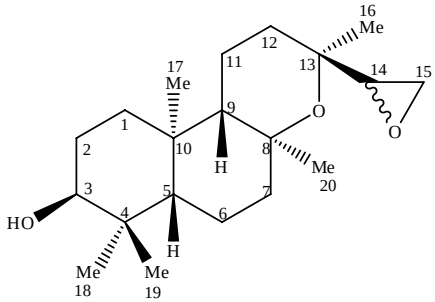

Compound **9**

Figure 31a The 300 MHz HMBC spectrum of compound 9 (in $CDCl_3$)

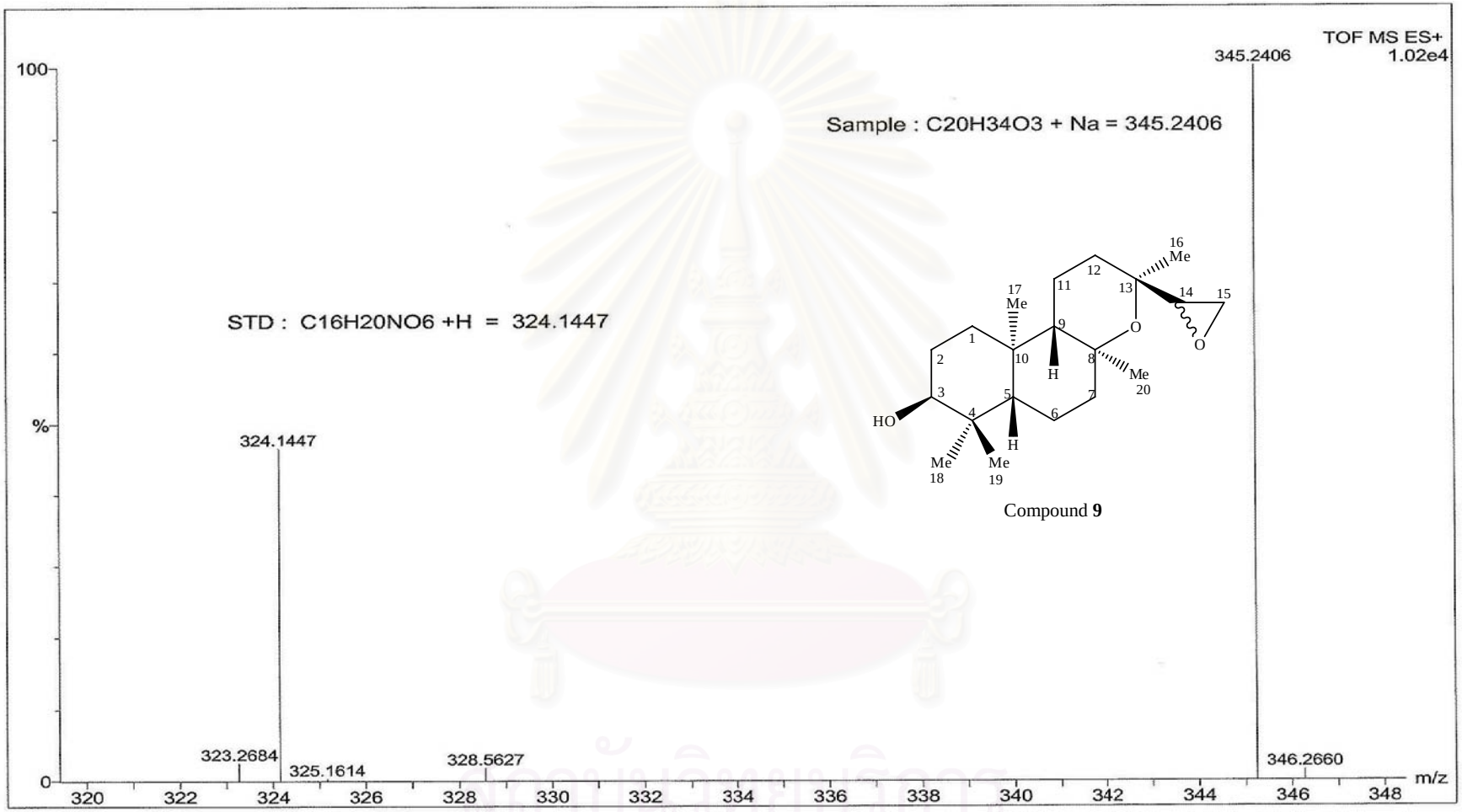

Compound **9**

Figure 32 The TOF-MS spectrum of compound 9

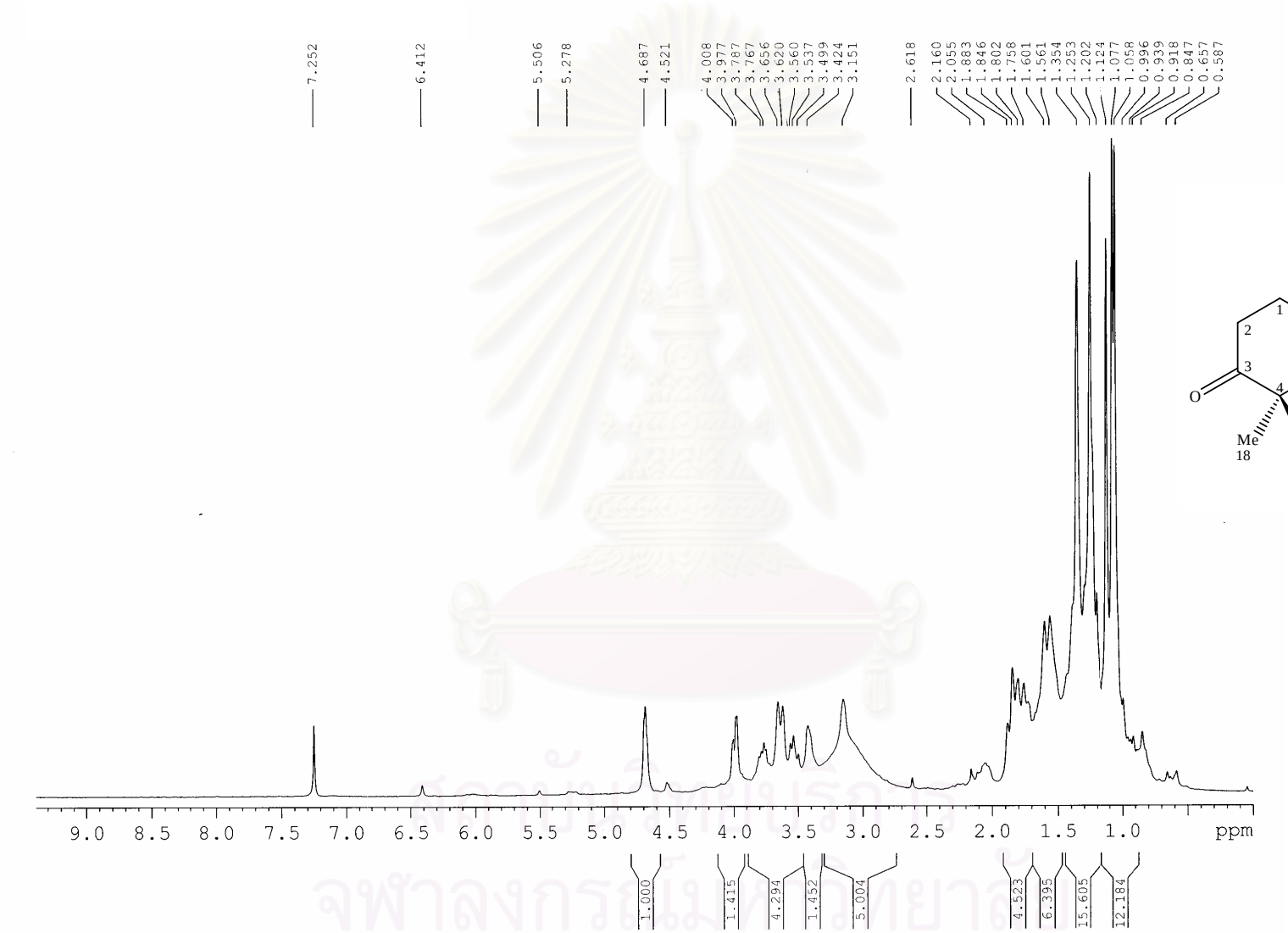

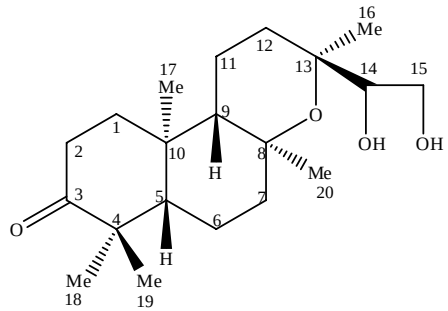

Compound **10**

Figure 33 The 300 MHz ^{1}H-NMR spectrum of compound **10**(in $CDCl_3$)

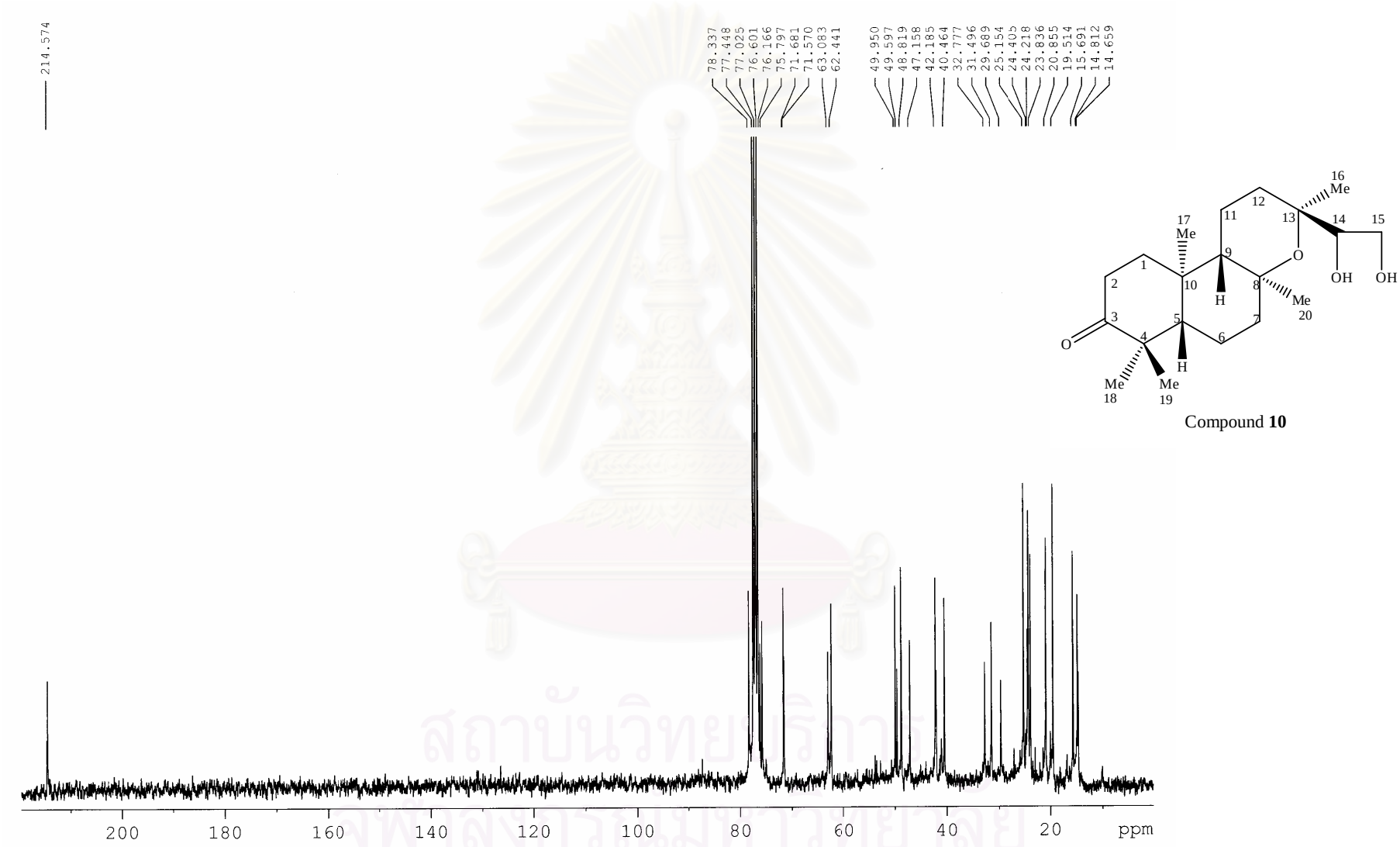

Compound **10**

Figure 34 The 75 MHz ^{13}C-NMR spectrum of compound **10**(in $CDCl_3$)

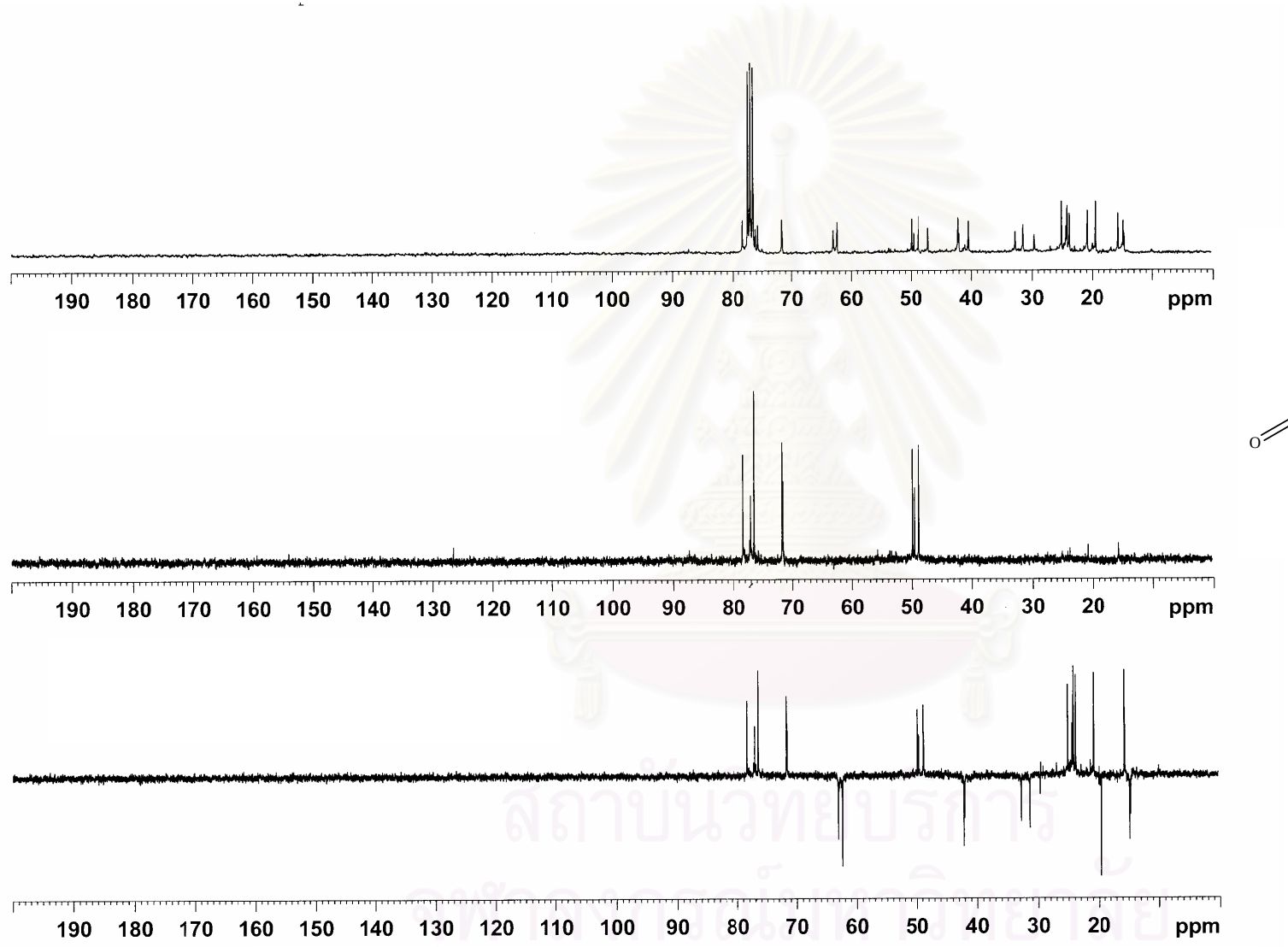

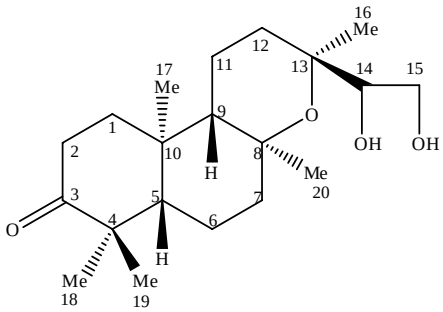

Compound **10**

Figure 35 The 75 MHz ^{13}C-NMR, DEPT-90 and DEPT-135 spectra of compound **10**

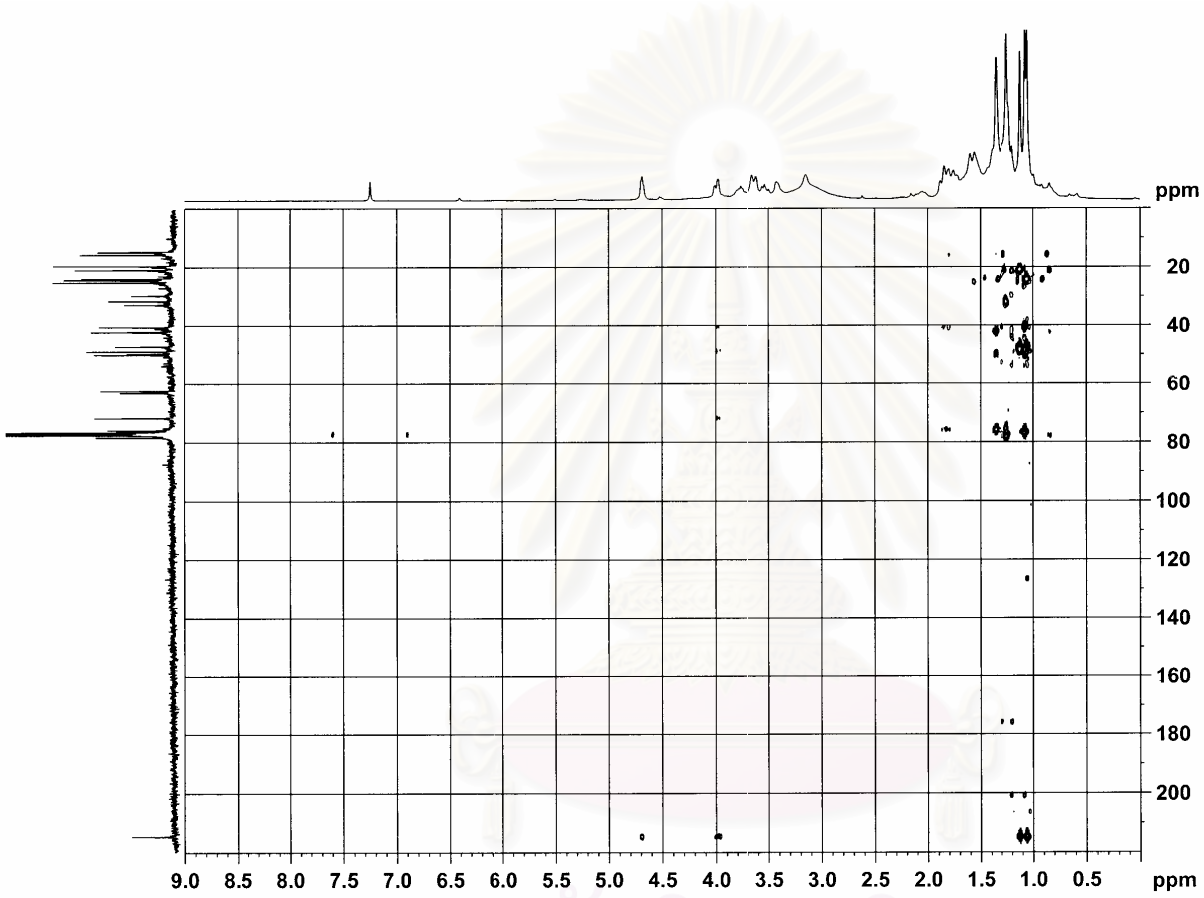

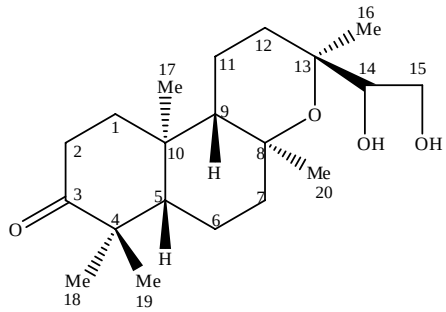

Compound **10**

Figure 36 The 300 MHz HMBC spectrum of compound **10** (in $CDCl_3$)

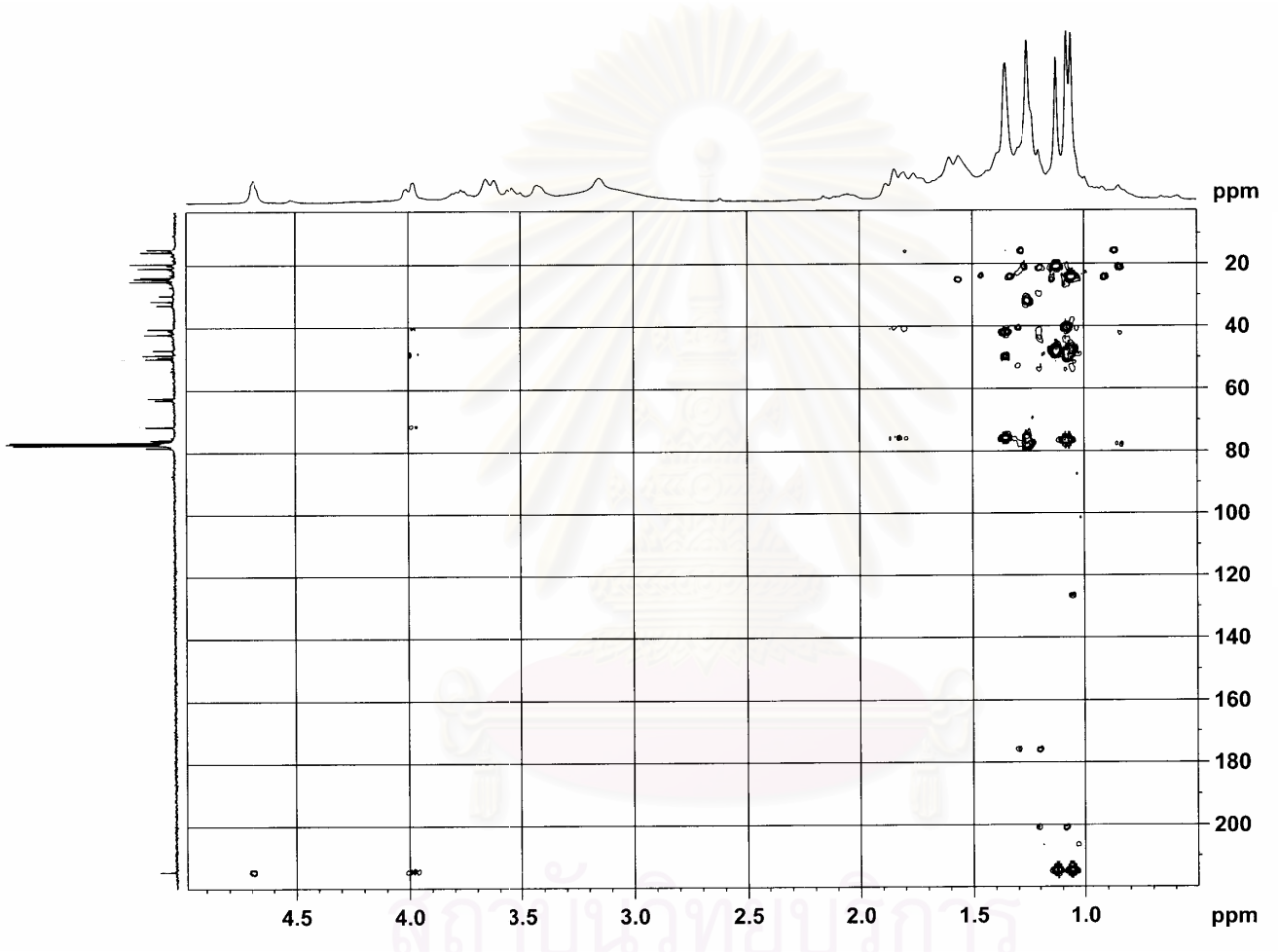

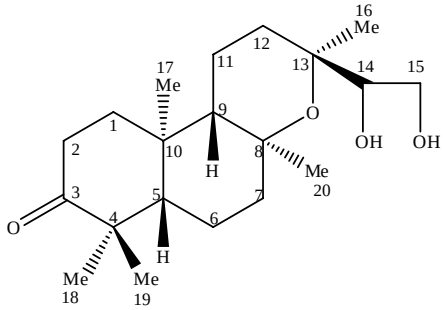

Compound **10**

Figure 36a The expand 300 MHz HMBC spectrum of compound **10** (in $CDCl_3$)

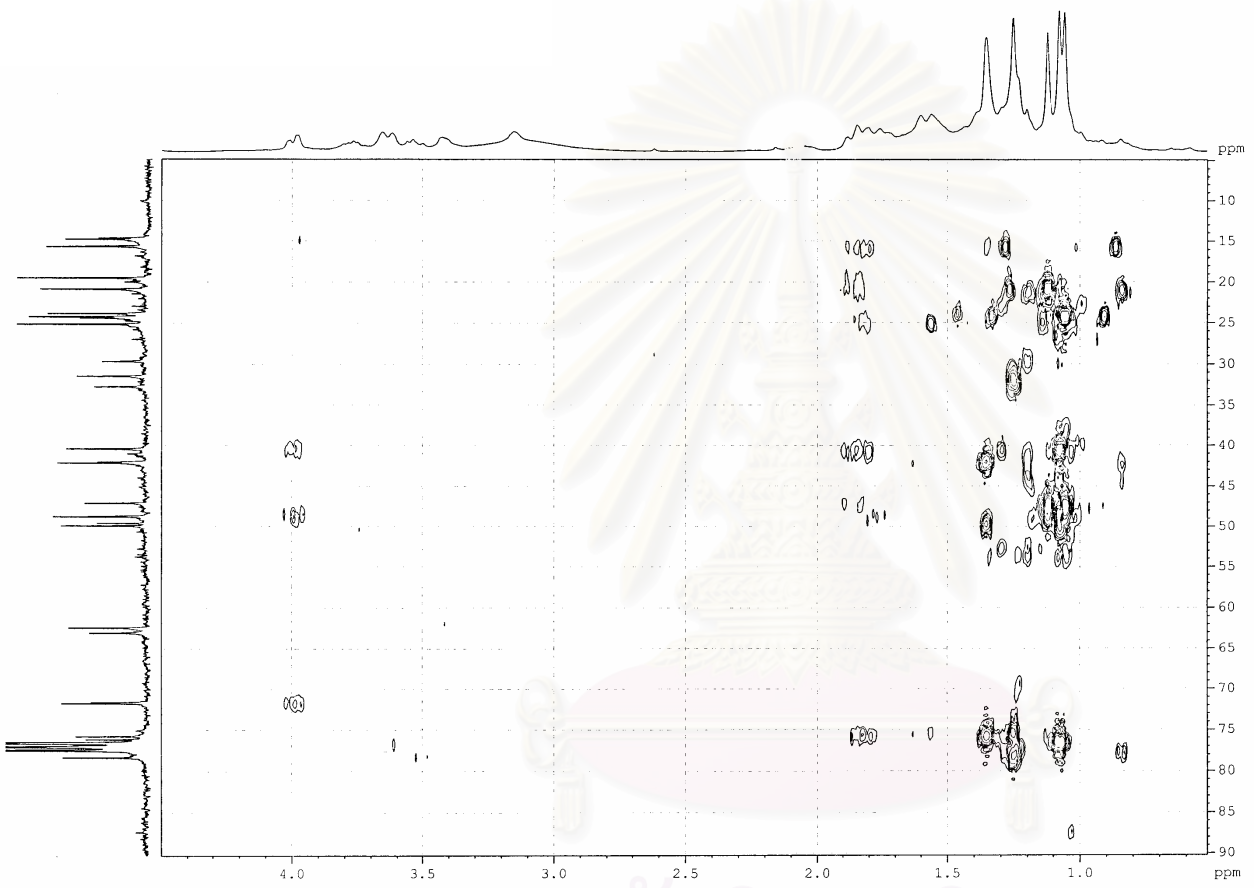

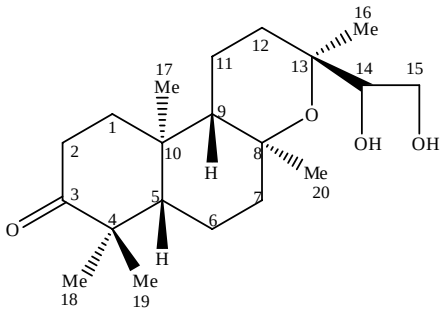

Compound **10**

Figure 36b The 300 MHz HMBC spectrum of compound **10** (in $CDCl_3$)

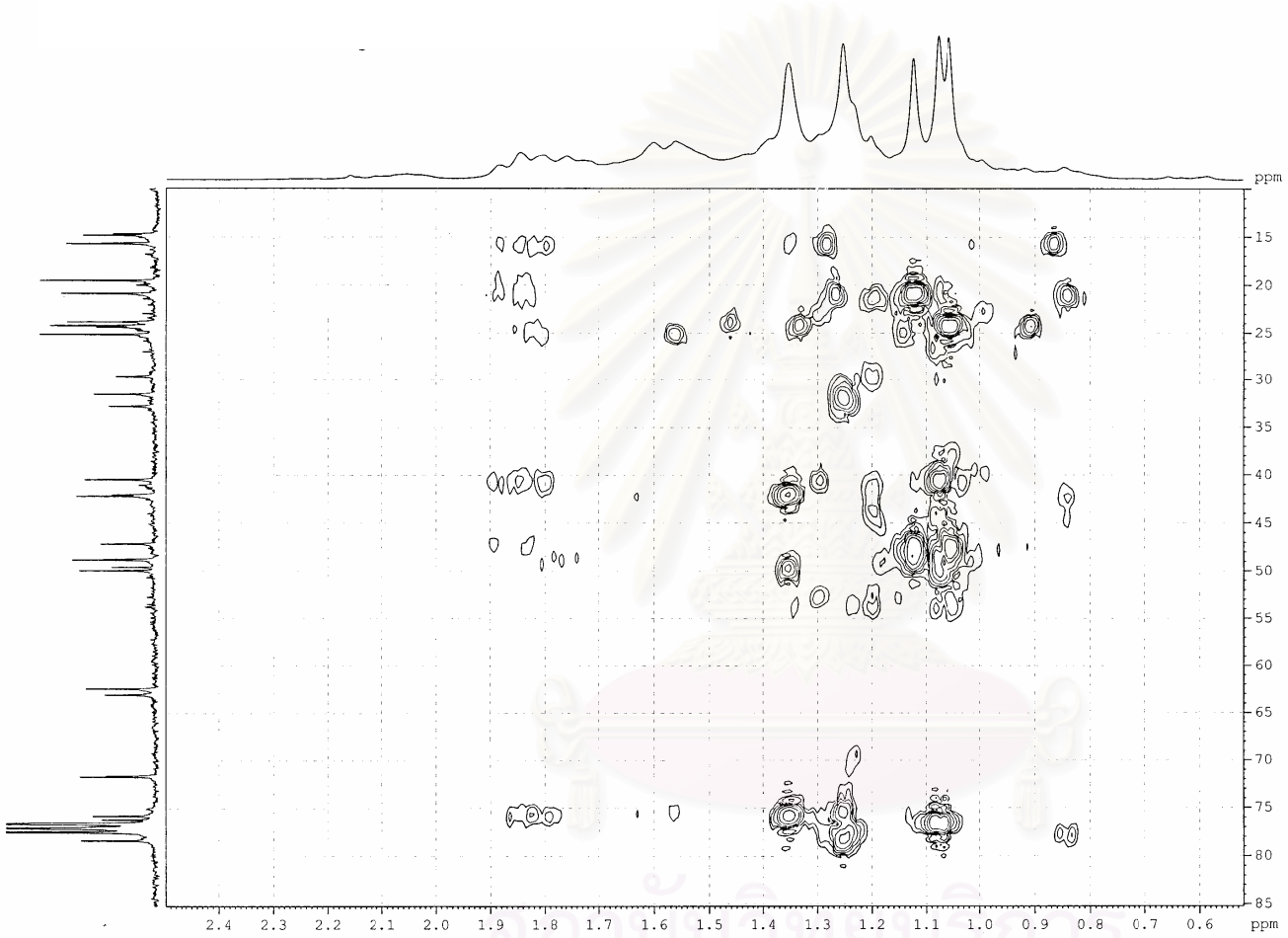

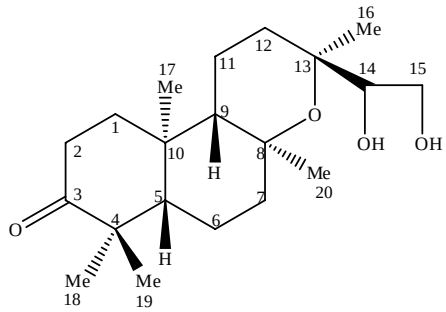

Compound **10**

Figure 36c The 300 MHz HMBC spectrum of compound **10** (in $CDCl_3$)

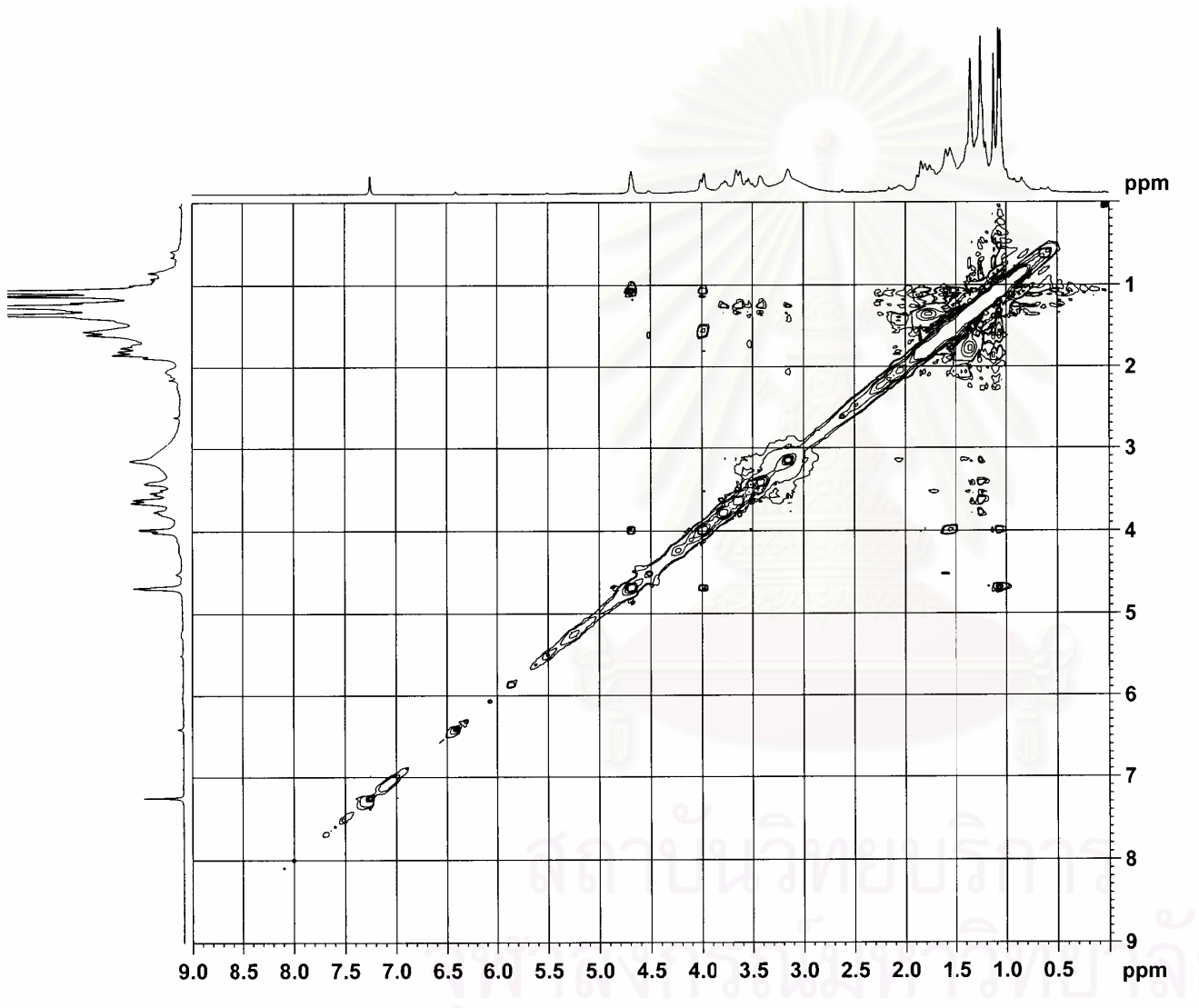

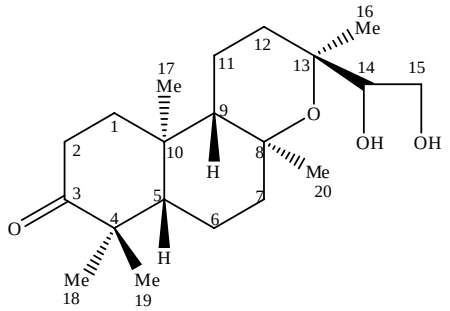

Compound **10**

Figure 37 The 300 MHz NOESY spectrum of compound **10** (in $CDCl_3$)

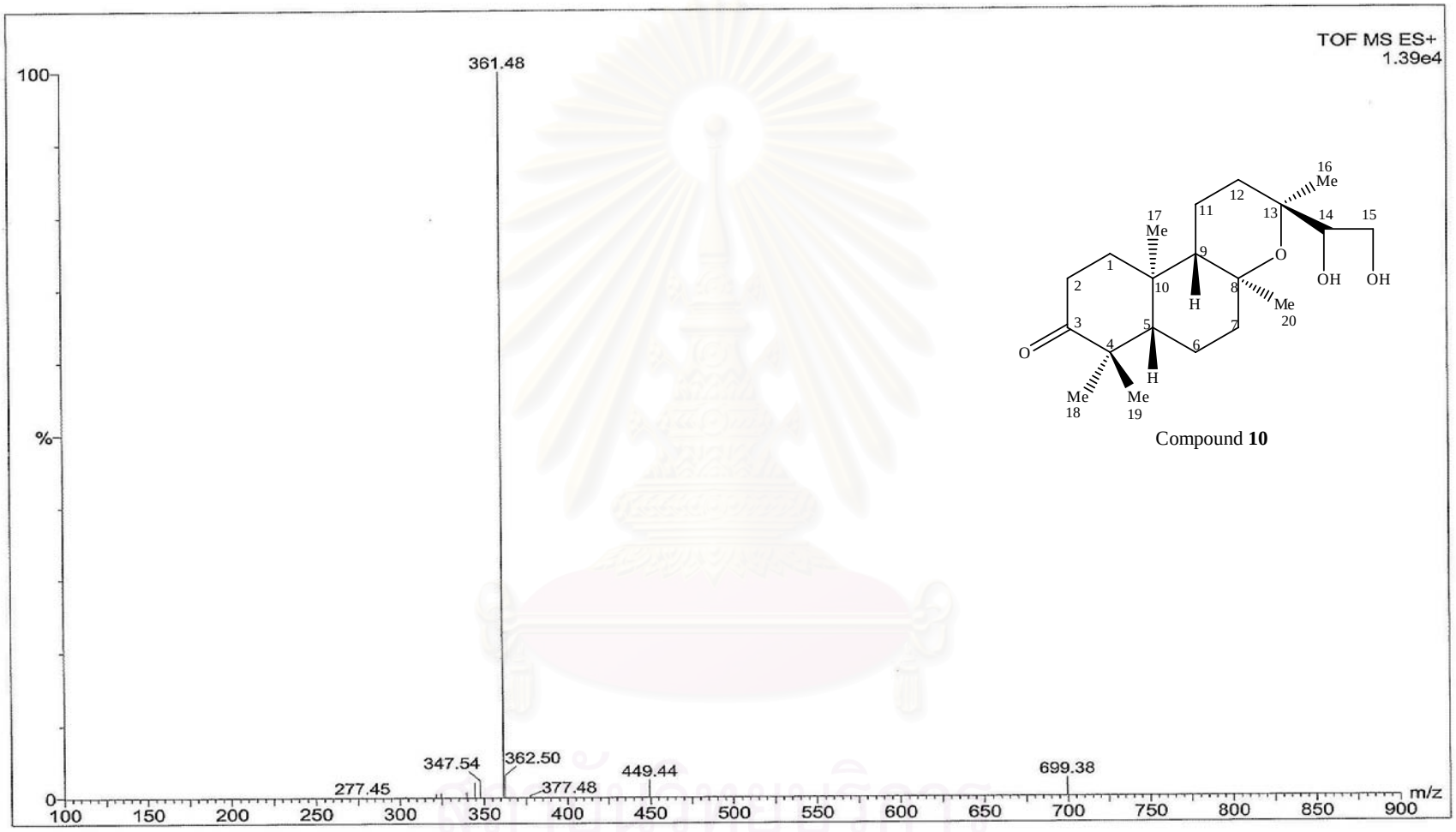

Compound **10**

Figure 38 The TOF-MS spectrum of compound **10**

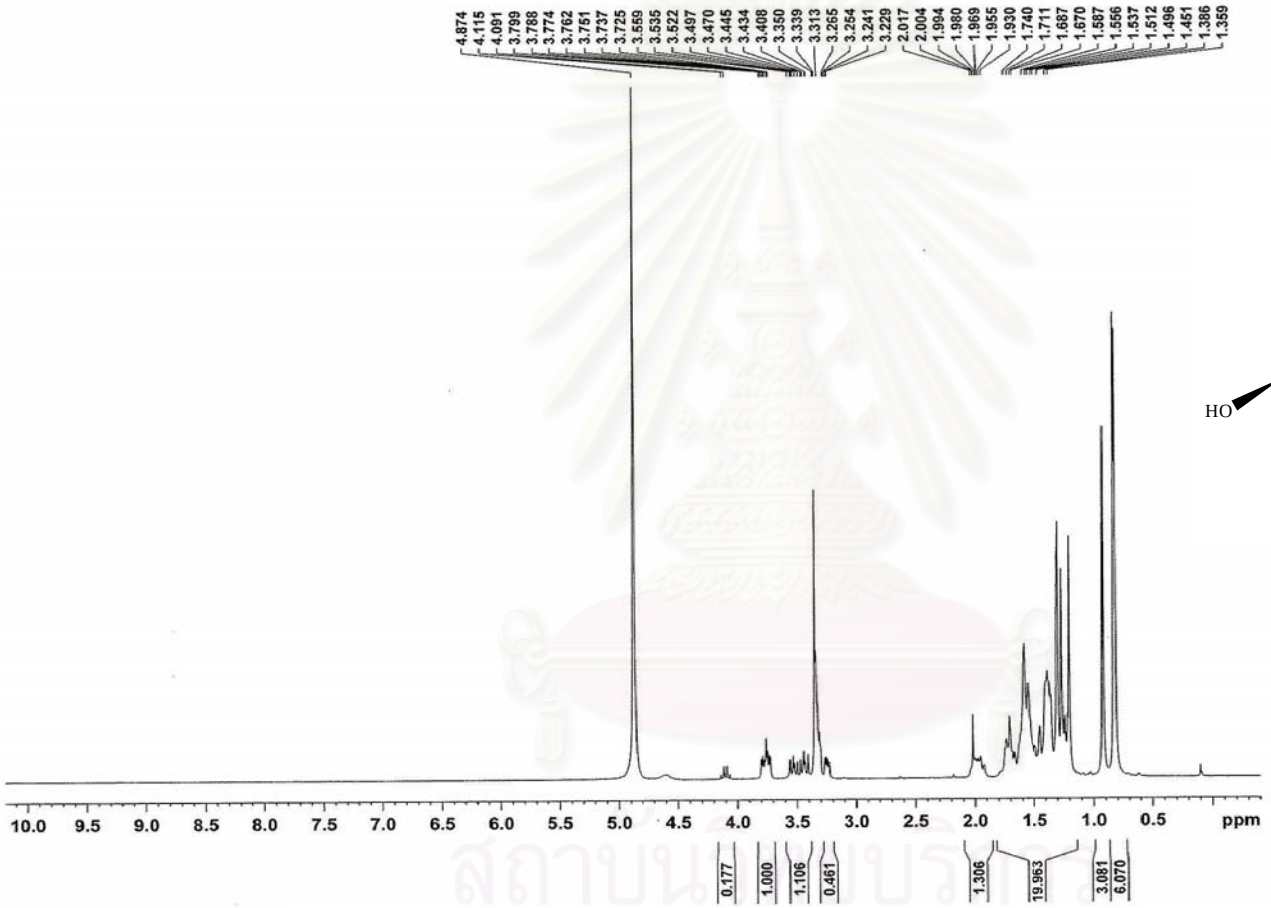

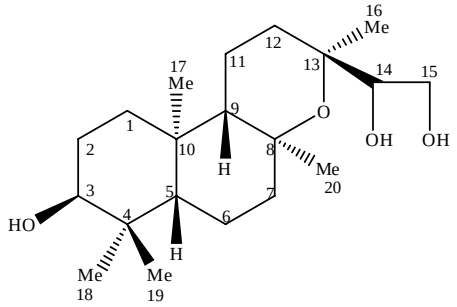

Compound **11**

Figure 39 The 300 MHz ^{1}H-NMR spectrum of compound **11** (in CD_3OD)

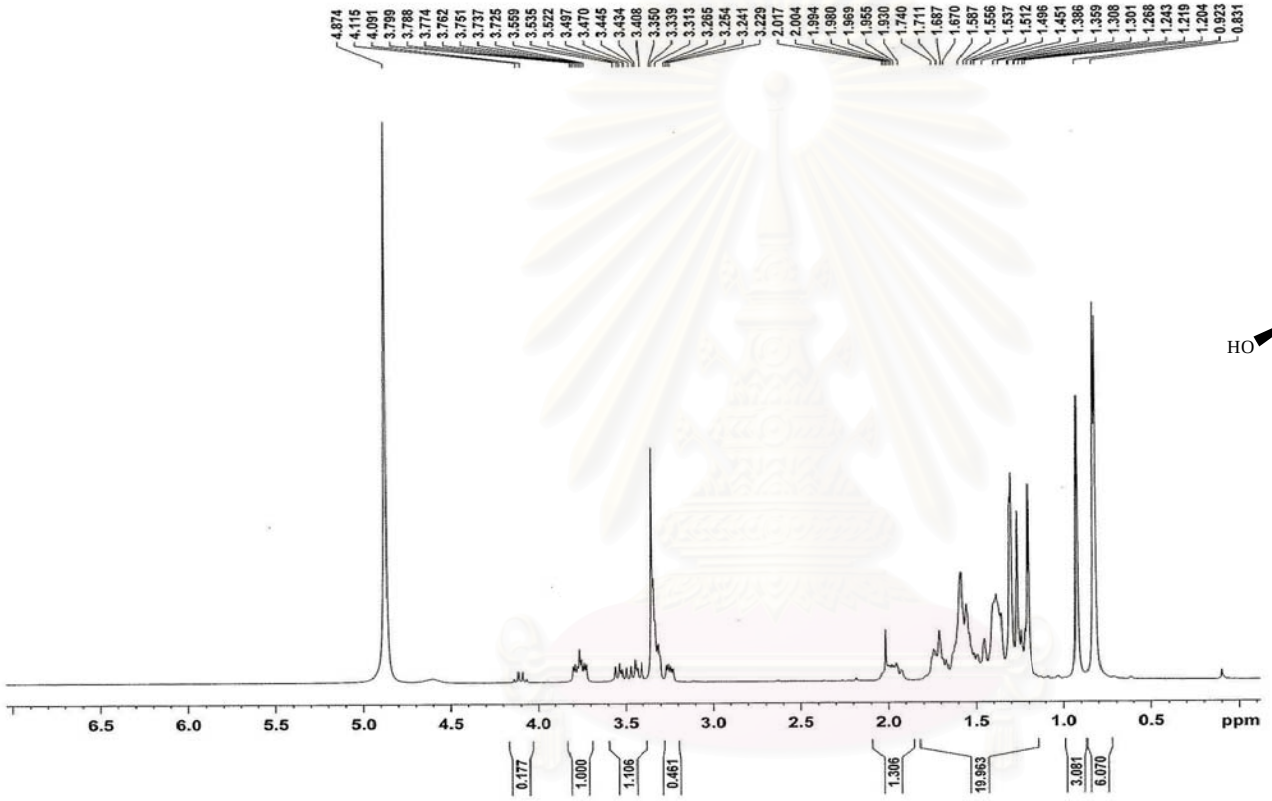

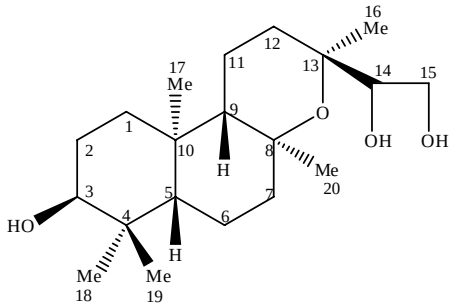

Compound **11**

Figure 39a The 300 MHz ^{1}H-NMR spectrum of compound **11** (in CD_3OD)

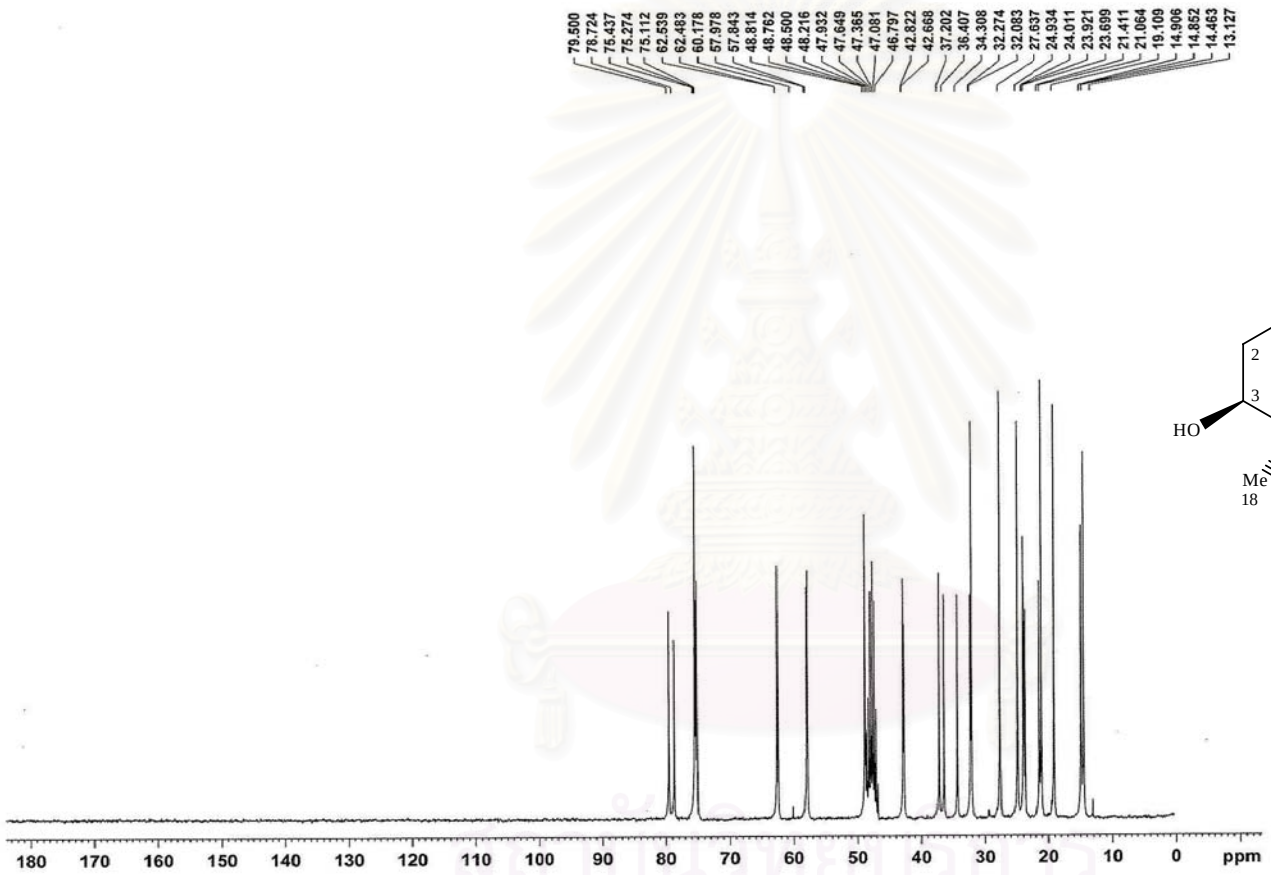

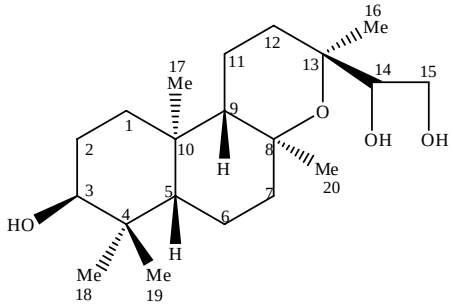

Compound **11**

Figure 40 The 75 MHz ^{13}C-NMR spectrum of compound **11** (in CD_3OD)

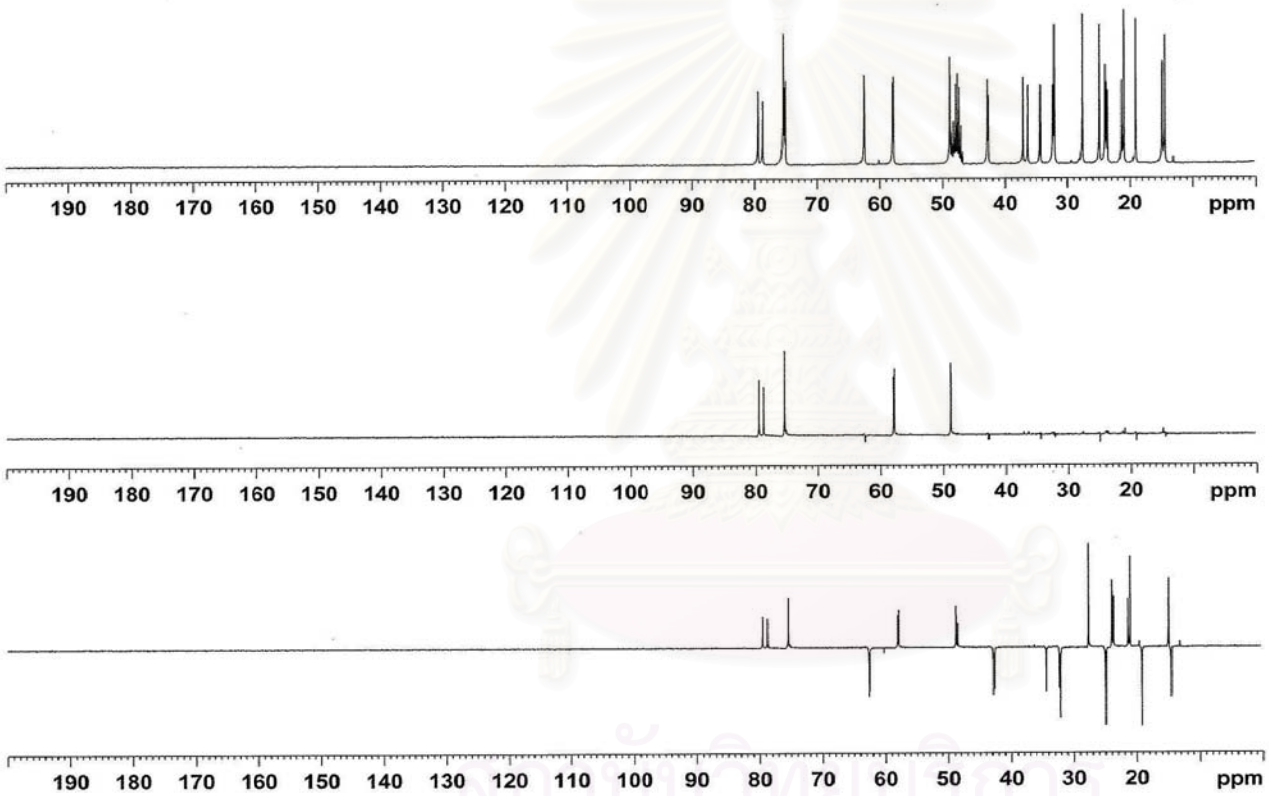

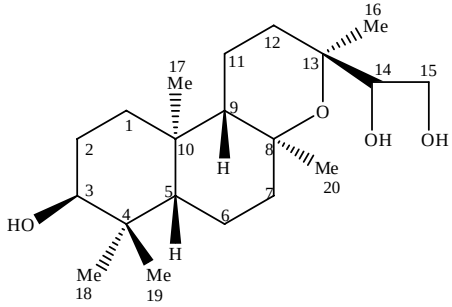

Compound **11**

Figure 41 The 75 MHz ^{13}C-NMR, DEPT-90 and DEPT-135 spectra of compound **11**

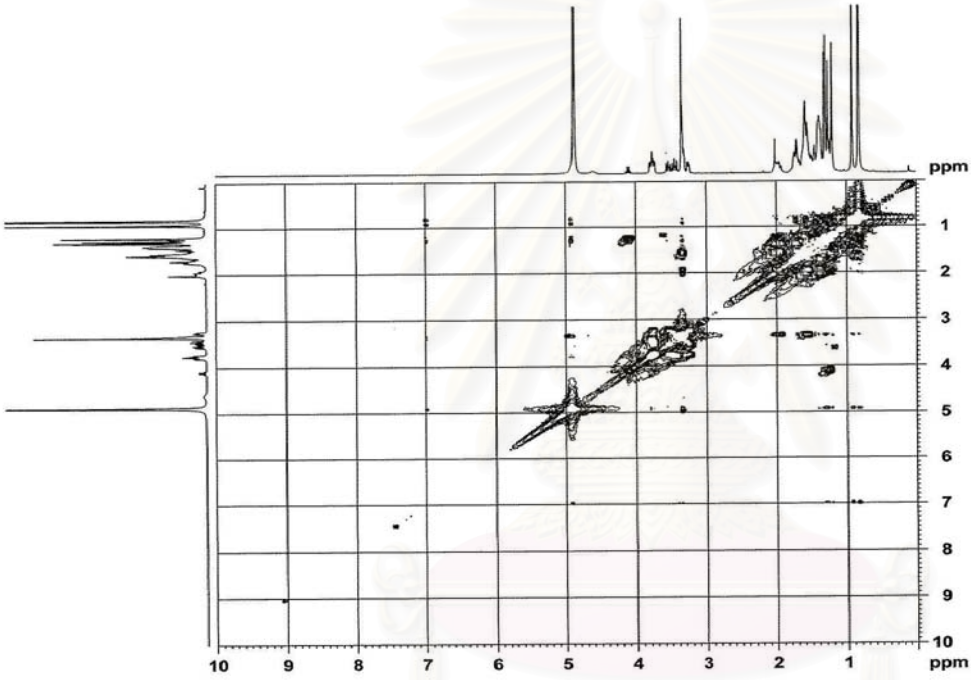

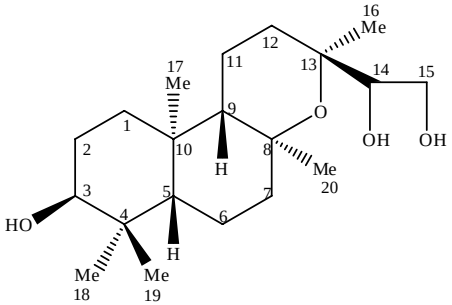

Compound **11**

Figure 42 The 300 MHz ^{1}H-^{1}H COSY NMR spectrum of compound **11** ((in CD_3OD)

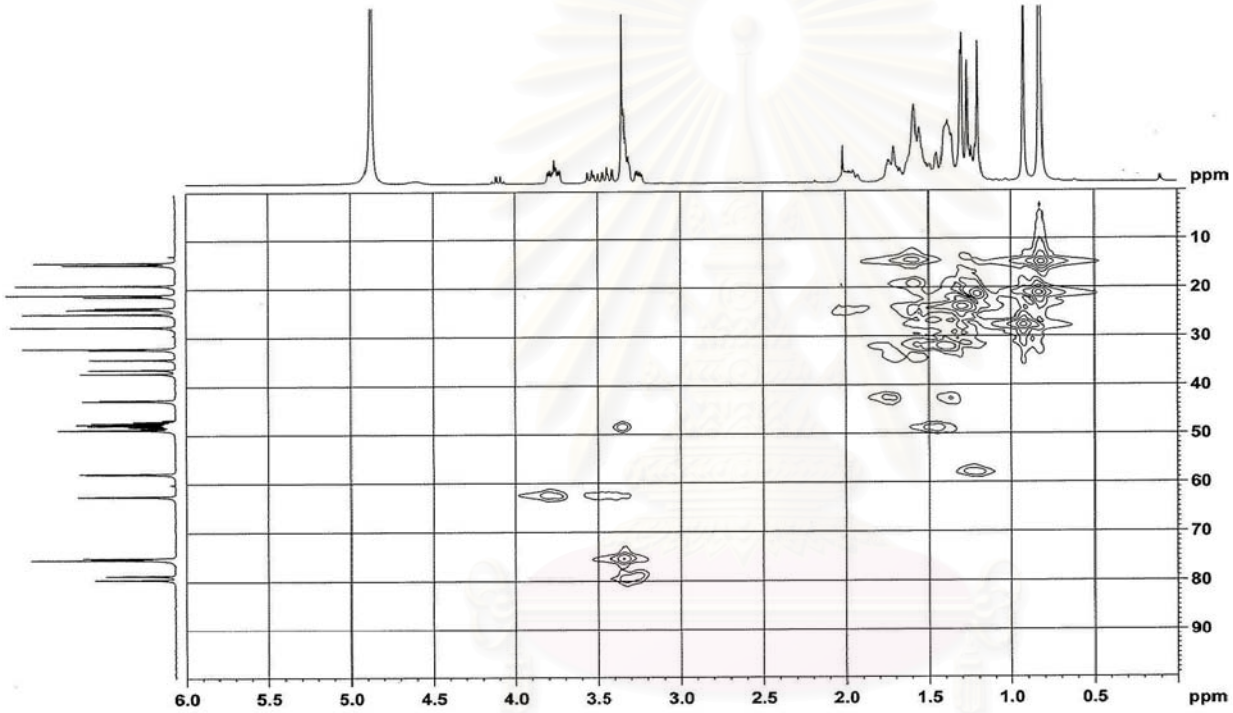

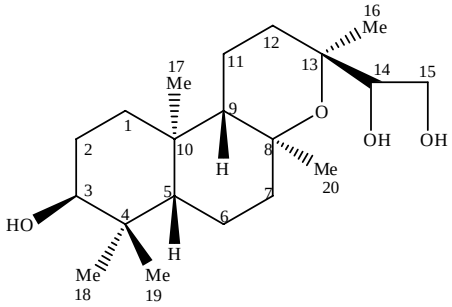

Compound **11**

Figure 43 The 300 MHz HMQC NMR spectrum of compound **11** (in CD_3OD)

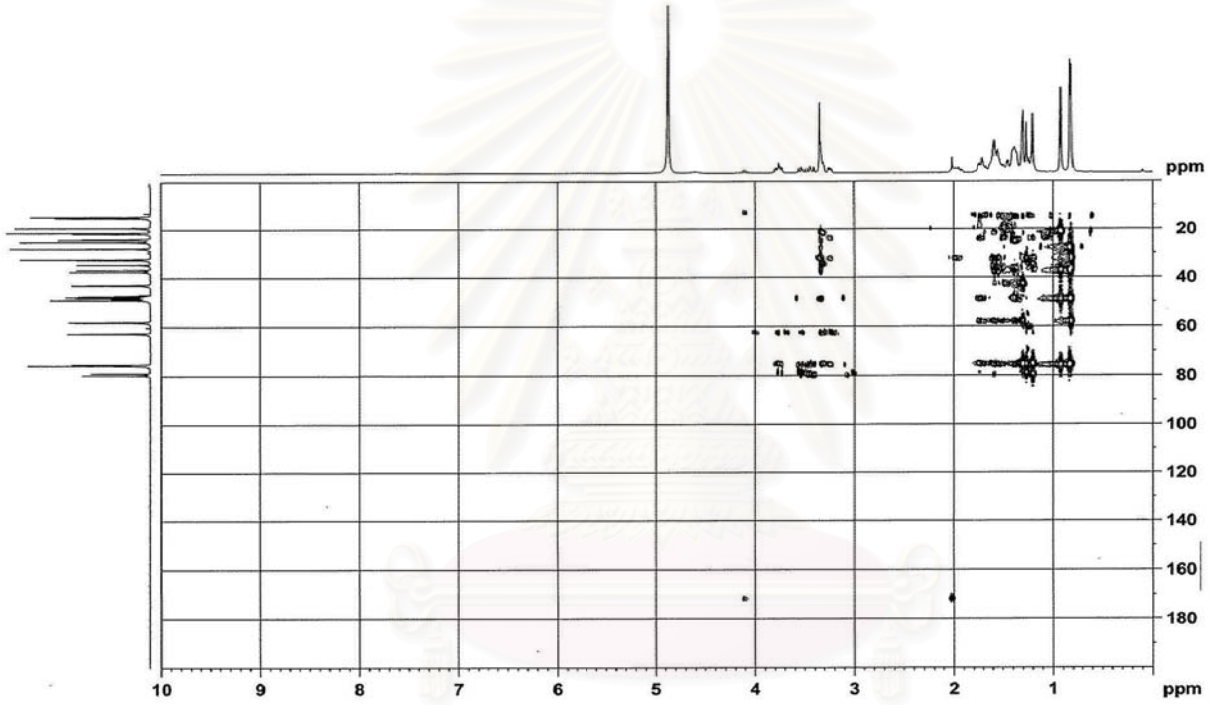

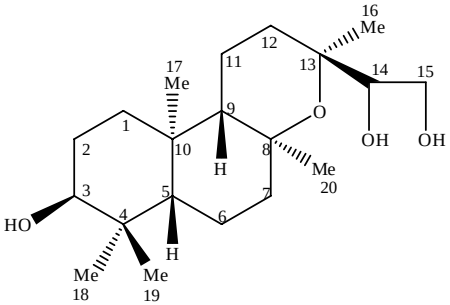

Compound **11**

Figure 44 The 300 MHz HMBC spectrum of compound **11** (in CD_3OD)

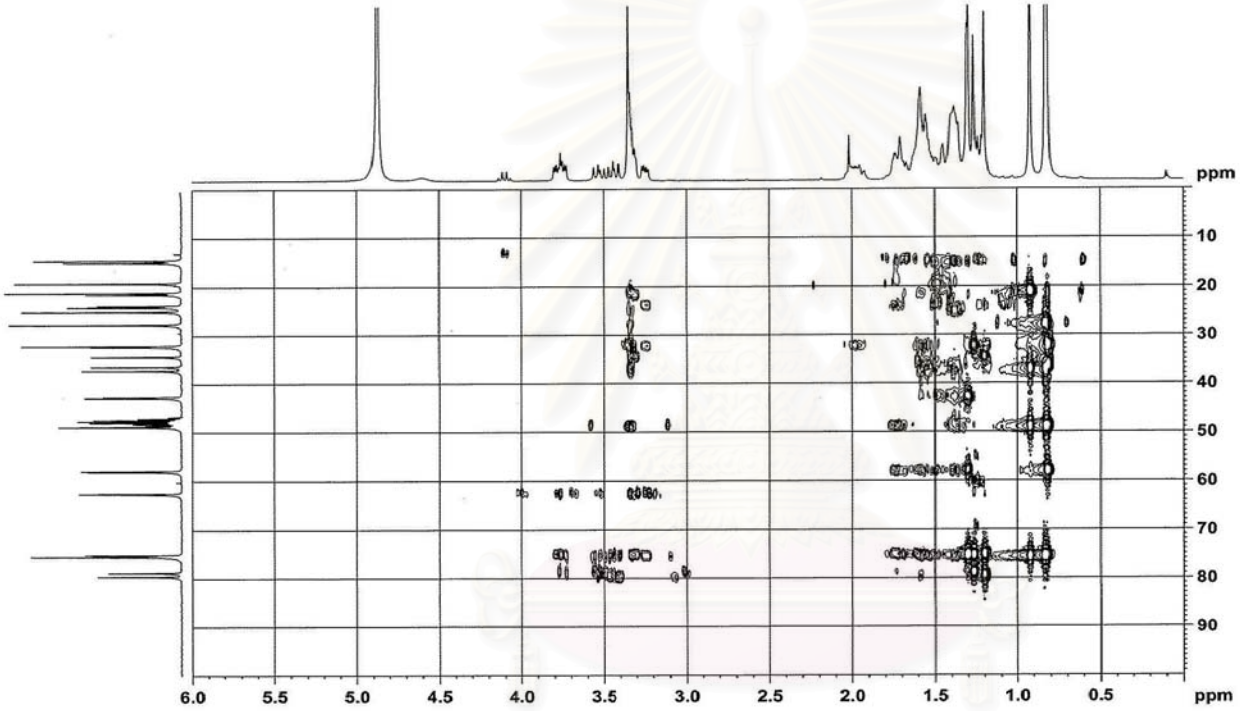

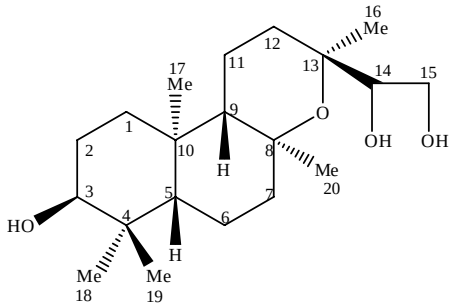

Compound **11**

Figure 44a The expanded 300 MHz HMBC spectrum of compound **11** (in CD_3OD)

(δ_H6.0-0.5 ppm, δ_C10 -90 ppm)

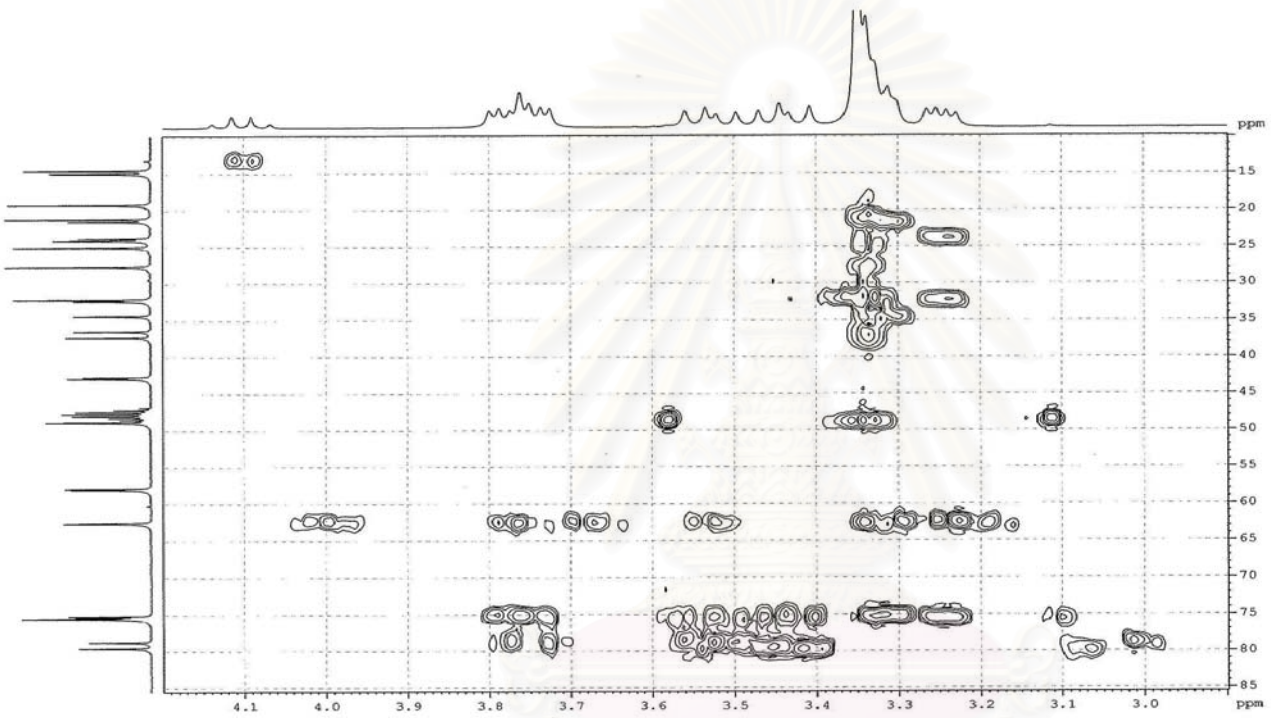

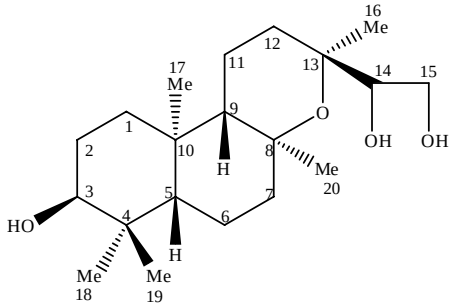

Compound **11**

Figure 44b The expanded 300 MHz HMBC spectrum of compound **11** (in CD_3OD)

(δ_H4.2-2.9 ppm, δ_C10 -85 ppm)

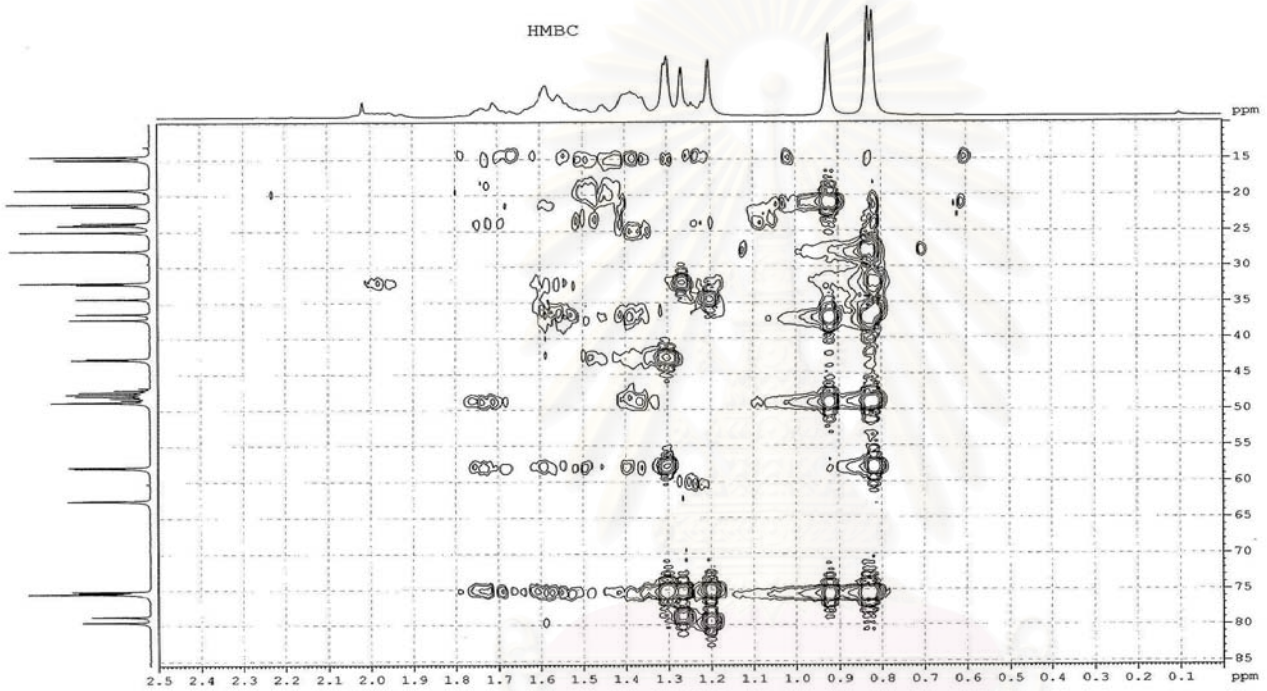

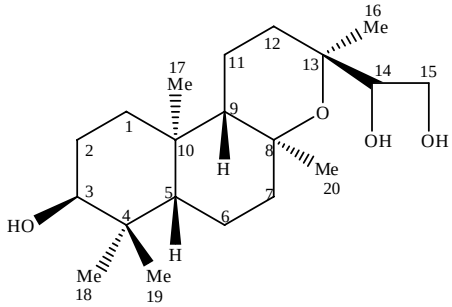

Compound **11**

Figure 44c The expanded 300 MHz HMBC spectrum of compound **11** (in CD_3OD)

(δ_H2.5-0.1 ppm, δ_C10 -85 ppm)

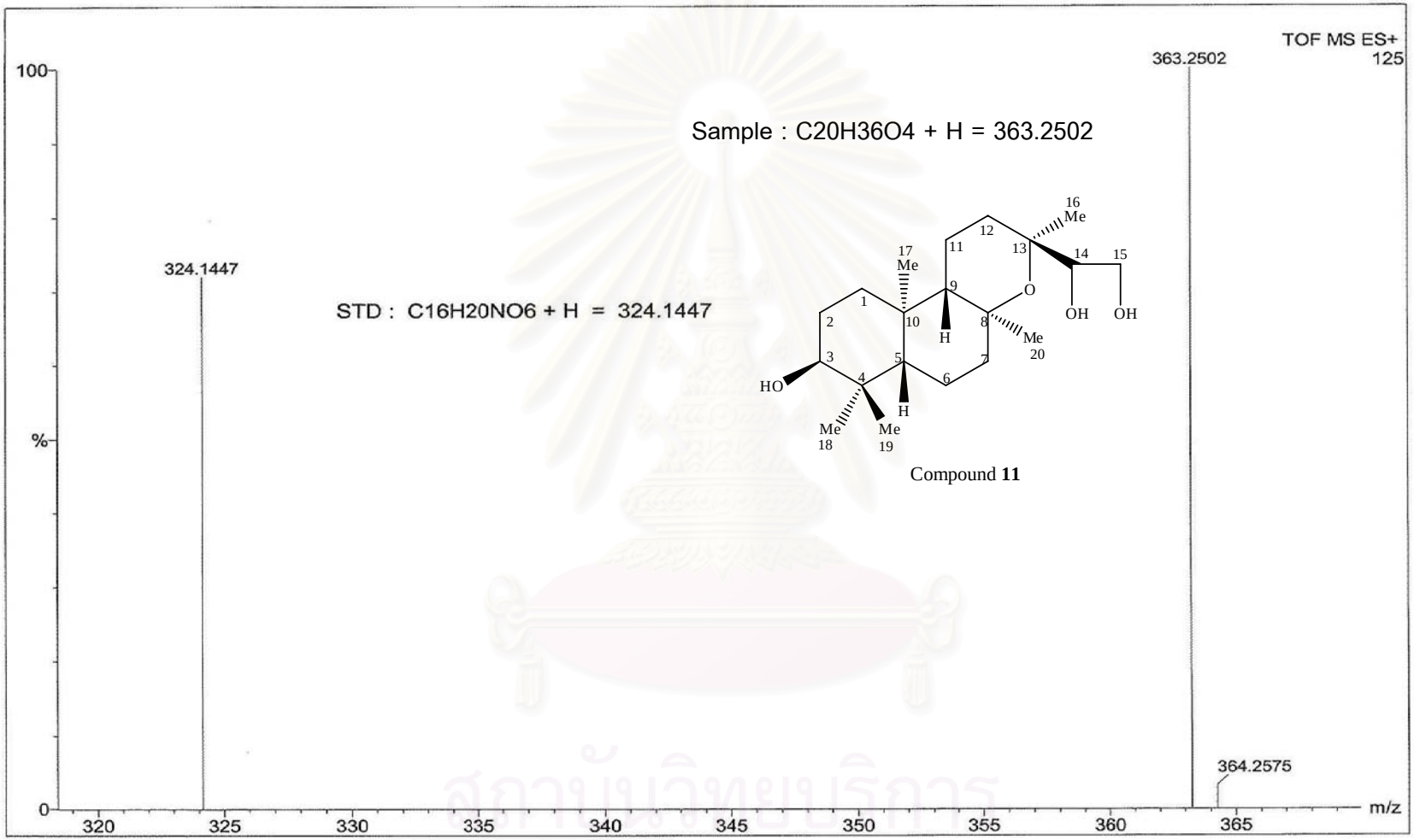

Figure 45 The TOF-MS spectrum of compound 11

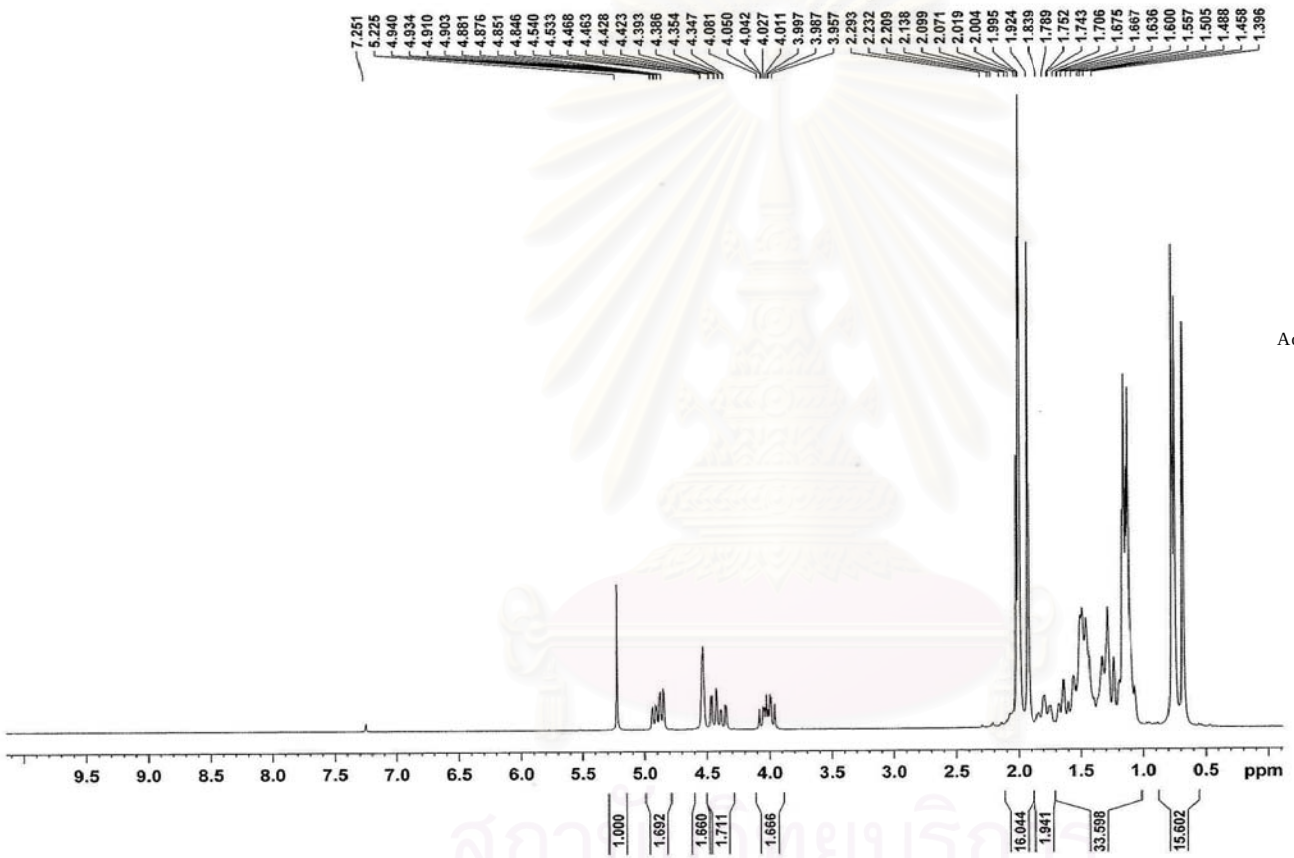

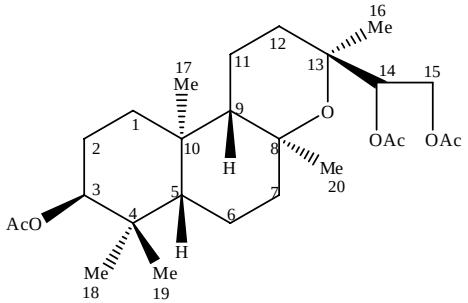

Compound **12**

Figure 46 The 300 MHz ^{1}H-NMR spectrum of compound **12** (in $CDCl_3$)

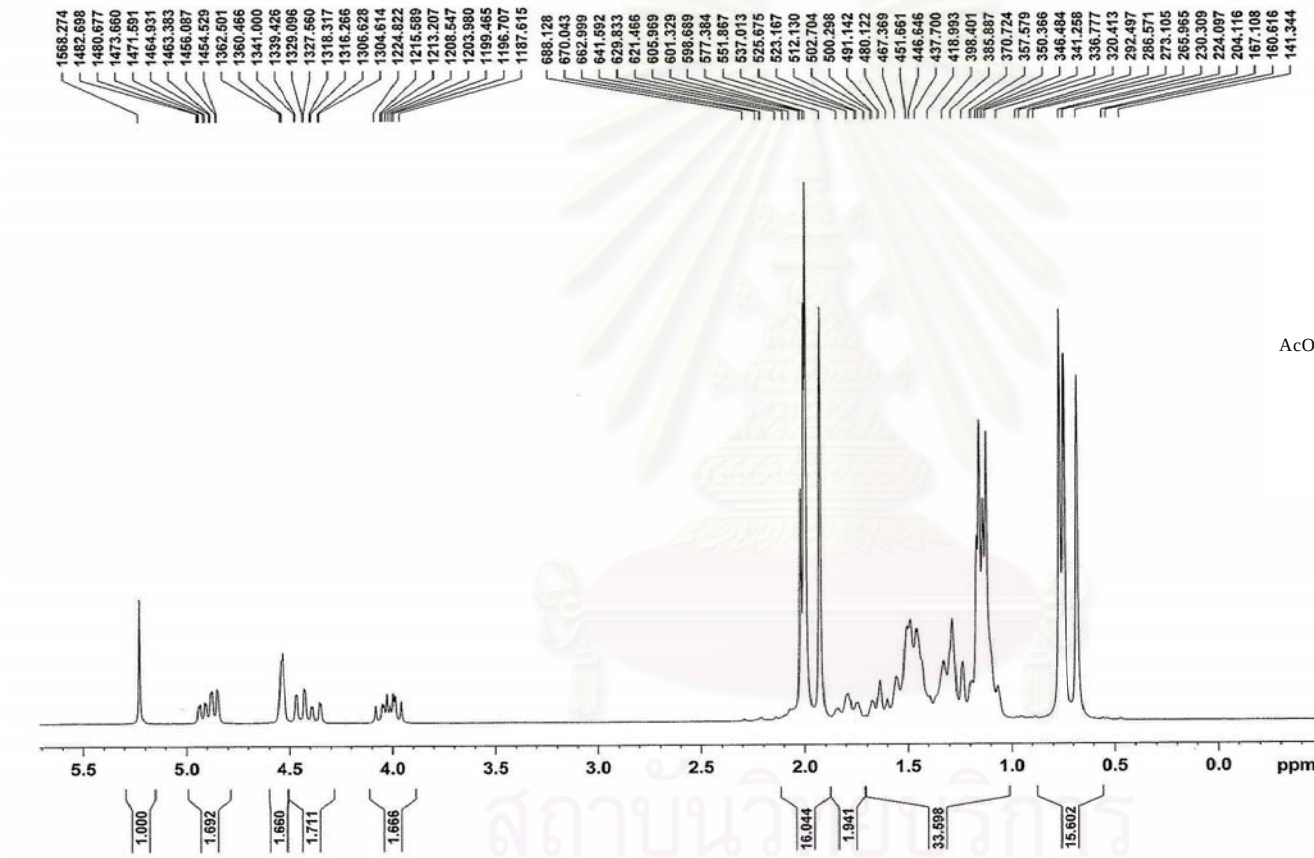

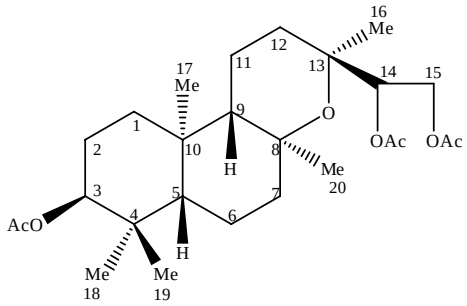

Compound **12**

Figure 46a The expanded 300 MHz ^{1}H-NMR spectrum of compound **12** (in $CDCl_3$)

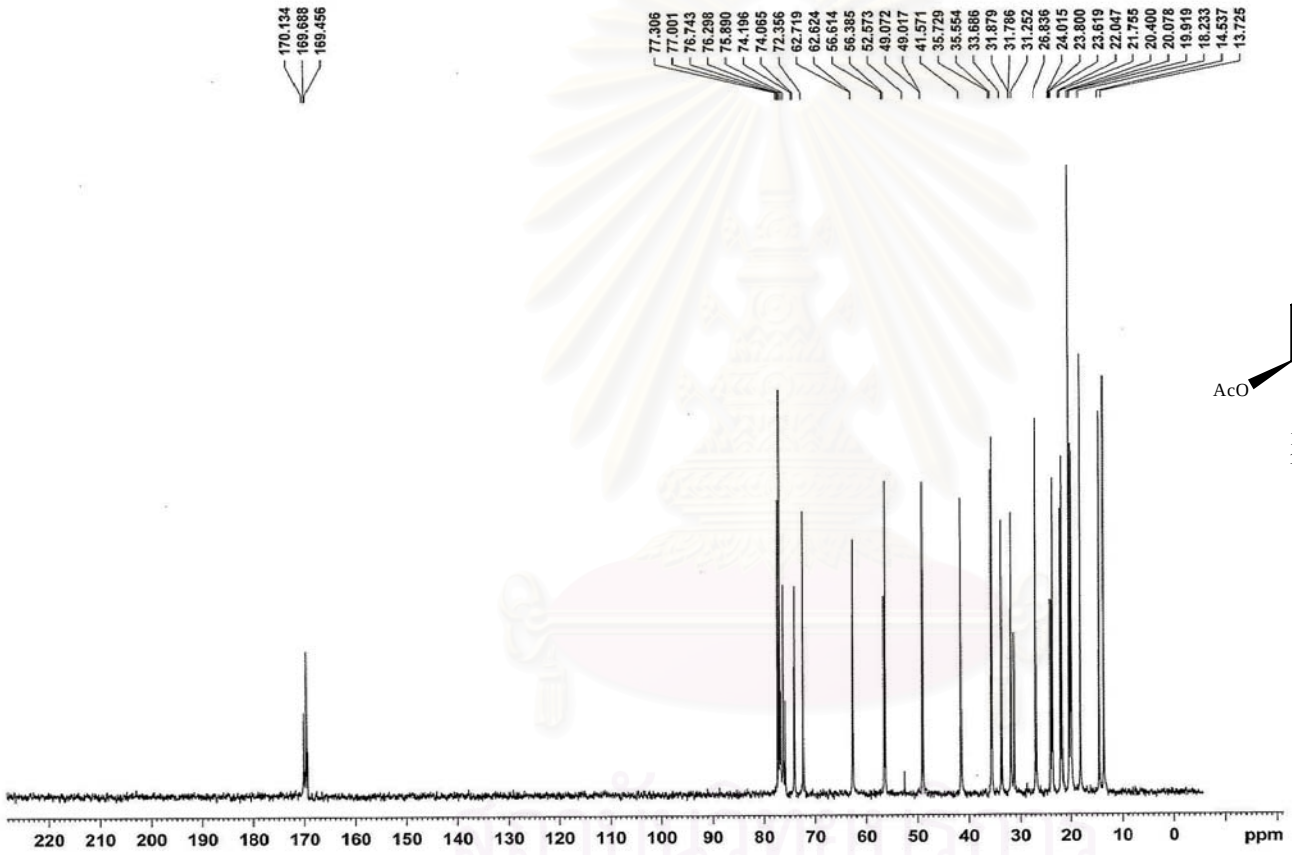

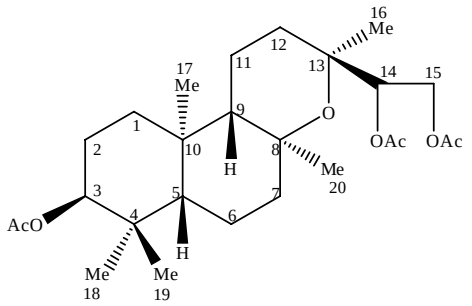

Compound **12**

Figure 47 The 75 MHz ^{13}C-NMR spectrum of compound **12**(in $CDCl_3$)

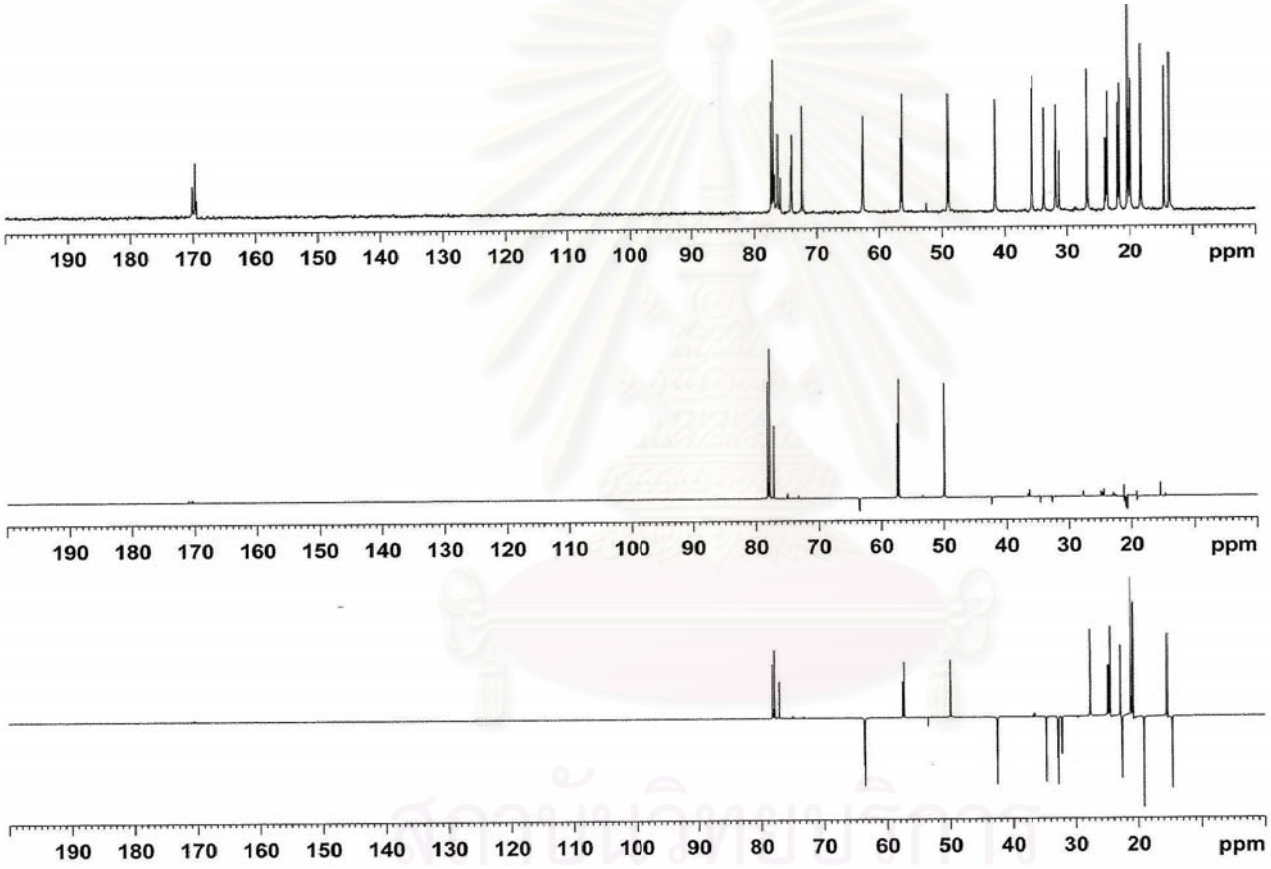

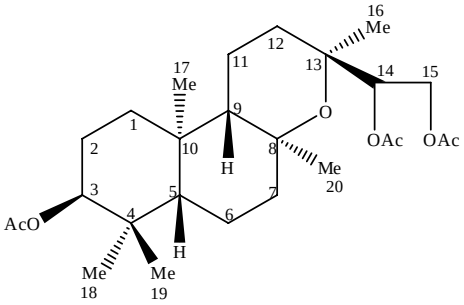

Compound **12**

Figure 48 The 75 MHz ^{13}C-NMR, DEPT-90 and DEPT-135 spectra of compound **12**

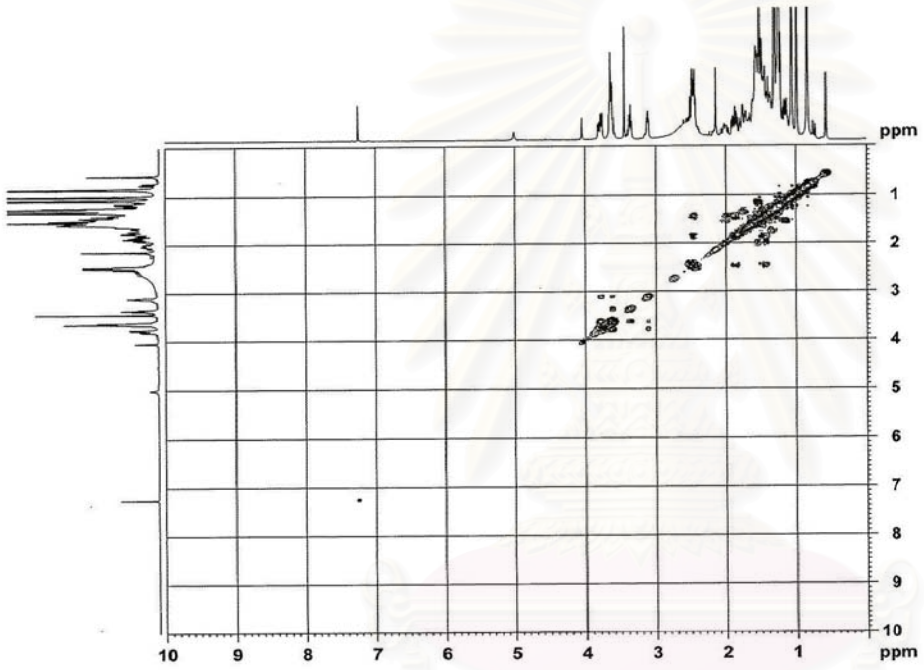

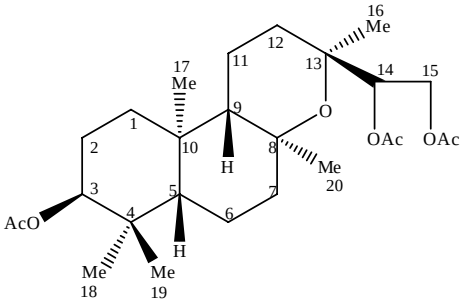

Compound **12**

Figure 49 The 300 MHz ^{1}H-^{1}H COSY NMR spectrum of compound **12**

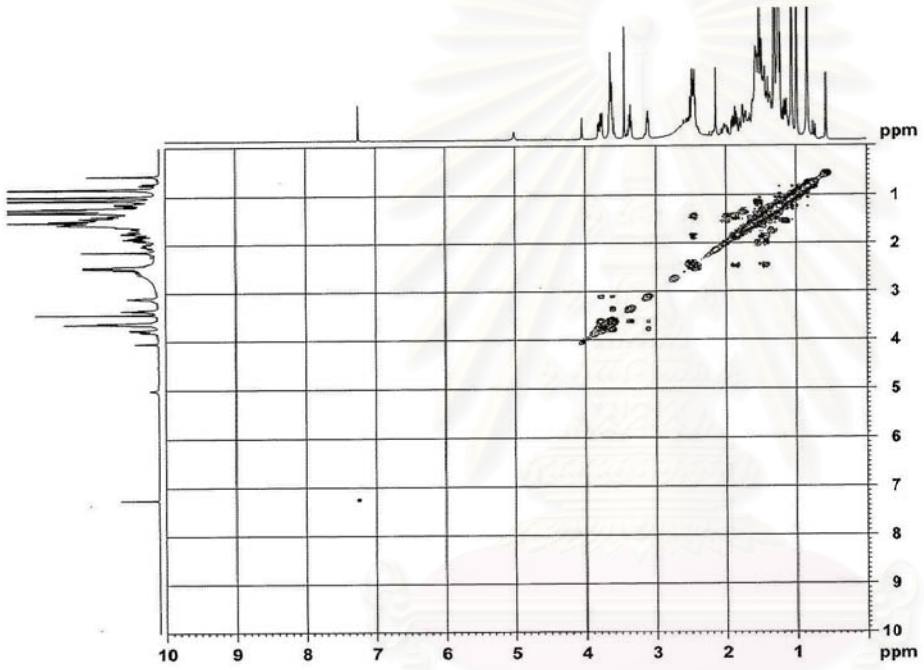

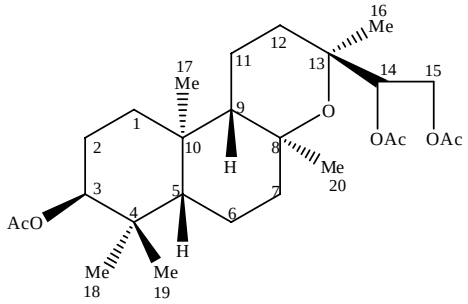

Compound **12**

Figure 49a The expanded 300 MHz ^{1}H-^{1}H COSY NMR spectrum of compound **12**

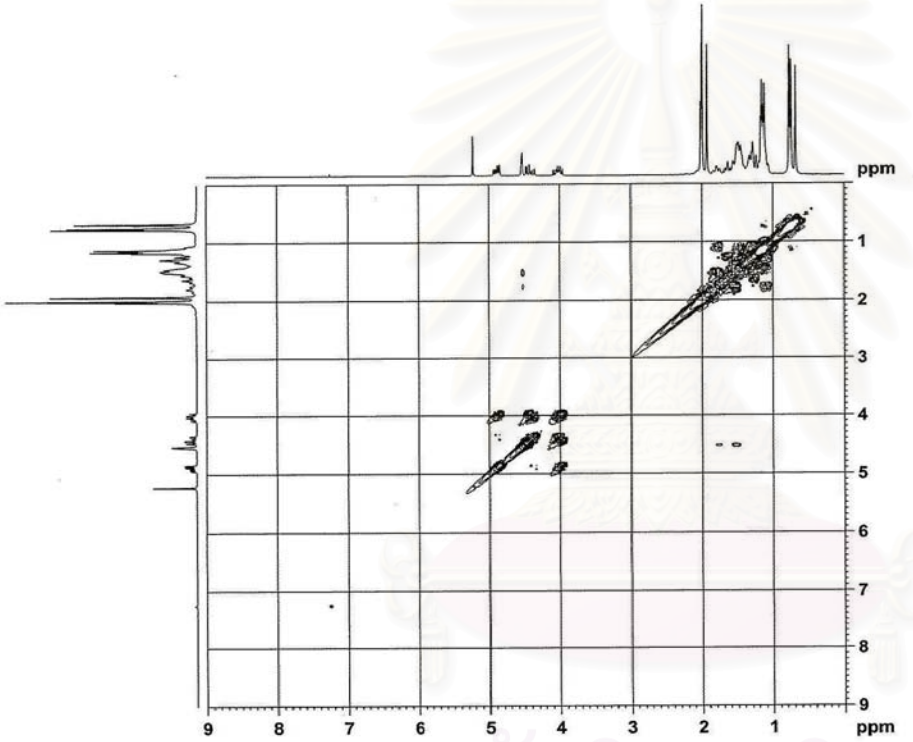

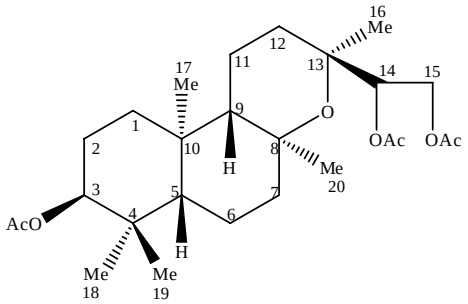

Compound **12**

Figure 49b The expanded 300 MHz ^{1}H-^{1}H COSY NMR spectrum of compound **12**

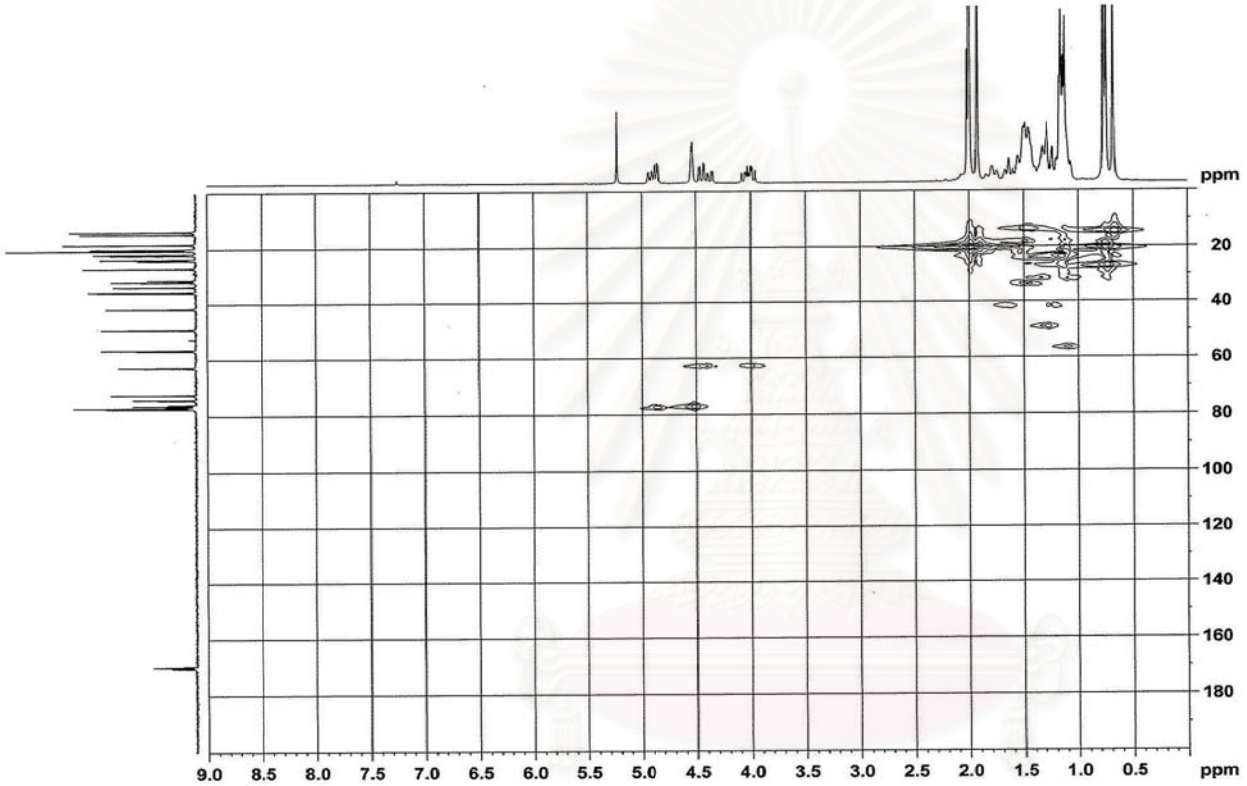

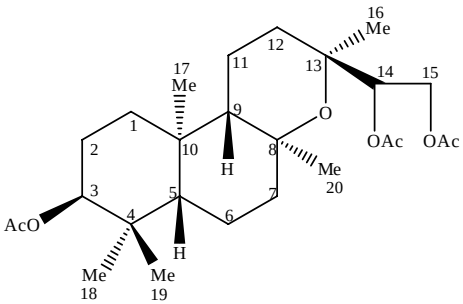

Compound **12**

Figure 50 The 300 MHz HMQC NMR spectrum of compound 12

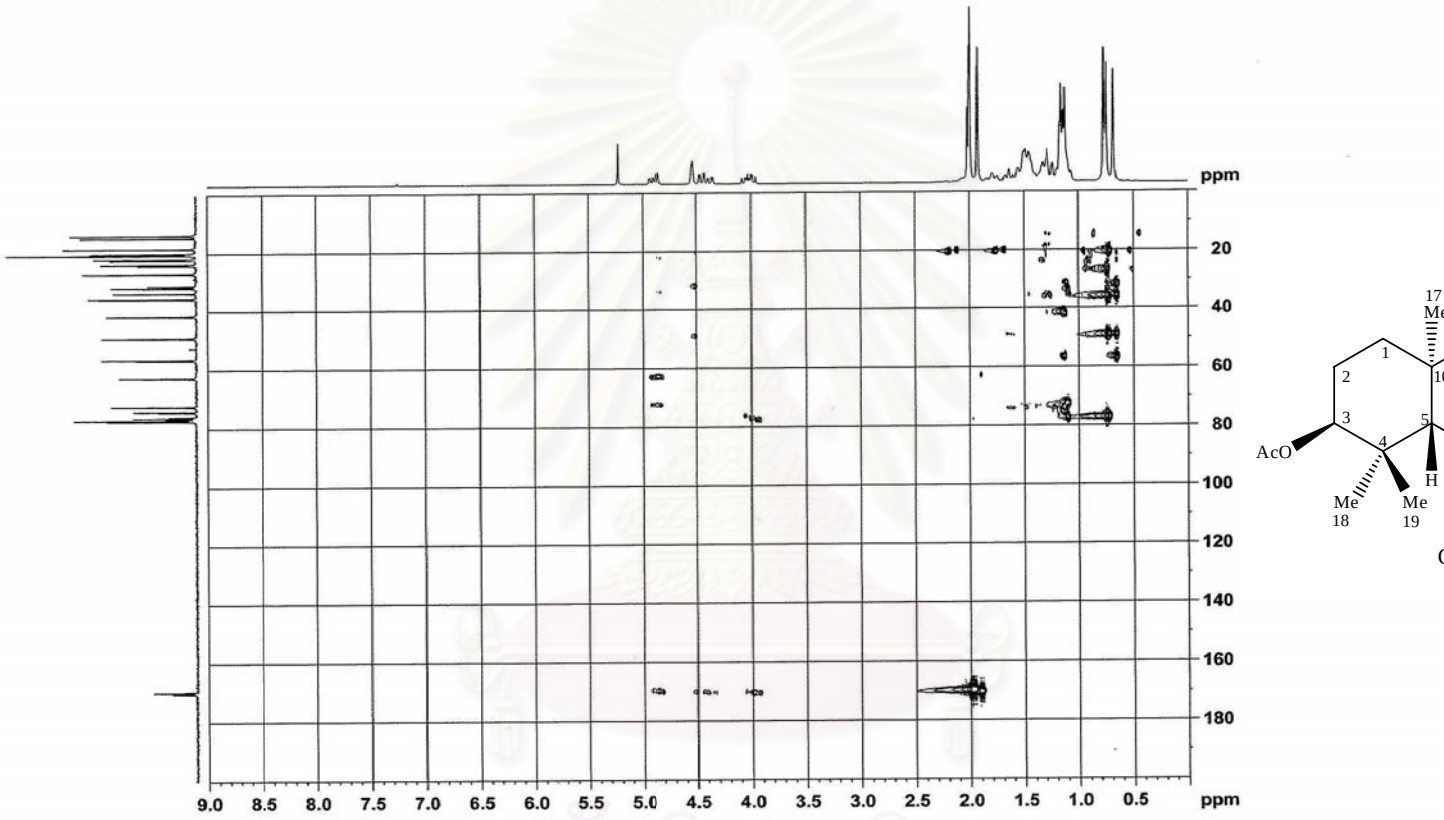

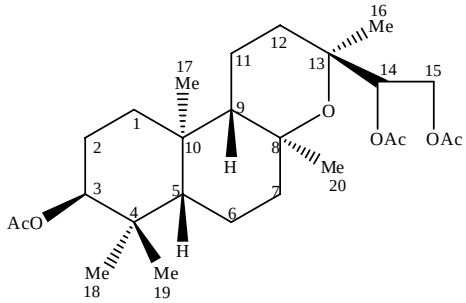

Compound **12**

Figure 52 The 300 MHz HMBC spectrum of compound **12** (in $CDCl_3$)

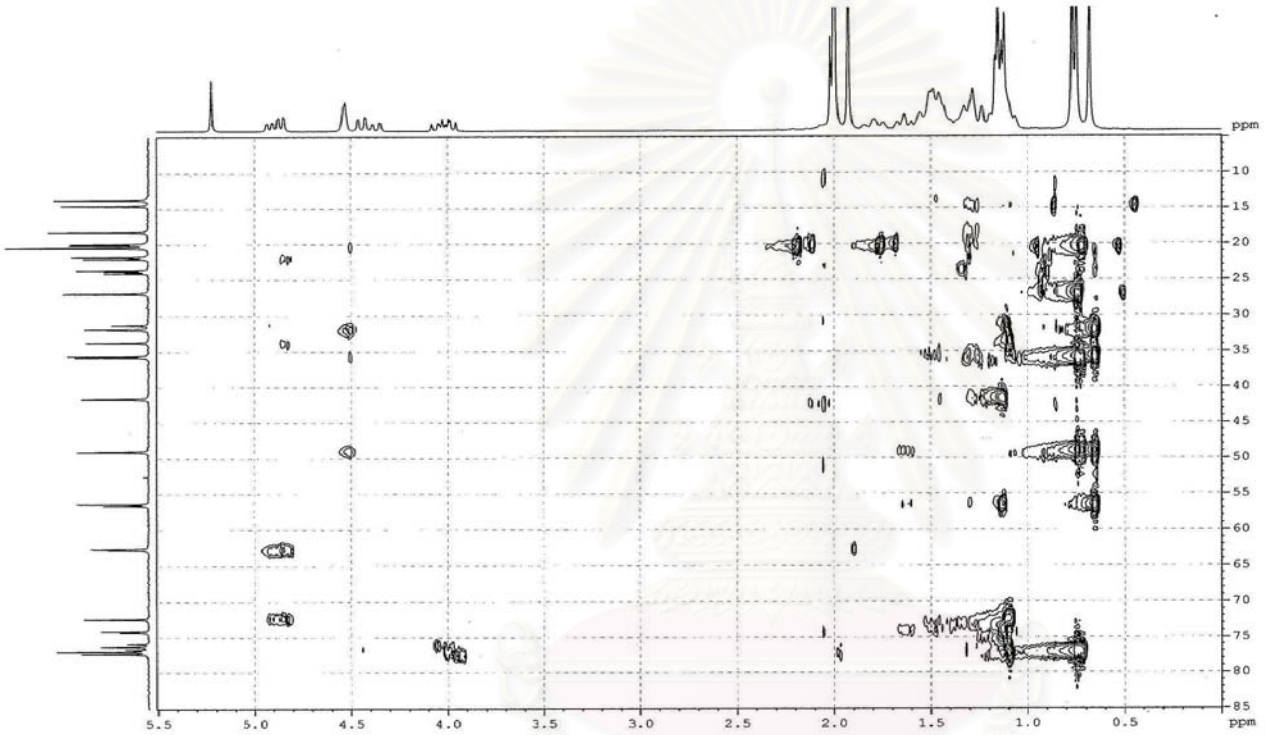

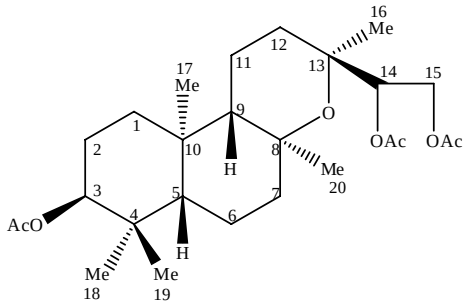

Compound **12**

Figure 51a The expanded 300 MHz HMBC spectrum of compound **12** (in $CDCl_3$)

(δ_H5.5-0.5 ppm, δ_C10 -85 ppm)

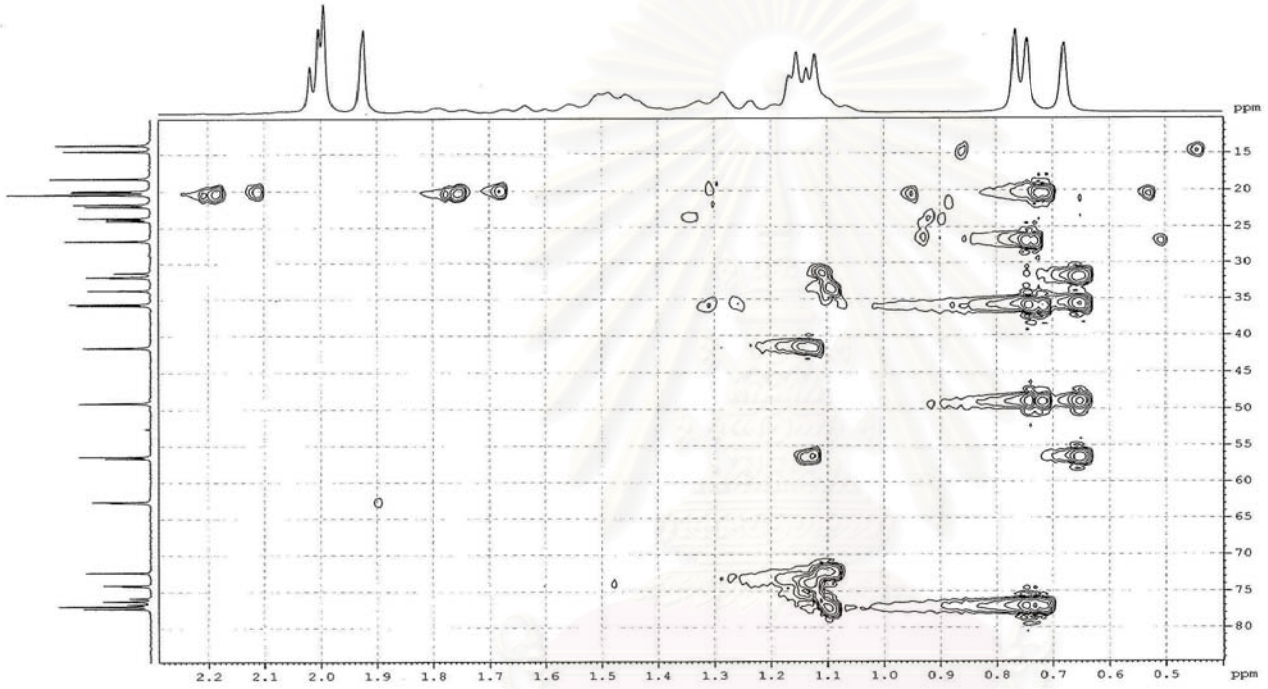

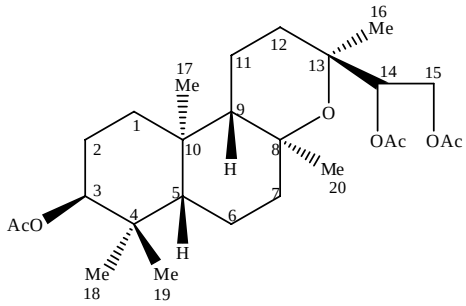

Compound **12**

Figure 51b The expanded 300 MHz HMBC spectrum of compound **12** (in $CDCl_3$)

(δ_H2.3-0.5 ppm, δ_C10 -80 ppm)

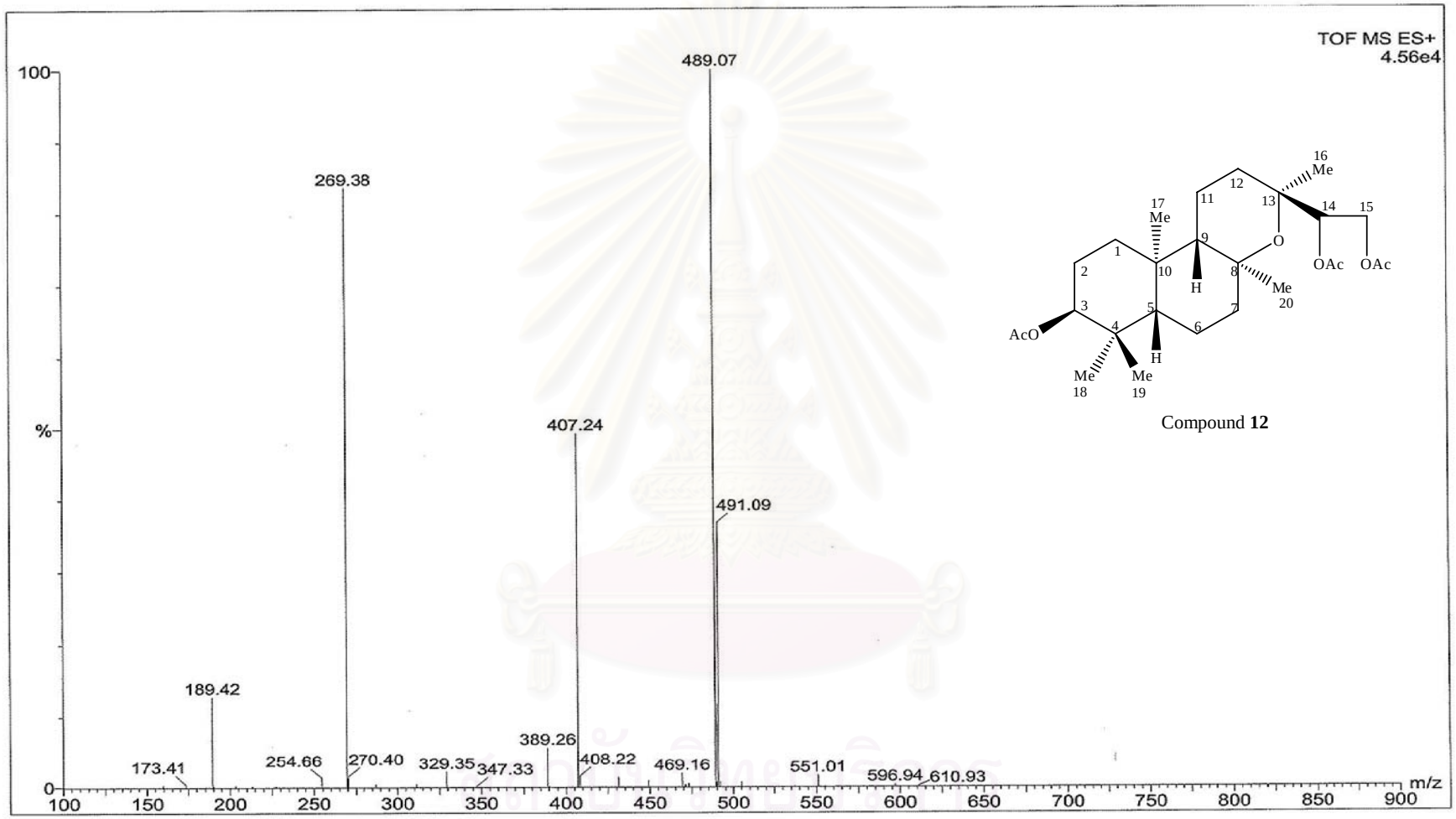

Compound **12**

Figure 52 The TOF-MS spectrum of compound **12**

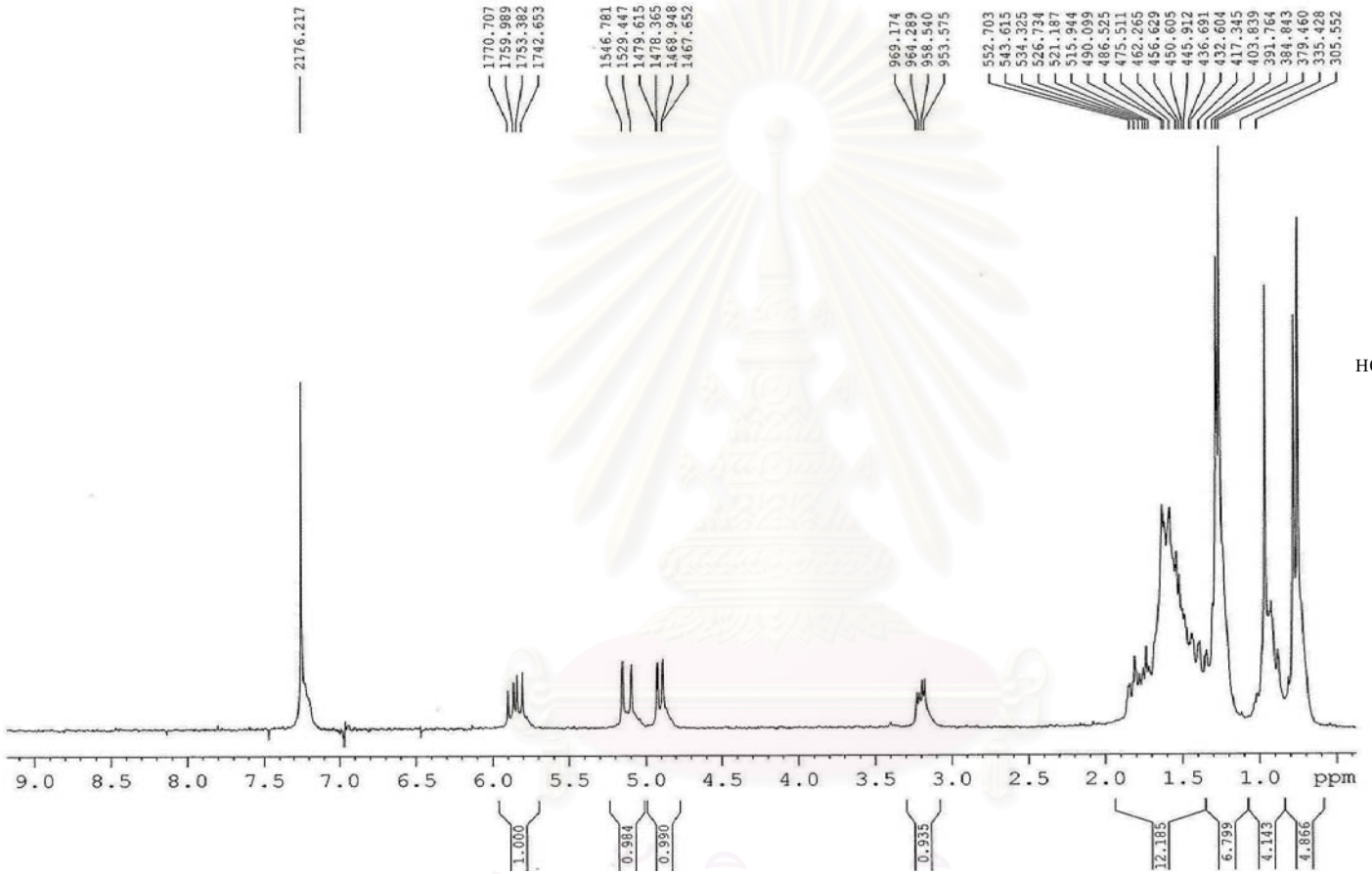

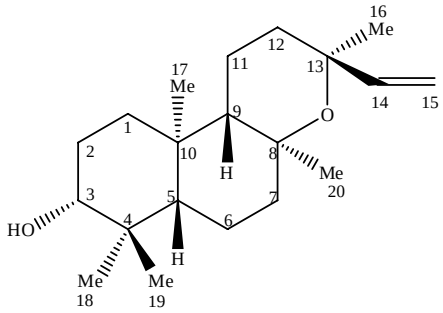

Compound **13**

Figure 53 The 300 MHz ^{1}H-NMR spectrum of compound **13** (in CDCl3)

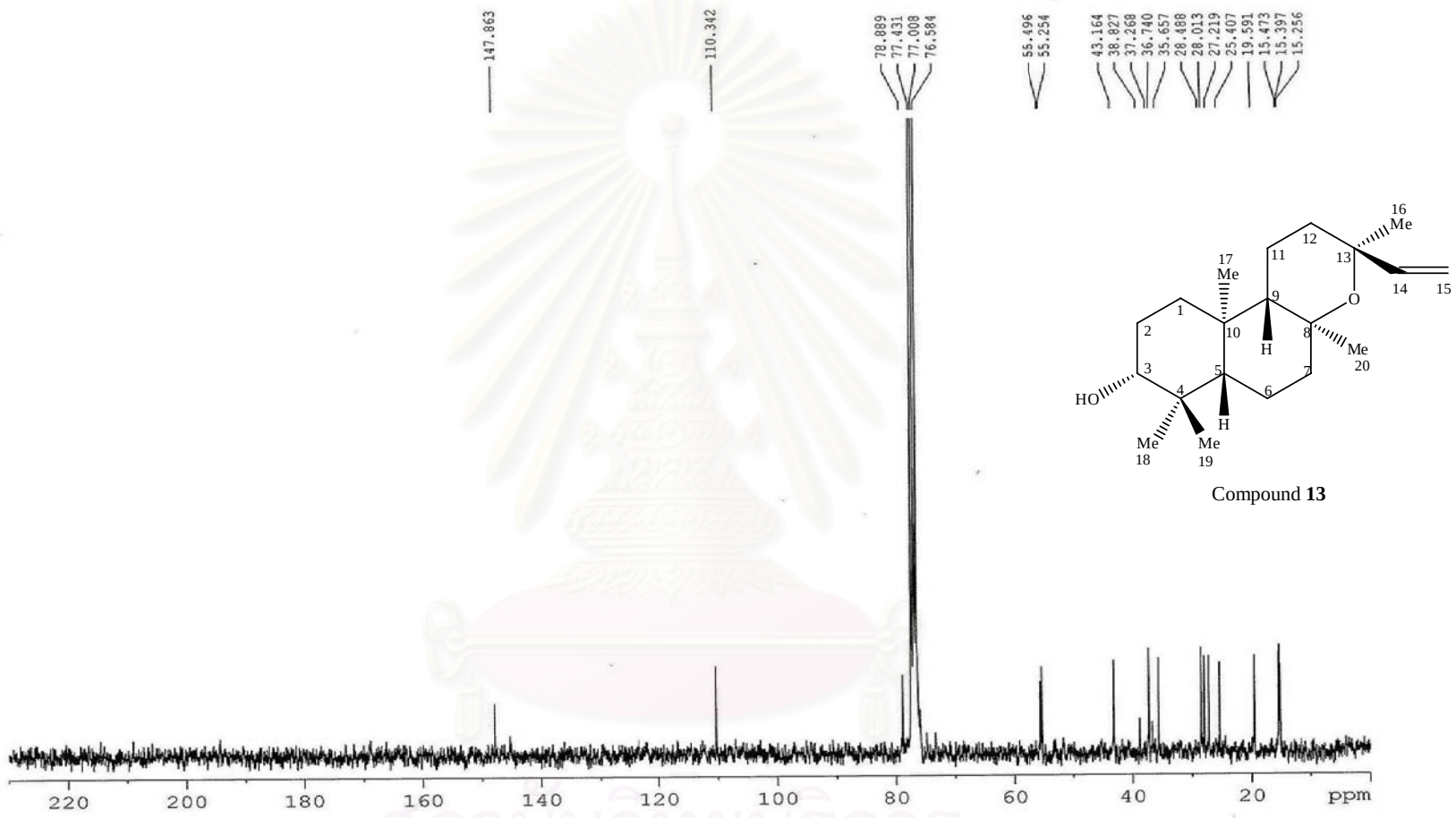

Compound **13**

Figure 54 The 75 MHz ^{13}C-NMR spectrum of compound **13** (in CDCl3)

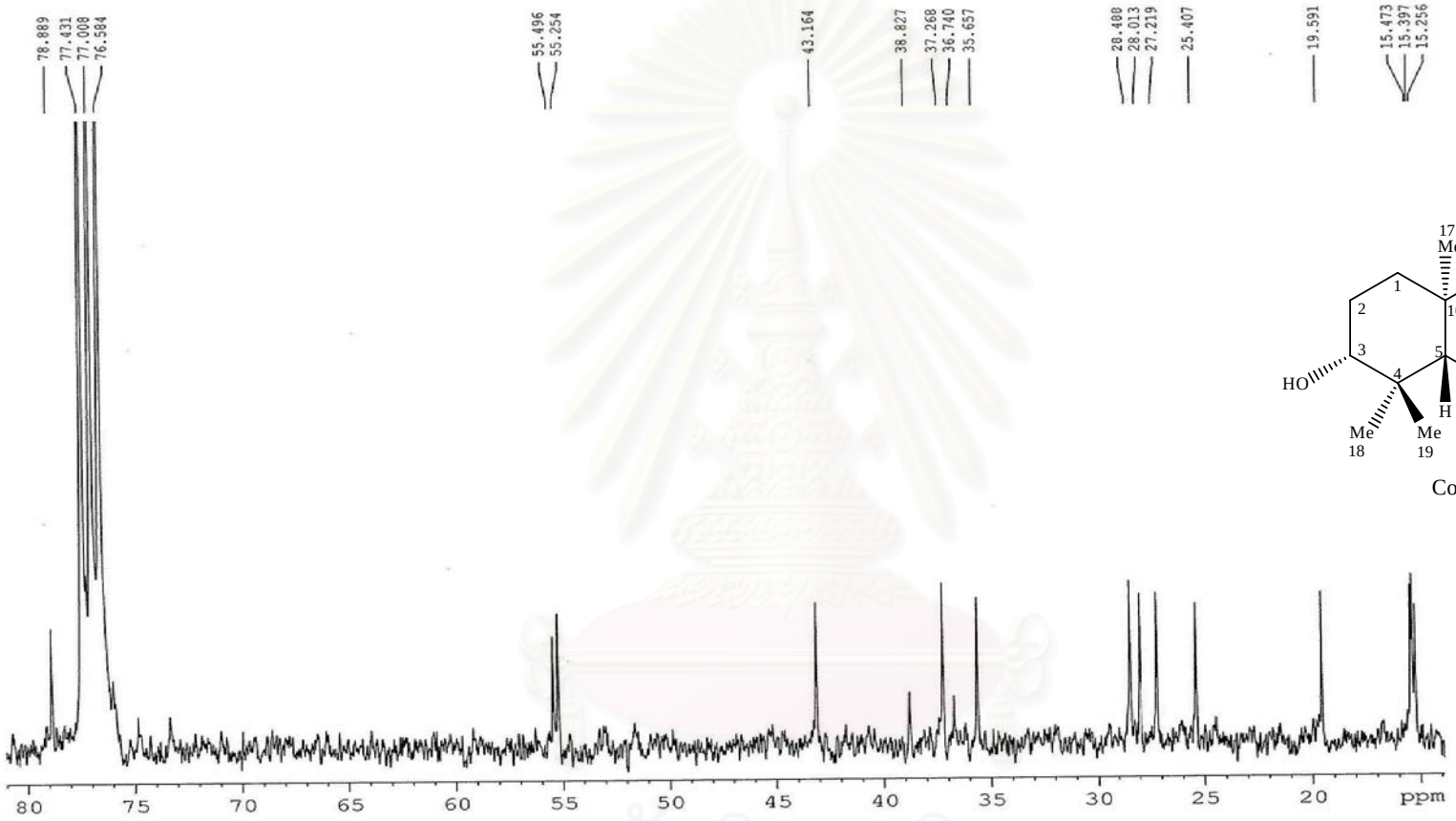

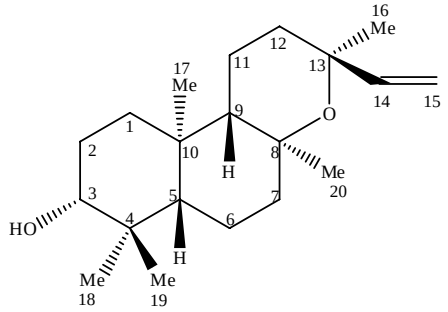

Compound **13**

Figure 54a The expanded 75 MHz ^{13}C-NMR spectrum of compound **13** (in $CDCl_3$)

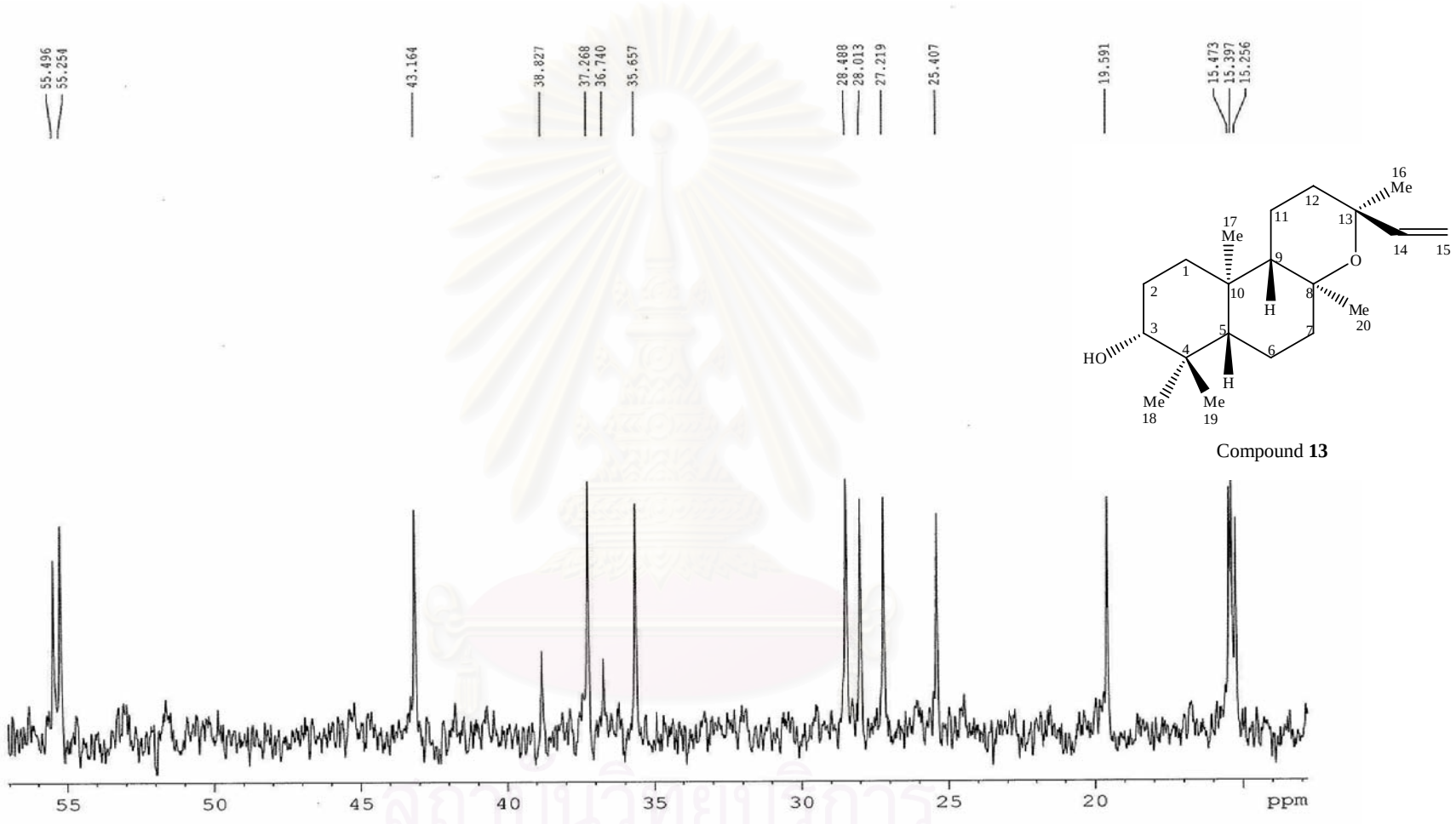

Compound **13**

Figure 54b The expanded 75 MHz ^{13}C-NMR spectrum of compound **13** (in $CDCl_3$)

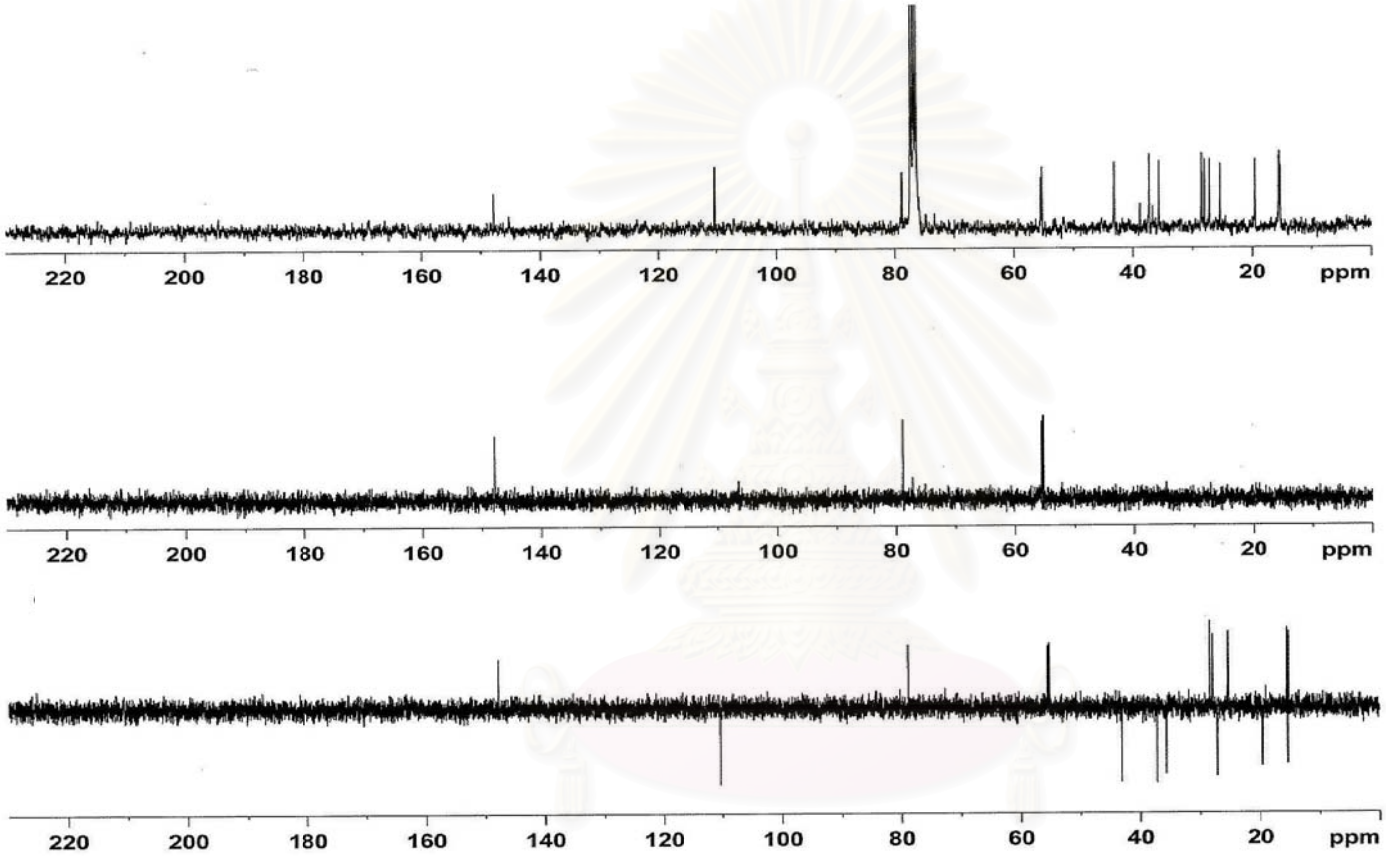

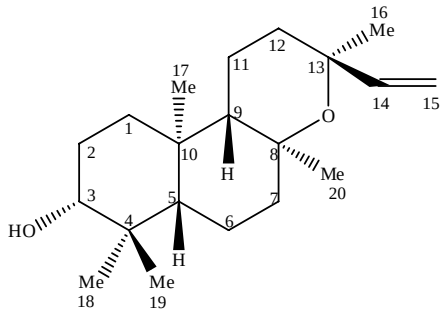

Compound **13**

Figure 55 The 75 MHz ^{13}C-NMR, DEPT-90 and DEPT-135 spectra of compound **13**

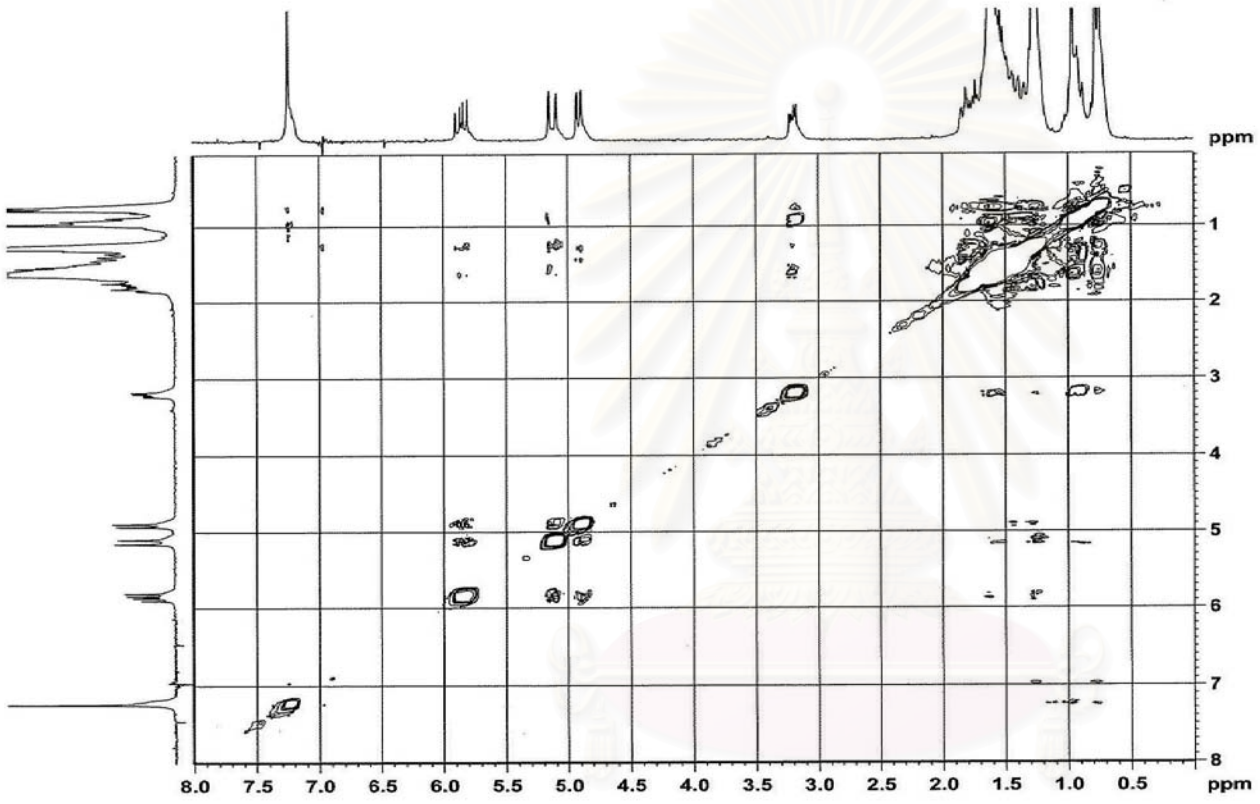

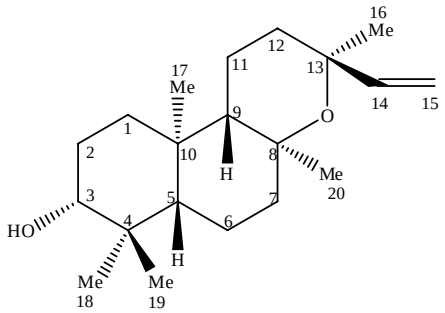

Compound **13**

Figure 56 The 300 MHz ^{1}H-^{1}H COSY NMR spectrum of compound **13** (in $CDCl_3$)

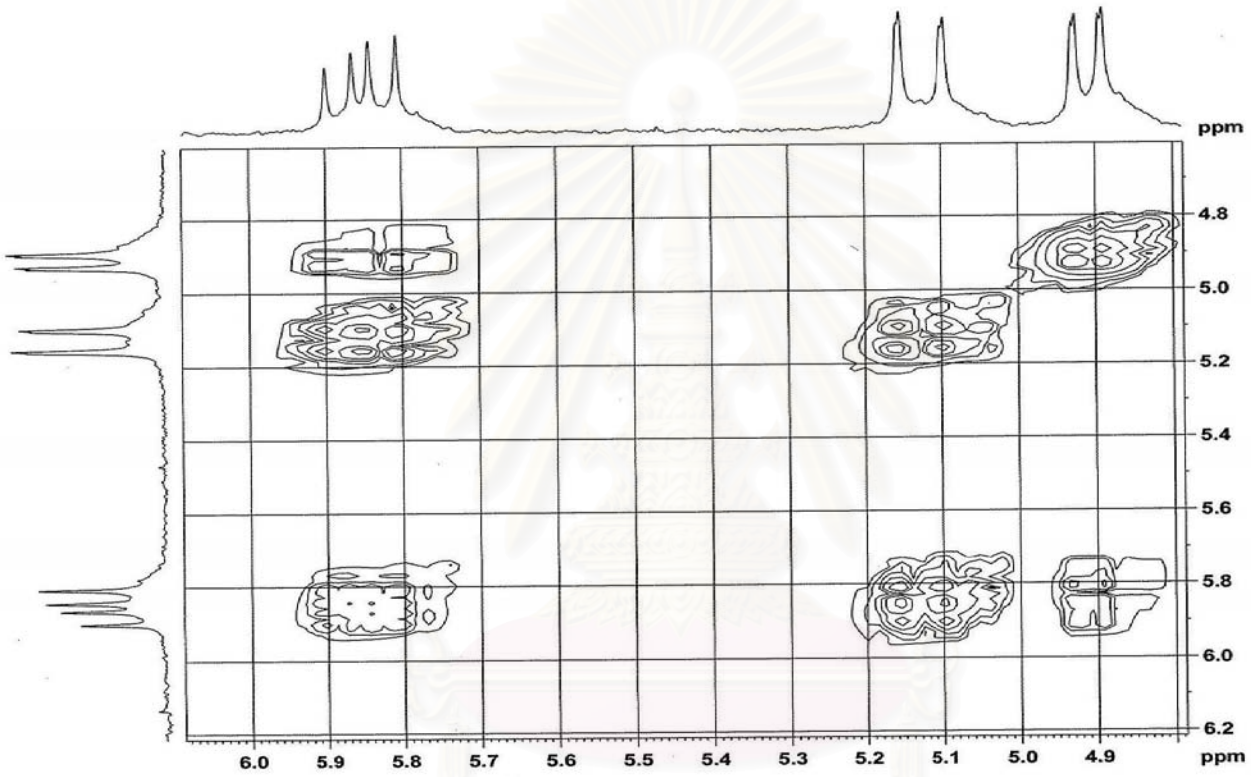

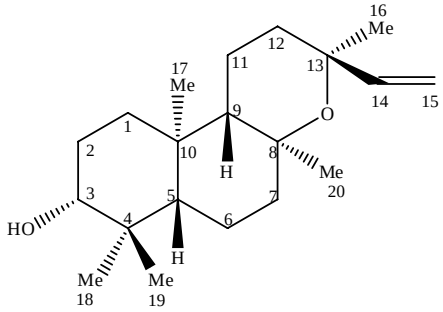

Compound **13**

Figure 56a The expanded 300 MHz ^{1}H-^{1}H COSY NMR spectrum of compound **13** (in $CDCl_3$) (δ_H6.2-4.8 ppm)

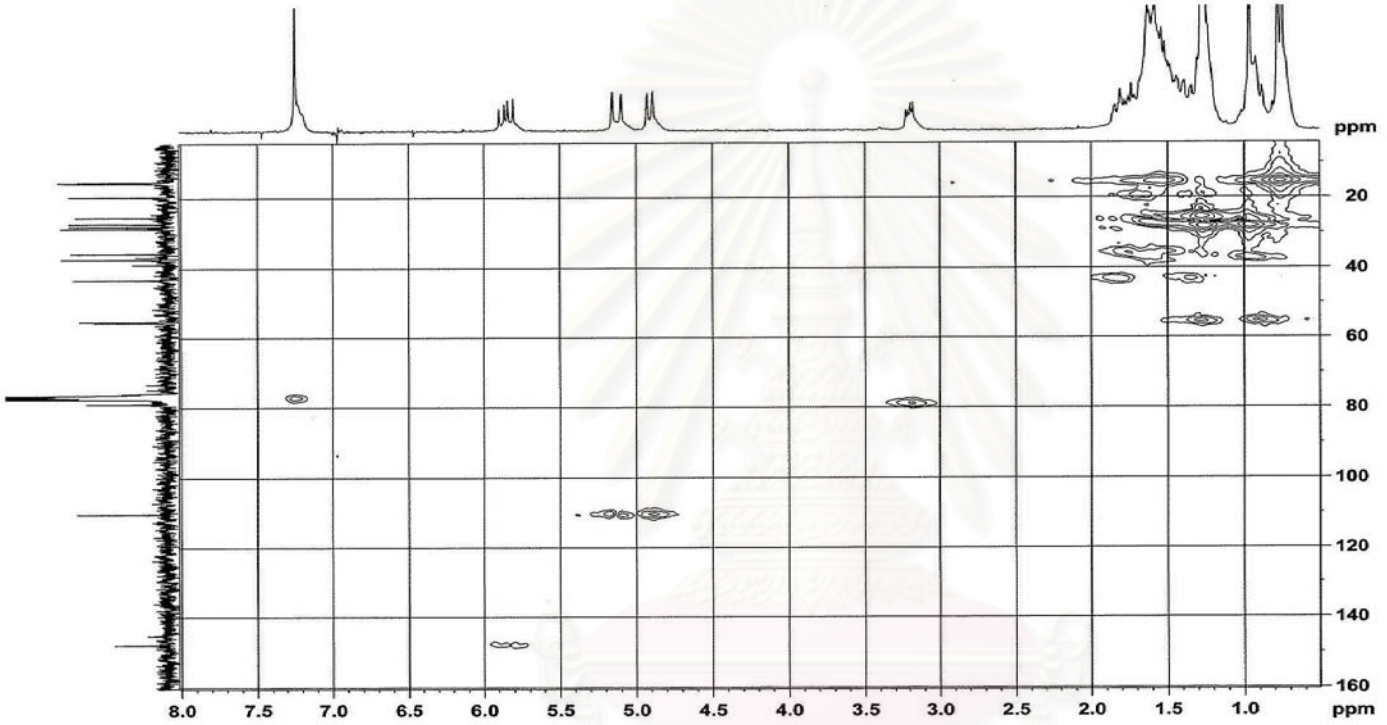

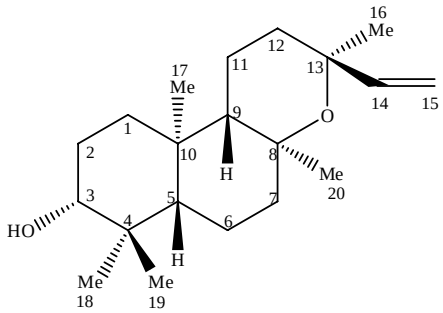

Compound **13**

Figure 57 The 300 MHz HMQC spectrum of compound **13** (in $CDCl_3$)

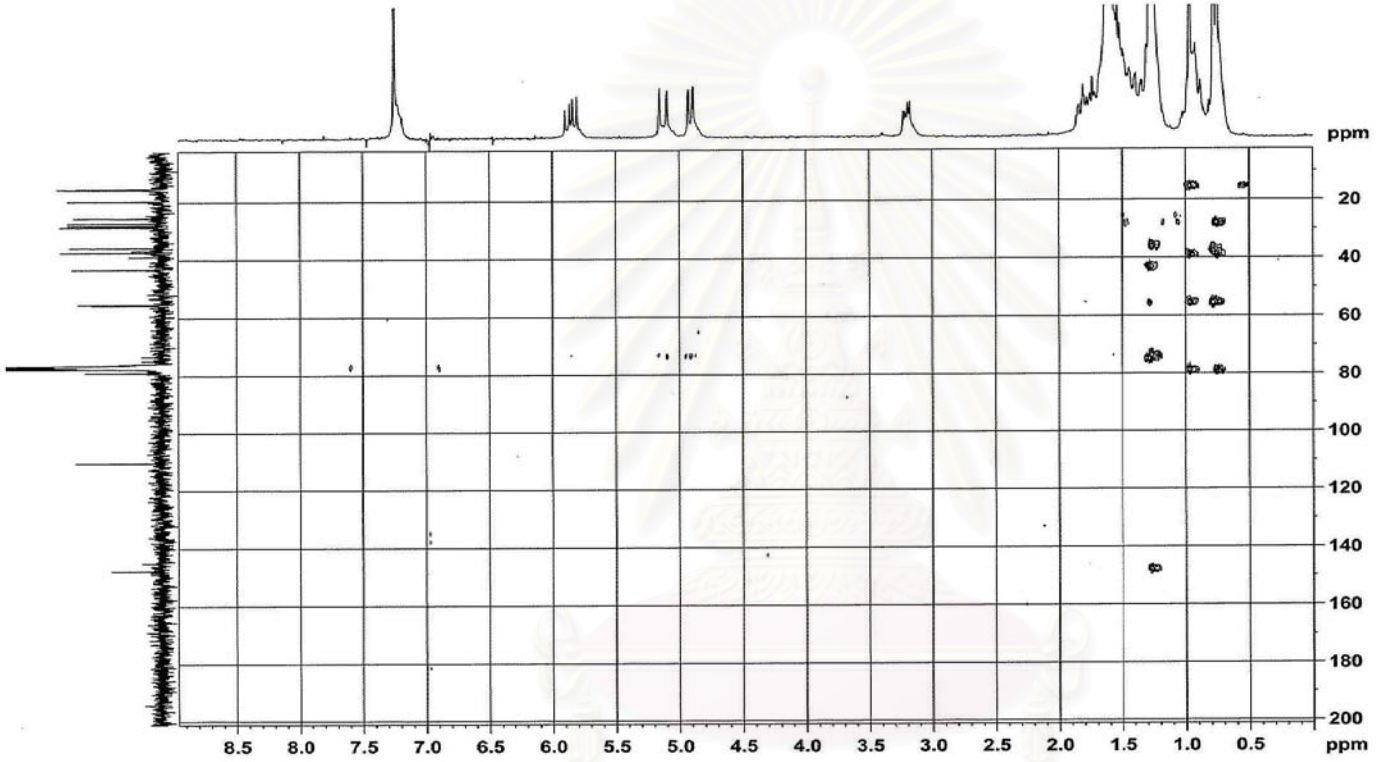

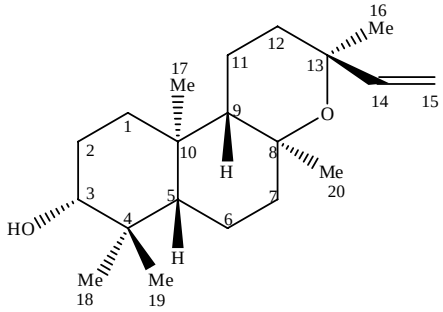

Compound **13**

Figure 58 The 300 MHz HMBC spectrum of compound **13** (in $CDCl_3$)

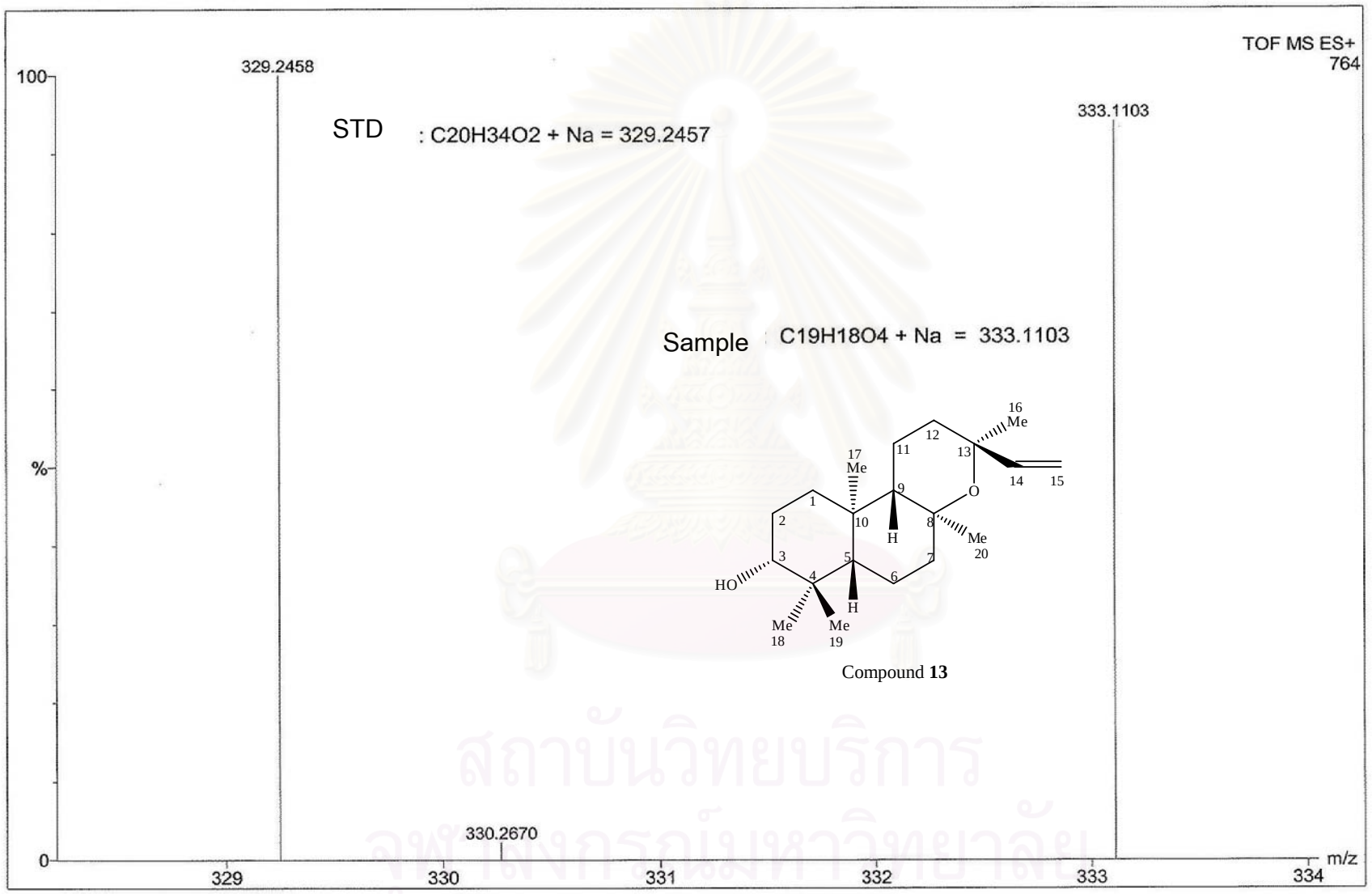

Compound **13**

Figure 59 The TOF-MS spectrum of compound 13

151

VITA

Miss Kavita Tundulawessa was born on September 2nd,1979 in Bangkok, Thailand. She received her Bachelor's degree of science in Pharmacy in 2001 from the Faculty of Pharmaceutical Sciences, Naresuan University, Thailand.